UMBC

DISSERTATION APPROVAL SHEET

Title of Dissertation: N-MYC DOWNSTREAM REGULATED GENE 1 (NDRG1): A MOLECULAR SWITCH FOR CELLULAR ADAPTATION TO HYPOXIA

Name of Candidate: Jong Park

Doctor of Philosophy, 2021

Graduate Program: NACS

Dissertation and Abstract Approved:

Rachel Brewster

Rachel Brewster

Biological Sciences

8/27/2021

8/27/2021 | 8:56:39 AM EDT

ABSTRACT

Title of Document: N-MYC DOWNSTREAM REGULATED GENE 1 (NDRG1): A MOLECULAR SWITCH FOR CELLULAR ADAPTATION TO HYPOXIA

Jong Sung Park, Ph.D., 2021

Directed By: Rachel Brewster, Ph.D.,

Associate Professor

Department of Biological Sciences

University of Maryland, Baltimore County

Lack of oxygen (hypoxia and anoxia) is detrimental to cell function and survival and underlies many disease conditions. Hence, metazoans have evolved mechanisms to adapt to low oxygen. One such mechanism, metabolic suppression, decreases the cellular demand for oxygen by downregulating ATP-demanding processes. However, the molecular mechanisms underlying this adaptation are poorly understood. Here, we report on the role of *ndrg1a* in hypoxia adaptation of the anoxia-tolerant zebrafish embryo. *ndrg1a* is expressed in the kidney and ionocytes, cell types that use large amounts of ATP

to maintain ion homeostasis. *ndrg1a* mutants are viable and develop normally when raised under normal oxygen. However, their survival and kidney function is reduced relative to WT embryos following exposure to prolonged anoxia. We further demonstrate that Ndrg1a binds to the energy-demanding sodium-potassium ATPase (NKA) pump under anoxia and is required for its degradation. Consequently, *ndrg1a* mutants that fail to downregulate NKA, have reduced ATP levels compared to WT embryos. Lastly, we show that sodium azide treatment, which increased lactate levels, was sufficient to trigger Ndrg1a-NKA degradation. These findings support a model whereby Ndrg1a functions as a molecular switch for long term adaptation to hypoxia via metabolic suppression.

N-MYC DOWNSTREAM REGULATED GENE 1 (NDRG1): A MOLECULAR SWITCH FOR CELLULAR ADAPTATION TO HYPOXIA

Jong Sung Park

Dissertation submitted to the Faculty of the Graduate School of the
University of Maryland, Baltimore County, in partial fulfillment
of the requirements for the degree of
Doctor of Philosophy
2021

Dedication

To my parents

for their unconditional love and support

TABLE OF CONTENTS

LIST OF TABLES

CHAPTER 1: INTRODUCTION

LIST OF FIGURES

CHAPTER 1: INTRODUCTION

APPENDIX

CHAPTER 1: INTRODUCTION

I. Life and oxygen: Origin of oxygen on earth

When earth formed approximately 4.5 billion years ago, its atmosphere was anoxic (devoid of oxygen) (Manhesa et al. 1980; Lindahl, 2008). Oxygen began to accumulate as ancestors of cyanobacteria evolved to generate this element through the process of photosynthesis **(Figure 1.1. Earth's geological time scale and oxygen concentration)** (Cardona et al. 2015). These oxygen-producing organisms are thought to have evolved about 2.45 billion years ago (Tomitani et al. 2006). The newly synthesized oxygen accumulated at high levels in earth's atmosphere and transformed it into an oxidizing environment (Sosa Torres et al. 2015). This event led to the extinction of many existing species (Hodgskiss et al. 2019) and was essential to the development of multicellular organisms (Gross and Bhattacharya 2010).

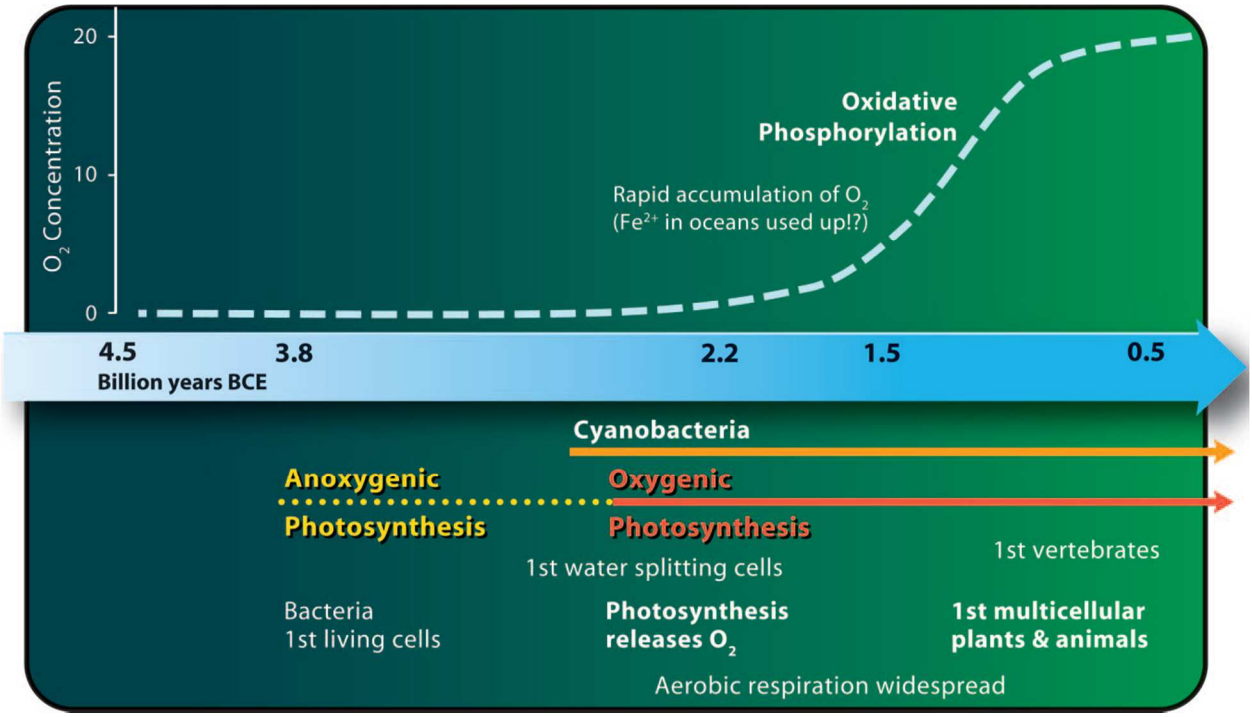

Figure 1.1. Earth's geological time scale and oxygen concentration. When earth was first formed 4.5 billion years ago, there was little to no oxygen present. The increase in oxygen concentration began as the ancestors of cyanobacteria developed the process of photosynthesis to generate oxygen. Image from Lindahl, 2008.

I.1. Role of oxygen in cellular metabolism

The increase in oxygen initiated an evolutionary race for the survival of the existing anoxic life, which took place over a period of 2 billion years and resulted in the current oxic life forms. Oxygen now comprises approximately 21% of atmospheric gas and serves as a critical molecule for the majority of life forms on earth. Specifically, oxygen serves as the terminal electron acceptor in the electron transport chain. In addition, it is used as a proximal signal in several molecular pathways, such as the well described stabilization of the hypoxia inducible factor.

I.1.1 Cellular respiration and oxidative phosphorylation

One of the important roles of oxygen in cellular metabolism is its participation in the oxidative phosphorylation step of cellular respiration. Cellular respiration is a set of biochemical reactions that are coupled together to transform macromolecules into the cell's energy currency, i.e. adenosine triphosphate (ATP). Briefly, cellular respiration consists of four major steps. The first step is glycolysis, during which glucose is broken down via various enzymatic reactions to form pyruvate **(Figure. Overview of glycolysis)**.

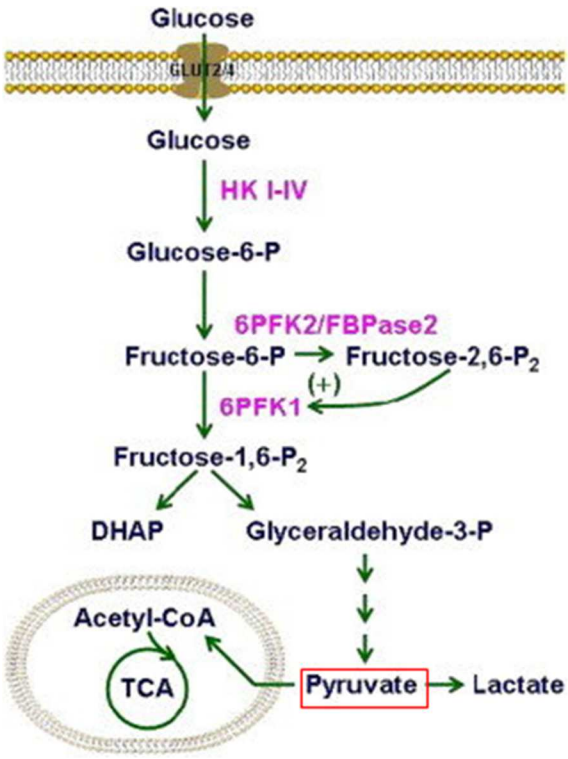

Figure 1.2. Overview of glycolysis. Following intake, glucose is processed by enzymes in the glycolysis pathway, resulting in the production of pyruvate molecules. Hexokinase (HK) and 6-phosphofructo-1-kinase (6PKF1), which phosphorylate glucose, are the rate limiting steps. DHAP: Dihydroxyacetone phosphate ,TCA: tricarboxylic acid cycle . Image from Guo et al., 2012.

The second step involves the transportation of pyruvate molecules derived from glycolysis into the mitochondrial matrix and their conversion into acetyl CoA, a non-reversible reaction. During the third step, known as the citric acid or Krebs cycle, acetyl CoA molecules are used as building blocks to produce citric acid in the mitochondrial matrix. Lastly, oxidative phosphorylation occurs on the inner membrane of the mitochondria via the transport of electrons derived from acetyl CoA through the electron transport chain, ultimately resulting in the production of ATP. This last step requires oxygen, which serves as the terminal electron acceptor of cytochrome c oxidase (complex IV) **(Figure 1.3. Oxygen is the terminal electron acceptor in the electron transport chain)** (Carreau et al. 2011; Ramsden et al. 2012; Rich, 2003). Oxidative phosphorylation specifically refers to a two-part process, namely oxidation of NADH and FADH2, followed by a phosphorylation step to produce ATP.

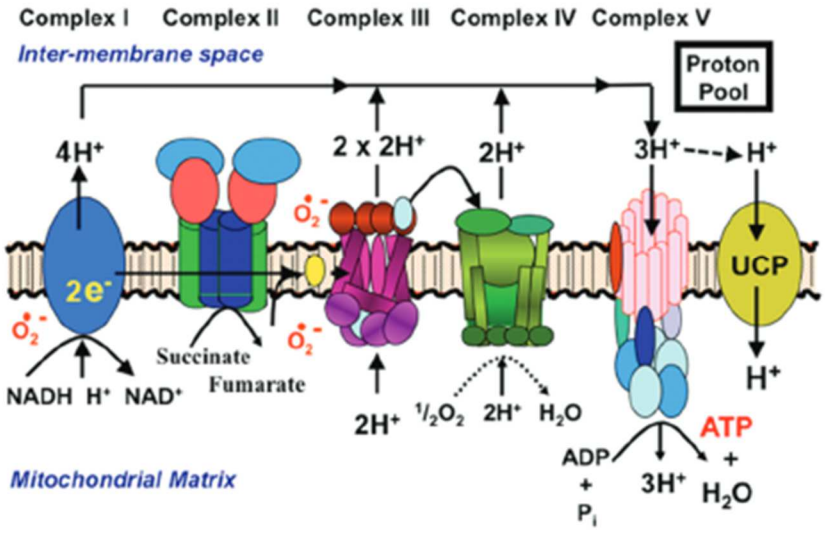

Figure 1.3. Oxygen is the terminal electron acceptor in the electron transport chain. Oxygen accepts electrons at the site of cytochrome c oxidase (complex IV) in the electron transport chain. Image from Ramsden et al., 2012.

Oxidative phosphorylation is fueled with 3 NADH and 1 FADH2 molecules for each turn of the citric acid cycle (glycolysis and pyruvate processing also generate NADH for oxidative phosphorylation). NADH oxidation results in a donation of electrons to protein complex I of the electron transport chain and the transport of protons against their gradient, from the matrix to the intermembrane space. The electrons received by protein complex I are transferred to another membrane-bound electron carrier in the electron transport chain called ubiquinone or simply Q. FADH2 oxidation and electron transfer are different from that of NADH. FADH2 directly donates electrons to Q via protein complex II and there is no associated hydrogen pumping with this process. The electrons from NADH via complex I-Q and electrons from FADH2 via complex II-Q are then transferred to protein complexes III and IV, which contribute to proton pumping into the intermembrane space. This accumulation of protons, also referred to as proton motive force (PMF), is how the cell stores the transformed energy from NADH and FADH2. The PMF powers the F0F1-ATP synthase, which uses the proton gradient energy to synthesize ATP. The F0F1-ATP synthase is composed of two main parts: F1 rotary knob structure, which contains catalytic subunit, and F0 stalk structure, which has a proton channel that spans the inner membrane of the mitochondria. The passage of protons from the intermembrane space through the F0 stalk structure feeds protons into the catalytic rotary F1 knob structure. It takes about 3 protons through the F1 catalytic rotary component of the ATP synthase to produce 1 ATP. Thus, via ATP synthase, the PMF is coupled with the phosphorylation of ADP to make ATP via ATP synthase. Lastly, electrons are transferred to oxygen, the final electron acceptor, at protein complex

IV of the electron transport chain. Therefore, without oxygen, oxidative phosphorylation cannot occur and ATP is not synthesized.

I.1.2 Oxygen-mediated cellular signaling: reactive oxygen species (ROS)

As discussed above, oxygen plays a critical role in cellular respiration, specifically, in oxidative phosphorylation where it serves as the terminal electron acceptor, allowing ATP-synthesizing machinery to run. However, oxygen also plays a role in the formation of reactive oxygen species and downstream cellular signaling. ROS was initially considered a detrimental byproduct of cellular respiration, as the accumulation of ROS can result in cellular damage and death. However, recent studies revealed that ROS plays a central role in key signaling pathways in physiological adaptation and homeostasis (Shadel and Hovath 2015).

In animal cells, there are several pathways in which ROS can be produced: mitochondrial ROS production, P450-dependent ROS production, and immune cell ROS production. For my thesis, I will only discuss the ROS produced in the mitochondria as it is the most relevant to my research focus. Mitochondrial ROS functions to regulate sodium-potassium ATPase activity when oxygen levels are low (discussed in further detail in section II.3). Due to its high affinity for electrons, oxygen readily accepts free electrons generated by the electron transport chain resulting in the production of ROS such as superoxide anion (O2*-) , hydroxyl radical (HO*), and hydrogen peroxide (H2O2) as byproducts (Devasagayam et al. 2004; Edreva 2005). Under optimal conditions, the flow of electrons to complex IV in the inner membrane of mitochondria results in the reduction of oxygen to water, a process that is coupled with ATP synthesis.

However, electrons can also react with oxygen prior to complex IV to form ROS if oxygen levels change suddenly, such as during reperfusion or reoxygenation events (Murphy 2009). In particular, complexes I and III are thought to be the main sites of mitochondrial ROS production, although recent findings suggest that other protein complexes in the mitochondria, including complex II, can participate in the production of ROS (Quinlan et al. 2013). It is possible that different sites of ROS production in the mitochondria can produce different species and amounts of ROS, which in turn participate in the physiological adaptation to changing environments **(Figure 1.4. Mitochondrial ROS signaling pathways)**.

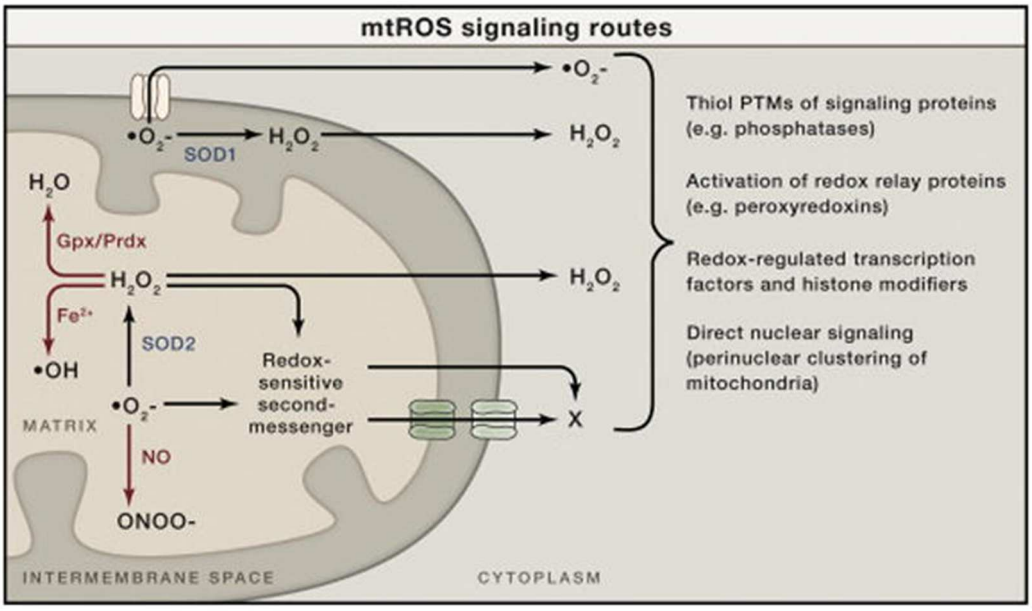

Figure 1.4. Mitochondrial ROS signaling pathways. Superoxide (oxygen-) can be turned into hydrogen peroxide (H2O2) by SOD. The resulting H2O2 can cross the mitochondrial membrane to induce signaling in the cytoplasm that can result in thiol PTM, activation of redox relay proteins, redox-regulation of transcription factors and histone modifiers. Furthermore, both superoxide and hydrogen peroxide can modify molecules in the mitochondria to induce ROS-signaling. Image from Shadel and Horvath, 2015.

Several studies have shown that these mitochondrial ROS are implicated in signaling pathways that either extend or inhibit aging in both invertebrates and vertebrates (Shulz et al. 2007; Weimer et al. 2014; Zarse et al. 2012; Dancy et al. 2014; Hekimi et al. 2011; Ristow and Schmeisser, 2011). In addition, mitochondrial ROS are implicated in other pathways including, but not limited to wound healing, intracellular pH balance, and survival under hypoxia (Xu and Chisholm 2014; Johnson et al. 2012; Schieber and Chandel, 2014).

II. Oxygen deprivation and hypoxia-induced responses

Oxygen deprivation results in decreased ATP levels via a reduction in oxidative phosphorylation, which is most acutely experienced in organs with high metabolic demands such as the brain, heart, and kidney. Hence it is not surprising that hypoxia and/or ischemia (inadequate blood supply to an organ) related injuries such as stroke and myocardial infarction cause major morbidity and mortality worldwide (Mozaffarian et al. 2016). Normal physiological oxygen levels in cells can be as low as 1.3% partial oxygen pressure (**Table 1.1. Values of normal physiological oxygen in different organs**) (Carreau et al. 2011) and hypoxia-induced adaptive responses are triggered when physiological oxygen levels decrease below their normal threshold.

	pO_2	
	mmHg	%
Air	160	21.1
Inspired air (in the tracheus)	150	19.7
Air in the alveoli	110	14.5
Arterial blood	100	13.2
Venous blood	40	5.3
Cell	9.9–19	1.3–2.5
Mitochondria	<9.9	<1.3
Brain	33.8 ± 2.6	4.4 ± 0.3
Lung	42.8	5.6
Skin (sub-papillary plexus)	35.2 ± 8	4.6 ± 1.1
Skin (dermal papillae)	24 ± 6.4	3.2 ± 0.8
Skin (superficial region)	8 ± 3.2	1.1 ± 0.4
Intestinal tissue	57.6 ± 2.3	7.6 ± 0.3
Liver	40.6 ± 5.4	5.4 ± 0.7
Kidney	72 ± 20	9.5 ± 2.6
Muscle	29.2 ± 1.8	3.8 ± 0.2
Bone marrow	48.9 ± 4.5	6.4 ± 0.6

Table 1.1. Values of normal physiological oxygen in different organs. Normal physiological oxygen levels vary widely depending on the location and function of the organs. Image from Carreau et al., 2011.

These responses can vary widely among species, at different developmental stages and among different tissue types within the same organism (Clegg, 1997; Dinkelacker, Costanzo and Lee, 2005; Duerr and Podrabsky, 2010; Meller and Podrabsky, 2013; Podrabsky and Wilson, 2016; Smith et al. 2009; Storey, 2007).

A common theme among organisms discussed below is the need to get rid of lactate build up. Lactate is a byproduct of glycolysis and that it can build up when organisms are deprived of oxygen for a long period. In turn, lactate causes acidosis, which is toxic to the cell. Hence, hypoxia-tolerant organisms have evolved mechanisms to get rid of lactate. Crucian carps (*Carassius carassius*) and goldfish (Carassius auratus) can survive without oxygen for days to months while overwintering in ponds that can become hypoxic during cold months (Vornanen, Stecyk, & Nilsson, 2009). These fish survive low oxygen conditions (hypoxia) or even the anoxia by turning the byproduct of glycolysis, lactate, into ethanol in skeletal muscle in order to continue to flux the glycolysis pathway and prevent lactic acidosis (**Figure 1.5. Lactate to ethanol pathway in the crucian carp under hypoxia**). Ethanol is secreted out of the fish through the gills.

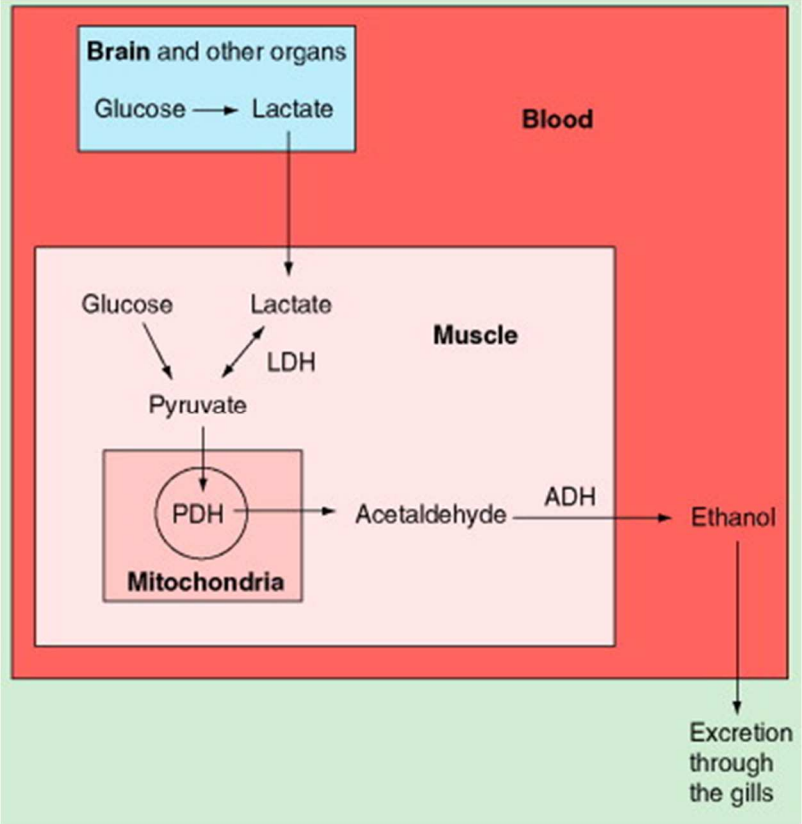

Figure 1.5. Lactate to ethanol pathway in the crucian carp under hypoxia. Ethanol is produced in muscle cells while all other cells produce lactate when exposed to hypoxia. The lactate molecules from other cells are turned into pyruvate in the muscle cell by lactate dehydrogenase (LDH). Then, pyruvate is further converted into acetaldehyde by pyruvate dehydrogenase (PDH). Finally, the acetaldehyde is turned into ethanol by alcohol dehydrogenase (ADH), which is a special enzyme that is only found in the muscle cells of crucian carp and closely related goldfish. Ethanol can easily diffuse across the plasma membrane and it enters the bloodstream to be eventually secreted by the gills. This process prevents the buildup of lactate and allows hypoxic glycolysis to continue for an extended period in the crucian carp. Image from Vornanen et al., 2009.

Furthermore, lamellae of the gill tissue protrude outward in response to hypoxia, resulting in an increased respiratory surface area for increased oxygen uptake (Sollid, 2003). Another adaptive mechanism in crucian carp is the extremely high oxygen affinity of haemoglobin (Stenslokken et al., 2014). In addition, these fish conserve ATP by reducing brain activity using inhibitory neuromodulators, GABA and adenosine (Nilsson, 1991; Stensløkken et al., 2014).

Painted turtles (Chrysemys picta) are also known for their remarkable hypoxia tolerance, surviving for several months trapped under ice or in anoxic mud (Jackson, 2002). This species allows a continuous flux of glycolysis by removing the excess buildup of lactate under anoxia via storage and buffering of lactate in their shell and skeleton (Jackson, 2004). Furthermore, painted turtles inhibit ion transporters to make their plasma membranes impermeable, a process known as channel arrest (Pamenter et al., 2008). Although channel arrest in neurons causes this organism to enter into a state of coma, this process allows conservation of ATP and survival of the organism. Channel arrest will be revisited in the Conclusion section of my thesis, as it may relate to Ndrg1 function. Furthermore, painted turtles, like crucian carps and goldfish, use adenosine and GABA to downregulate neuronal activity (Buck, Hogg, Rodgers-Garlick, & Pamenter, 2012; Lutz & Leone-Kabler, 1995; Pék & Lutz, 1997; Pérez-Pinzón, Lutz, Sick, & Rosenthal, 1993).

In contrast to these aquatic organisms, naked mole rats, which live underground in dry and arid regions, survive anoxia by switching from glucose to fructose-mediated glycolysis. Upregulation of GLUT5 (a fructose transporter) and ketohexokinase allows mole rats to use fructose to drive glycolysis and avoid feedback inhibition on

phosphofructokinase due to lactic acidosis (**Figure 1.6. GLUT5 up-regulation and ketohexokinase allow mole rats to use fructose to drive glycolysis and avoid feedback inhibition on phosphofructokinase due to lactic acidosis**) (Park et al., 2017).

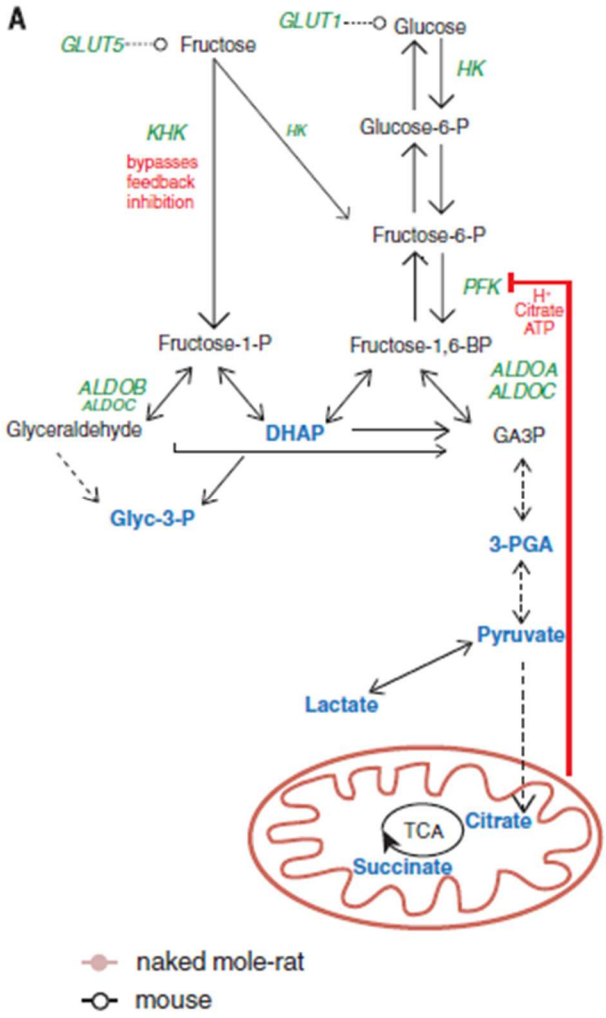

Figure 1.6. GLUT5 up-regulation and ketohexokinase allow mole rats to use fructose to drive glycolysis and avoid feedback inhibition on phosphofructokinase due to lactic acidosis. Fructose enters cells via GLUT5 and ketohexokinase (KHK) phosphorylates fructose at a higher rate than hexokinase (HK). Fructose-1-P is metabolized into trioses via aldolase B (ALDOB) or aldolase C (ALDOC), bypassing the feedback inhibition on phosphofructokinase (PFK) by the buildup of lactate. Glyceraldehyde-3-phosphate (GA3P), tricarboxylic acid (TCA). Image from Park et al., 2017.

The examples provided above illustrate overlapping yet distinct adaptive responses to hypoxia between organisms. The outcome of hypoxia responses can also vary within the same organism depending on how far below the norm the levels of oxygen are (e.g. hypoxia vs. anoxia). In *C. elegans*, the response to severe hypoxia (0.1 kPa oxygen) and anoxia is dramatically different. Under anoxia, the majority of organisms survive while most of them die when exposed to severe hypoxia. A postulated key difference between these treatments is that anoxia elicits metabolic arrest but severe hypoxia does not. Thus, while neither treatment allows for ATP levels to be maintained at normoxic values (glycolysis produces less ATP than oxidative phosphorylation), anoxia preserves energy by shutting down metabolically demanding processes. (**Figure 1.7. Survival of *C. elegans* to low oxygen is discontinuous**) (Nystul & Roth, 2004). These observations further suggest that the differential response to low oxygen is qualitative and may not simply be the result of a passive response to oxygen deprivation.

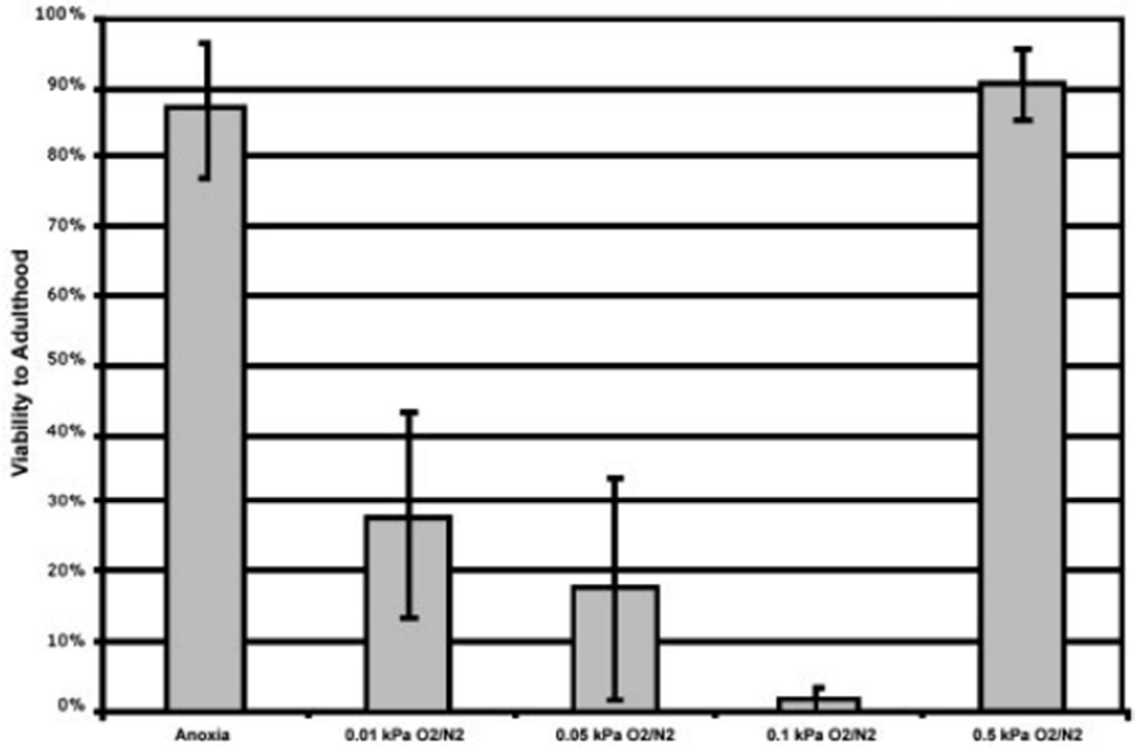

Figure 1.7. Survival of *C. elegans* to low oxygen is discontinuous. *C. elegans* were subjected to different oxygen concentrations for 24 hours. From left to right, Anoxia (0% oxygen); .01 kPa oxygen; .05 kPa oxygen; .1 kPa oxygen; .5kPa oxygen. Survival was scored using three independent experiments. Image from Nystul and Roth, 2004.

While the examples provided above highlight unique adaptive mechanisms to low oxygen in different organisms, especially those involved in metabolic reprogramming (switching to and maintaining glycolysis), currently there are very little findings on mechanisms that induce metabolic arrest, which is the focus of my thesis.

Metabolic arrest or hypometabolism is the concept that ATP can be preserved via reduction of its turnover rate by downregulating ATP demanding processes in the cell. There are reports of downregulation of transcription and translation as examples of hypoxia adaptation (K. B. Storey & Storey, 2007). In addition, hypoxia-tolerant organisms such as the painted turtle, crucian carp, and goldfish have the ability to reduce cell membrane permeability to ions - specifically in neurons, which may reduce ATP demand. However, these underlying mechanisms remain poorly understood.

Interestingly, human cells and organs are not thought to perform active metabolic suppression - although controversially, they do downregulate sodium-potassium pump (NKA), a protein that consumes high levels of ATP.

For my thesis, I will investigate the impact of downregulation of NKA under anoxia in the zebrafish kidney, an organ with very high ATP demand that relies heavily on NKA activity.

II.1. Causes and types of hypoxia in humans

There are many different ways in which hypoxia can manifest itself in humans. Mainly, any dysfunction in the lung tissues, including alveoli and the surrounding tissues can impair oxygen diffusion. In addition, inefficient vascular circulation can also cause hypoxia. The following are some of the well-known causes of hypoxia in humans:

premature birth (underdeveloped lungs), sleep apnea, sickle cell anemia, and life at high altitude. In addition, underlying pathophysiology such as pneumonia, COVID19, asthma, or chronic obstructive pulmonary disease (COPD) may result in insufficient air exchange resulting in hypoxia. Furthermore, any condition that reduces the function or the amount of haemoglobin to support normal oxygen levels can cause hypoxia. Such conditions include iron deficiency, hemorrhage, methemoglobinemia, carbon monoxide poisoning. Also, improper blood flow caused by sickle cell anemia, edema, heart attack or ischemic stroke can cause hypoxia in the downstream target tissues. Lastly, chemical agents such as cyanide block the process of oxidative phosphorylation to suffocate the cell in the presence of oxygen.

Terminology that is often used interchangeably to indicate low oxygen includes hypoxia, anoxia, hypoxemia, and ischemia. However, these terms are not synonymous. Hypoxia and anoxia have been previously defined, but in detail, hypoxia refers to the state in which the oxygen supply is below the normal threshold to maintain normal cell or tissue function while the term anoxia refers to a state where there is a complete absence of oxygen supply in the cell. The normal physiological oxygen values for different organs can be found in (**Table 1.1. Values of normal physiological oxygen in different organs**). The term hypoxemia refers to arterial oxygen supply that is below a normal threshold (West, 1977). Hence, there may be hypoxemia without the onset of hypoxia or anoxia in tissues if hypoxemia is a recent occurrence. Lastly, ischemia refers to disruption or insufficient blood flow to the target tissue, which can cause hypoxia in those affected cells and tissues.

In addition, hypoxia can be classified as either a generalized or local event. Generalized hypoxia affects the whole body while local hypoxia affects specific tissues or organs of the body. Signs and symptoms of hypoxia vary depending on the severity and onset, but in general, hypoxia results in cyanosis or bluing of the affected tissues, confusion, hypertension, headache, fainting, polycythemia (chronic hypoxia) and tachycardia (fast heart rate). In the case of severe hypoxia, if the affected tissues or organs are not adequately oxygenated within a few minutes, then most tissues will suffer from irreparable damage and, in severe cases, death may occur.

II.2. Hypoxia-induced responses and molecular pathways

While the previous section above described the general hypoxia adaptive strategies such as metabolic reprogramming and hypometabolism in non-human organisms, this section will focus on molecular pathways of hypoxia-induced responses.

Endogenous hypoxia-induced responses can be activated when oxygen levels decrease below the normal threshold of oxygen concentration depending on tissue types. There are several major hypoxia pathways that are well studied, including the hypoxia inducible factor pathway, the discovery of which earned Kaelin, Ratcliffe and Semanza the 2019 Nobel prize in physiology and medicine. In addition, AMPK and NF-kB are well studied hypoxia responsive molecules, which will be further described below. Although there are other hypoxia induced responses, I will not cover them as they are less well understood and not directly relevant to my thesis.

II.2.1 The hypoxia inducible factor (HIF)

Specific hypoxia responsive genes are upregulated in response to stabilization of the hypoxia inducible factor (HIF). HIF is a member of the basic helix-loop-helix (bHLH) per-arnt-sim (PAS) domain-containing transcription factors (Dengler et al. 2014). The active form of the transcription factor is composed of two HIF subunits, one alpha and one beta subunit (Semenza and Wang, 1992; Wang et al., 1995). Under normoxia, the alpha subunit or HIF-1a, is hydroxylated by the prolyl-hydroxylase enzyme (PHD2) using oxygen as a substrate (Ivan et al., 2001; Jaakkola et al., 2001; Bruick and McKnight, 2001; Epstein et al., 2001; Ivan et al., 2002). When HIF-1a is hydroxylated, it can be recognized and ubiquitinated by the Von-Hippel Lindau tumor suppressor (E3 ubiquitin ligase) and subsequently targeted for proteasomal degradation (**Figure 1.8. HIF degradation pathway**) (Maxwell et al., 1999; Cockman et al., 2000; Kamura et al., 2000; Krieg et al., 2000; Ohh et al., 2000; Tanimoto et al., 2000). However, under hypoxia, the low levels of molecular oxygen prevents PHD2 from hydroxylating HIF-1a and the resulting stabilized HIF-1a can localize to the nucleus where it dimerizes with its partner, HIF-1b, and regulates the expression of genes that contain hypoxia-responsive elements (HRE) in their promoter region. In addition, it has been found that HIF can also be stabilized by ROS (Jung et al., 2008). Many of the genes that are upregulated by HIF control angiogenesis, erythropoiesis, glycolysis, and cell survival pathways.

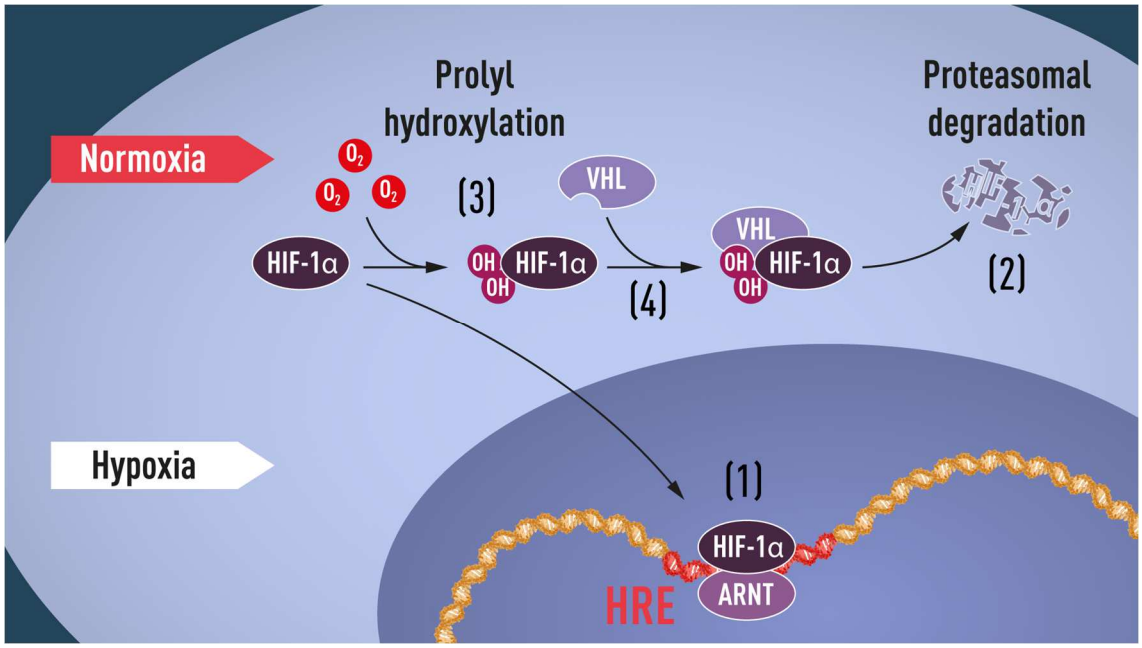

Figure 1.8. HIF degradation pathway. Under normoxia, oxygen is used as a substrate for hydroxylation of HIF-1a by the prolyl hydroxylase enzyme (PHD). Following hydroxylation, HIF-1a is subsequently ubiquitinated by Von-Hippel Lindau tumor suppressor (E3 ubiquitin ligase) and targeted for proteasomal degradation. Under low oxygen , HIF-1a is protected from degradation and accumulates in the nucleus where it associates with HIF-1b or ARNT to bind to hypoxia-response element (HRE) sequences to regulate hypoxia responsive genes. Image from Nobelprize.org.

II.2.2 The AMP-activated protein kinase (AMPK)

In addition to HIF, AMP-activated protein kinase (AMPK) plays an important role in the hypoxia adaptive response. AMPK is a well characterized energy sensor that is present in both vertebrates and invertebrates, (Hawley et al., 1996; Hardie and Ashford, 2014; Hardie et al., 2016). Although its function is not completely understood, it is well established that AMPK can act as an energy sensor by sensing the AMP/ATP ratio in the cell. Under stressful conditions such as hypoxia or the presence of oxidative phosphorylation inhibitors (Corton et al., 1994; Hardie et al., 2016), the cell's energy supply (ATP) drops below its normal threshold. This directly changes the AMP/ATP ratio - specifically, AMP levels rise while ATP levels decrease. This increase in AMP/ATP ratio results in the binding of AMP to the gamma subunit of AMPK, which results in allosteric activation of the alpha subunit of AMPK via phosphorylation at the Thr182 residue. Thus the energy currency of the cell, ATP, and its dephosphorylated form, AMP, are tightly coupled to the activity of AMPK (Hardie and Ashford, 2014). However, previous reports have also proposed that AMPK can be activated by ROS acting on redox-sensitive cysteine residues on the alpha subunit of AMPK (Zmijewski et al., 2010). Another study confirmed that the role of ROS in activating AMPK is merely an indirect one (Hinchy et al., 2018). Regardless of how AMPK is activated, it regulates the activity of target proteins via phosphorylation to reprogram metabolism. Mainly, it deactivates energy-consuming processes and promotes glycolysis to maintain adequate levels of ATP despite reduced oxygen (Hardie and Ashford, 2014; Lang and Foller, 2014). There are many studies that document the activation of AMPK in hypoxia-induced pathologies in the heart, brain, and gut and downstream events that promote cell survival

(Russell et al., 2004; Seo-Mayer et al., 2011; Cai et al., 2019; Hu et al., 2019; Michiels 2004; Kondo et al., 2019).

III. N-myc downstream regulated genes (NDRGs)

N-myc downstream regulated genes (NDRGs) consist of four members (NDRG1-4). NDRGs are members of the alpha/beta hydrolase superfamily that contain alpha/beta hydrolase fold motifs in their structure (Melotte et al., 2010) (**Figure 1.9. Structural outline of the human NDRG proteins 1-4**).

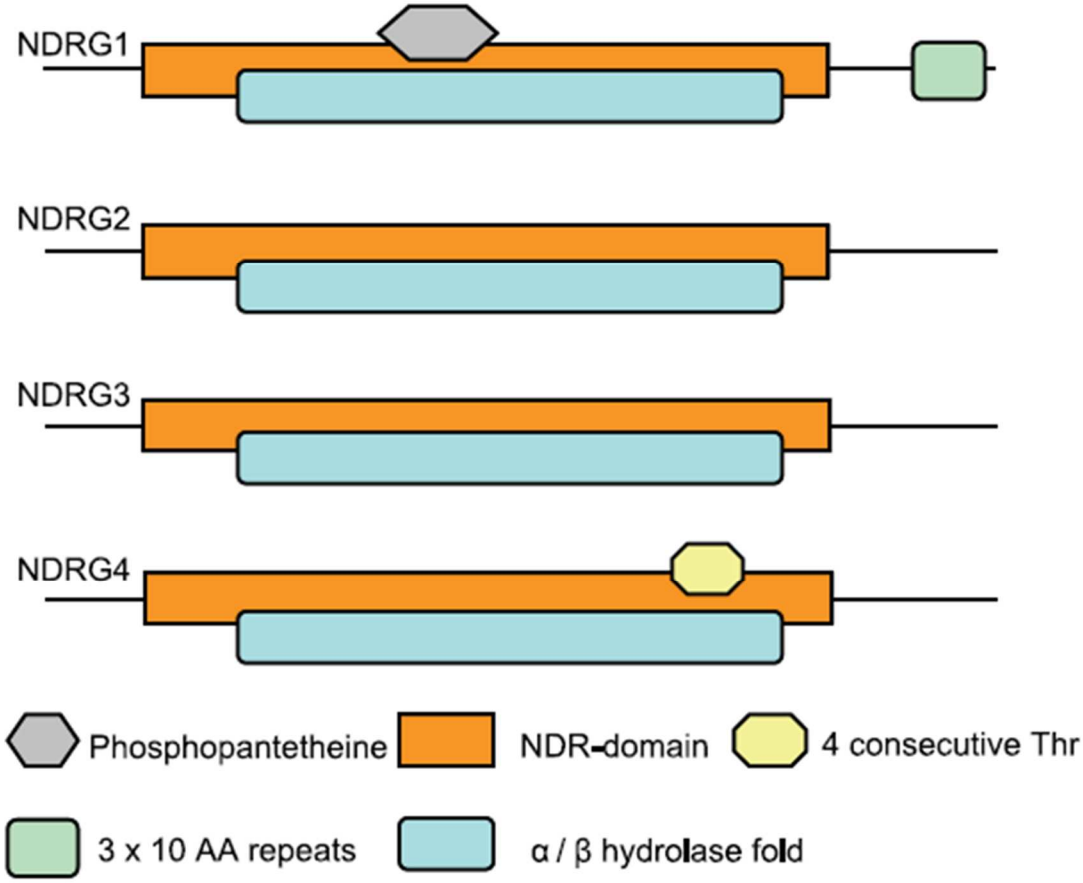

Figure 1.9. Structural outline of the human NDRG proteins 1-4. Schematic of different domains present in each of the NDRG family members. Image from Melotte et al., 2010.

The different NDRG paralogs share about 53-65% protein homology while each member of the NDRG family (NDRG1 in different species) are highly conserved among different organisms (**Figure 1.10. Phylogenetic tree of the NDRG family**). For example, human and mouse NDRG1, NDRG2, and NDRG3 share a sequence homology of 94%, 92%, and 96%, respectively (Zhou et al. 2001).

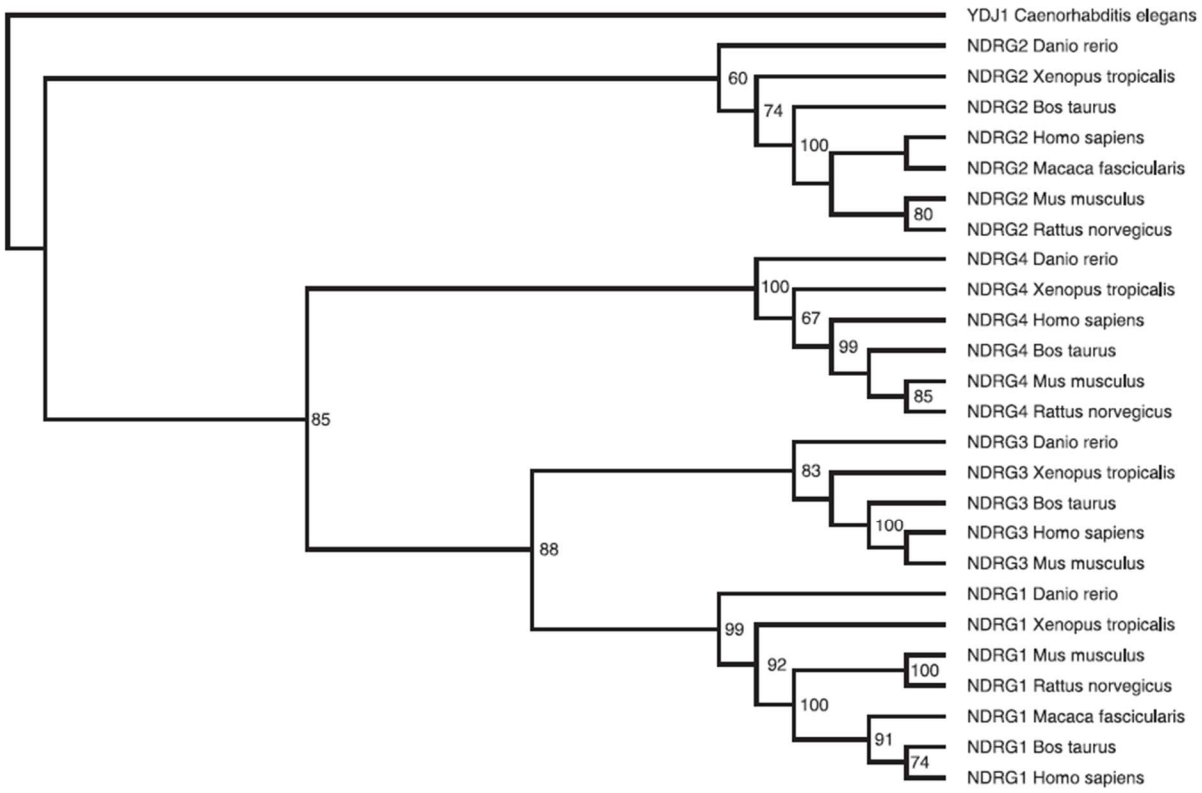

Figure 1.10. Phylogenetic tree of the NDRG family. NDRG proteins 1-4 from human (*Homo sapiens*), crab-eating macaque (*Macaca fascicularis*), Cow (*Bos taurus*), mouse (*Mus musculus*), rat (*Rattis norvegicus*), lipid frog (*Xenopus tropicalis*), and zebrafish (*Danio rerio*) are from UniProt/Swiss-Prot database. For outgroup, a closely related protein from *Caenorhabditis elegans* was selected (YDJ1). Image from Melotte et al., 2010.

Furthermore, NDRG homologs are also found in plants (Krauter-Canhame et al. 1997) and are conserved (**Figure 1.11. Amino acid comparison of NDRG1 among different species**). In sunflowers, the *ndrg1* homolog is known as the *sf21*; it is thought that the protein acts in pollen-pistil interaction (Krauter-Canhame et al., 1997). For the rest of the document, NDRG refers to NDRGs in mammals and members of this family in general while Ndrgs refers to members of the family in zebrafish specifically.

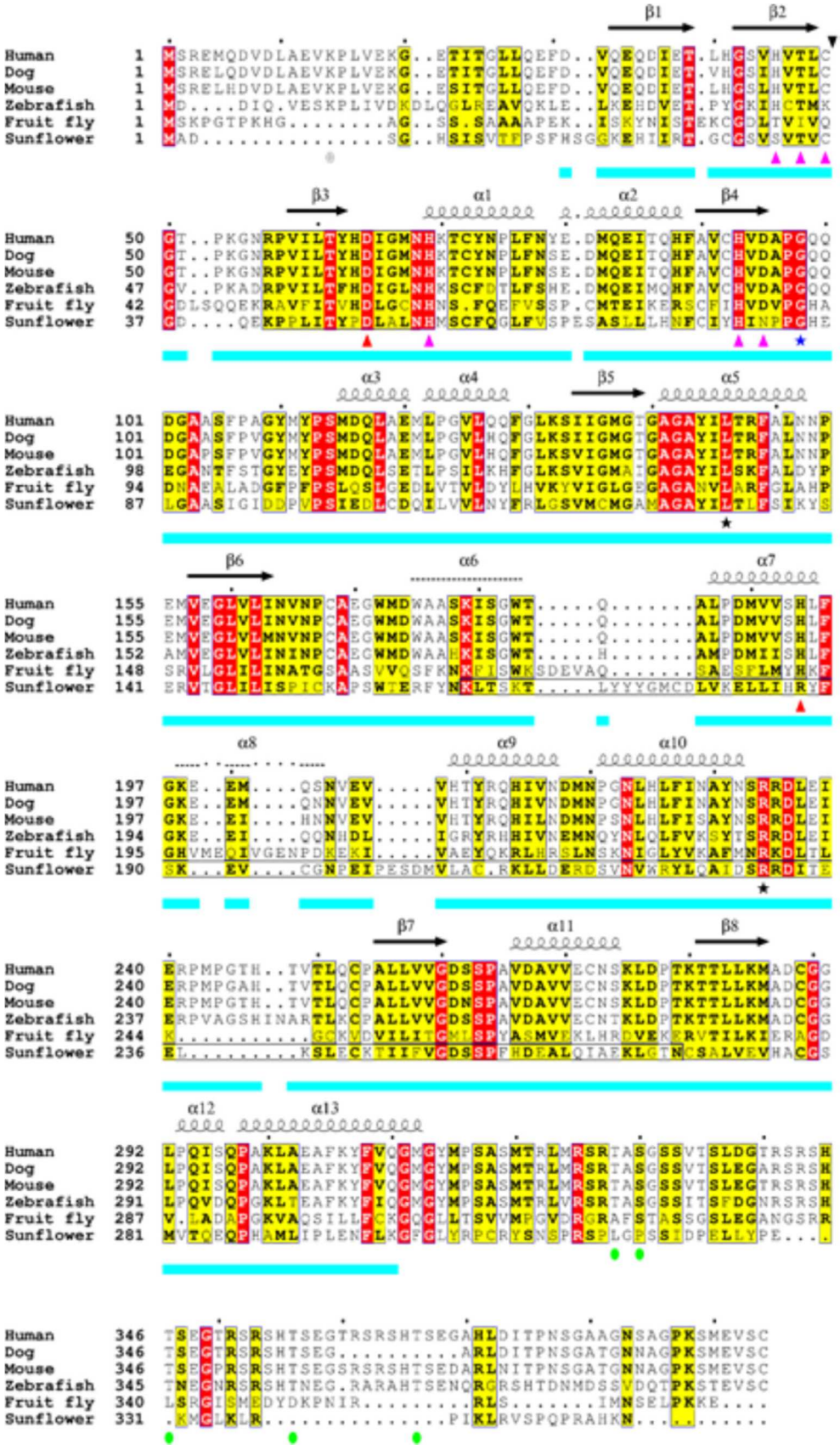
β1
β2
β3
α1
α2
β4
α3
α4
β5
α5
β6
α6
α7
α8
α9
α10
β7
α11
β8
α12
α13
Human
Dog
Mouse
Zebrafish
Fruit fly
Sunflower

Figure 1.11. Amino acid comparison of NDRG1 among different species. Putative catalytic residues are in red triangles, putative metal-binding residues in pink triangles, phosphorylation sites in green circles, SUMOylation site in grey circle and a predicted proteolytic cleavage site are in black triangle. UniProtKB accession numbers were as follows: dog NDRG1 (L7V3M2-1), mouse NDRG1 (Q62433-1), zebrafish NDRG1 (Q6A3P5-1), fruit fly BcDNA : GH02439 (Q9Y164-1) and sunflower pollen-specific protein SF21 (Q23969-1). Image from Mustonen et al., 2021.

Interestingly, despite belonging to the alpha/beta hydrolase family, NDRGs lack key amino acids required for the catalytic activity of the alpha/beta hydrolase (Shaw et al., 2002; Hwang et al., 2011). However, the recent crystal structure of NDRG1 suggests that this family member contains putative catalytic residues (Mustonen et al., 2021) (**Figure 1.12. New crystal structure of NDRG1 reveals putative catalytic amino acids that were once thought to be absent**).

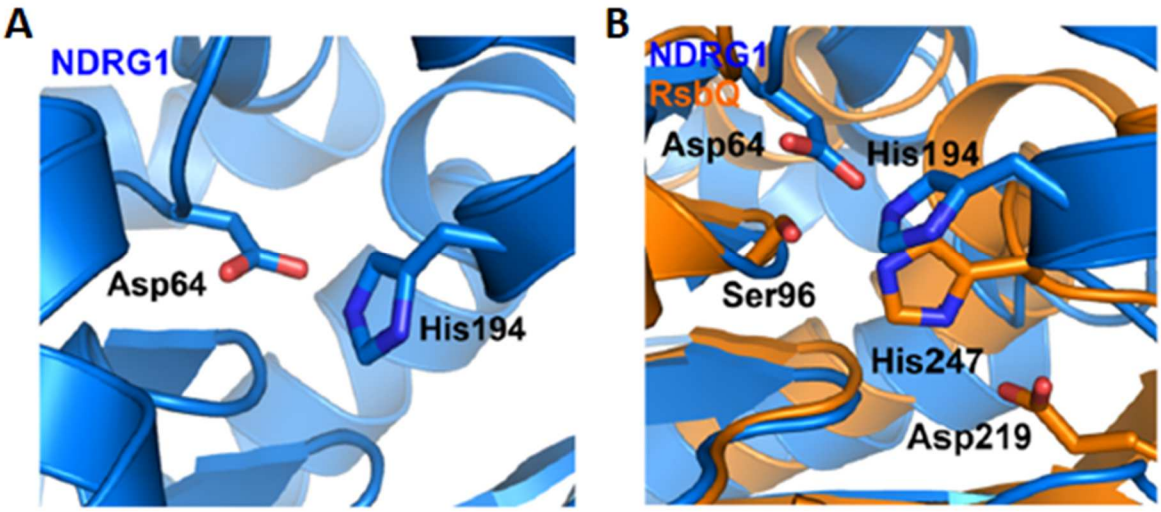

Figure 1.12. New crystal structure of NDRG1 reveals putative catalytic amino acids that were once thought to be absent. Panels A and B were prepared using PyMOL. (A) The 3D structure of NDRG1 reveals that the canonical catalytic sites are not present in NDRG1, however, amino acids Asp64 and His194 are in close enough proximity to function as putative catalytic residues. (B) Overlap between the 3D structure of NDRG1 and a well known catalytic site of *Bacillus subtilis* stress-response regulator, RsbQ (in orange), supports the model for NDRG1 putative catalytic activity. Image from Mustonen et al., 2021.

Previously, NDRGs have been proposed to function as molecular scaffolds that mediate protein-protein interactions and signaling among different binding protein partners (Kim et al. 2020). Such an adapter function for NDRGs could in principle enable context-dependent functions - acting as a switch between normoxia and hypoxia by interacting with different sets of proteins in these environments. In addition, the different tissue-specific expression patterns of NDRGs (Okuda et al. 1999; Zhou et al. 2001) suggest that members of this family function in a context specific manner.

III.1. NDRG background and history

Although the cellular function of the NDRG family is not completely clear, our understanding has grown over the past decade. There is enough evidence to suggest that NDRGs are stress-responsive genes regulated by hypoxia, both transcriptionally and post-translationally (unpublished Le et al.). Other studies also revealed that NDRGs have a normoxic role in vesicle trafficking (Askautrud et al. 2014, Kacchap et al. 2007, Pietiainen et al. 2013, Fontenas et al. 2016), cytoskeletal interaction (Croessmann et al., 2015, Kim et al., 2004) and cell proliferation (Jin et al., 2014; Lu et al., 2015; Liu et al., 2012; Ai et al., 2016). NDRG1 was the first family member to be discovered and so named because it is negatively regulated by the proto-oncogenes MYC and N-MYC (Shimono et al. 1999). NDRG1 has a rich nomenclature history, as it was renamed multiple times; its former names are: reducing agents and tunicamycin-responsive protein (RTP), reduced in tumor, 42kDa (Rit42), calcium associated protein 43kDa (Cap43), downregulated gene 1 (Drg1), and protein regulated by oxygen 1 (PROXY1) (Kokame et al., 1996; Kurdistani et al., 1998; Zhou et al., 1998; Piquemal et al.,1999; Shimono et al.,

1999; Kitowska and Pawelczyk, 2010). Much of the previous work on NDRG1 has focused on its role in cancer progression, as either an oncogene or a tumor suppressor (van Belzen et al. 1997; Kurdistani et al. 1998). *NDRG1* has also been implicated in several neuropathies and mutations in this gene have been identified in patients with Charcot-Marie Tooth Disease Type 4D (CMT4D), a demyelinating disease. In this context, NDRG1, which is expressed in Schwann cells, mediates the endosomal trafficking that supports myelination and the considerable demands of nerve growth (Piatianinen et al. 2013).

Thus far, the majority of studies on NDRG1 have revealed normoxic functions. Hence, our current understanding of the role of NDRG family members in physiological adaptation to hypoxia is quite incomplete. For my thesis, I aim to unravel the molecular role of NDRG1 in hypoxia tolerance. I propose two general models for NDRG1 as a molecular switch for hypoxia adaptation, which are partly informed by its known normoxic roles: a quantitative model, in which the normoxic function of NDRG1 is enhanced under hypoxia, and a qualitative model, whereby NDRG1 acquires new properties in response to hypoxia that are distinct from those it has under normoxic conditions. These models, which are not mutually exclusive, will be further discussed in the sections below.

III.2. Hypoxic regulation of NDRGs

III.2.1 Transcriptional regulation of NDRGs. As the name suggests, both *NDRG1* and *2* can be transcriptionally downregulated by Myc via Miz-1 (transcriptional factor) dependent interaction with the *NDRG1* and *2* promoter regions. In fact, both N-Myc and

c-Myc can downregulate human *NDRG1* at the transcriptional level (Zhang et al., 2008). Furthermore, NDRGs can be regulated by many different signals including hypoxia, nickel, cobalt, reducing agents, and as a result of DNA damage (Kokame et al., 1996; Park et al., 2000; Said et al., 2017; Stein et al., 2004; Wang et al., 2013; Zhou et al., 1998). Hence it is not surprising that *NDRGs* are targets of both p53 (a tumor suppressor associated transcription factor), and aryl hydrocarbon receptor (AHR, also known as HIF-1b) (Stein et al., 2004). Furthermore, hypoxia-responsive elements (HREs) have been identified in the promoter region of human and zebrafish *NDRG* family members (Wang et al., 2013; Greenland et al., 2015). Specifically, both the *NDRG1* and *NDRG2* promoter regions have been reported to contain HRE motifs (Wang et al., 2008; Wang et al., 2013). Furthermore, a long non-coding transcript of *NDRG1* functions to inhibit transcription and translation of *NDRG1* itself under hypoxia, identifying another layer of complexity in the regulation of *NDRG1* (Lin et al., 2017).

Furthermore, work from the Brewster lab on the transcriptional regulation of zebrafish *ndrgs* revealed that members of this family are responsive to hypoxia in concentration-dependent manner and that *ndrg1* is the most robustly up-regulated member (Le et al., unpublished).

III.2.2 Post-translational regulation of NDRGs

NDRG1 and *NDRG2* are the only members of the *NDRG* family known to be transcriptionally up-regulated in a HIF-dependent manner under hypoxia (Wang et al., 2008; Wang et al., 2013). However, it is possible that additional NDRG family members are post-translationally modified in response to hypoxia. Indeed, several post-

translational modifications (PTMs) that change the localization, stability or/and activity of these proteins (NDRG1 and NDRG3 in particular) have been reported to occur under both normoxic and hypoxic conditions. The focus here will be on the hypoxia-induced PTMs of NDRGs, although studies reporting on the normoxic PTMs of NDRGs are more abundant.

A study by Shi et al. revealed that NDRG1 redistributes to the nucleus and endoplasmic reticulum from the cytosol under hypoxia in a phosphopantetheine attachment site (PPAS)-dependent manner (Shi et al. 2013). In bacterial systems, the phosphopantetheine (Ppant) prosthetic group is post-translationally added to the PPAS by a phosphopantetheinyl transferase enzyme (Copp et al., 2006). The addition of the flexible Ppant arm to target proteins in this organism assists with the processing of metabolite intermediates by allowing dynamic spatial movement within the complex (Marahiel et al., 1997; Quadri et al., 1998). Although the potential function of the PPAS site on NDRG1 can only be gleaned from bacterial studies, this study suggests a potential role for the Ppant PTM in regulating NDRG1 subcellular distribution in response to hypoxia.

Another study by Park and colleagues showed that NDRG1 is phosphorylated at serine 330 and threonine 346 following the induction of HIF-1a using potential anti-cancer treatment agents DFO, Dp44mT, and DpC (Park et al. 2018). These compounds function by binding to cellular iron. Furthermore, NDRG1 phosphorylation at serine 330 resulted in NDRG1 localization to the nucleus, while phosphorylation at the threonine 346 correlated with the localization of NDRG1 to the cytoplasm. It is possible that the

induction of HIF activity by these anti-cancer agents may result in kinase upregulation that results in the phosphorylation of NDRG1.

Several studies have also alluded to the possibility of a cytochrome C hypoxia-mediated PTM of NDRG1 with no known function. Sugiki et al. identified a cytochrome C heme-binding motif on NDRG1 (Sugiki et al. 2004) (**Figure 1.13. Location of phosphorylation, phosphopantetheine (PPAS), and putative cytochrome C family heme-binding motif in the NDRG1 core domain**).

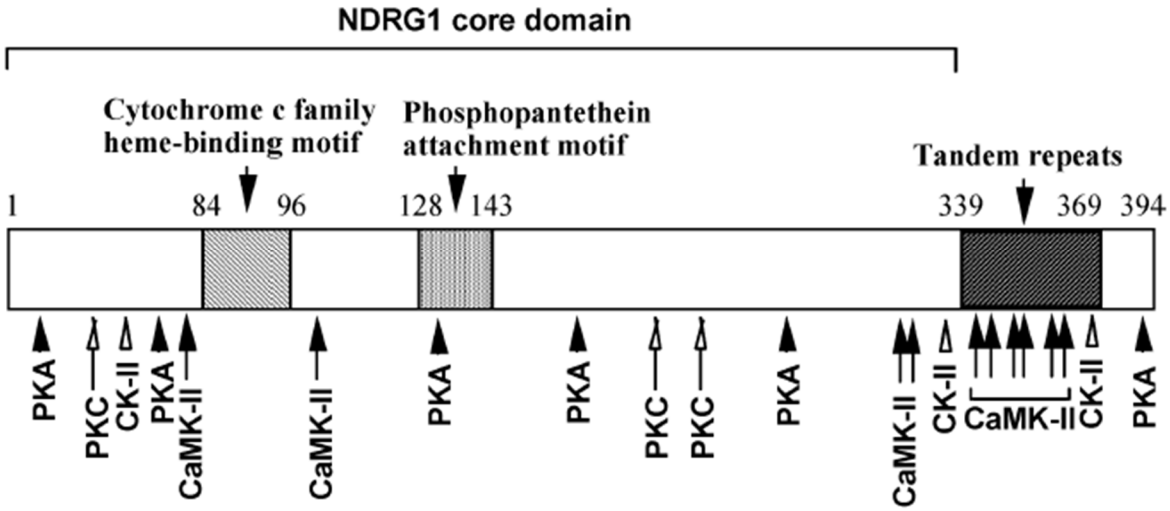

Figure 1.13. Location of phosphorylation, phosphopantetheine (PPAS), and putative cytochrome C family heme-binding motif in the NDRG1 core domain. Bottom arrows indicate the location of possible phosphorylation sites for PKA, PKC, CK-II, and CaMK-II. In addition, the location of phosphopantetheine (PPAS) and cytochrome C family heme-binding motifs are depicted above the protein sequence. Image from Sugiki et al., 2004.

In support of this finding, a study by Naro et al. in 1993 reported the release of cytochrome C from the inner mitochondrial membrane during hypoxia (Naro et al. 1993). As the release of cytochrome C often leads to apoptosis (Cai et al. 1998), it is possible that the cytochrome C interaction with NDRG1 under stressful hypoxic environments may trigger an initial protective cellular adaptation before the eventual apoptosis of the cell.

Another study by Lee et al. demonstrated that the stability and functional regulation of NDRG3 is mediated by hypoxic PTMs, which have been compared to those of HIF-1a. Under normoxic conditions, NDRG3, much like HIF-1a, is degraded by the 26S proteasome in a PHD2-VHL-dependent manner (Lee et al. 2015) (**Figure 1.14. Signaling role of lactate in the adaptive response of cancer cells to hypoxia**).

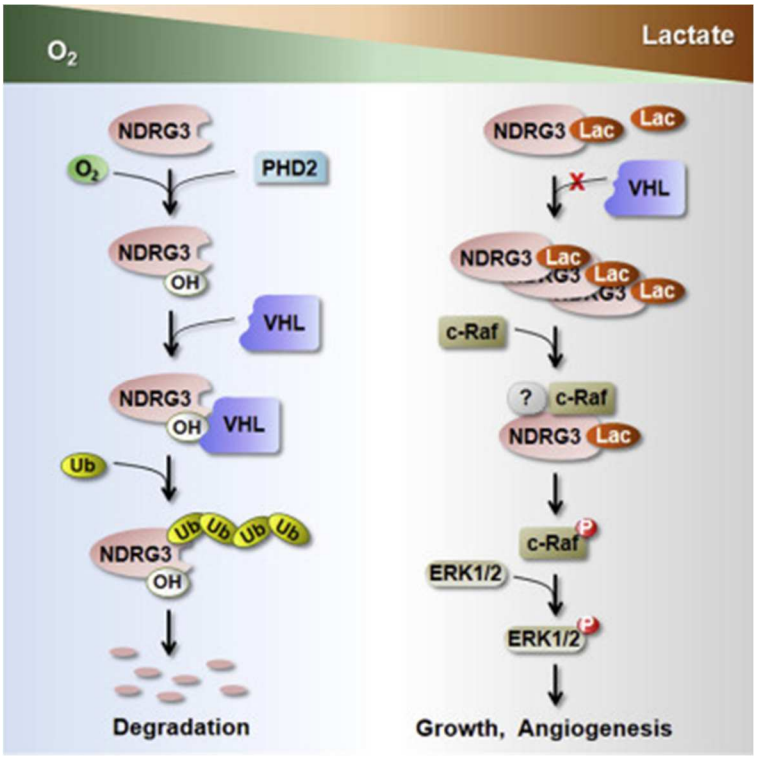

Figure 1.14. Signaling role of lactate in the adaptive response of cancer cells to hypoxia. Under normoxia, NDRG3 is degraded in a PHD and VHL-dependent manner. As oxygen levels drop and lactate levels rise, NDRG3 is stabilized by the binding of lactate, which prevents VHL mediated degradation. Once stable, NDRG3 signals through Raf/ERK to promote growth and angiogenesis in cancer. Image from Lee et al., 2015.

However, the accumulation of lactate resulting from prolonged hypoxia mediates the stabilization of NDRG3 by conferring protection against the PHD2-VHL degradation pathway. Once stable, NDRG3 signals through Raf/ERK to promote growth and angiogenesis in cancer under hypoxia. Interestingly, the NDRG3 residues that bind lactate are also conserved in NDRG1 (unpublished observation), suggesting that this metabolite may play a role in lactate-NDRG1 signaling.

As demonstrated by these examples, hypoxic PTMs regulate the localization, stability and activity of NDRGs. It is possible that these PTMs induce conformational changes in NDRGs that enable NDRGs to interact and bind with new protein partners under hypoxia. These PTMs would allow NDRGs to serve as adapter proteins to confer novel functions under low oxygen conditions.

III.3. Molecular functions of NDRGs

Most NDRG studies have been performed under normoxia or hypoxia, but seldom both, making it difficult to parse out whether NDRG function is the same across different oxygen concentrations or different.

In an attempt to address these unknowns, I propose two different models, a quantitative model and a qualitative model, for NDRG1 activation under hypoxia, both of which are supported by the literature (**Figure 1.15. Illustration of simplified quantitative and qualitative models**). In the quantitative model, the normoxic function of NDRG1 is heightened under hypoxia due to increases in NDRG1 protein levels, resulting from transcriptional upregulation (Le et al., unpublished). This model assumes

that NDRG1 has no other unique functions under hypoxia other than enhanced activity levels brought on by the increased levels of NDRG1.

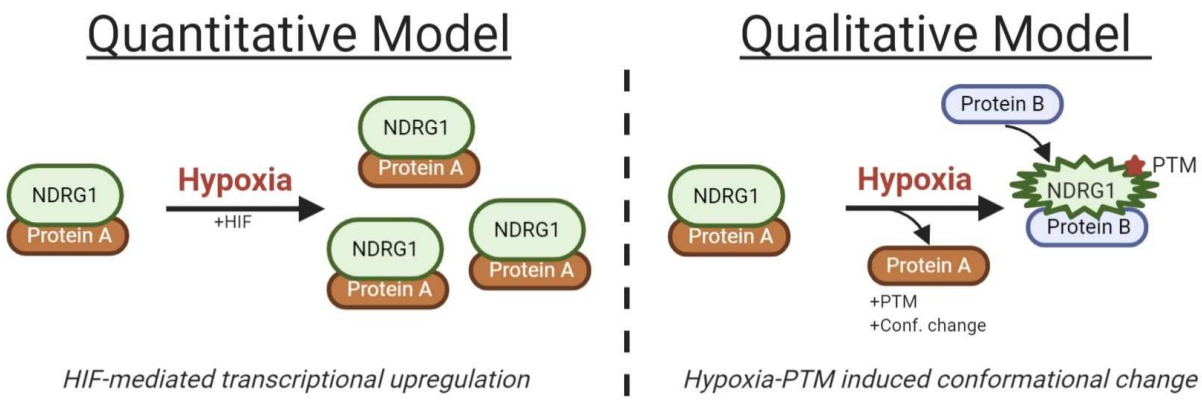

Figure 1.15. Illustration of simplified quantitative and qualitative models. In the quantitative model, the normoxic function in NDRG1 is maintained but enhanced due to an increase in the amount of NDRG1 following transcriptional up-regulation and stabilization . In the qualitative model, NDRG1 acquires different properties and functions than those effective under normoxia via conformational change following PTMs, which modify the binding affinity of NDRG1.

In the qualitative model, NDRG1 acquires properties and functions that are distinct from those exhibited under normoxic conditions. These may be acquired through PTMs (Lee et al., 2015) that result in changes in protein conformation or binding partners (Chapter 2, Figure 5). These two models are not mutually exclusive since they may both occur during the transition to a hypoxic environment. It is interesting to note that NDRG1 interacts with a diverse class of proteins in human prostate cancer cells. Among them, is the alpha subunit of the NKA, which my thesis has focused on the functional relevance of Ndrg1 interaction with nka in the kidney (**Table 1.2. List of NDRG1-interacting proteins in normoxic prostate cancer cells identified by immunoprecipitation and LC/MS/MS**).

TABLE I

Proteins identified from NDRG1 IP complex by LC-MS/MS analysis

Gene symbol	Total no. of peptides	No. of independent experiments	IPI	RefSeq accession no.	Protein description	Amino acid coverage
						%
NDRG1	23	3	IPI00022078	NP_006087	NDRG1	28.2
Chaperon protein						
HSPCA	57	3	IPI00382470	NP_005339	Heat shock protein HSP 90-α	44.7
HSPA5 (GRP78)	79	3	IPI00003362	NP_005338	Heat shock 70 kDa protein 5	42
VCP	19	3	IPI00022774	NP_009057	Transitional endoplasmic reticulum ATPase	23.2
CANX	18	3	IPI00020984	NP_001737	Calnexin	21.5
Ubiquitin-dependent protein catabolism	22	3	IPI00018398	NP_002795	26S protease regulatory subunit 6A	32.1
PSMC2	17	3	IPI00021435	NP_002794	26S protease regulatory subunit 7	25.5
PSMD2	32	3	IPI00012268	NP_002799	26S proteasome non-ATPase regulatory subunit 2	37.1
DNA repair proteins						
XRCC6 (Ku70)	32	3	IPI00465430	NP_001460	ATP-dependent DNA helicase II	48.8
RUVBL2	8	3	IPI00009104	NP_006657	RuvB-like 2	21.9
Transcriptional factor						
ILF3 (NFAT90)	16	3	IPI00219330	NP_036350	Interleukin enhancer-binding factor 3	19.5
SEC23A	19	3	IPI00017375	NP_006355	Protein transport protein Sec23A	23
COPB2	54	3	IPI00220219	NP_004757	Coatomer β subunit	36.7
CLTC	86	3	IPI00024067	NP_004850	Similar to clathrin heavy chain	27.2
AP2M1	5	3	IPI00022256	NP_004059	AP-2 complex subunit μ-1	12.5
AP1M2	28	3	IPI00002552	NP_005489	Splice isoform 1 of AP-1 complex subunit μ-2	31
Cell adhesion and cytoskeleton organization	38	3	IPI00247063	NP_009218	Neprilysin	40.9
CTNNB1	39	3	IPI00017292	NP_001895	Splice isoform 1 of β-catenin	38.7
ACTB	50	3	IPI00021440	NP_001605	Actin	60.5
KIF5B	12	3	IPI00012837	NP_004512	Kinesin heavy chain	13.6
Signal transduction						
PPP2R2A	17	3	IPI00332511	NP_002708	Serine/threonine protein phosphatase 2A	31.3
TLE3	3	3	IPI00219368	NP_005069	Splice isoform 1 of transducin-like enhancer protein 3	3.4
Metabolic enzymes, mitochondria precursors, and carrier HSD17B4	11	3	IPI00019912	NP_000405	Peroxisomal multifunctional enzyme type 2	16.5
CNDP2	31	3	IPI00177728	NP_060705	Cytosolic nonspecific dipeptidase	33.5
DARS	38	3	IPI00216951	NP_001340	Aspartyl-tRNA synthetase	48.1
DLST	14	3	IPI00420108	NP_001924	Dihydrolipoyllysine-residue succinyl-transferase	13.9
ACSL3	16	3	IPI00401055	NP_004448	acyl-CoA synthetase long chain family member 3	16.7
FASN	33	3	IPI00645907	NP_004095	Fatty acid synthase	11.5
MAOA	26	3	IPI00008483	NP_000231	Amine oxidase (flavin containing) A	25.2
LDHA	14	3	IPI00217966	NP_005557	Lactate dehydrogenase A	22.6
PKM2	41	3	IPI00479186	NP_002645	Pyruvate kinase 3 isoform 1	40.9
RPN2	18	3	IPI00301271	NP_002942	Dolichyl-diphosphooligosaccharide—protein glycosyltransferase 63 kDa subunit precursor	31.9
TARS	29	3	IPI00329633	NP_689508	Threonyl-tRNA synthetase, cytoplasmic	23.7
SHMT2	11	3	IPI00002520	NP_005403	Serine hydroxymethyltransferase, mitochondrial precursor	19.8
SLC25A6	3	3	IPI00291467	NP_001627	Solute carrier family 25,ADP/ATP translocase 3	16.8
ATP1A1	23	3	IPI00006482	NP_000692	Sodium/potassium-transporting ATPase α-1	17.4
Protein translation regulators EEF2	37	3	IPI00186290	NP_001952	Elongation factor 2	28.7
EEF1G	38	3	IPI00000875	NP_001395	Similar to elongation factor 1-gamma	37.2
EIF2S3	15	3	IPI00297982	NP_001406	Eukaryotic translation initiation factor 2 subunit 3	33.1

						%
EIF3S6	11	3	IPI00013068	NP_001559	Eukaryotic translation initiation factor 3 subunit 6	24.7
PABPC1	52	3	IPI00008524	NP_002559	Splice isoform 1 of polyadenylate-binding protein 1	42.9
Ribosomal proteins						
RPS3	35	3	IPI00011253	NP_000996	40S ribosomal protein S3	57.2
RPS6	17	3	IPI00021840	NP_001001	40S ribosomal protein S6	21.3
RPL24	7	3	IPI00306332	NP_000977	60S ribosomal protein L24	13.4
RPL3	31	3	IPI00550021	NP_000958	60S ribosomal protein L3	34.3
RPS16	15	3	IPI00221092	NP_001011	40S ribosomal protein S16	24.8
RPS8	13	3	IPI00216587	NP_001003	40S ribosomal protein S8	31.9
RPS20	6	3	IPI00012493	NP_001014	40S ribosomal protein S20	25.2
RPS9	18	3	IPI00221088	NP_001004	40S ribosomal protein S9	30.6
RPL4	79	3	IPI00003918	NP_000959	60S ribosomal protein L4	39.2
RPS26	9	3	IPI00655650	NP_001020	40S ribosomal protein S26	21.1
RNA processing						
NCL	21	3	IPI00444262	NP_005372	Nucleolin	25.2
HNRPF	25	3	IPI00003881	NP_004957	Heterogeneous nuclear ribonucleoprotein F	20.5
HNRPU	22	3	IPI00644079	NP_114032	Heterogeneous nuclear ribonucleoprotein U	18.5
HNRPH1	25	3	IPI00013881	NP_005511	Heterogeneous nuclear ribonucleoprotein H1	20.5
DDX1	22	3	IPI00293655	NP_004930	ATP-dependent helicase DDX1	29.5
DDX5	6	3	IPI00017617	NP_004387	Probable RNA-dependent helicase p68	17.6
UPF1	21	3	IPI00034049	NP_002902	Regulator of nonsense transcripts 1	19.2
EWSR1	11	3	IPI00009841	NP_005234	EWS-B of RNA-binding protein EWS	15.5

Table 1.2. List of NDRG1-interacting proteins in normoxic prostate cancer cells identified by immunoprecipitation and LC/MS/MS. Several classes of proteins were identified from this mass-spectrometry study investigating binding partners of NDRG1. The following are general categories of cell function in which these identified proteins can be grouped: Chaperon proteins, Ubiquitin-dependent protein catabolism, DNA repair proteins, Transcriptional factors, Cell cytoskeletal organizations, Signal transduction, Metabolic enzymes, Translation machinery, Ribosomal proteins, RNA processing. The alpha subunit of NKA is boxed in green. Image from Tu et al., 2007.

III.3.1 NDRGs as regulators of vesicular trafficking

Vesicular Trafficking Overview

Cells have evolved complex signaling pathways and mechanisms that regulate vesicular trafficking between the plasma membrane and organelles to maintain membrane structure and function. Translation of the vast majority of proteins in eukaryotic cells begins in the cytosol. For proteins bound for the plasma membrane, translation ends in the ER, then those fully translated proteins are modified through multiple layers of the Golgi apparatus. These organelles function to further modify membrane-bound proteins. In addition, these proteins are checked for misfolding during these initial synthesis steps and if any mistakes are found, the misfolded proteins are targeted for degradation.

Once at the plasma membrane, the proteins can subsequently be endocytosed, then recycled back to the membrane, or be processed for degradation via either the lysosome or proteasome depending on the cellular condition and needs. The endocytosis of membrane proteins can be initiated by ubiquitination (Foot et al., 2017). When membrane proteins are ubiquitinated, this PTM triggers the entry into vesicles at the plasma membrane (Hicke and Dunn, 2003). Hence ubiquitination is an important step in the initiation of plasma membrane protein degradation. However, as mentioned previously, depending on further modification of these vesicles, the cargo can either be recycled back to the plasma membrane or further ubiquitination can serve as a signal for proteolysis by the lysosome (Bonifacino and Traub, 2003). Many types of membrane proteins are regulated by ubiquitination, including ion transporters and channels.

A review of the current literature reveals that NDRGs play an essential role in regulating vesicular trafficking. The following section compares and contrasts the normoxic and hypoxic role of NDRGs in vesicular trafficking.

Normoxic role of NDRGs in Vesicular Trafficking

NDRGs have been shown to regulate both exocytic and endocytic pathways. In particular, a global gene expression profiling study by Askautrud and colleagues revealed that NDRG1 levels in breast epithelial cell lines, SUM102 and ME16C2, negatively correlated with the expression levels of vesicular trafficking genes in both exocytic and endocytic pathways (Askautrud et al. 2014). Specifically, the study identified 21 differentially expressed genes related to ER, Golgi, endosomes, or vesicular transport among these organelles and found that 19 of these were upregulated in cells with NDRG1 knockdown, and downregulated in cell populations with ectopic overexpression of NDRG1 (Askautrud et al., 2014). The authors proposed that NDRG1 may increase cell survival during hypoxia by downregulating secretory or endocytic functions of the cell to conserve energy. It is currently not known how NDRG1 regulates these genes, but an NDRG1 protein interactome study (Tu et al., 2007) revealed that NDRG1 physically interacts with the members of the transcription processes (**Table 1.2. List of NDRG1-interacting proteins in normoxic prostate cancer cells identified by immunoprecipitation and LC/MS/MS)**. It is tempting to speculate that NDRG1 may regulate the mRNA levels of other genes via interaction with transcription factors

In addition to transcriptionally regulating vesicular trafficking genes, NDRG1 appears to directly interact with the proteins involved in vesicular trafficking. It is also

interesting to note that the localization of NDRG1 protein to cellular compartments such as ER and endosomal compartments is consistent with the proposed role of NDRG1 in regulating vesicular trafficking.

One of the first reported normoxic roles of NDRGs in regulating vesicular trafficking was demonstrated for the exocytosis pathway. In this study, NDRG1 was described as a Rab4a effector protein that recycled E-cadherin back to the membrane (Kacchap et al. 2007). Specifically, NDRG1 stabilized the levels of E-cadherin at the membrane by binding to recycling endosomes and interacting with membrane-bound Rab4aGTPase. Another study by Fontenas and colleagues demonstrated that NDRG4 also promotes exocytosis via regulation of snap25 and NSF expression. In this manner, NDRG4 was shown to regulate sodium channel clustering in nodes of Ranvier in zebrafish (Fontenas et al. 2016).

The role of NDRG1-in mediating exocytosis of select targets, and more precisely in recycling specific proteins from early endosomes back to the plasma membrane, is further confirmed in the work by Pietiainen and colleagues. In this study, NDRG1 was shown to maintain steady LDLR levels on the plasma membrane. Specifically, silencing NDRG1 resulted in reduced LDLR levels on the plasma membrane and an accumulation of LDLR in EEA1-positive endosomes. (Pietiainen et al. 2013). Thus, NDRG1 can regulate the trafficking of target proteins both indirectly via the modulation of the transcript levels of proteins implicated in vesicular trafficking, and directly by mediating the delivery of specific target proteins to the plasma membrane.

NDRG and membrane protein degradation

In addition to their role in exocytosis, members of the NDRG family also mediate endocytosis and degradation. First, the previously mentioned study by Pietiainen and colleagues hints at the possible role of NDRG1 in the endocytosis-degradation pathway. In addition to finding that LDLR was not recycled back to the membrane in the absence of NDRG1, the authors also demonstrated that LDLR degradation was reduced in NDRG1-depleted epithelial cells. Furthermore, there is correlative physiological evidence for NDRGs mediating membrane protein degradation. Kultz and colleagues showed that NDRG1 levels were negatively correlated with ion transporter protein levels in the gills of tilapia, a fresh water fish. Specifically, in high salinity, ion transporters were found to be upregulated to compensate for high ion homeostasis, while NDRG1 was strongly down-regulated (Kultz et al. 2013, 2014). In addition, in a correlative clinical study, Ma et al. demonstrated that NDRG2 expression is associated with glucose transporter degradation and a positive prognosis in breast carcinomas (Ma et al. 2014). Wang et al. further revealed that NDRG1 is required for the fusion of vesicles with lysosomes (Wang et al. 2017) (Figure) and a zebrafish study revealed that NDRG1a promotes the ubiquitination and degradation of IFN (interferon) regulatory factor 7 (IRF7) (Lu et al., 2018).

Lastly, Menezes et al. showed that NDRG1 is involved in the endocytic-lysosomal mediated degradation pathway of epidermal growth factor receptor (EGFR) by upregulating mitogen-inducible gene 6 (MIG6). Specifically, the authors demonstrated that the overexpression of NDRG1 resulted in increased levels of MIG6, which in turn facilitates lysosomal processing and degradation of EGFR. Briefly, MIG6 is a cytoplasmic EGFR inhibitor that binds to the EGFR dimers to lock EGFR in catalytically

inactive conformation. It has been previously reported that MIG6 can initiate the endocytosis and degradation of EGFR via a lysosomal mechanism (Menezes et al. 2019; Frosi et al., 2010).

Currently, no published studies address the role of NDRGs in vesicular trafficking in the context of hypoxia, but interestingly the NDRG1 interaction study by Tu and colleagues revealed that NDRG1 binds to several components of vesicular trafficking and degradation pathways (**Table 1.2. List of NDRG1-interacting proteins in normoxic prostate cancer cells identified by immunoprecipitation and LC/MS/MS)**. My thesis work will address this in the context of downregulation of the NKA in response to hypoxia, a key mechanism for hypoxia adaptation.

III.4. Zebrafish NDRGs

In zebrafish, there are 6 *ndrg* genes: *ndrg 1a, 1b, 2, 3a, 3b,* and *4*. It is likely that the genome duplication event in zebrafish resulted in the paralogs of *ndrg*s (*ndrg1b, 3b*) that are not present in other species (Taylor et al., 2003; Postlethwait et al., 2004). However, all members of the zebrafish *ndrg* family have high homology to mammalian *NDRGs* as well as invertebrate homologs of *ndrgs*.

Thus far, studies specifically on zebrafish *ndrgs* have been few and far between and most of then have focused on Ndrg localization or expression (Takita et al., 2016; Le et al., unpublished; Schonkeren et al., 2019) with very sparse functional studies (Lu et al., 2018; Fontenas et al. 2016).

It is interesting to note that NDRGs are expressed in ATP-demanding tissues such as the kidney, heart, brain, and muscle in zebrafish, amphibians and mammals (Melotte et

al., 2010; Zhong et al., 2015, Le et al., unpublished). Ndrg1a, the focus of my thesis, is primarily expressed in the embryonic kidney (pronephric duct) and ionocytes (**Chapter 2, Figure 1**).

Kidney cells reabsorb ions in part through active transcellular transport. Likewise, ionocytes, specialized cells in the skin of zebrafish embryos, facilitate active absorption of electrolytes from the environment (Kersten & Arjona, 2017).

IV. Zebrafish as a model organism

Zebrafish is an ideal model organism to use for developmental hypoxia tolerance. First and foremost, zebrafish embryos are hypoxia tolerant (discussed in more detail in section IV.1 below). Zebrafish is also an inexpensive vertebrate model organism that reaches adulthood in three months. Female zebrafish can produce hundreds of embryos in a single spawning that are transparent and externally fertilized, which facilitates imaging of deep tissues and real-time imaging. Furthermore, a large array of genetic and molecular tools are available for this model organism. In contrast, other hypoxia-tolerant models such as carps and turtles are not genetically tractable.

IV.1. Zebrafish embryos are hypoxia-tolerant

Zebrafish embryos maintain function and homeostasis in decreasing levels of physiological oxygen by transitioning into a hypometabolic state, characterized by a dramatic reduction in metabolic rate and energy production (Lant & Storey, 2010). In zebrafish embryos, hypometabolism is manifested by a delay or an arrest in development in young embryos and by suppression of physiological responses in older embryos

(Figure 1.16. Hypoxia-induced developmental and physiological arrest in zebrafish embryos) (Padilla & Roth, 2001).

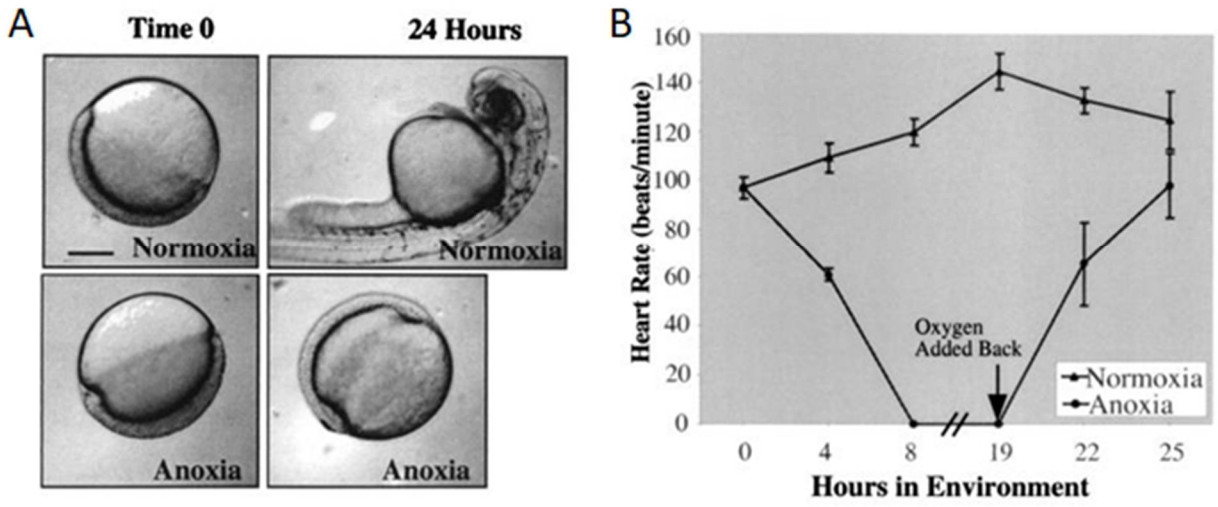

Figure 1.16. Hypoxia-induced developmental and physiological arrest in zebrafish embryos. (A) shows embryos developmentally arrest under anoxia and that this arrest is reversible. (B) shows reversible physiological arrest under anoxia in 29 hpf stage zebrafish embryo. Image from Padilla and Roth, 2001.

Remarkably, young (pre-gastrula) zebrafish embryos can survive for up to 50 hours of anoxia in this arrested state and resume normal development upon return to normoxic conditions (Mendelsohn et al., 2008). Previous studies suggest that a proximal signal that induces hypometabolism is triggered by the blockage of the electron transport chain (ETC). Indeed, the Gitlin laboratory and a research group at Novartis both showed that exposure to chemical ETC blockers results in reversible developmental arrest in zebrafish embryos under normoxic conditions (Lai et al., 2013; Mendelsohn et al., 2008). Given that ETC blockage and anoxia have a similar effect on the embryo and ETC is disrupted under severe hypoxia, these findings suggest that a yet-to-be-identified endogenous signaling molecule(s) is produced downstream of ETC blockage. It is tempting to speculate that this molecule might be hydrogen sulfide and/or lactate, as both are produced endogenously and are known to contribute to hypoxia adaptation (Olson et al., 2010*)*.

Interestingly, a field study investigating the oxygen concentration of water bodies where zebrafish live revealed that these water can be severely hypoxic (Suriyampola et al., unpublished; e-mail correspondence) (**Table 1.3. Dissolved oxygen levels in the body of water containing zebrafish in nature**). That said, adult zebrafish do not survive severe hypoxia as long as zebrafish embryos, indicating that hypoxia-tolerance, in this organism, is developmental stage specific. However, considering that carp and turtles maintain very high hypoxia tolerance as adults, it is unlikely that the developmental stage specificity observed in zebrafish can be accounted for solely by higher ratios of progenitor and stem cells in embryos versus adults. Irrespective of the underlying reason,

this developmental stage specificity could be exploited to facilitate the identification of underlying signaling pathways.

Water body	DO[2] (mg/L)	Depth (cm)
Slow-flowing stream 1	8.5-8.75	10 to 18
Slow-flowing stream 2	6.7-7.65	6 to 32
Slow-flowing stream 3	7	5
Paddy field	4.48	2
Irrigation channel 1	0.42-0.62	10 to 22
Irrigation channel 2	4.85-6	4 to 30

Table 1.3. Dissolved oxygen levels in the body of water containing zebrafish in nature. Levels of dissolved oxygen measured in (mg/L) corresponding to water depth at different water bodies. All of the field sites contained live zebrafish. Data from Suriyampola et al., unpublished - email correspondence; Martins lab.

IV.2. Kidney development and function in terrestrial and aquatic vertebrates

ndrg1 is prominently expressed in the kidney of zebrafish, thus I will discuss kidney development and function in zebrafish. Zebrafish is an aquatic vertebrate that lives in a hypotonic freshwater environment and must therefore constantly maintain bodily fluid and ionic homeostasis. Freshwater fish have highly concentrated blood (akin to mammals) (~290 mOs; concentration of salts) and live in a freshwater environment of about ~20 mOs. Hence freshwater fish are constantly at risk for osmotic swelling. The primary function of the kidney in these fishes is therefore to prevent excessive water influx and retain salts. Therefore, defective kidney function in zebrafish typically leads to interstitial edema due to constant influx of water from the environment (Maceina and Shireman, 1979*)*.

In both non-mammalian and mammalian vertebrates, the kidney plays an essential physiological role in the removal of unwanted metabolites, balancing water, ionic and acid-base systems, and regulation of blood pressure (McCampbell and Wingert, 2014). Mammals or humans have a pair of bean-shaped kidneys located in the back abdominal cavity. Nephrons, which are the functional units of the kidney, are packed neatly in arrays. Each nephron is composed of 3 major components: 1. The filter, also known as the glomerulus, and 2. The tubule, which is composed of various segments expressing diverse transporters that can function to either secrete or reabsorb specific molecules and 3. The collecting duct, where excretion of unwanted solute along with water occurs (**Figure 1.17. Mammalian kidney structure depicting filter, tubule, and duct**).

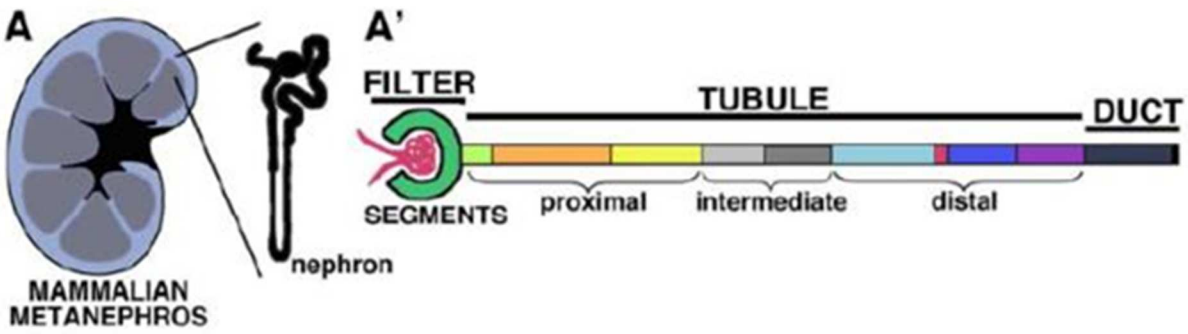

Figure 1.17. Mammalian kidney structure depicting filter, tubule, and duct. Panel A shows a depiction of a typical mammalian kidney structure, which consists of millions of nephrons. A' reveals an individual nephron with key components labeled: filter, tububle, and the duct. Image from McCampbell and Wingert, 2014.

The components of the nephron are conserved, however, differences are found even in closely related mammals (Reilly et al., 2007). During normal development, the mammalian kidney differentiates sequentially into three distinct kidney structures, namely, the pronephros, the mesonephros, and the metanephros (Dressler, 2006). In mammals, the metanephros is the adult kidney form that contains the most complex arrangement of nephrons. However, in lower vertebrates such as frogs and zebrafish, the mesonephros is the terminally differentiated kidney form that serves as the adult organ (Vize et al., 1997; Drummond, 2003; Chan and Asashima, 2006; Gerlach and Wingert, 2013). In zebrafish, the pronephros consists of 2 nephrons only. When the pronephros differentiates into the mesonephros, the zebrafish gains several hundred nephrons that are added on top of the initial pronephros structure (Gerlach and Wingert, 2013). Interestingly, the zebrafish nephrons contain proximal and distal tubule domains that are highly similar to the mammalian nephron counterparts and share similar histological characteristics with mammals. These similarities suggest that kidney development and function are likely conserved, although there are some structures and segments that are absent in the zebrafish (Wingert, Selleck, Yu et al., 2007) (**Figure 1.18. The zebrafish pronephros is highly similar to the human nephron**).

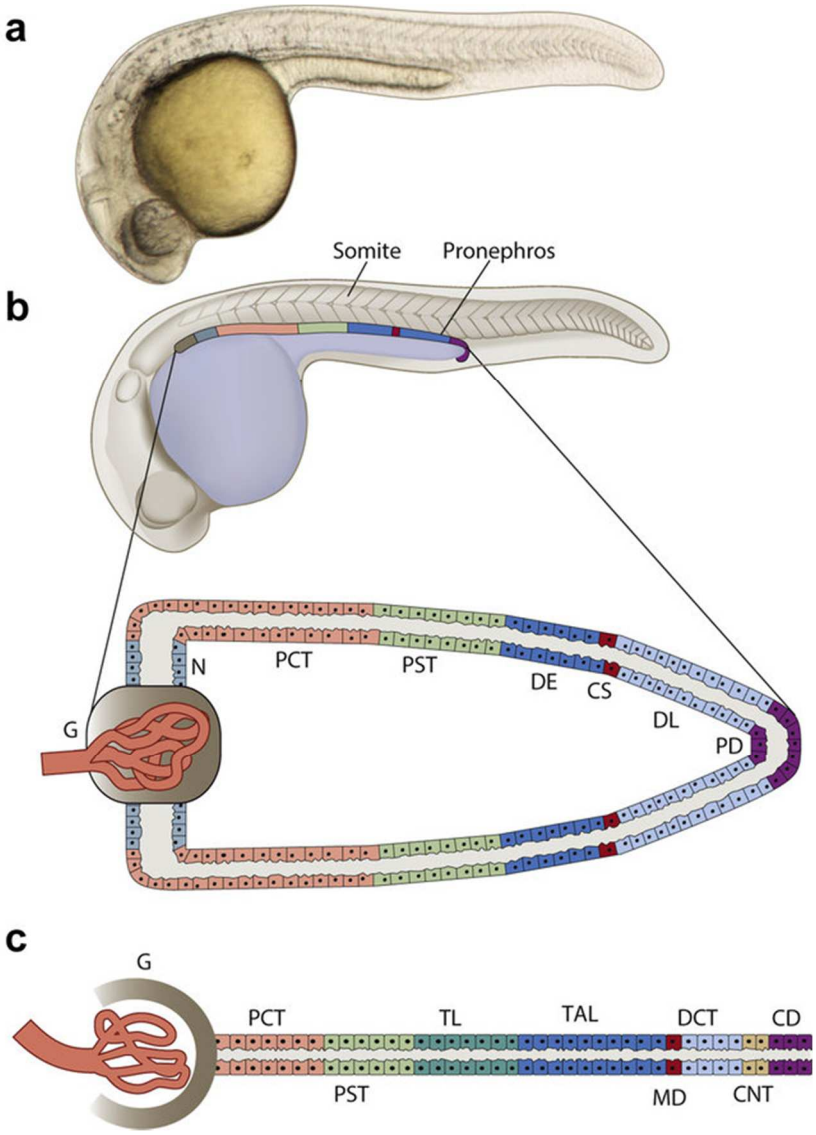

Figure 1.18. The zebrafish pronephros is highly similar to the human nephron. (A) shows a 24 hpf old embryo. (B) is an illustration of lateral view of the pronephros in a 24hpf embryo. (C) shows a dorsal view of the pronephros, which reveals the bilateral pronephros with each of the segments represented in different color schematics: glomerulus (G), neck (N), proximal convoluted tubule (PCT), proximal straight tubule (PST), distal early (DE), corpuscle of Stannius (CS), distal late (DL), and pronephric duct (PD). Panel C represents a diagram of a human nephron with each of the segments represented in different color schematics: glomerulus (G), proximal convoluted tubule (PCT), proximal straight tubule (PST), thin limb (TL), thick ascending limb (TAL), macula densa (MD), distal convoluted tubule (DCT), connecting tubule (CNT), and collecting duct (CD). The segment color schematics that are matching between the zebrafish and human indicate genetic conservation. Image from Poureetezadi and Wingert, 2016.

The cellular architecture of kidney tubule cells is equally well conserved across vertebrates. These cells are highly polarized with distinct ions channels and pumps distributed on either apical, lateral, or baso-lateral surfaces (Kersten and Arjona, 2017; Takvam et al., 2021). Of particular interest, the NKA is on the basolateral surface of the kidney, which is the surface that is closest to the blood vessels. Basolateral NKA activity results in Na+ being pumped out of the kidney cells and into the blood. This creates a gradient for Na+ ions to enter the kidney cell from the apical surface of the kidney that is closest to the lumen. Hence the polarity of the kidney is also integral to the function of the kidney. Without this polarized distribution of NKA, Na+ ions would not be able to be transported through the kidney cell in a directional manner (**Figure. 1.19. Overview of the localization of ion and water transporters in freshwater teleost kidney**).

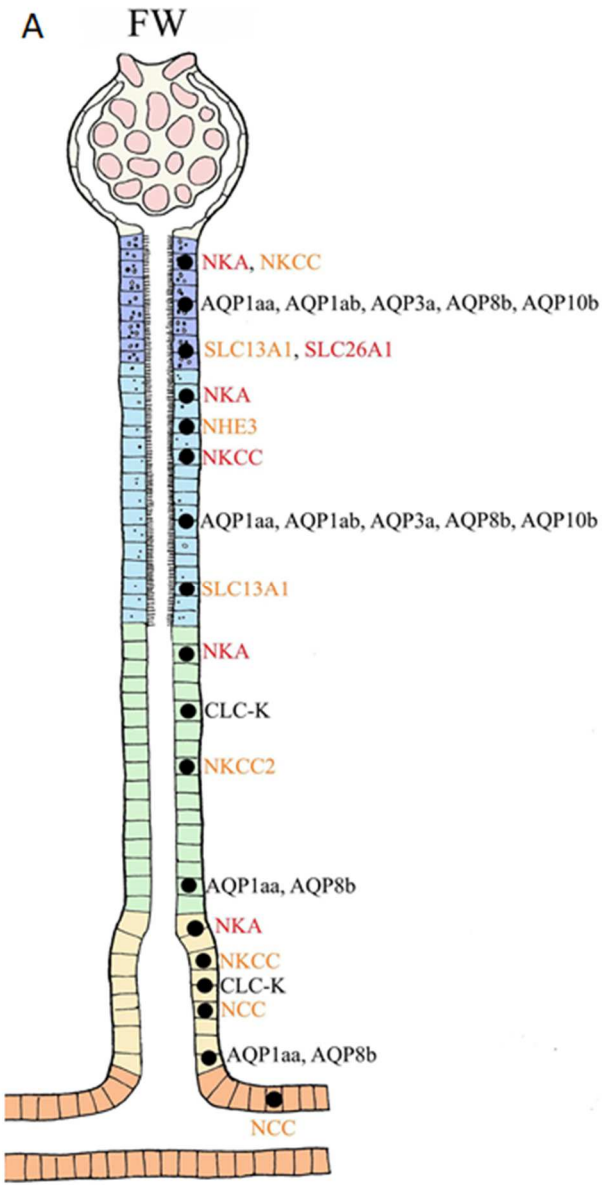

Figure. 1.19. Overview of the localization of ion and water transporters in freshwater teleost kidney. (A) shows localization of various ion and water transporters that have been molecularly detected at different segments (Anterior to posterior; top to bottom) of the freshwater teleost kidney. Transporters in yellow are located at the apical membrane, those labeled in red are expressed on the basolateral surface, and lastly transporters in black are found in multiple locations. Interestingly, NKA is localized to the basolateral membrane along the kidney. Abbreviations: NKCC (Na-K-Cl cotransporter), AQP (aquaporin), SLC13A1 (Sodium/sulfate symporter), SLC26A1 (Sulfate transporter), NHE3 (Sodium-hydrogen exchanger), CLC-K (Chloride ion channel), NCC (Sodium-chloride symporter). Image from Takvam et al., 2021.

Interestingly, there appears to be increased Na+ ion transport into the blood at the distal (posterior) ends of the kidney compared to the proximal (anterior) kidney (**Figure 1.20. Movement of Na+ ions across freshwater teleost kidney**).

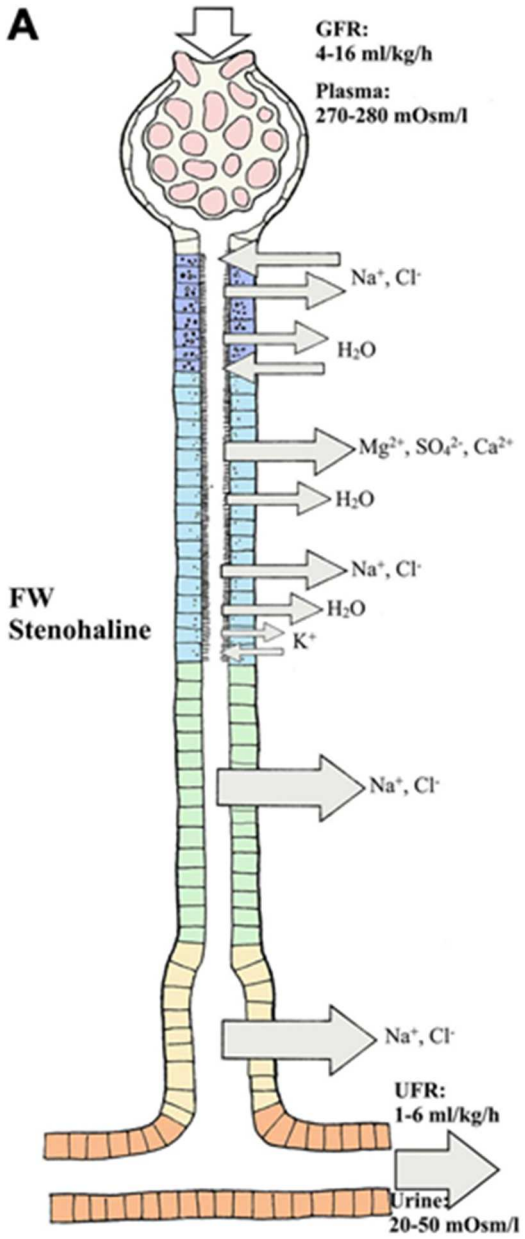

Figure 1.20. Movement of Na+ ions across freshwater teleost kidney. (A) shows type and magnitude of ions or water movement along different segments of freshwater teleost kidney. Interestingly, the posterior kidney (green and yellow) segments show higher magnitude of Na+ movement into the blood. Image from Takvam et al., 2021.

IV.2.1 *Ionocyte development and function in zebrafish*

Both aquatic and terrestrial vertebrates have evolved mechanisms to regulate ion and fluid homeostasis in their bodily fluids to allow efficient physiological function. In the terrestrial vertebrates, ion and fluid homeostasis is maintained mainly by the kidney. However, aquatic vertebrates also use their gills and ionocytes as major non-kidney organs that balance ions and maintain fluid homeostasis (Evans et al., 2008; Hwang et al., 2011; Hwang and Perry, 2010).

Four types of ionocytes have been identified in the developing zebrafish: 1, H+ ATPase-rich, 2. Na+K+ ATPase-rich, 3. Na+Cl- cotransporter-expressing, and 4. K+ secreting cells, which perform transepithelial H+ secretion/Na+ uptake/NH4+ excretion, Ca2+ uptake, Na+/Cl- uptake, and K+ secretion, respectively (Hwang and Chou, 2013; Chang and Hwang, 2011)(**Figure 1.21. Comparison of models between zebrafish ionocytes and mammalian kidney cells**). Interestingly, these ionocytes are similar to various renal tubular cells in terms of their composition of ion transporters as well as their functions.

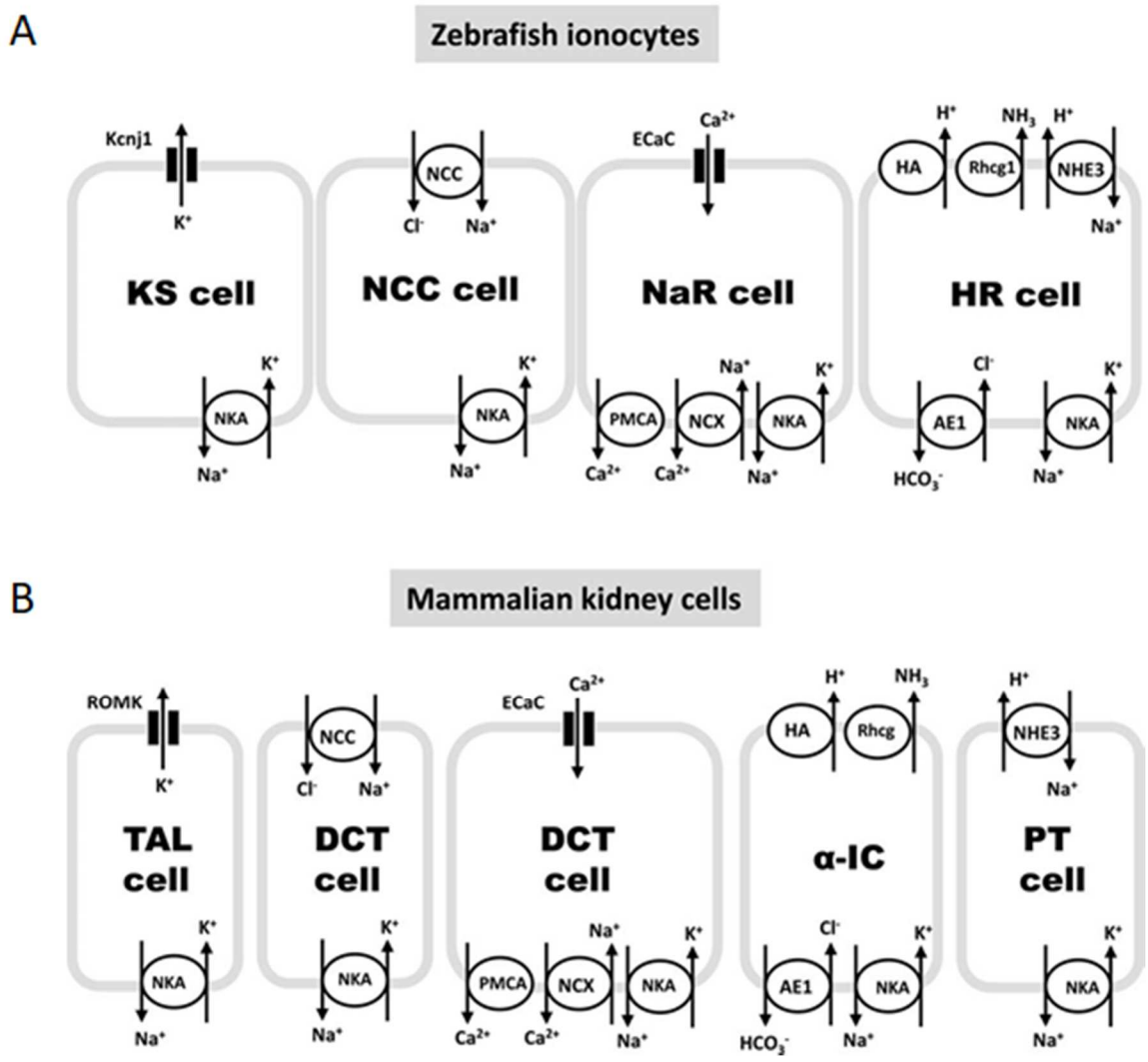

Figure 1.21. Comparison of models between zebrafish ionocytes and mammalian kidney cells. (A) Different types of zebrafish ionocytes containing ion transporters; from left to right: (KS cell): K+ secreting cells, (NCC cell): Na+ Cl- cotransporter, (NaR cell): Na+ K+ ATPase-rich, (HR cell): H+ ATPase-rich. Note that all the ionocytes contain a different isoform of the sodium potassium pump alpha subunit (ATP1a); KS cell contains NKA.4, NCC cells contain NKA.2, NaR cells contain NKA.1, and HR cells contain NKA.5 isoform of the NKA alpha subunit (Hwang and Chou, 2013). (Bottom panels). Different cells of mammalian kidney with their ion transporters; left from left to right: thick ascending limb (TAL), distal convoluted tubule (DCT), alpha-intercalated cell (a-IC), proximal tubular (PT) cell. Image from Chang and Hwang, 2011.

In the early stages of development before the gills are functional, ionocytes differentiate from ionocyte progenitors that are derived from epidermal stem cells and become functional around 24 hpf (Hwang and Chou, 2013). Given their properties, which are similar to renal tubule cells, and their direct exposure to the outside environment, ionocytes can be readily treated with different drugs and ion concentrations, making this cell type an ideal model to study ion and fluid homeostasis. Ionocytes therefore add to the benefits of using zebrafish as a model organism.

Although there are many ion transporters present in the zebrafish kidney and ionocytes, for the purpose of my dissertation thesis, I will focus on the NKA, which is expressed throughout the entire length of the embryonic kidney in addition to the ionocytes (Figure in Chapter 2). Briefly, the NKA is an energetically demanding pump that uses 1 ATP to move 3 Na+ ions out of the cell, while transporting 2 K+ ions into the cell. The Na+ and K+ gradients established by NKA are critical for ion and water homeostasis and regulate the functions of other ion channels in the kidney. Under energy demanding conditions such as hypoxia, NKA is targeted for downregulation to conserve energy in many hypoxia tolerant organisms (Buck and Hochachka, 1993; Hylland et al., 1997; De Angelis et al., 1998; Stecyk et al., 2017). Also in human lung cells, hypoxia decreases the number of active NKA at the plasma membrane, although it is not commonly thought to be an adaptive mechanism (Dada et al., 2013; Gusarova et al., 2009; Gusarova et al., 2011). Given that NDRG1 is hypoxia-responsive protein expressed in the zebrafish pronephros and ionocytes (Figure Chapter 2), and is known to bind ATP1a (Tu et al., 2007), it is possible that NDRG1 regulates ATP1a under hypoxia, a hypothesis I will explore in my thesis.

V. Hypotheses and Specific Aims

The molecular mechanisms that trigger entry into hypometabolism in zebrafish and other anoxia-tolerant organisms are for the most-part unknown. However, current literature suggests that anoxia-induced hypometabolism is accomplished by an intricate balancing act between ATP demand and anoxia-diminished ATP supply and may involve multiple signaling pathways acting downstream of ETC blockage or anoxia itself (Padilla & Roth, 2001; Mendelsohn et al., 2008; Lai et al., 2013). In an effort to identify a proximal signal that induces hypometabolism, we collaborated with Dr. Young-Sam Lee at Johns Hopkins University, and performed a mass spectrometry (MS) experiment to identify metabolites whose levels change in response to anoxia. It was reasoned that metabolites would serve as ideal signaling molecules as their levels change rapidly in response to fluctuations in the environment. Global metabolite MS screening revealed several metabolites implicated in the glycolytic pathway whose levels changed in response to anoxia, among which was lactate (**Chapter 2, Figure 6**). Further analysis using a fluorometric lactate detection assay revealed a rapid increase in lactate levels in 24 hour-post fertilization (hpf) zebrafish embryos exposed to a short duration of anoxia.

In support of our finding, studies from the Gitlin laboratory also showed that both anoxia and blockage of the ETC resulted in accumulation of lactate in zebrafish embryos (**Figure 1.22. Rate of lactate build up in 24 hpf embryos following incubation in different chemical ETC blockers or anoxia**) (Mendelsohn et al., 2008).

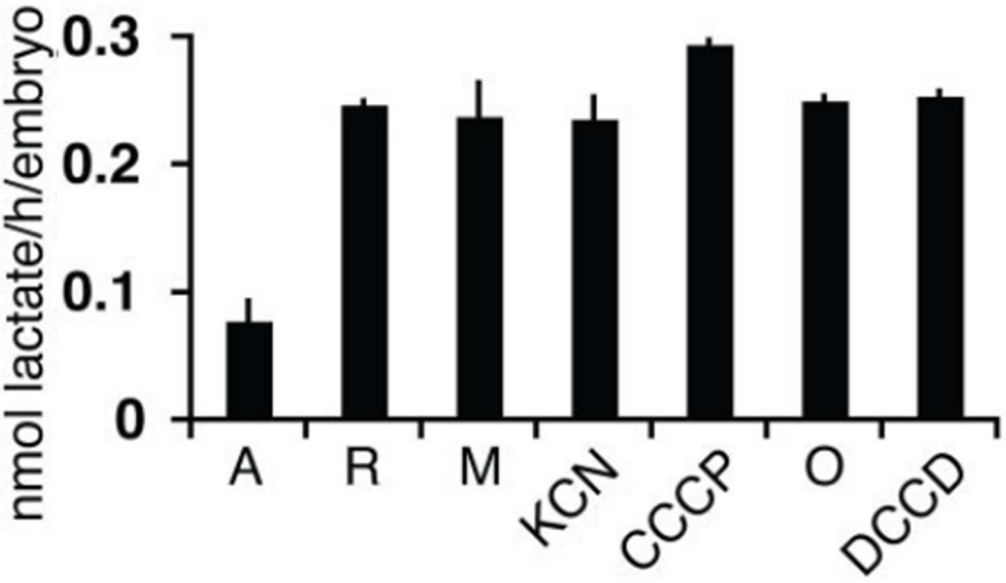

Figure 1.22. Rate of lactate build up in 24 hpf embryos following incubation in different chemical ETC blockers or anoxia. A, anoxia; R, rotenone; M, myxothiazole; O, oligomycin. The chemical ETC blockers resulted in a higher rate of lactate accumulation than in anoxia. Image from Mendelsohn et al., 2008.

While lactate is generally thought of as a byproduct of glycolysis, increasing evidence suggests that this metabolite also plays an important signaling role. For instance, lactate was shown to bind to a GPCR olfactory receptor, Olfr78, in the carotid body to stimulate hyperventilation in response to hypoxia (Chang et al., 2015). Furthermore, as mentioned in the section on post-translational modification of NDRGs, another study revealed that lactate binds to and stabilizes N-myc downstream-regulated gene 3 (NDRG3) to promote cellular adaptation in hypoxic cancer cells via Raf-ERK signaling pathway (**Figure 1.14. Signaling role of lactate in adaptive response of cancer cells to hypoxia**) (Lee et al., 2015; Park et al., 2015); indicating that lactate-NDRG signals promote cellular adaptation to low oxygen. Other than the study by Lee and colleagues (2015), the physiological role of NDRG family members under low oxygen has not been investigated. While the role of NDRG1 in cancer progression is being slowly uncovered, its contribution to normal physiology, more specifically, in intact organisms, is mostly unknown.

The observations that lactate levels increase dramatically under hypoxia and the study by Lee et and colleagues revealing a lactate-NDRG signaling axis were the starting point of my thesis work. I became interested in understanding the role of Ndrg1 in the hypoxia response and more specifically, its potential function in lactate-mediated adaptation to low oxygen. Although both Ndrg1 and Ndrg3 are expressed in the kidney, there was an interesting protein-protein mass spectrometry study (**Table 1.2. List of NDRG1-interacting proteins in normoxic prostate cancer cells identified by immunoprecipitation and LC/MS/MS**) (Tu et al., 2007) for Ndrg1 that further solidified my interest in pursuit of Ndrg1.

My thesis thus explores the physiological significance of lactate/NDRG signaling in the developing zebrafish embryo. More specifically, I have investigated the role of lactate/NDRG1 signaling in regulating the metabolic and physiological responses in the pronephros and ionocytes.

The following hypotheses will be tested:

Hypothesis 1: NDRG1 promotes tissue and organismal protection under hypoxia.

Hypothesis 2: NDRG1 downregulates the ATP-demanding sodium potassium ATPase pump under hypoxia.

Hypothesis 3: Lactate is a proximal signal downstream of hypoxia that can activate NDRG1.

VI. Chapter 1 References

1. Ai R, Sun Y, Guo Z, et al. NDRG1 overexpression promotes the progression of esophageal squamous cell carcinoma through modulating Wnt signaling pathway. *Cancer Biol Ther*. 2016;17(9):943-954. doi:10.1080/15384047.2016.1210734
2. Askautrud HA, Gjernes E, Gunnes G, et al. Global gene expression analysis reveals a link between NDRG1 and vesicle transport. *PLoS One*. 2014;9(1):e87268. Published 2014 Jan 31. doi:10.1371/journal.pone.0087268
3. Buck LT, Hochachka PW. Anoxic suppression of Na(+)-K(+)-ATPase and constant membrane potential in hepatocytes: support for channel arrest. Am J Physiol. 1993 Nov;265(5 Pt 2):R1020-5. doi: 10.1152/ajpregu.1993.265.5.R1020. PMID: 8238602.
4. Buck, L. T., Hogg, D. W. R., Rodgers-Garlick, C., & Pamenter, M. E. (2012). Oxygen sensitive synaptic neurotransmission in anoxia-tolerant turtle cerebrocortex. In Advances in Experimental Medicine and Biology (Vol. 758, pp. 71–79). https://doi.org/10.1007/978-94-007-4584-1-10
5. Bonifacino JS, Traub LM. Signals for sorting of transmembrane proteins to endosomes and lysosomes. Annu Rev Biochem. 2003;72:395-447. doi: 10.1146/annurev.biochem.72.121801.161800. Epub 2003 Mar 6. PMID: 12651740.
6. Cai J, Yang J, Jones DP. Mitochondrial control of apoptosis: the role of cytochrome c. Biochim Biophys Acta. 1998 Aug 10;1366(1-2):139-49. doi: 10.1016/s0005-2728(98)00109-1. PMID: 9714780.

7. Cai C.-C., Zhu J.-H., Ye L.-X., Dai Y.-Y., Fang M.-C., Hu Y.-Y., Pan S.-L., Chen S., Li P.-J., Fu X.-Q., et al. Glycine Protects against Hypoxic-Ischemic Brain Injury by Regulating Mitochondria-Mediated Autophagy via the AMPK Pathway. *Oxid. Med. Cell. Longev.* 2019;2019:4248529. doi: 10.1155/2019/4248529.
8. Carreau, A., Hafny-Rahbi, B. El, Matejuk, A., Grillon, C., & Kieda, C. (2011). Why is the partial oxygen pressure of human tissues a crucial parameter? Small molecules and hypoxia. Journal of Cellular and Molecular Medicine, 15(6), 1239–1253. https://doi.org/10.1111/j.1582-4934.2011.01258.x
9. Cardona, T.; Murray, J. W.; Rutherford, A. W. (May 2015). "Origin and Evolution of Water Oxidation before the Last Common Ancestor of the Cyanobacteria". *Molecular Biology and Evolution*. 32 (5): 1310–1328. doi:10.1093/molbev/msv024. PMC 4408414. PMID 25657330.
10. Chan T, Asashima M. Growing kidney in the frog. Nephron Exp Nephrol 2006;103:e81–5.
11. Chang WJ, Hwang PP. Development of zebrafish epidermis. Birth Defects Res C Embryo Today. 2011 Sep;93(3):205-14. doi: 10.1002/bdrc.20215. PMID: 21932430.
12. Chang, A. J., Ortega, F. E., Riegler, J., Madison, D. V, & Krasnow, M. A. (2015). Oxygen control of breathing by an olfactory receptor activated by lactate. Nature, 527(7577), 240–244. https://doi.org/10.1038/nature15721
13. Clegg. (1997). Embryos of Artemia franciscana survive four years of continuous anoxia: the case for complete metabolic rate depression. The Journal of

Experimental Biology, 200(3), 467–75. Retrieved from http://www.ncbi.nlm.nih.gov/pubmed/9318130

14. Cockman, M.E., Masson, N., Mole, D.R., Jaakkola, P., Chang, G.W., Clifford, S.C., Maher, E.R., Pugh, C.W., Ratcliffe, P.J., and Maxwell, P.H. (2000). Hypoxia inducible factor-alpha binding and ubiquitylation by the von Hippel-Lindau tumor suppressor protein. J Biol Chem *275*, 25733-25741.
15. Copp JN, Neilan BA. The phosphopantetheinyl transferase superfamily: phylogenetic analysis and functional implications in cyanobacteria. *Appl Environ Microbiol*. 2006;72(4):2298-2305. doi:10.1128/AEM.72.4.2298-2305.2006
16. Corton J.M., Gillespie J.G., Hardie D.G. Role of the AMP-activated protein kinase in the cellular stress response. *Curr. Biol.* 1994;4:315–324. doi: 10.1016/S0960-9822(00)00070-1.
17. Croessmann, Sarah, et al. "*NDRG1* Links p53 with Proliferation-Mediated Centrosome Homeostasis and Genome Stability." *Proceedings of the National Academy of Sciences of the United States of America*, vol. 112, no. 37, 2015, pp. 11583–11588. *JSTOR*, www.jstor.org/stable/26465061. Accessed 10 June 2021.
18. Cymerman, A; Rock, PB, *Medical Problems in High Mountain Environments. A Handbook for Medical Officers*, USARIEM-TN94-2, US Army Research Inst. of Environmental Medicine Thermal and Mountain Medicine Division Technical Report, archived from the original on 2009-04-23, retrieved 2009-03-05
19. Dancy BM, Sedensky MM, Morgan PG. Effects of the mitochondrial respiratory chain on longevity in C. elegans. Exp Gerontol. 2014 Aug;56:245-55. doi: 10.1016/j.exger.2014.03.028. Epub 2014 Apr 5. PMID: 24709342.

20. Danielson PB (December 2002). "The cytochrome P450 superfamily: biochemistry, evolution and drug metabolism in humans". *Current Drug Metabolism*. 3 (6): 561–97.
21. De Angelis C, Haupert GT Jr. Hypoxia triggers release of an endogenous inhibitor of Na(+)-K(+)-ATPase from midbrain and adrenal. Am J Physiol. 1998 Jan;274(1):F182-8. doi: 10.1152/ajprenal.1998.274.1.F182. PMID: 9458838.
22. Dengler VL, Galbraith M, Espinosa JM. Transcriptional regulation by hypoxia inducible factors. *Crit Rev Biochem Mol Biol*. 2014;49(1):1-15. doi:10.3109/10409238.2013.838205
23. Devasagayam TP, Tilak JC, Boloor KK, Sane KS, Ghaskadbi SS, Lele RD (October 2004). "Free radicals and antioxidants in human health: current status and future prospects". *The Journal of the Association of Physicians of India*. 52: 794–804. PMID 15909857
24. Dinkelacker, S. A., Costanzo, J. P., & Lee, R. E. (2005). Anoxia tolerance and freeze tolerance in hatchling turtles. Journal of Comparative Physiology B: Biochemical, Systemic, and Environmental Physiology, 175(3), 209–217. https://doi.org/10.1007/s00360-005-0478-0
25. Dressler GR. The cellular basis of kidney development. Annu Rev Cell Dev Biol 2006;22:509–29.
26. Drummond I. Making a zebrafish kidney: a tale of two tubes. Trends Cell Biol 2003;13:357–65.
27. Duerr, J. M., & Podrabsky, J. E. (2010). Mitochondrial physiology of diapausing and developing embryos of the annual killifish Austrofundulus limnaeus:

Implications for extreme anoxia tolerance. Journal of Comparative Physiology B: Biochemical, Systemic, and Environmental Physiology, 180(7), 991–1003. https://doi.org/10.1007/s00360-010-0478-6

28. Edreva, Aglika (2 April 2005). "Generation and scavenging of reactive oxygen species in chloroplasts: a submolecular approach". *Agriculture, Ecosystems & Environment*. 106 (2): 119–133. doi:10.1016/j.agee.2004.10.022. ISSN 0167-8809

Engineering ToolBox, (2004). *Air Solubility in Water*. [online] Available at: https://www.engineeringtoolbox.com/air-solubility-water-d_639.html

29. Evans DH (2011) Freshwater fish gill ion transport: august Krogh to morpholinos and microprobes. Acta Physiol 202:349–359

Fondriest Environmental, Inc. “Dissolved Oxygen.” Fundamentals of Environmental Measurements. 19 Nov. 2013. Web. < https://www.fondriest.com/environmental-measurements/parameters/water-quality/dissolved-oxygen/ >.

30. Fontenas L, De Santis F, Di Donato V, et al. Neuronal Ndrg4 Is Essential for Nodes of Ranvier Organization in Zebrafish. *PLoS Genet*. 2016;12(11):e1006459. Published 2016 Nov 30. doi:10.1371/journal.pgen.1006459
31. Foot N, Henshall T, Kumar S. Ubiquitination and the Regulation of Membrane Proteins. Physiol Rev. 2017 Jan;97(1):253-281. doi: 10.1152/physrev.00012.2016. PMID: 27932395.
32. Frosi Y, Anastasi S, Ballarò C, Varsano G, Castellani L, Maspero E, Polo S, Alemà S, Segatto O. A two-tiered mechanism of EGFR inhibition by

RALT/MIG6 via kinase suppression and receptor degradation. J Cell Biol. 2010 May 3;189(3):557-71. doi: 10.1083/jcb.201002032. Epub 2010 Apr 26. PMID: 20421427; PMCID: PMC2867293.

33. Gerlach GF, Wingert RA. Kidney organogenesis in the zebrafish: insights into vertebrate nephrogenesis and regeneration.Wiley interdiscip Rev Dev Biol 2013;2:559–85.
34. Gonzalez FJ, Gelboin HV (November 1992). "Human cytochromes P450: evolution and cDNA-directed expression". *Environmental Health Perspectives*. 98: 81–5.
35. Greenald, D., Jeyakani, J., Pelster, B. *et al.* Genome-wide mapping of Hif-1α binding sites in zebrafish. *BMC Genomics* 16, 923 (2015). https://doi.org/10.1186/s12864-015-2169-x
36. Gross, J.; Bhattacharya, D. (August 2010). "Uniting sex and eukaryote origins in an emerging oxygenic world". *Biol. Direct*. 5: 53. doi:10.1186/1745-6150-5-53. PMC 2933680. PMID 20731852.
37. Xin Guo, Honggui Li, Hang Xu, Shihlung Woo, Hui Dong, Fuer Lu, Alex J. Lange, Chaodong Wu. Glycolysis in the control of blood glucose homeostasis, Acta Pharmaceutica Sinica B, Volume 2, Issue 4, 2012, Pages 358-367, ISSN 2211-3835, https://doi.org/10.1016/j.apsb.2012.06.002.
38. Hanukoglu I, Rapoport R, Weiner L, Sklan D (September 1993). "Electron leakage from the mitochondrial NADPH-adrenodoxin reductase-adrenodoxin-P450scc (cholesterol side chain cleavage) system". *Archives of Biochemistry and Biophysics*. 305 (2): 489–98.

39. Hardie D.G., Ashford M.L.J. AMPK: Regulating energy balance at the cellular and whole body levels. *Physiology.* 2014;29:99–107. doi: 10.1152/physiol.00050.2013.

40. Hardie D.G., Schaffer B.E., Brunet A. AMPK: An Energy-Sensing Pathway with Multiple Inputs and Outputs. *Trends Cell Biol.* 2016;26:190–201. doi: 10.1016/j.tcb.2015.10.013.

41. Hawley S.A., Davison M., Woods A., Davies S.P., Beri R.K., Carling D., Hardie D.G. Characterization of the AMP-activated protein kinase kinase from rat liver and identification of threonine 172 as the major site at which it phosphorylates AMP-activated protein kinase. *J. Biol. Chem.* 1996;271:27879–27887. doi: 10.1074/jbc.271.44.27879.

42. Hekimi S, Lapointe J, Wen Y. Taking a "good" look at free radicals in the aging process. *Trends Cell Biol*. 2011;21(10):569-576. doi:10.1016/j.tcb.2011.06.008

43. Hicke L, Dunn R. Regulation of membrane protein transport by ubiquitin and ubiquitin-binding proteins. Annu Rev Cell Dev Biol. 2003;19:141-72. doi: 10.1146/annurev.cellbio.19.110701.154617. PMID: 14570567.

44. Hinchy EC, Gruszczyk AV, Willows R, et al. Mitochondria-derived ROS activate AMP-activated protein kinase (AMPK) indirectly. *J Biol Chem*. 2018;293(44):17208-17217. doi:10.1074/jbc.RA118.002579

45. Hodgskiss, Malcolm S. W.; Crockford, Peter W.; Peng, Yongbo; Wing, Boswell A.; Horner, Tristan J. (27 August 2019). "A productivity collapse to end Earth's Great Oxidation". *PNAS*. 116 (35): 17207–17212.

Bibcode:2019PNAS..11617207H. doi:10.1073/pnas.1900325116. PMC 6717284. PMID 31405980.

46. Hu H., Li X., Ren D., Tan Y., Chen J., Yang L., Chen R., Li J., Zhu P. The cardioprotective effects of carvedilol on ischemia and reperfusion injury by AMPK signaling pathway. *Biomed. Pharmacother.* 2019;117:109106. doi: 10.1016/j.biopha.2019.109106.
47. Huang, A.M., Rubin, G.M. (2000). A misexpression screen identifies genes that can modulate RAS1 pathway signaling in Drosophila melanogaster. *Genetics* **156(3)**: 1219--1230.
48. Hwang J, Kim Y, Kang HB, Jaroszewski L, Deacon AM, Lee H, Choi WC, Kim KJ, Kim CH, Kang BS, Lee JO, Oh TK, Kim JW, Wilson IA, Kim MH. Crystal structure of the human N-Myc downstream-regulated gene 2 protein provides insight into its role as a tumor suppressor. J Biol Chem. 2011 Apr 8;286(14):12450-60. doi: 10.1074/jbc.M110.170803. Epub 2011 Jan 18. PMID: 21247902; PMCID: PMC3069448.
49. Hwang PP, Lee TH, Lin LY (2011) Ion regulation in fish gills: recent progress in the cellular and molecular mechanisms. Am J Physiol Regul Integr Comp Physiol 301:R28–R47
50. Hwang PP, Perry SF (2010) Ionic and acid–base regulation. In: Perry SF, Ekker M, Farrell AP, Brauner CJ (eds) Fish physiology Vol. 29. Zebrafish. Academic, San Diego, pp 311–343

51. Hwang PP, Chou MY. Zebrafish as an animal model to study ion homeostasis. Pflugers Arch. 2013 Sep;465(9):1233-47. doi: 10.1007/s00424-013-1269-1. Epub 2013 Apr 9. PMID: 23568368; PMCID: PMC3745619.

52. Hylland P, Milton S, Pek M, Nilsson GE, Lutz PL. Brain Na+/K+-ATPase activity in two anoxia tolerant vertebrates: crucian carp and freshwater turtle. Neurosci Lett. 1997 Oct 10;235(1-2):89-92. doi: 10.1016/s0304-3940(97)00727-1. PMID: 9389603.

53. Ivan, M., Kondo, K., Yang, H., Kim, W., Valiando, J., Ohh, M., Salic, A., Asara, J.M., Lane, W.S., and Kaelin, W.G., Jr. (2001). HIFalpha targeted for VHL-mediated destruction by proline hydroxylation: implications for oxygen sensing. Science *292*, 464-468.

54. Jaakkola, P., Mole, D.R., Tian, Y.M., Wilson, M.I., Gielbert, J., Gaskell, S.J., Kriegsheim, A., Hebestreit, H.F., Mukherji, M., Schofield, C.J.*, et al.* (2001). Targeting of HIF-alpha to the von Hippel-Lindau ubiquitylation complex by oxygen-regulated prolyl hydroxylation. Science *292*, 468-472.

55. Jackson, D. C. (2002). Hibernating without oxygen: physiological adaptations of the painted turtle. The Journal of Physiology, 543(Pt 3), 731–7. https://doi.org/10.1113/jphysiol.2002.024729

56. Jackson, D. C. (2004). Surviving extreme lactic acidosis: The role of calcium lactate formation in the anoxic turtle. In Respiratory Physiology and Neurobiology

57. Jamieson C, Sharma M, Henderson BR. Wnt signaling from membrane to nucleus: β-catenin caught in a loop. Int J Biochem Cell Biol. 2012 Jun;44(6):847-50. doi: 10.1016/j.biocel.2012.03.001. Epub 2012 Mar 14. PMID: 22433990.

58. Jin R, Liu W, Menezes S, Yue F, Zheng M, Kovacevic Z, Richardson DR. The metastasis suppressor NDRG1 modulates the phosphorylation and nuclear translocation of β-catenin through mechanisms involving FRAT1 and PAK4. J Cell Sci. 2014 Jul 15;127(Pt 14):3116-30. doi: 10.1242/jcs.147835. Epub 2014 May 14. PMID: 24829151.

59. Johnson D, Allman E, Nehrke K. Regulation of acid-base transporters by reactive oxygen species following mitochondrial fragmentation. *Am J Physiol Cell Physiol*. 2012;302(7):C1045-C1054. doi:10.1152/ajpcell.00411.2011

60. Jung SN, Yang WK, Kim J, Kim HS, Kim EJ, Yun H, Park H, Kim SS, Choe W, Kang I, Ha J. Reactive oxygen species stabilize hypoxia-inducible factor-1 alpha protein and stimulate transcriptional activity via AMP-activated protein kinase in DU145 human prostate cancer cells. Carcinogenesis. 2008 Apr;29(4):713-21. doi: 10.1093/carcin/bgn032. Epub 2008 Feb 6. PMID: 18258605.

61. Kachhap SK, Faith D, Qian DZ, Shabbeer S, Galloway NL, Pili R, et al. (2007) The N-Myc Down Regulated Gene1 (NDRG1) Is a Rab4a Effector Involved in Vesicular Recycling of E-Cadherin. PLoS ONE 2(9): e844. https://doi.org/10.1371/journal.pone.0000844

62. Kamura, T., Sato, S., Iwai, K., Czyzyk-Krzeska, M., Conaway, R.C., and Conaway, J.W. (2000). Activation of HIF1alpha ubiquitination by a reconstituted

von Hippel-Lindau (VHL) tumor suppressor complex. Proc Natl Acad Sci U S A *97*, 10430-10435.

63. Kersten, S., & Arjona, F. J. (2017). Ion transport in the zebrafish kidney from a human disease angle: possibilities, considerations, and future perspectives. American Journal of Physiology - Renal Physiology, 312(1), F172–F189. https://doi.org/10.1152/ajprenal.00425.2016
64. Kyung-tae Kim, Pat P. Ongusaha, Young-Kwon Hong, Siavash K. Kurdistani, Masafumi Nakamura, Kun Ping Lu, Sam W. Lee. Function of Drg1/Rit42 in p53-dependent Mitotic Spindle Checkpoint*, Journal of Biological Chemistry, Volume 279, Issue 37, 2004, Pages 38597-38602
65. Kim YJ, Yoon SY, Kim JT, Song EY, Lee HG, Son HJ, Kim SY, Cho D, Choi I, Kim JH, Kim JW. NDRG2 expression decreases with tumor stages and regulates TCF/beta-catenin signaling in human colon carcinoma. Carcinogenesis. 2009 Apr;30(4):598-605. doi: 10.1093/carcin/bgp047. Epub 2009 Feb 23. PMID: 19237607; PMCID: PMC2664458.
66. Kim KR, Kim KA, Park JS, et al. Structural and Biophysical Analyses of Human N-Myc Downstream-Regulated Gene 3 (NDRG3) Protein. *Biomolecules*. 2020;10(1):90. Published 2020 Jan 6. doi:10.3390/biom10010090
67. Kitowska A, Pawełczyk T. N-myc downstream regulated 1 gene and its place in the cellular machinery. Acta Biochim Pol. 2010;57(1):15-21. Epub 2010 Mar 19. PMID: 20300662.

68. Kokame K, Kato H, Miyata T (1996) Homocysteine-respondent genes in vascular endothelial cells identified by differential display analysis. GRP78/BiP and novel genes. *J Biol Chem* 271:29659–29665

69. Kondo Y., Sueyoshi K., Zhang J., Bao Y., Li X., Fakhari M., Slubowski C.J., Bahrami S., Ledderose C., Junger W.G. Adenosine 5'-Monophosphate Protects From Hypoxia By Lowering Mitochondrial Metabolism and Oxygen Demand. *Shock.* 2019 doi: 10.1097/SHK.0000000000001440.

70. Kräuter-Canham R, Bronner R, Evrard J-L, Hahne G, Friedt W, Steinmetz A (1997) A transmitting tissue- and pollen-expressed protein from sunflower with sequence similarity to the human RTP protein. Plant Science 129:191–202

71. Krieg, M., Haas, R., Brauch, H., Acker, T., Flamme, I., and Plate, K.H. (2000). Up-regulation of hypoxia-inducible factors HIF-1alpha and HIF-2alpha under normoxic conditions in renal carcinoma cells by von Hippel-Lindau tumor suppressor gene loss of function. Oncogene *19*, 5435-5443.

72. Kültz D, Li J, Gardell A, Sacchi R. Quantitative molecular phenotyping of gill remodeling in a cichlid fish responding to salinity stress. *Mol Cell Proteomics*. 2013;12(12):3962-3975. doi:10.1074/mcp.M113.029827

73. Kurdistani SK, Arizti P, Reimer CL, Sugrue MM, Aaronson SA, Lee SW (1998) Inhibition of tumor cell growth by RTP/rit42 and its responsiveness to p53 and DNA damage. *Cancer Res* 58:4439–4444

74. Lai, K., Selinger, D. W., Solomon, J. M., Wu, H., Schmitt, E., Serluca, F. C., … Benson, J. D. (2013). Integrated compound profiling screens identify the mitochondrial electron transport Chain as the molecular target of the natural

products manassantin, sesquicillin, and arctigenin. ACS Chemical Biology, 8(1), 257–267. https://doi.org/10.1021/cb300495e

75. Lang F., Föller M. Regulation of ion channels and transporters by AMP-activated kinase (AMPK) *Channels.* 2014;8:20–28. doi: 10.4161/chan.27423.

76. Lant, B., & Storey, K. B. (2010). An overview of stress response and hypometabolic strategies in Caenorhabditis elegans: Conserved and contrasting signals with the mammalian system. International Journal of Biological Sciences, 6(1), 9–50. https://doi.org/10.7150/ijbs.6.9

77. Lee DC, Sohn HA, Park ZY, Oh S, Kang YK, Lee KM, Kang M, Jang YJ, Yang SJ, Hong YK, Noh H, Kim JA, Kim DJ, Bae KH, Kim DM, Chung SJ, Yoo HS, Yu DY, Park KC, Yeom YI. A lactate-induced response to hypoxia. Cell. 2015 Apr 23;161(3):595-609. doi: 10.1016/j.cell.2015.03.011. Epub 2015 Apr 16. PMID: 25892225.

78. Li, J., & Kultz, D. (2014). Quantitative label-free proteomics of tilapia gill epithelium: confirmation of established and identification of novel responses to salinity change (1182.4). *The FASEB Journal*, *28*(s1). https://doi.org/https://doi.org/10.1096/fasebj.28.1_supplement.1182.4

79. Lin HC, Yeh CC, Chao LY, et al. The hypoxia-responsive lncRNA *NDRG-OT1* promotes NDRG1 degradation via ubiquitin-mediated proteolysis in breast cancer cells. *Oncotarget*. 2017;9(12):10470-10482. Published 2017 Dec 28. doi:10.18632/oncotarget.23732

80. Lindahl SG. Oxygen and life on earth: an anesthesiologist's views on oxygen evolution, discovery, sensing, and utilization. Anesthesiology. 2008 Jul;109(1):7-13. doi: 10.1097/ALN.0b013e31817b5a7e. PMID: 18580166.

81. Lu WJ, Chua MS, Wei W, So SK. NDRG1 promotes growth of hepatocellular carcinoma cells by directly interacting with GSK-3β and Nur77 to prevent β-catenin degradation. *Oncotarget*. 2015;6(30):29847-29859. doi:10.18632/oncotarget.4913

82. Lu LF, Li S, Wang ZX, Liu SB, Chen DD, Zhang YA. Zebrafish NDRG1a Negatively Regulates IFN Induction by Promoting the Degradation of IRF7. J Immunol. 2019 Jan 1;202(1):119-130. doi: 10.4049/jimmunol.1800490. Epub 2018 Nov 30. PMID: 30504422.

83. Liu W, Xing F, Iiizumi-Gairani M, Okuda H, Watabe M, Pai SK, Pandey PR, Hirota S, Kobayashi A, Mo YY, Fukuda K, Li Y, Watabe K. N-myc downstream regulated gene 1 modulates Wnt-β-catenin signalling and pleiotropically suppresses metastasis. EMBO Mol Med. 2012 Feb;4(2):93-108. doi: 10.1002/emmm.201100190. Epub 2012 Jan 13. PMID: 22246988; PMCID: PMC3306556.

84. Lutz, P. L., & Leone-Kabler, S. L. (1995). Upregulation of the GABAA/benzodiazepine receptor during anoxia in the freshwater turtle brain. The American Journal of Physiology, 268(5 Pt 2), R1332-5. Retrieved from http://www.ncbi.nlm.nih.gov/pubmed/7771598

85. Ma, J., Liu, W., Guo, H. *et al.* N-myc downstream-regulated gene 2 expression is associated with glucose transport and correlated with prognosis in breast carcinoma. *Breast Cancer Res* 16, R27 (2014). https://doi.org/10.1186/bcr3628

86. MacDonald BT, Tamai K, He X. Wnt/beta-catenin signaling: components, mechanisms, and diseases. Dev Cell. 2009 Jul;17(1):9-26. doi: 10.1016/j.devcel.2009.06.016. PMID: 19619488; PMCID: PMC2861485.

87. Maceina, M.J. and Shireman, J.V. (1979), Grass Carp: Effects of Salinity on Survival, Weight Loss, and Muscle Tissue Water Content. The Progressive Fish-Culturist, 41: 69-73. https://doi.org/10.1577/1548-8659(1979)41[69:GCOSOS]2.0.CO;2

88. Manhesa, Gérard; Allègre, Claude J.; Dupréa, Bernard & Hamelin, Bruno (1980). "Lead isotope study of basic-ultrabasic layered complexes: Speculations about the age of the earth and primitive mantle characteristics". *Earth and Planetary Science Letters*. 47 (3): 370–382. Bibcode:1980E&PSL..47..370M. doi:10.1016/0012-821X(80)90024-2.

89. Marahiel MA, Stachelhaus T, Mootz HD. Modular Peptide Synthetases Involved in Nonribosomal Peptide Synthesis. Chem Rev. 1997 Nov 10;97(7):2651-2674. doi: 10.1021/cr960029e. PMID: 11851476.

90. Maxwell, P.H., Wiesener, M.S., Chang, G.W., Clifford, S.C., Vaux, E.C., Cockman, M.E., Wykoff, C.C., Pugh, C.W., Maher, E.R., and Ratcliffe, P.J. (1999). The tumour suppressor protein VHL targets hypoxia-inducible factors for oxygen-dependent proteolysis. Nature *399*, 271-275.

91. McCampbell KK, Wingert RA. New tides: using zebrafish to study renal regeneration. Transl Res. 2014 Feb;163(2):109-22. doi: 10.1016/j.trsl.2013.10.003. Epub 2013 Oct 14. PMID: 24183931; PMCID: PMC3946610.

92. Meller, C. L., & Podrabsky, J. E. (2013). Avoidance of Apoptosis in Embryonic Cells of the Annual Killifish Austrofundulus limnaeus Exposed to Anoxia. PLoS ONE, 8(9), 1–9. https://doi.org/10.1371/journal.pone.0075837

93. Melotte, V., Qu, X., Ongenaert, M., van Criekinge, W., de Bruïne, A. P., Baldwin, H. S., & van Engeland, M. (2010). The N-myc downstream regulated gene (NDRG) family: diverse functions, multiple applications. The FASEB Journal : Official Publication of the Federation of American Societies for Experimental Biology, 24(11), 4153–4166. https://doi.org/10.1096/fj.09-151464

94. Mendelsohn, B. A., Kassebaum, B. L., & Gitlin, J. D. (2008). The zebrafish embryo as a dynamic model of anoxia tolerance. Developmental Dynamics, 237(7), 1780–1788. https://doi.org/10.1002/dvdy.21581

95. Menezes SV, Kovacevic Z, Richardson DR. The metastasis suppressor NDRG1 down-regulates the epidermal growth factor receptor via a lysosomal mechanism by up-regulating mitogen-inducible gene 6. J Biol Chem. 2019 Mar 15;294(11):4045-4064. doi: 10.1074/jbc.RA118.006279. Epub 2019 Jan 24. Erratum in: J Biol Chem. 2019 Aug 2;294(31):11675. PMID: 30679310; PMCID: PMC6422098.

96. Michiels C. Physiological and pathological responses to hypoxia. *Am. J. Pathol.* 2004;164:1875–1882. doi: 10.1016/S0002-9440(10)63747-9.

97. Mozaffarian, D., Benjamin, E. J., Go, A. S., Arnett, D. K., Blaha, M. J., Cushman, M., … Turner, M. B. (2016). Heart Disease and Stroke Statistics—2016 Update. Circulation, 133(4), e38–e360. https://doi.org/10.1161/CIR.0000000000000350 [doi]

98. Murphy MP. How mitochondria produce reactive oxygen species. Biochem J. 2009 Jan 1;417(1):1-13. doi: 10.1042/BJ20081386. PMID: 19061483; PMCID: PMC2605959.

99. Mustonen V, Muruganandam G, Loris R, Kursula P, Ruskamo S. Crystal and solution structure of NDRG1, a membrane-binding protein linked to myelination and tumour suppression. FEBS J. 2021 Jun;288(11):3507-3529. doi: 10.1111/febs.15660. Epub 2021 Jan 22. PMID: 33305529.

100. Nakayama, K., and Kataoka, N. (2019) Regulation of Gene Expression under Hypoxic Conditions. International Journal of Molecular Sciences 20, 3278

101. Naro F, Fazzini A, Grappone C, Citro G, Dini G, Giotti A, Malatesta F, Franconi F, Brunori M. Release of cytochromes from hypoxic and reoxygenated guinea pig heart. Cardioscience. 1993 Sep;4(3):177-84. PMID: 8400026.

102. Nilsson, G. E. (1991). The adenosine receptor blocker aminophylline increases anoxic ethanol excretion in crucian carp. The American Journal of Physiology, 261(4 Pt 2), R1057–R1060.

103. Nystul, T. G., & Roth, M. B. (2004). Carbon monoxide-induced suspended animation protects against hypoxic damage in Caenorhabditis elegans. Proceedings of the National Academy of Sciences of the United States of America, 101(24), 9133–6. https://doi.org/10.1073/pnas.0403312101

104. Ohh, M., Park, C.W., Ivan, M., Hoffman, M.A., Kim, T.Y., Huang, L.E., Pavletich, N., Chau, V., and Kaelin, W.G. (2000). Ubiquitination of hypoxia-inducible factor requires direct binding to the beta-domain of the von Hippel-Lindau protein. Nat Cell Biol *2*, 423-427.

105. Okuda T, Kondoh H (1999) Identification of new genes Ndr2 and Ndr3 which are related to Ndr1/RTP/Drg1 but show distinct tissue specificity and response to N-myc. *Biochem Biophys Res Commun* 266:208–215

106. Olson KR, Whitfield NL, Bearden SE, St Leger J, Nilson E, Gao Y, Madden JA. Hypoxic pulmonary vasodilation: a paradigm shift with a hydrogen sulfide mechanism. Am J Physiol Regul Integr Comp Physiol. 2010 Jan;298(1):R51-60. doi: 10.1152/ajpregu.00576.2009. Epub 2009 Nov 4. PMID: 19889863; PMCID: PMC2806212.

107. Padilla, P. a, & Roth, M. B. (2001). Oxygen deprivation causes suspended animation in the zebrafish embryo. Proceedings of the National Academy of Sciences of the United States of America, 98(13), 7331–7335. https://doi.org/10.1073/pnas.131213198

108. Pamenter ME, Shin DS, Buck LT. AMPA receptors undergo channel arrest in the anoxic turtle cortex. Am J Physiol Regul Integr Comp Physiol. 2008 Feb;294(2):R606-13. doi: 10.1152/ajpregu.00433.2007. Epub 2007 Dec 5. PMID: 18056983.

109. Park H, Adams MA, Lachat P, Bosman F, Pang SC, Graham CH. Hypoxia induces the expression of a 43-kDa protein (PROXY-1) in normal and malignant

cells. Biochem Biophys Res Commun. 2000 Sep 16;276(1):321-8. doi: 10.1006/bbrc.2000.3475. PMID: 11006124.

110. Park, K. C., Lee, D. C., & Yeom, Y. Il. (2015). NDRG3-mediated lactate signaling in hypoxia. BMB Reports, 48(6), 301–2. https://doi.org/10.1016/j.cell.2015.03.011.of

111. Park, T. J., Reznick, J., Peterson, B. L., Blass, G., Omerbašić, D., Bennett, N. C., … Lewin, G. R. (2017). Fructose-driven glycolysis supports anoxia resistance in the naked mole-rat. Science, 356(6335), 307–311. https://doi.org/10.1126/science.aab3896

112. Park KC, Menezes SV, Kalinowski DS, Sahni S, Jansson PJ, Kovacevic Z, Richardson DR. Identification of differential phosphorylation and sub-cellular localization of the metastasis suppressor, NDRG1. Biochim Biophys Acta Mol Basis Dis. 2018 Aug;1864(8):2644-2663. doi: 10.1016/j.bbadis.2018.04.011. Epub 2018 Apr 19. PMID: 29679718.

113. Pék, M., & Lutz, P. L. (1997). Role for adenosine in channel arrest in the anoxic turtle brain. The Journal of Experimental Biology, 200(Pt 13), 1913–7. Retrieved from http://www.ncbi.nlm.nih.gov/pubmed/9232005

114. Pérez-Pinzón, M. A., Lutz, P. L., Sick, T. J., & Rosenthal, M. (1993). Adenosine, a “retaliatory” metabolite, promotes anoxia tolerance in turtle brain. Journal of Cerebral Blood Flow and Metabolism : Official Journal of the International Society of Cerebral Blood Flow and Metabolism, 13(4), 728–32. https://doi.org/10.1038/jcbfm.1993.93

115. Pietiäinen V, Vassilev B, Blom T, Wang W, Nelson J, Bittman R, Bäck N, Zelcer N, Ikonen E. NDRG1 functions in LDL receptor trafficking by regulating endosomal recycling and degradation. J Cell Sci. 2013 Sep 1;126(Pt 17):3961-71. doi: 10.1242/jcs.128132. Epub 2013 Jun 26. PMID: 23813961.

116. Piquemal D, Joulia D, Balaguer P, Basset A, Marti J, Commes T (1999) Differential expression of the RTP/Drg1/Ndr1 gene product in proliferating and growth arrested cells. *Biochim Biophys Acta* 1450:364–373

117. Podrabsky, J. E., & Wilson, N. E. (2016). Hypoxia and Anoxia Tolerance in the Annual Killifish Austrofundulus limnaeus. In Integrative and Comparative Biology (Vol. 56, pp. 500–509). https://doi.org/10.1093/icb/icw092

118. Postlethwait J, Amores A, Cresko W, Singer A, Yan YL (2004) Subfunction partitioning, the teleost radiation and the annotation of the human genome. Trends in Genetics 20: 481–490.

119. Poureetezadi SJ, Cheng CN, Chambers JM, Drummond BE, Wingert RA. Prostaglandin signaling regulates nephron segment patterning of renal progenitors during zebrafish kidney development. Elife. 2016 Dec 20;5:e17551. doi: 10.7554/eLife.17551. PMID: 27996936; PMCID: PMC5173325.

120. Quinlan CL, Perevoshchikova IV, Hey-Mogensen M, Orr AL, Brand MD. Sites of reactive oxygen species generation by mitochondria oxidizing different substrates. Redox Biol. 2013 May 23;1(1):304-12. doi: 10.1016/j.redox.2013.04.005. PMID: 24024165; PMCID: PMC3757699.

121. Quadri LE, Weinreb PH, Lei M, Nakano MM, Zuber P, Walsh CT. Characterization of Sfp, a Bacillus subtilis phosphopantetheinyl transferase for

peptidyl carrier protein domains in peptide synthetases. Biochemistry. 1998 Feb 10;37(6):1585-95. doi: 10.1021/bi9719861. PMID: 9484229.

122. Ramsden, D. B., Ho, P. W. L., Ho, J. W. M., Liu, H. F., So, D. H. F., Tse, H. M., … Ho, S. L. (2012). Human neuronal uncoupling proteins 4 and 5 (UCP4 and UCP5): Structural properties, regulation, and physiological role in protection against oxidative stress and mitochondrial dysfunction. Brain and Behavior. https://doi.org/10.1002/brb3.55

123. Reilly RF, Bulger RE, KrizW. Structural-functional relationships in the kidney. Diseases of the kidney and urinary tract. Philadelphia: Lippincott Williams & Wilkins, 2007:2–53.

124. Rich, P. R. (2003). The molecular machinery of Keilin's respiratory chain. Biochemical Society Transactions, 31(Pt 6), 1095–1105. https://doi.org/10.1042/BST0311095

125. Ristow M, Schmeisser S. Extending life span by increasing oxidative stress. Free Radic Biol Med. 2011 Jul 15;51(2):327-36. doi: 10.1016/j.freeradbiomed.2011.05.010. Epub 2011 May 14. PMID: 21619928.

126. Russell R.R., Li J., Coven D.L., Pypaert M., Zechner C., Palmeri M., Giordano F.J., Mu J., Birnbaum M.J., Young L.H. AMP-activated protein kinase mediates ischemic glucose uptake and prevents postischemic cardiac dysfunction, apoptosis, and injury. *J. Clin. Investig.* 2004;114:495–503. doi: 10.1172/JCI19297.

127. Said HM, Safari R, Al-Kafaji G, Ernestus RI, Löhr M, Katzer A, Flentje M, Hagemann C. Time- and oxygen-dependent expression and regulation of

NDRG1 in human brain cancer cells. Oncol Rep. 2017 Jun;37(6):3625-3634. doi: 10.3892/or.2017.5620. Epub 2017 May 3. PMID: 28498432.

128. Sawai S, Shimono A, Wakamatsu Y, Palmes C, Hanaoka K, Kondoh H 1993. Defects of embryonic organogenesis resulting from targeted disruption of the N-*myc* gene in the mouse. *Development* 117: 1445–1455

129. Schieber M, Chandel NS. TOR signaling couples oxygen sensing to lifespan in C. elegans. Cell Rep. 2014 Oct 9;9(1):9-15. doi: 10.1016/j.celrep.2014.08.075. Epub 2014 Oct 2. PMID: 25284791; PMCID: PMC4194168.

130. Semenza, G.L., and Wang, G.L. (1992). A nuclear factor induced by hypoxia via de novo protein synthesis binds to the human erythropoietin gene enhancer at a site required for transcriptional activation. Mol Cell Biol *12*, 5447-5454.

131. Seo-Mayer P.W., Thulin G., Zhang L., Alves D.S., Ardito T., Kashgarian M., Caplan M.J. Preactivation of AMPK by metformin may ameliorate the epithelial cell damage caused by renal ischemia. *Am. J. Physiol. Ren. Physiol.* 2011;301:F1346–F1357. doi: 10.1152/ajprenal.00420.2010.

132. Shadel GS, Horvath TL. Mitochondrial ROS signaling in organismal homeostasis. Cell. 2015 Oct 22;163(3):560-9. doi: 10.1016/j.cell.2015.10.001. Epub 2015 Oct 22. PMID: 26496603; PMCID: PMC4634671.

133. Shaw E, McCue LA, Lawrence CE & Dordick JS (2002) Identification of a novel class in the alpha/beta hydrolase fold superfamily: the N-myc differentiation related proteins. Proteins Struct Funct Genet 47, 163–168.

134. Shi XH, Larkin JC, Chen B, Sadovsky Y. The expression and localization of N-myc downstream-regulated gene 1 in human trophoblasts. *PLoS One*. 2013;8(9):e75473. Published 2013 Sep 16. doi:10.1371/journal.pone.0075473

135. Shi J, Zheng H, Yuan L. High NDRG3 expression facilitates HCC metastasis by promoting nuclear translocation of β-catenin. *BMB Rep*. 2019;52(7):451-456. doi:10.5483/BMBRep.2019.52.7.201

136. Shimono A, Okuda T, Kondoh H (1999) N-myc-dependent repression of *Ndr1*, a gene identified by direct subtraction of whole mouse embryo cDNAs between wild type and *N-myc* mutant. *Mech Dev* 83:39–52

137. Schonkeren SL, Massen M, van der Horst R, Koch A, Vaes N, Melotte V. Nervous NDRGs: the N-myc downstream-regulated gene family in the central and peripheral nervous system. Neurogenetics. 2019 Oct;20(4):173-186. doi: 10.1007/s10048-019-00587-0. Epub 2019 Sep 4. PMID: 31485792; PMCID: PMC6754360.

138. Smith, R. W., Cash, P., Ellefsen, S., & Nilsson, G. E. (2009). Proteomic changes in the crucian carp brain during exposure to anoxia. Proteomics, 9(8), 2217–2229. https://doi.org/10.1002/pmic.200800662

139. Sollid, J. (2003). Hypoxia induces adaptive and reversible gross morphological changes in crucian carp gills. Journal of Experimental Biology, 206(20), 3667–3673. https://doi.org/10.1242/jeb.00594

140. Sosa Torres, Martha E.; Saucedo-Vázquez, Juan P.; Kroneck, Peter M.H. (2015). "Chapter 1, Section 2: The rise of dioxygen in the atmosphere". In Kroneck, Peter M.H.; Sosa Torres, Martha E. (eds.). *Sustaining Life on Planet*

Earth: Metalloenzymes Mastering Dioxygen and Other Chewy Gases. Metal Ions in Life Sciences volume 15. 15. Springer. pp. 1–12. doi:10.1007/978-3-319-12415-5_1. ISBN 978-3-319-12414-8. PMID 25707464.

141. Stecyk JA, Farrell AP, Vornanen M. Na+/K+-ATPase activity in the anoxic turtle (Trachemys scripta) brain at different acclimation temperature. Comp Biochem Physiol A Mol Integr Physiol. 2017 Apr;206:11-16. doi: 10.1016/j.cbpa.2017.01.002. Epub 2017 Jan 13. PMID: 28089857.

142. Stein S, Thomas EK, Herzog B, Westfall MD, Rocheleau JV, Jackson RS 2nd, Wang M, Liang P. NDRG1 is necessary for p53-dependent apoptosis. J Biol Chem. 2004 Nov 19;279(47):48930-40. doi: 10.1074/jbc.M400386200. Epub 2004 Sep 17. PMID: 15377670.

143. Stensløkken, K. O., Ellefsen, S., Vasieva, O., Fang, Y., Farrell, A. P., Olohan, L., … Cossins, A. R. (2014). Life without oxygen: Gene regulatory responses of the crucian carp (Carassius carassius) heart subjected to chronic anoxia. PLoS ONE, 9(11). https://doi.org/10.1371/journal.pone.0109978

144. Storey, K. B. (2007). Anoxia tolerance in turtles: Metabolic regulation and gene expression. Comparative Biochemistry and Physiology - A Molecular and Integrative Physiology. https://doi.org/10.1016/j.cbpa.2006.03.019

145. Storey, K. B., & Storey, J. M. (2007). Tribute to P. L. Lutz: putting life on `pause' - molecular regulation of hypometabolism. Journal of Experimental Biology, 210(10), 1700–1714. https://doi.org/10.1242/jeb.02716

146. Sugiki T, Murakami M, Taketomi Y, Kikuchi-Yanoshita R, Kudo I. N-myc downregulated gene 1 is a phosphorylated protein in mast cells. Biol Pharm Bull. 2004 May;27(5):624-7. doi: 10.1248/bpb.27.624. PMID: 15133234.

147. Takita, S., Wada, Y. & Kawamura, S. Effects of NDRG1 family proteins on photoreceptor outer segment morphology in zebrafish. *Sci Rep* 6, 36590 (2016). https://doi.org/10.1038/srep36590

148. Takvam M, Wood CM, Kryvi H, Nilsen TO. Ion Transporters and Osmoregulation in the Kidney of Teleost Fishes as a Function of Salinity. Front Physiol. 2021 Apr 20;12:664588. doi: 10.3389/fphys.2021.664588. PMID: 33967835; PMCID: PMC8098666.

149. Tanimoto, K., Makino, Y., Pereira, T., and Poellinger, L. (2000). Mechanism of regulation of the hypoxia-inducible factor-1 alpha by the von Hippel-Lindau tumor suppressor protein. EMBO Journal *19*, 4298-4309.

150. Taylor JS, Braasch I, Frickey T, Meyer A, Van de Peer Y (2003) Genome duplication, a trait shared by 22000 species of ray-finned fish. Genome Res 13: 382–390.

151. Tepekoy F, Akkoyunlu G, Demir R. The role of Wnt signaling members in the uterus and embryo during pre-implantation and implantation. *J Assist Reprod Genet*. 2015;32(3):337-346. doi:10.1007/s10815-014-0409-7

152. Tomitani, Akiko (April 2006). "The evolutionary diversification of cyanobacteria: Molecular–phylogenetic and paleontological perspectives". *PNAS*. 103 (14): 5442–5447. Bibcode:2006PNAS..103.5442T. doi:10.1073/pnas.0600999103. PMC 1459374. PMID 16569695.

153. Tu LC, Yan X, Hood L, Lin B. Proteomics analysis of the interactome of N-myc downstream regulated gene 1 and its interactions with the androgen response program in prostate cancer cells. Mol Cell Proteomics. 2007 Apr;6(4):575-88. doi: 10.1074/mcp.M600249-MCP200. Epub 2007 Jan 12. PMID: 17220478.

154. van Belzen N, Dinjens WN, Diesveld MP, Groen NA, van der Made AC, Nozawa Y, Vlietstra R, et al. (1997) A novel gene which is up-regulated during colon epithelial cell differentiation and down-regulated in colorectal neoplasms. *Lab Invest* 77:85–92

155. Vize PD, Seufert DW, Carroll TJ,Wallingford JB. Model systems for the study of kidney development: use of the pronephros in the analysis of organ induction and patterning. Dev Biol 1997;188: 189–204.

156. Vornanen, M., Stecyk, J. A. W., & Nilsson, G. E. (2009). Chapter 9 The Anoxia-Tolerant Crucian Carp (Carassius Carassius L.). Fish Physiology, 27(C), 397–441. https://doi.org/10.1016/S1546-5098(08)00009-5

157. Wang, G.L., Jiang, B.H., Rue, E.A., and Semenza, G.L. (1995). Hypoxia-inducible factor 1 is a basic-helix-loop-helix-PAS heterodimer regulated by cellular oxygen tension. Proceedings of the National Academy of Sciences of the United States of America *92*, 5510-5514.

158. Wang, G.L., and Semenza, G.L. (1995). Purification and characterization of hypoxia-inducible factor 1. Journal of Biological Chemistry *270*, 1230-1237.

159. Wang L, Liu N, Yao L, Li F, Zhang J, Deng Y, Liu J, Ji S, Yang A, Han H, Zhang Y, Zhang J, Han W, Liu X. NDRG2 is a new HIF-1 target gene necessary for hypoxia-induced apoptosis in A549 cells. Cell Physiol Biochem. 2008;21(1-3):239-50. doi: 10.1159/000113765. Epub 2008 Jan 16. PMID: 18209490.

160. Wang Q, Li LH, Gao GD, Wang G, Qu L, Li JG, Wang CM. HIF-1α up-regulates NDRG1 expression through binding to NDRG1 promoter, leading to proliferation of lung cancer A549 cells. Mol Biol Rep. 2013 May;40(5):3723-9. doi: 10.1007/s11033-012-2448-4. Epub 2013 Mar 25. PMID: 23526365.

161. Wang, H., Li, W., Xu, J. *et al.* NDRG1 inhibition sensitizes osteosarcoma cells to combretastatin A-4 through targeting autophagy. *Cell Death Dis* 8, e3048 (2017). https://doi.org/10.1038/cddis.2017.438

162. Weimer S, Priebs J, Kuhlow D, Groth M, Priebe S, Mansfeld J, Merry TL, Dubuis S, Laube B, Pfeiffer AF, Schulz TJ, Guthke R, Platzer M, Zamboni N, Zarse K, Ristow M. D-Glucosamine supplementation extends life span of nematodes and of ageing mice. Nat Commun. 2014 Apr 8;5:3563. doi: 10.1038/ncomms4563. PMID: 24714520; PMCID: PMC3988823.

163. West, John B. (1977). *Pulmonary Pathophysiology: The Essentials*. Williams & Wilkins. p. 22. ISBN 978-0-683-08936-3.

164. Wingert RA, Selleck R,Yu J, et al. The cdx genes and retinoic acid control the positioning and segmentation of the zebrafish pronephros. PLoS Genet 2007;3:1922–38.

165. Xu S, Chisholm AD. C. elegans epidermal wounding induces a mitochondrial ROS burst that promotes wound repair. Dev Cell. 2014 Oct 13;31(1):48-60. doi: 10.1016/j.devcel.2014.08.002. PMID: 25313960; PMCID: PMC4197410.

166. Zarse K, Schmeisser S, Groth M, Priebe S, Beuster G, Kuhlow D, Guthke R, Platzer M, Kahn CR, Ristow M. Impaired insulin/IGF1 signaling extends life span by promoting mitochondrial L-proline catabolism to induce a transient ROS signal. Cell Metab. 2012 Apr 4;15(4):451-65. doi: 10.1016/j.cmet.2012.02.013. PMID: 22482728; PMCID: PMC4844853.

167. Zhang J, Chen S, Zhang W, Zhang J, Liu X, Shi H, Che H, Wang W, Li F, Yao L. Human differentiation-related gene NDRG1 is a Myc downstream-regulated gene that is repressed by Myc on the core promoter region. Gene. 2008 Jul 1;417(1-2):5-12. doi: 10.1016/j.gene.2008.03.002. Epub 2008 Mar 12. PMID: 18455888.

168. Zhong, C., Zhou, Y. K., Yang, S. S., Zhao, J. F., Zhu, X. L., Chen, Z. H., Huang, X. (2015). Developmental expression of the N-myc downstream regulated gene (Ndrg) family during Xenopus tropicalis embryogenesis. International Journal of Developmental Biology, 59(10–12), 511–517. https://doi.org/10.1387/ijdb.150178xh

169. Zhou D, Salnikow K, Costa M (1998) *Cap43*, a novel gene specifically induced by Ni2+ compounds. *Cancer Res* 58:2182–2189

170. Zhou RH, Kokame K, Tsukamoto Y, Yutani C, Kato H, Miyata T. Characterization of the human NDRG gene family: a newly identified member,

NDRG4, is specifically expressed in brain and heart. Genomics. 2001 Apr 1;73(1):86-97. doi: 10.1006/geno.2000.6496. PMID: 11352569.

171. Zmijewski JW, Banerjee S, Bae H, Friggeri A, Lazarowski ER, Abraham E. Exposure to hydrogen peroxide induces oxidation and activation of AMP-activated protein kinase. J Biol Chem. 2010 Oct 22;285(43):33154-33164. doi: 10.1074/jbc.M110.143685. Epub 2010 Aug 20. PMID: 20729205; PMCID: PMC2963401.

CHAPTER 2: N-myc Downstream Regulated Gene 1 (NDRG1): A molecular switch for cellular adaptation to hypoxia

Jong Park[1], Austin M. Gabel[1], Lois Kang[1], Bryanna Canales[1], Polina Kassir[1], Afia Osei-Ntansah[1], Neil D. Tran[1], Anya Viswanathan[1], Young-Sam Lee[2] and Rachel Brewster[1*]

1. Department of Biological Sciences, University of Maryland Baltimore County, Baltimore, Maryland

2. Department of Biology, Johns Hopkins University, Baltimore, Maryland

* Corresponding author

ABSTRACT

Lack of oxygen (hypoxia and anoxia) is detrimental to cell function and survival and underlies many disease conditions. Hence, metazoans have evolved mechanisms to adapt to low oxygen. One such mechanism, metabolic suppression, decreases the cellular demand for oxygen by downregulating ATP-demanding processes. However, the molecular mechanisms underlying this adaptation are poorly understood. Here, we report on the role of *ndrg1a* in hypoxia adaptation of the anoxia-tolerant zebrafish embryo. *ndrg1a* is expressed in the kidney and ionocytes, cell types that use large amounts of ATP to maintain ion homeostasis. *ndrg1a* mutants are viable and develop normally when raised under normal oxygen. However, their survival and kidney function is reduced relative to WT embryos following exposure to prolonged anoxia. We further demonstrate that Ndrg1a binds to the energy-demanding sodium-potassium ATPase (NKA) pump under anoxia and is required for its degradation. Consequently, *ndrg1a* mutants that fail to downregulate NKA, have reduced ATP levels compared to WT embryos. Lastly, we show that sodium azide treatment, which increased lactate levels, was sufficient to trigger Ndrg1a-NKA degradation. These findings support a model whereby Ndrg1a functions as a molecular switch for long term adaptation to hypoxia via metabolic suppression.

INTRODUCTION

Hypoxia contributes to multiple disease conditions, including acute kidney injury (Shu et al., 2019), pulmonary hypertension (Bosc, Resta, Walker, & Kanagy, 2010), obstructive sleep apnea (Douglas et al., 2010), neurodegenerative disease (Peers et al., 2009), and

ischemia/stroke (Won, Kim, & Gwag, 2002). Despite these hypoxia-related pathological outcomes, low oxygen is encountered in many environments, such as at high altitude, overwintering in frozen ponds, embryonic development in utero and in the center of solid tumors. Hence, metazoans have evolved mechanisms to adapt to hypoxia and maintain homeostasis. These adaptations differ among cell types and species and the degree of protection they confer, however, they generally involve enhanced oxygen delivery, autophagy to recycle cellular constituents, and metabolic reprogramming (switch from oxidative phosphorylation to glycolysis) (Bellot et al., 2009; Guillemin & Krasnow, 1997; Semenza, 2001; Xie & Simon, 2017). Important mediators of such responses include hypoxia inducible factor 1α (Hif1α), a transcription factor that is stabilized by low oxygen (Semenza, 2012) and AMP-activated kinase (AMPK), whose activation is triggered by an increase in AMP or reactive oxygen species levels (Dengler, 2020). In addition, cells adapt to chronic and severe hypoxia by reducing their metabolic rate via suppression of ATP-consuming processes (Hochachka & Lutz, 2001). This regulation allows cells to maintain steady ATP levels even though ATP production is decreased. As ion pumps are major utilizers of cellular ATP, a key aspect of metabolic suppression is reduction in ion pumping via downregulation of NKA (Bogdanova, Petrushanko, Hernansanz-Agustin, & Martinez-Ruiz, 2016; Buck & Hochachka, 1993; Gusarova et al., 2011). In alveolar cells, this process depends on activation of AMPK (Gusarova et al., 2011).

The NDRG family consists of four members (NDRG 1-4) that belong to the α−β hydrolase superfamily, however, they lack the catalytic domain to be enzymatically active (Shaw, McCue, Lawrence, & Dordick, 2002). Several members of this family have

altered expression in cancer cells and tumor suppressor or oncogenic functions that impact cell proliferation, differentiation and metastasis (Melotte et al., 2010). NDRGs are also implicated in stress response and some members are transcriptionally up-regulated, in a Hif1α -dependent manner, following exposure to hypoxia (Angst et al., 2006; Cangul, 2004; Chen, Nelson, & Sadovsky, 2006; Melotte et al., 2010; Park et al., 2000). In hypoxic cancer cells, NDRG3 is stabilized by lactate and promotes angiogenesis and cell growth via activation of the Raf-ERK pathway (Lee et al., 2015). NDRG1 (formerly known as Drg1, Cap43, Rit42, RTP, and PROXY-1) protects human trophoblasts from hypoxic injury by triggering an anti-apoptotic response (Chen et al., 2006; Choi, Oh, Kim, Sadovsky, & Roh, 2007; Roh, Budhraja, Kim, Nelson, & Sadovsky, 2005). While NDRGs are clearly implicated in the stress response, their physiological roles in hypoxia adaptation of normal cells are mostly unknown.

The zebrafish genome encodes six *ndrg* family members that are highly homologous to mammalian *NDRGs* (Melotte et al., 2010). We have previously shown that *ndrg1a* mRNA is up-regulated nine fold in zebrafish embryos exposed to prolonged anoxia (Le et al., under revision), despite a general suppression of transcription under severe hypoxia (Storey & Storey, 2007). These observations suggest that *ndrg1a* plays an essential role in hypoxia adaptation. *ndrg1a* is primarily expressed in the embryonic kidney (pronephric duct or PD) and ionocytes (Le et al., under revision), cell types that maintain ion homeostasis via the activity of membrane pumps and ion transporters (Hwang & Chou, 2013).

We report here on the function of *ndrg1a* in the anoxia-tolerant zebrafish embryo, which can survive up to 50 hours of anoxia in a state of reversible arrest (Mendelsohn, Kassebaum, & Gitlin, 2008; Padilla & Roth, 2001). While *ndrg1a* is expressed in the PD and ionocytes, it is not required for the differentiation or function of these cells under normal conditions (normoxia). We rather found that *ndrg1a* promotes organismal survival and protects the kidney from hypoxic injury following exposure to prolonged anoxia. We further show that, under normoxic conditions, Ndrg1a spatially overlaps with NKA in the PD and ionocytes and that NKA degradation is accelerated in response to prolonged anoxia, in an Ndrg1a-dependent manner. Given that *ndrg1a* mutants have reduced ATP levels relative to WT embryos post-anoxia, we propose that activation of Ndrg1a contributes to metabolic suppression. Lastly, we show that an increase in intracellular lactate, the end product of glycolysis, may be sufficient to trigger NKA degradation. These findings support a model whereby Ndrg1a functions as a molecular switch for long term adaptation to hypoxia via metabolic suppression.

METHODS

Zebrafish husbandry and use

Wild type (WT) zebrafish (*Danio rerio*) of the AB strain were reared and manipulated using protocols approved by the Institutional Animal Care and Use Committee at the University of Maryland Baltimore County. Fish were maintained in UV-irradiated, filtered running water and exposed to a 12:12 light/dark cycle. Male and female fish were separated by a partition that was removed after the first light to initiate spawning.

Embryos were collected and staged according to previously described methods (Kimmel et al., 1995). Both age and stage-matched controls were used for hypoxia/anoxia -treated embryos. The sex of the embryos used is unknown.

CRISPR/Cas9 mutagenesis to generate *ndrg1a* mutants

Target Selection. The online bioinformatics tool CHOPCHOP (https://chopchop.cbu.uib.no/) was used to identify three unique CRISPR targets for *ndrg1a* (NM_001128353, isoform 1; GRCz10). Each guide RNA (gRNA) target sequence was chosen based on homology to other sequences in the published zebrafish genome, predicted off-target effects, and self-complementation. Two gRNAs were used to target the intron-exon splice junctions of *ndrg1a* exons 4 (gRNA1) and 5 (gRNA2), and a third gRNA was complementary to coding sequence in exon 7 (gRNA3) (Supplemental Fig. 1A).

The CRISPR target sequences are as follows:

gRNA1*: 5'-CCACGTCATGTTCCTACACGGGG-3'*

gRNA2*: 5'-AGGCAATGTAACTCACCCAGTGG-3'*

gRNA3*: 5'-CTTAGAAAGGATGTAAGCACCGG-3'*

Generation of insertion-deletions (indels). Embryos were mutagenized using active ribonucleoproteins (RNPs) consisting of the Alt-R CRISPR/Cas9 high fidelity nuclear-targeted Cas9 protein (HF-nCas9) and synthetic gRNAs according to the manufacturer's

recommendations (Integrated DNA Technologies; IDT). RNPs were co-injected in one-cell stage embryos in the animal pole for multiplexed editing of *ndrg1a*.

CRISPR mutant identification and characterization of the ndrg1a^{mbc1} allele. Genomic DNA sequencing of one of the F2 females identified 1-9 bp deletions in the vicinity of each of the gRNAs (Supplemental Fig. 1B). Sequencing of the corresponding cDNA revealed a large deletion spanning exons 4-15 (likely caused by gRNA1) (Supplemental Fig. 1C), which resulted in a truncated protein product that lacks the α−β hydrolase fold in addition to the C-terminal three tandem repeats and the phosphopantetheine sequence which are characteristic of NDRG1 (14) (Supplemental Fig. 1D). A homozygous mutant line was established for this allele, *ndrg1a*^{mbc1} (designated as *ndrg1a* $^{-/-}$). Immunolabeling and western blotting using anti-NDRG1 (directed against AA 82-203 of human NDRG1; UniProt accession no. Q92597) did not detect any signal in *ndrg1a* $^{-/-}$ mutants (Supplemental Fig. 1E, G). In contrast, wholemount *in situ* hybridization (riboprobe targeting the 3' end of the gene and 3'UTR) revealed that the transcript is expressed at normal levels (Supplemental Fig. 1F). The failure to detect protein is therefore likely to be a consequence of protein truncation.

Morpholino-mediated Ndrg1a knockdown

Morpholinos (MOs) targeting the translational start site of *ndrg1a* (Supplemental Fig. 1A) and the human β-globin gene (standard, control MO) (Schmajuk, Sierakowska, & Kole, 1999) were commercially obtained (Gene Tools, LLC) and administered at 2nl/embryo using 0.1mM working solution. Each MO was injected at the 1–4 cell stages

into the yolk margin just underneath the embryo proper. The MO sequences are as follows:

ndrg1a (MO1): 5'- CGTCCATTCTCAACGAGGACACCCG -3'

Standard control MO: 5'-CCTCTTACCTCAGTTACAATTTATA-3'

Specificity of the *ndrg1a* MO1 was confirmed using immunolabeling and western blotting, which revealed that Ndrg1a protein was absent or greatly reduced in MO-injected embryos (Supplemental Fig 1E, G). As expected, *ndrg1a* transcript levels, detected using whole-mount *in situ* hybridization, appeared normal in *ndrg1a* MO-injected embryos Supplemental Fig 1F).

Whole-mount *in situ* hybridization

Embryos were fixed in 4% paraformaldehyde (PFA) at the desired stages and processed for *in situ* hybridization as previously described (Thisse and Thisse, 2008), using riboprobes against zebrafish *atp1a1a1.2, kcnj1a.1, ndrg1a, slc12a3, slc20a1a*. Primers used for probe design were as follows: The underlined font indicates the T7 RNA polymerase binding site.

atp1a1a1.2:

FWD: 5'-CTTATGGAATCCAGGTGGCATC-3'

REV: 5'-<u>TAATACGACTCACTATAG</u>GCAGTACCTTCAACACAGTTGG-3'

kcnj1a.1:

FWD: 5’-CCTGGAGGTGTGGCTTTGAT-3’

REV: 5’-TAATACGACTCACTATAGAGCCATGCCATCGAGGAAAA-3’

ndrg1a:

FWD: 5’-AGCTCACACCTCCGAAAACC-3’

REV: 5’-TAATACGACTCACTATAGACGATGTCTCTGTGCTGCAT-3’

slc12a3:

FWD: 5’-ATGGGAATCCAAGGCCCAAG-3’

REV: 3’-TAATACGACTCACTATAGACACAGGAGCCAATGGTAGC-3’

slc20a1a:

FWD: 5’-ACCATCTTTGAGACAGTGGGTG-3’

REV: 5’-TAATACGACTCACTATAGCAGCCCAGTGAGATTAGCAGGG-3’

Immunolabeling and other labeling procedures

Immunolabeling. Embryos were fixed in 4% paraformaldehyde (PFA) at 4°C overnight and washed in 1x PBS for 30 min. Fixed embryos were permeabilized with cooled acetone for 5 min at -20°C, followed by a 5 min wash in 1x PBS. Embryos were subsequently incubated in Inoue blocking solution (Inoue & Wittbrodt, 2011) (5 % Normal Goat Serum (NGS) (Abcam, cat# ab7481, lot# GR325285-5), 2% BSA (Fisher Scientific, cat# BP1600-100, lot# 196941), 1.25% Triton X-100 (Fisher Scientific, cat#

BP151-500, lot# 172611) in 1x PBS for 1 hour at room temperature (RT) on a rotating platform (80 RPM). Incubation in primary antibodies was performed in I-buffer solution (1% normal goat serum, 2% bovine serum albumin, 1.25 % Triton X-100, in 1x PBS) for 2 days at 4°C on a rotating platform (80 RPM). Embryos were then washed three times, 30 min each, with 1x PBS at room temperature. Secondary antibodies, diluted in I-buffer, were applied for 1 day at 4°C on a rotating platform (80 RPM). After secondary antibody incubation, embryos were washed three times with 1x PBS for 30 min.

Primary antibodies: anti-NDRG1 @ 1:500 (Sigma Aldrich, catalog # HPA006881, lot# A69409, rabbit polyclonal), anti-ATP1A1A @ 1:500 (DHSB, catalog # a5s, lot# 10/17/19, mouse monoclonal), anti-GFP @ 1:500 (Invitrogen, cat# A21311, lot# 2207528, rabbit polyclonal, Alexa Fluor 488 conjugated), anti-ZO-1 @ 1:500 (Invitrogen, cat#40-220D*, lot# UB280595, rabbit polyclonal). Secondary antibodies: Goat anti-rabbit Alexa Fluor 594 (Abcam, cat# ab150080, lot# GR3373513-1), Goat anti-mouse Alexa Fluor 488 @ 1:500 (Abcam, catalog # ab150113, Lot#GR3373409-1). Other labels added after secondary antibodies. Phalloidin-Alexa 594 (Invitrogen, cat#A12381, lot# 2256805), Phalloidin-Alexa 405 (Invitrogen, cat#A30104, lot# 2277734) and DAPI (Thermo Scientific, cat# 62248, lot# WD3246961) were used according to the manufacturer's instructions.

Whole-mount proximity ligation assay (PLA). To identify *in situ* protein-protein interactions, PLA was performed using the PLA Duolink kit (Sigma Aldrich, catalog# DUO92101). The protocol was performed according to the manufacturer's instructions with the following modifications: All steps were performed in 96-well plates, 40 mM final volume, at RT, rotating (80 RPM). Embryos were incubated in primary antibody

solution at RT overnight. Embryos were then treated with Duolink PLA probes at RT overnight, followed by incubation in the ligation solution at RT overnight and an additional 1 hour at 37°C. Between primary antibody, Duolink PLA probe, and ligation solution incubations, samples were washed with 1x Wash Buffer A at RT for 3 x 20 min. Embryos were incubated in the amplification solution at RT overnight, followed by 1 hour at 37°C. Lastly, samples were washed in 1x Wash Buffer B at RT for 3 x 20 min, then in 0.01x Wash Buffer B at RT for 20 min.

Sectioning and microscopy

Sectioning embryos. Transverse sections (40 μm) of fixed and labeled embryos were obtained using a vibratome (Vibratome, 1500). Embryos were mounted in agarose (4 %) blocks prior to sectioning. Sections through the anterior and posterior pronephric duct were distinguished based on tissue morphology, as the distance between the two tubules is larger in the anterior region.

Compound microscopy. Live, dechorionated embryos were immobilized using the sedative tricaine methanesulfonate at 0.001% w/v in embryo medium E3 (5mM NaCl, 0.33mM CaCl2, 0.17mM KCl, 0.33mM MgSO4). Sedated or fixed embryos were mounted on depression slides in E3 medium. Lateral views of 24-48 hpf embryos were viewed at 50X magnification using an Axioskop II compound microscope (Carl Zeiss, Axioscope II) and imaged with an AxioCam (Carl Zeiss, 504 CCD camera).

Confocal microscopy. For lateral views, 24-48 hpf embryos were mounted in E3 medium on glass-bottom culture dishes with size #1.5 coverslips (Mattek, cat# P50GC-1.5-14-F). Images were captured with a 5X air objective lens using an inverted SP5 laser scanning

confocal microscope (Leica Microsystems). For imaging transverse sections of embryos, a 63X oil objective lens was used. Images were analyzed and processed using FIJI ImageJ (National Institutes of Health) and PowerPoint (Microscope). When comparing protein levels between embryos in the same experimental repeat, all specimens were processed using identical settings, including gain.

Western blot Analysis

Embryos were dechorionated and mechanically lysed in precooled cOmplete Protease Inhibitor Cocktail (Millipore Sigma, catalog# 11836145001). The bicinchoninic acid (BCA) protein assay was used to determine the total protein concentration in embryo lysates. Western blot analysis was performed by loading 7.5 g of total protein per lane into 7.5% Tris-glycine SDS-PAGE gels (Bio-Rad, catalog #4561026) and transferring to methanol-activated PVDF membranes (Bio-rad, cat# 1620177. Specific protein detection was performed using diluted primary antibodies as follows: anti-NDRG1 @ 1:5000 (Sigma-Aldrich, catalog# HPA006881, rabbit polyclonal); anti-GAPDH @1:5000 (GeneTex, catalog #GTX124503; batch: RRID:AB_11165273, rabbit polyclonal). The secondary antibody used is Goat anti-rabbit @ 1:10,000 (Cell Signaling Technology, catalog #7074; RRID:AB_2099233). Molecular weights were determined using pre-stained protein ladders (Thermo Fisher Scientific, catalog #26616; GE Healthcare, catalog #RPN800E). Protein abundance was detected on membranes using the SuperSignal West Femto enhanced chemiluminescence kit (Thermo Fisher Scientific, catalog #34095) and Blu-C high-contrast autoradiography film (Stellar Scientific, catalog #BLC-57-100).

Drug treatments

Sodium Azide (NaN3) (catalog #S2002-5G) was used at 300 μM concentration in E3 embryo medium to increase endogenous lactate levels, as previously described (Oginuma et al., 2017). Since Sodium Azide arrests or delays development, age and stage-matched untreated controls were used.

Protease inhibitor MG-132 (EMD Millipore Corp, cat# 474791-5MG, lot# 3537249) and autophagy inhibitor Chloroquine (Sigma Aldrich, cat# C6628-50G, batch # 0000090940) were used at 100 μM and 1 mM, respectively in E3 embryo medium.

Hypoxia and anoxia treatments

For all hypoxia experiments, oxygen levels were controlled using a PLAS LABS' Controlled Environmental Chamber (model# 856-HYPO). A combination of pure nitrogen (N2) (Airgas) and room air was perfused into the chamber and resulting oxygen concentrations were measured using the PLAS LABS' built-in oxygen sensor. Additionally, a handheld portable oxygen meter (Yellow Springs Instruments (YSI) Item# 626972) was placed inside of the hypoxia chamber to directly monitor oxygen levels in E3 embryo medium. E3 medium was placed in the PLAS LABS chamber in a beaker and aerated using an air pump to accelerate equilibration of dissolved oxygen levels with the chamber's ambient oxygen level for 12 hours before experimentation.

Survival tests

Anoxia survival. Survival was assayed immediately following anoxia exposure. Embryos were examined for severe tissue necrosis and deterioration using bright field imaging.

Anoxia + re-oxygenation survival. Embryos that survived anoxia were transferred to normoxic water and examined after two days of re-oxygenation for signs of viability, including heartbeat and response to touch. The surviving embryos were further categorized into either mild or severe edema cases. All survival experiments were performed at least three times with > 25 embryos per experiment.

Kidney clearance assay

Kidney function was examined in WT and *ndrg1a*$^{-/-}$ mutants using the kidney clearance assay (KCA) (Christou-Savina, Beales, & Osborn, 2015).

KCA using embryos raised under normoxic conditions. WT embryos and *ndrg1a*$^{-/-}$ mutants were injected at 48 hpf in the pericardial cavity with rhodamine dextran (10,000 MW; Invitrogen, cat# D1824, lot# 2270252; working concentration of 5 mg/ml in distilled water). Fluorescence in the heart chamber of injected embryos was imaged and quantified 3 and 24 hours post-injection (hpi) using an Axioskop II compound microscope (Carl Zeiss) and AxioCam 504 CCD camera (Carl Zeiss). Embryos were imaged at 50 X total magnification using identical exposure settings. Images were taken in an area of interest centered on the heart and analyzed and processed using ImageJ (National Institutes of Health).

KCA using embryos exposed to anoxia followed by re-oxygenation. Same procedure as described above but with the following modifications: 24 hpf WT embryos and *ndrg1a*$^{-/-}$ mutants were exposed to 12 h of anoxia, followed by injection of rhodamine dextran (under normal oxygen) and two days of re-oxygenation.

ATP assay

24 hpf WT embryos and *ndrg1a*$^{-/-}$ mutants were exposed to 0, 6, 12, 18 and 24 h of anoxia and snap-frozen in liquid nitrogen immediately post-anoxia treatment and removal of E3 medium. Metabolites were extracted and ATP concentration (nmol/embryo) measured using a luminescent ATP Detection Assay kit (Abcam, catalog # ab113849), according to the manufacturer's instructions.

Lactate assay

Lactate levels were measured in 24 hpf WT and *ndrg1a*$^{-/-}$ mutant embryos exposed to either anoxia or Sodium Azide. For each treatment group, 20 embryos were snap-frozen in liquid nitrogen after embryo medium removal and kept at - 80°C until further processing. The L-lactate fluorometric kit (BioVision, catalog #K607) was used according to the manufacturer's instructions for small biological samples. No-sample background control fluorescence was subtracted from the experimental samples' fluorescence to account for background fluorescence.

Metabolomic analysis

A metabolomic analysis was performed on 5 hpf WT embryos exposed to 1 hour of anoxia and age-matched normoxic controls (5 hpf). 400 µl of methanol and 400 µl of water were added as a polar solvent to decant the embryos over ice. After decanting, 400 µl of isopropanol was added as a nonpolar solvent. Samples were rocked at 4º C for 20 min and centrifuged at 13,000 g for 5 min. The water-soluble metabolites (top of phase separation) was extracted and stored at - 80ºC. Four biological replicates were obtained

and 10 embryos were used per sample. Mass spectra were acquired using a Phenomenox Luna NH2 column connected to an Agilent 1200 HPLC and Agilent 6210 ESI-TOF mass spectrometer in a negative ion mode. Data were analyzed with Agilent software packages (MassHunter, Mass Profiler, Profinder and Mass Profiler Professional) using 1,000 ion counts as an arbitrary cutoff. An extracted ion chromatograph (EIC) was then generated for each ion. Ions that did not show clear peaks were discarded from the subsequent analysis. Ions were identified by comparing molar mass against Mzed database (Draper et al., 2009). The lactate peak (observed: 89.0240, calculated mass for M-H ions is 89.0239) was extracted, and the area was used for comparison.

Alignment of NDRG Family Members

The protein sequences of several vertebrate NDRG family members (human: NDRG3, NP_114402.1; mouse: NDRG3, NP_038893.1, zebrafish: Ndrg1a, NP_998513.2, zebrafish: Ndrg1b: NP_956986.2, zebrafish Ndrg3a: NP_955811.1, zebrafish Ndrg3b: XP_005162043.1) were aligned using the Clustal Omega Multiple Sequence Alignment software (https://www.ebi.ac.uk/Tools/msa/clustalo/) to identify homologous regions of interest.

Measurements

Fluorescence intensity measurements of the pronephric duct. Fluorescence intensity corresponding to ATP1A1A protein levels in the anterior and posterior pronephric duct was measured using lateral views of immunolabeled embryos. Two regions of interest (ROI) centered along the anterior or posterior halves of the pronephric duct were delineated for intensity measurements using ImageJ (FIJI) software.

Fluorescence intensity measurements of ionocytes. Fluorescence intensity corresponding to ATP1A1A protein levels in ionocytes was measured by drawing a tight ROI around individual ionocytes (5-10) in the yolk ball and flank region demarcated by the distal ends of the yolk extension using ImageJ (FIJI).

***Ionocyte length*:** Ionocyte length (micron) was measured by drawing a line along the longest axis of the cell.

Experimental design and statistical analysis

Graphing and statistical analysis were performed using Prism 9 (Graph Pad). Statistical significance was declared in circumstances where $p < \text{or} = 0.05$. Experiments comparing three or more groups were analyzed using a two-way ANOVA test. An unpaired t-test was used when comparing means of two independent groups. Data were reported as the mean +/- SEM unless otherwise indicated.

RESULTS

ndrg1a is not required for kidney and ionocyte differentiation or function

We have previously shown that *ndrg1a* is a hypoxia-responsive gene whose transcript levels increase proportionately with the severity and duration of hypoxia (Le et al., under review), suggesting that *ndrg1a* is implicated in hypoxia adaptation. However, others have shown that NDRG1 plays a key role in kidney cell differentiation in *Xenopus* (Kyuno, Fukui, Michiue, & Asashima, 2003; Zhang, Guo, & Chen, 2013), which, if

conserved, would preclude directly testing the function of this NDRG family member in cell physiology. We therefore began by investigating whether differentiation of PD cells and ionocytes is impaired in Ndrg1a-deficient zebrafish embryos.

Ndrg1a was targeted using a translation-blocking morpholino (MO) and CRISPR/Cas 9 mutagenesis to produce a null allele, *ndrg1a*^{mbc1} (Supplemental Fig. 1). *ndrg1a*^{mbc1} mutants (henceforth referred to as *ndrg1a*$^{-/-}$) are homozygous viable and morphologically normal (Supplemental Fig. 1E, F). Please see Appendix Section II for more details on CRISPR *ndrg1a*$^{-/-}$ mutant generation.

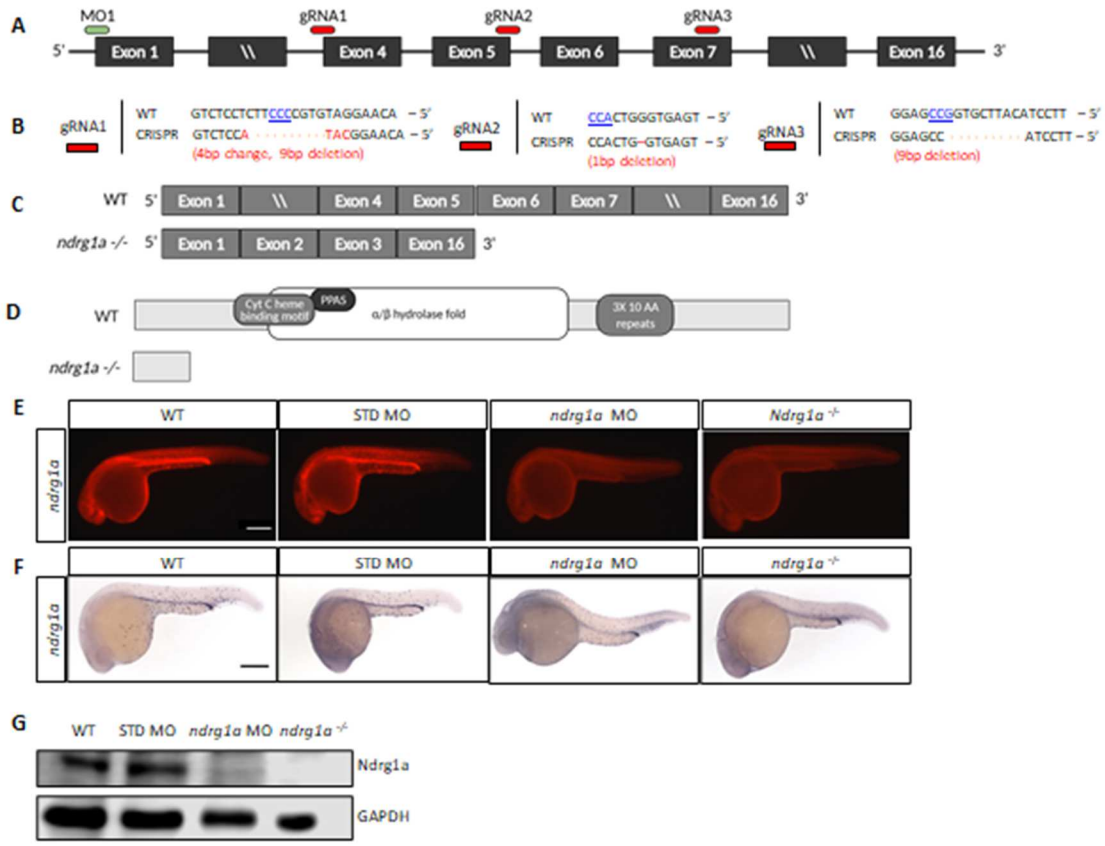

Supplemental Figure 1. Generation of *ndrg1a* loss of function tools.

(A) Schematic of the *ndrg1a* locus showing 5' and 3' untranslated regions, exons (black boxes), and the target sites for the *ndrg1a* translation-blocking morpholino (MO1, green bar) and the three CRISPR-Cas9 guide RNAs (gRNA 1-3, red bars). (B) Genomic DNA sequences of WT embryos and *ndrg1a*^{mbc1} homozygous mutants at the CRISPR-Cas9 gRNA target sites. PAM sequences are in blue, underlined font and insertion/deletion mutations are shown in red. (C) Illustration of exons included in the WT and *ndrg1a*^{mbc1} mutant alleles. (D) Structure of the WT and *ndrg1a* mutant proteins showing domains present and missing in the mutant. Domains present in WT include: α/β hydrolase fold, cytochrome c heme binding motif, NDR, phosphopantetheine attachment site (PPAS) and 3 X 10 AA repeats. (E) Lateral views of 24 hpf WT, standard (STD, control) morpholino (MO)-injected, *ndrg1a* MO-injected and *ndrg1a*^{mbc1} homozygous mutants, immunolabeled with anti-NDRG1. Scale bar 300 mM. n= 3 embryos imaged per treatment group. (F) Lateral views of 24 hpf WT, STD MO-injected, *ndrg1a* MO-injected and *ndrg1a*^{mbc1} homozygous mutants labeled by whole-mount *in situ* hybridization using an *ndrg1a* riboprobe. Scale bar 300 mM. n= 3 embryos imaged per treatment group (G) Western blot analysis of Ndrg1a protein levels in 24 hpf WT, STD MO-injected, *ndrg1a* MO-injected and *ndrg1a*^{mbc1} homozygous mutants. GAPDH was used as a loading control. n= 2 repeats.

Whole-mount *in situ* hybridization (WISH) using several markers (*slc20a1a*: anterior PD, *slc12a3*: posterior PD, *atp1a1a,* the catalytic subunit of NKA: entire length of the PD and all ionocytes and *kcnj1a.1*: middle part of the PD and ionocytes), revealed that the distribution of these transcripts is normal in *ndrg1a* loss-of-function (LOF) embryos at 24 hpf, when PDs are fully formed (Kimmel, Ballard, Kimmel, Ullmann, & Schilling, 1995) (Fig. 1A). Furthermore, the expression of *slc20a1a* and *atp1a1a* is properly maintained in 48 hpf *ndrg1a* LOF embryos (Supplemental Fig. 2A), when the kidney becomes fully functional (Drummond et al., 1998). Immunofluorescence using anti-ATP1A1A and anti-GFP in the transgenic line Tg[*enpep:GFP*] (entire length of the PD) further confirmed proper protein expression in the PD (Fig. 1B).

Kidney physiology is tightly linked to cell polarity, which enables the directional flow of ions. Analysis of the subcellular distribution of polarity markers F-actin and Zonula-Occludens-1 (ZO-1) showed that *ndrg1a* is not required for apico-basal polarization of PD cells (Supplemental Fig. 2B).

We next tested the function of the embryonic kidney using a kidney clearance assay (KCA) (Christou-Savina et al., 2015). Rhodamine dextran was injected into the pericardial cavity of 48 hpf embryos and the ability of the kidney to clear the rhodamine dextran was tested by measuring fluorescence intensity after 3 and 24 hours post-injection. This analysis revealed that kidney filtration is normal in *ndrg1a*$^{-/-}$ mutants (Supplemental Fig. 2C, D).

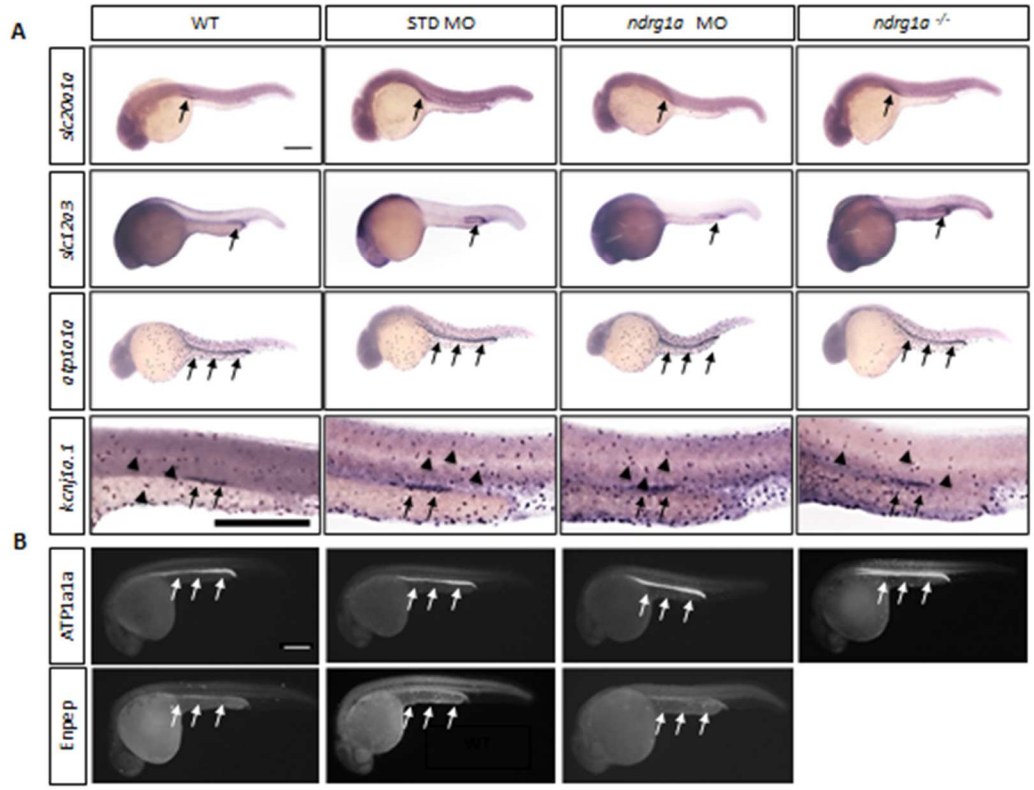

Figure 1. Ndrg1a is not required for the differentiation of the pronephric duct and ionocytes.

(A, B) Lateral views of 24 hpf WT, standard MO-injected, *ndrg1a* MO-injected and *ndrg1a*$^{-/-}$ mutant embryos labeled using (A) wholemount *in situ* hybridization to detect the mRNA distribution of *slc20a1a, slc12a3, atp1a1a and kcnj1a.1* and (B) immunolabeling with anti-ATP1A1A or anti-GFP (Tg[*enpep:GFP* transgenic line). n = 3 embryos imaged for each probe. Scale bar 300 μm for *slc20a1a*, *kcnj1a.1*, and ATP1a1a. Annotations: arrows point to signal in the pronephric duct; arrowheads: ionocytes.

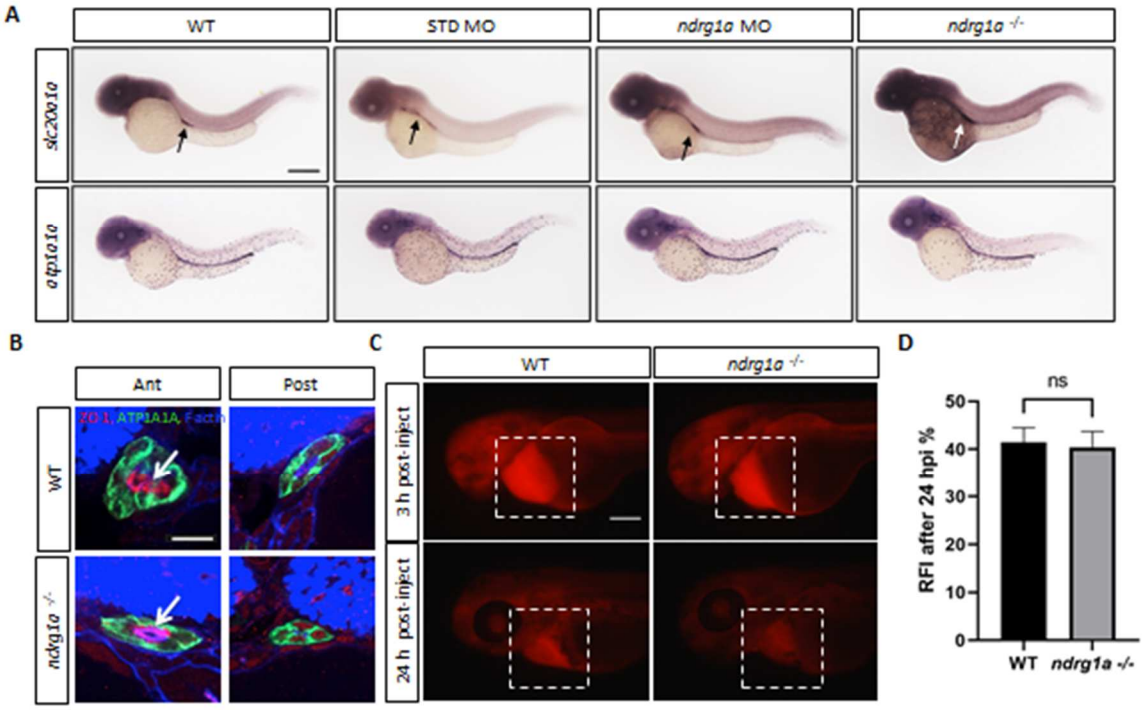

Supplemental Figure 2. The morphology, differentiation and function of the pronephric duct are normal in Ndrg1a loss-of-function embryos.

(A) Lateral views of 48 hpf WT, STD MO-injected, *ndrg1a* MO-injected and *ndrg1a*$^{-/-}$ mutant embryos labeled by whole-mount *in situ* hybridization using *slc20a1a* and *atp1a1a* riboprobes. Scale bar 300 mM. Annotations: arrows point to signal in the pronephric duct. n= 3 embryos imaged per treatment group. (B) Transverse views of the anterior and posterior pronephric duct of WT embryos and *ndrg1a*$^{-/-}$ mutants, labeled with anti-ATP1A1A (green), anti-ZO-1 (apical pole, red), and phalloidin (F-actin, blue). Scale bar 10 mM. Annotations: arrows point to the apical surface. n = 3 embryos imaged per treatment group. (C) Kidney clearance assay using 48 hpf WT embryos and *ndrg1a*$^{-/-}$ mutants raised under normoxic conditions. Embryos were injected at 48 hpf in the pericardial sac with rhodamine dextran. Lateral views of injected embryos were taken 3 and 24 hours post-injection (hpi). White boxes indicate where fluorescence measurements were taken. Scale bar 200 μm. (D) Quantification of kidney clearance assay. No significant difference between WT and mutants was observed 24 hpi (unpaired t test; p value = 0.8192, ns). n = 10 embryos analyzed per group.

These findings indicate that *ndrg1a* is neither required for the differentiation of the PD and ionocytes nor for the function of the PD under normoxic conditions, enabling us to directly test the function of *ndrg1a* in physiological adaptation to hypoxia.

Ndrg1a promotes organismal and cell survival under prolonged hypoxia

To test whether *ndrg1a* promotes hypoxia survival, we exposed 24 hpf embryos to increasing durations of anoxia (6, 12, 18 and 24 h) and scored viability immediately post-treatment. This analysis showed that WT embryos survived prolonged anoxia exposure somewhat better than *ndrg1a* $^{-/-}$ mutants (18 h: WT 78.5% vs. *ndrg1a* $^{-/-}$ 52.6%; 24 h: WT 47.8% vs. *ndrg1a* $^{-/-}$ 23.2%) (Fig. 2A). However, when surviving embryos were returned to normal oxygen for 2 days, we noticed a dramatic reduction in viability of *ndrg1a* $^{-/-}$ mutants relative to WT embryos (18h: WT 79.0% vs. *ndrg1a* $^{-/-}$ 35.5%; 24h: WT 58.8% vs. *ndrg1a* $^{-/-}$ 7.1%) (Fig. 2B). Furthermore, a large percentage of the *ndrg1a* $^{-/-}$ mutants that survived immediately post-anoxia developed mild or severe edema (Fig. 2C) (6h: WT 97.3% no edema, 2.7% mild edema, 0% severe edema vs. *ndrg1a* $^{-/-}$ 69.5% no edema, 30.5% mild edema, 0% severe edema; 12h: WT 94.5% no edema, 5.5% mild edema, 0% severe edema vs. *ndrg1a* $^{-/-}$ 65.2% no edema, 28.2% mild edema, 6.6% severe edema; 18h: WT 93.1% no edema, 6.9% mild edema, 0% severe edema vs. *ndrg1a* $^{-/-}$ 50% no edema, 8.8% mild edema, 41.2% severe edema). Edema results from water retention and has multiple proximal causes, including malfunction of the PD (Elmonem et al., 2018) and ionocytes (Hwang & Chou, 2013). We therefore tested whether renal damage occurred post-anoxia using the kidney clearance assay. 24 hpf embryos were subjected to 12 h of anoxia and 2 days of re-oxygenation, following which rhodamine dextran was injected into their pericardial cavity and fluorescence measurements were

made 3 and 24 hours post-injection. This analysis revealed that *ndrg1a* $^{-/-}$ mutants retained more rhodamine dextran than WT embryos post-anoxia (WT: 44.3% fluorescence vs. *ndrg1a* $^{-/-}$ mutants: 60.3% fluorescence) (Fig. 2D, E), indicative of reduced kidney filtration capability.

Together, these data suggest that *ndrg1a* protects the kidney (and possibly ionocytes) from hypoxia-induced cellular damage, which reduces edema formation and enhances survival.

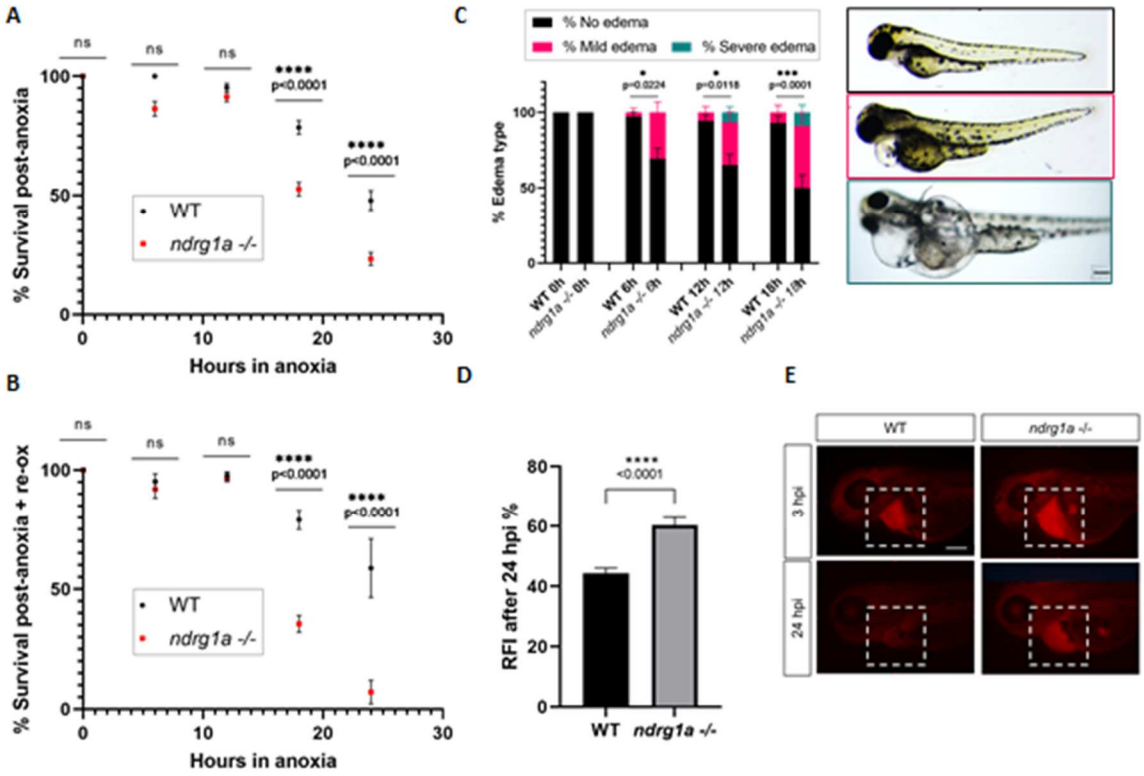

Figure 2. *ndrg1a* confers protection from hypoxic injury

(A) % Survival of WT embryos and *ndrg1a*$^{-/-}$ mutants immediately following 6, 12, 18 and 24 h of anoxia exposure. Embryos were 24 hpf at the time of exposure. A significant difference between WT and mutants was observed for 12 and 18 h of anoxia (Two-way ANOVA analysis was performed; 0 h WT vs. *ndrg1a*$^{-/-}$: p value > 0.9999, ns; 6 h WT vs. *ndrg1a*$^{-/-}$: p value = 0.1275, ns; 12 h WT vs. *ndrg1a*$^{-/-}$: p value = 0.9940, ns; 18 h WT vs. *ndrg1a*$^{-/-}$: p value < 0.0001, ****; 24 h WT vs. *ndrg1a*$^{-/-}$: p value < 0.0001, ****). n = average of 30 embryos per experimental group; n > 5 experiments. (B) % Survival of WT embryos and *ndrg1a*$^{-/-}$ mutants following 6, 12, 18 and 24 h of anoxia exposure and 2 days of re-oxygenation (re-ox). Embryos were 24 hpf at the time of initial anoxia exposure. A significant difference between WT and mutants was observed for 18 and 24 h of anoxia + 2 days re-ox (Two-way ANOVA analysis was performed; 0 h + re-ox WT vs. *ndrg1a*$^{-/-}$: p value > 0.9999, ns; 6 h + re-ox WT vs. *ndrg1a*$^{-/-}$: p value > 0.9999, ns; 12h + re-ox WT vs. *ndrg1a*$^{-/-}$: p value >0.9999, ns; 18 h + re-ox WT vs. *ndrg1a*$^{-/-}$: p value < 0.0001, ****; 24 h + re-ox WT vs. *ndrg1a*$^{-/-}$: p value < 0.0001, ****). n = average of 9-26 embryos per experimental group; n = 2-5 experiments. (C, left) % Edema observed in WT embryos and *ndrg1a*$^{-/-}$ mutants following 0, 6, 12, 18 and 24 h of anoxia exposure and 2 days re-ox. Edema phenotypes were divided into 3 categories: no edema, mild edema and severe edema. A significant difference between WT and mutants was

observed for 6, 12, and 18 h of anoxia + 2 days re-ox for the presence of either mild or severe edema (Two-way ANOVA analysis was performed; 0h + re-ox WT vs. *ndrg1a*$^{-/-}$: p value > 0.9999, ns; 6 h + re-ox WT vs. *ndrg1a*$^{-/-}$: p value = 0.0224, *; 12 h + re-ox WT vs. *ndrg1a*$^{-/-}$: p value = 0.0118, *; 18 h + re-ox WT vs. *ndrg1a*$^{-/-}$: p value = 0.0001, ***). (C, right) Representative images of embryos in each phenotypic category. n = average of 9-26 embryos per experimental group; n = 2-3 experiments. Scale bar 200 μm. (D) Quantification of kidney clearance assay using 48 hpf WT embryos and *ndrg1a*$^{-/-}$mutants exposed to 12 h of anoxia, followed by 2 days re-ox and injection with rhodamine dextran. A significant difference between WT and mutants was observed 24 hpi (unpaired t test; p value < 0.0001, ****. n = average of 9 embryos per experimental group; each experiment was repeated 2 times. (E) Lateral views of injected embryos were taken 3 and 24 h post-injection (hpi). White boxes indicate where fluorescence measurements were taken. Scale bar 200 μm.

NKA is downregulated following prolonged anoxia

The expression of *ndrg1a* in the PD and ionocytes and the edema observed in mutants exposed to severe and prolonged hypoxia suggest that Ndrg1a plays a regulatory role, perhaps by controlling ion homeostasis. Of the multiple ion channels and pumps expressed in these cells (e.g. Fig. 1), the catalytic subunit of the NKA pump, ATP1A1A, was selected for further analysis. This enzyme is estimated to consume 30% of the cell's energy in maintaining Na^+ and K^+ gradients (Pirahanchi, Jessu, & Aeddula, 2021). Given this high-energy demand, an evolutionarily conserved response of cells exposed to low oxygen is to downregulate NKA activity or to degrade the pump itself (Bogdanova et al., 2016; Buck & Hochachka, 1993; Gusarova et al., 2011).

To address whether Ndrg1a and ATP1A1A interact in the zebrafish embryo, we began by examining their distribution. There are five genes encoding the alpha 1 subunit in the zebrafish genome (*atp1a1a.1-atp1a1a.5*), each with a distinct expression profile (Blasiole et al., 2002; Canfield et al., 2002). The distribution of *atp1a1a.2* is very similar to that of *ndrg1a*, both of which are expressed in the PD and ionocytes (Fig. 3a1,a2). Double immunolabeling using anti-NDRG1 and anti-ATP1A1A (against the chick alpha 1 subunit) confirmed that Ndrg1a and ATP1A1A are co-expressed in the kidney and ionocytes (Fig. 3a3), although a small percentage of ionocytes are positive for only Ndrg1a or ATP1A1A (magnified image Fig 3a3, colored boxes in Fig. 4a1).

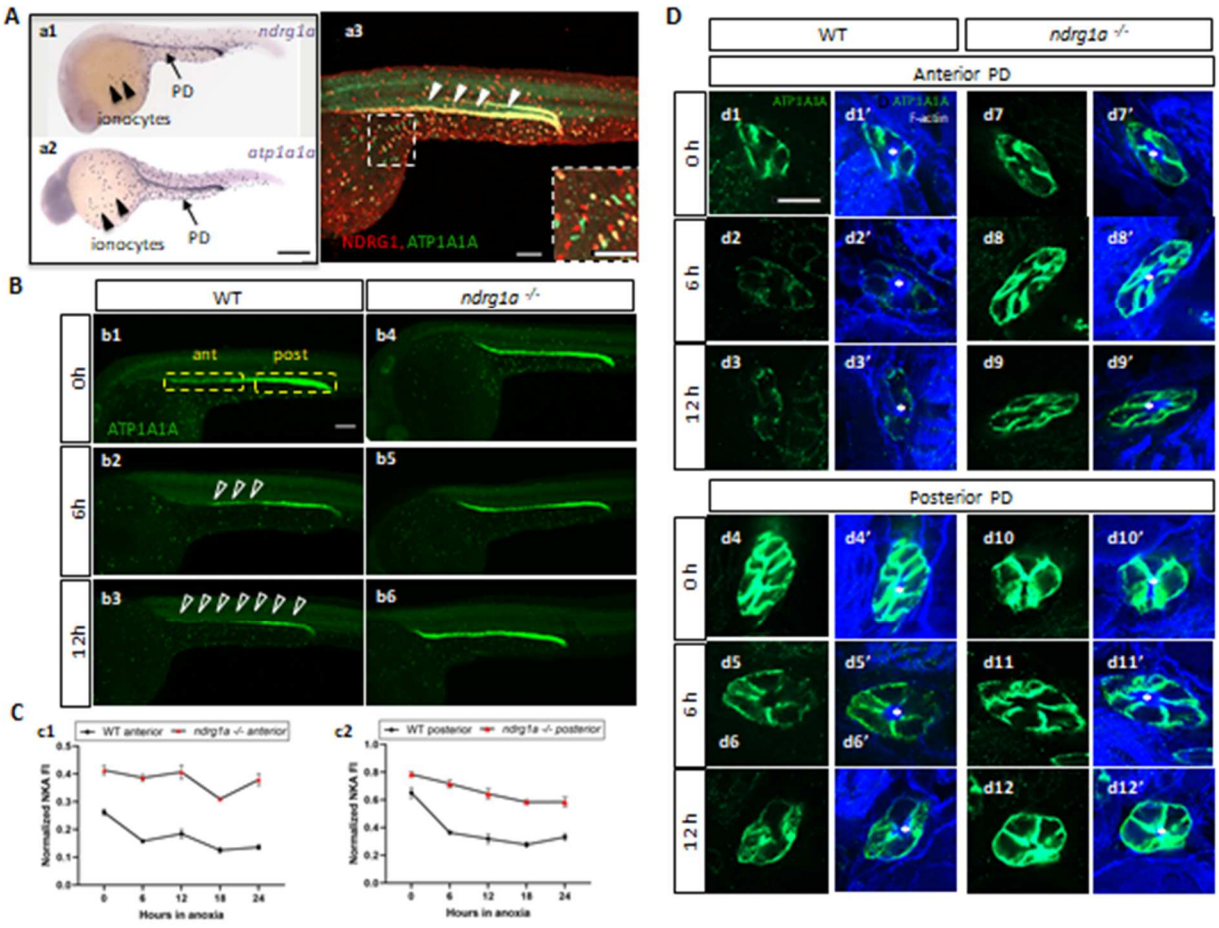

Figure 3. NKA downregulatation in the pronephric duct in response to anoxia is *ndrg1a*-dependent

(A) Lateral views of 24 hpf WT embryos revealing (a.1,2) *ndrg1a* and *atp1a1a* transcript distribution using whole-mount *in situ* hybridization. (a.3) Ndrg1a and ATP1A1A protein distribution using double immunolabeling. Scale bars: a1, a2: 300 mM, a3: 100 mM for both wholemount and inset. (B) Lateral views of WT embryos and *ndrg1a*$^{-/-}$ mutants exposed at 24 hpf to increasing duration of anoxia: (b1, b4) 0 h; (b2, b5) 6 h; (b3, b6) 12 h and immunolabeled to reveal ATP1A1A. n = average of 5 embryos per experimental group; n=2 experiments. Scale bar 100 µm. Abbreviations: ant = anterior, post = posterior. Annotations: yellow boxes show where anterior and posterior pronephric duct measurements were taken. Arrowheads indicate decreased signal. (C) Normalized fluorescence intensity in the (c1) anterior and (c2) posterior pronephric duct of WT embryos and *ndrg1a*$^{-/-}$ mutants. Embryos were exposed at 24 hpf to increasing duration of anoxia (0, 6, 12, 18 and 24 h) and immunolabeled to reveal ATP1A1A levels. n = average of 5 pronephric duct per experimental group; n=2 experiments. (D) Cross sections views of the anterior (d1-d3', d7-d9') and posterior (d4-d6', d10-d12') pronephric ducts in WT embryos (d1-d3', d4-d6') and *ndrg1a*$^{-/-}$ mutants (d7-d9', d10-d12'), labeled with anti-ATP1A1A and phalloidin (F-actin). Scale bar 20 mM. Annotations: asterisks indicate the

lumen (apical surface of PD cells). n = average of 6 pronephric ducts imaged per treatment group or 3 embryos; each experiment was repeated 2 times.

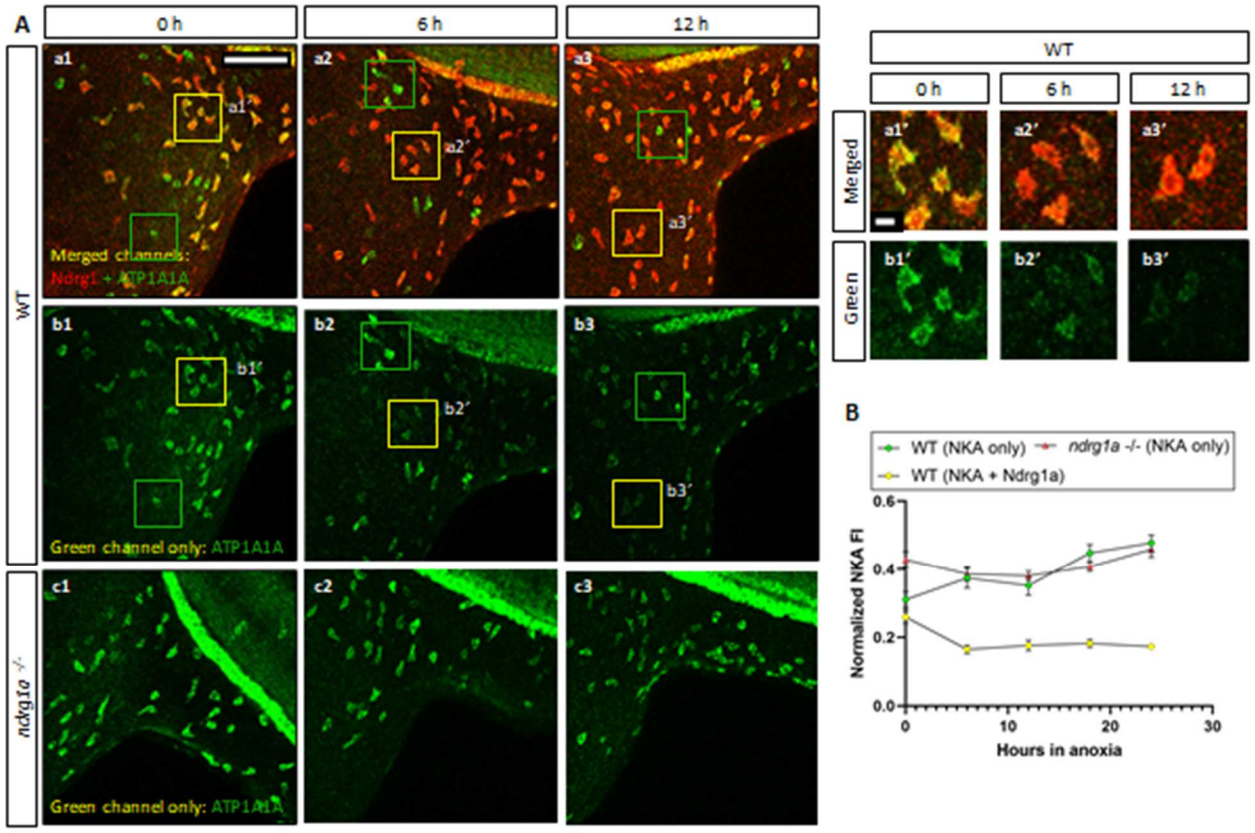

Figure 4. **NKA is co-expressed with Ndrg1a in a subset of ionocytes and downregulated under anoxia in an *ndrg1a*-dependent manner**

(A, left) Lateral views of WT embryos (a1-b3) and *ndrg1a*$^{-/-}$ mutants (c1-c3) exposed to anoxia for 0 h (a1-c1), 6 h (a2-c2), 12 h (a3-c3) and immunolabeled with anti-ATP1A1A (green) and anti-Ndrg1a (red); (a1-a3) show merged channels, while (b1-c3) show the green (ATP1A1A) channel only. Annotations: yellow and green boxes identify ionocytes that are positive for Ndrg1a and ATP1A1A (yellow) or ATP1A1A-only (green). Scale bar: a1: 100µm; a1': 2µm. (A, right) Higher magnification images of yellow boxed in areas in a1-b3, showing merged channels (a1-a3') and green channel only (b1-b3'). (B) Normalized fluorescence intensity of ATP1A1A in ionocytes of WT embryos and *ndrg1a*$^{-/-}$ mutants exposed to anoxia for 0, 6, 12, 18, and 24h.

We next tested whether NKA is hypoxia-responsive in zebrafish by examining ATP1A1A levels in embryos that were exposed to different durations of anoxia. Under normoxic conditions (0 h time point), ATP1A1A was distributed along the entire length of the PD but its levels were noticeably higher in the posterior PD (Fig. 3b1). Following 6 h of anoxia, the intensity of the signal was reduced throughout the PD, but most noticeably in the anterior region (open arrowheads in Fig. 3b2; quantified in Fig. 3C). By 12 h of anoxia, ATP1A1A levels were further decreased along the full anterior-posterior extent of the PD (open arrowheads in Fig. 3b3; quantified in Fig. 3C). Additional timepoints of anoxia (18 and 24 h) resulted in further NKA downregulation (WT anterior PD: 48% reduction of NKA level between 0h and 24h anoxia; WT posterior PD: 49% reduction of NKA level between 0h and 24h anoxia) (Fig. 3C), but not complete depletion, consistent with prior observations in human and rat lung cells (Wodopia et al., 2000). Transverse sections of WT embryos subjected to anoxia and double labeled with anti-ATP1A1A and the cell surface marker phalloidin (cortical F-actin) revealed that NKA levels were gradually reduced in the baso-lateral plasma membrane compartment of anterior (Fig. 3d1-d3', top panels) and posterior (Fig. 3d4-d6', bottom panels) PD cells.

ATP1A1A was also downregulated under anoxia in ionocytes that co-expressed Ndrg1a (33% reduction of NKA level between 0h and 24h anoxia), (yellow boxes in Fig. 4a1-b3, a1'-b3', quantified in Fig. 4B). In contrast, ionocytes that were Ndrg1a-negative retained high levels of ATP1A1A following 6 and 12 h of anoxia (green boxes in Fig 4a1-b3, quantified in Fig. 4B). These observations reveal a negative correlation between the presence of Ndrg1a and ATP1A1A levels.

We also observed that the downregulation of ATP1A1A is reversible. Indeed, following 18 h of anoxia, ATP1A1A levels in both the PD and ionocytes increased steadily when embryos were re-introduced to normoxia, plateauing at 6 h post-re-oxygenation (anterior PD) (Supplemental Fig. 3).

Overall, these data indicate that downregulation of NKA is a gradual, long-term response to anoxia that is reversible when oxygen levels return to normal.

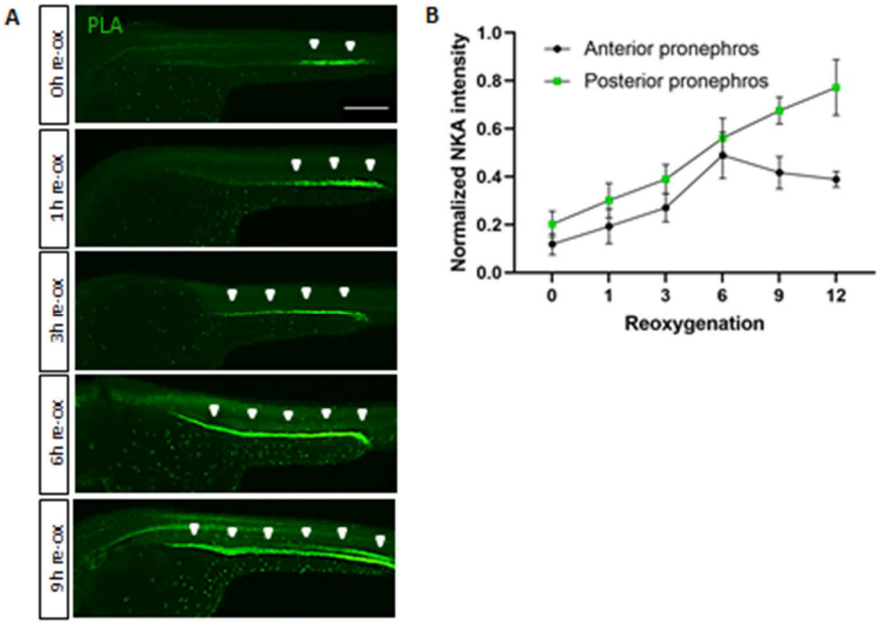

Supplemental Figure 3. NKA downregulation is reversible upon reoxygenation.

(A) Lateral views of WT embryos exposed at 24 hpf to 18 h of anoxia followed by 1, 3, 6 and 9 h of re-oxygenation and immunolabeled with anti-ATP1A1A. Scale bar 200 μm. n= average of 3 embryos per experimental group; n=3 experiments. (B) Quantification of ATP1A1A levels during reoxygenation. n= average of 3 embryos per experimental group; n=3 experiments. Annotations: arrowheads point to PLA signal in the pronephric duct.

Degradation of NKA is Ndrg1a-dependent

The spatial overlap between Ndrg1a and ATP1A1A and the negative correlation between the levels of these proteins in ionocytes, suggested that Ndrg1a may control NKA abundance under hypoxia. To test this, *ndrg1a* $^{-/-}$ mutants were exposed to different durations of anoxia and ATP1A1A levels were quantified. Unexpectedly, analysis of normoxic controls (0 h anoxia time point) revealed that the PD (Fig. 3b1 vs. b4, C) and ionocytes (Fig. 4b1 vs. a1', B) of mutants expressed higher levels of ATP1A1A than cells in WT embryos (58% and 20% increase in anterior and posterior PD of mutants vs. WT), suggesting that Ndrg1a regulates ATP1A1A levels, even under normal oxygen. However, despite these elevated normoxic levels, the relative amount of ATP1A1A in the PD of mutants was only marginally reduced following prolonged anoxia compared to WT embryos in which ATP1A1A levels decreased proportionately to time in anoxia (24 h anoxia, anterior PD: 8.3% reduction for *ndrg1a* $^{-/-}$ vs. 48% reduction for WT; 24 h anoxia, posterior PD: 25% reduction for *ndrg1a* $^{-/-}$ vs. 49% reduction for WT) (Fig. 3b2,b3 vs. b5, b6, C) and even slightly increased in ionocytes (7% increase) (Fig. 4B).

Furthermore, analysis of cross sections double-labeled with phalloidin showed that ATP1A1A mostly remained localized in the baso-lateral membrane of PD cells (Fig. 3D) in *ndrg1a* $^{-/-}$ mutants, suggesting that the pump is not endocytosed.

These data suggest that Ndrg1a negatively regulates NKA abundance in the plasma membrane under normal oxygen and that this activity is somehow enhanced or accelerated in response to prolonged anoxia.

Ndrg1a and NKA interact under severe hypoxia

A previous study identified ATP1A1A as a potential binding partner of NDRG1 in human prostate cancer cells (Tu, Yan, Hood, & Lin, 2007), raising the question of whether Ndrg1a physically interacts with ATP1A1A to bring about its downregulation. ATP1A1A is a transmembrane protein, in contrast to NDRG1 whose peptide sequence does not include an obvious membrane localization signal (Shi, Larkin, Chen, & Sadovsky, 2013). Furthermore, NDRG1 intracellular distribution appears to vary between cell types and in response to environmental signals, including hypoxia (Caruso et al., 2004; Kim et al., 2004; Kurdistani et al., 1998; Lachat et al., 2002; Shi et al., 2013; Sibold et al., 2007; Song et al., 2010). Given that ATP1A1A downregulation is triggered downstream of hypoxia, in an Ndrg1a-dependent manner, we reasoned that these proteins may co-localize near the cell cortex. This was confirmed in embryos that were double-labeled with anti-NDRG1 and anti-ATP1A1A. Under normoxic conditions, we observed that Ndrg1a was distributed throughout the cytosol and overlapped extensively with ATP1A1A at the cell cortex of ionocytes (Fig 4a1 (inset)) and PD cells (Fig. 5a1, a4). The overlap was reduced following 6 and 12 h of anoxia in both the ionocytes (insets in Fig. 4a2, a3) and the anterior PD, coinciding with significant downregulation of ATP1A1A (Fig. 5a2, a3). In contrast to the anterior PD, the posterior kidney showed extensive overlap of Ndrg1a and ATP1A1A at the cell cortex, even after 12 h of anoxia (Fig 5a5, a6), which is consistent with retention of NKA in the distal kidney tubule (Fig. 3b3, d6) and indicative of distinct physiological properties of these cells.

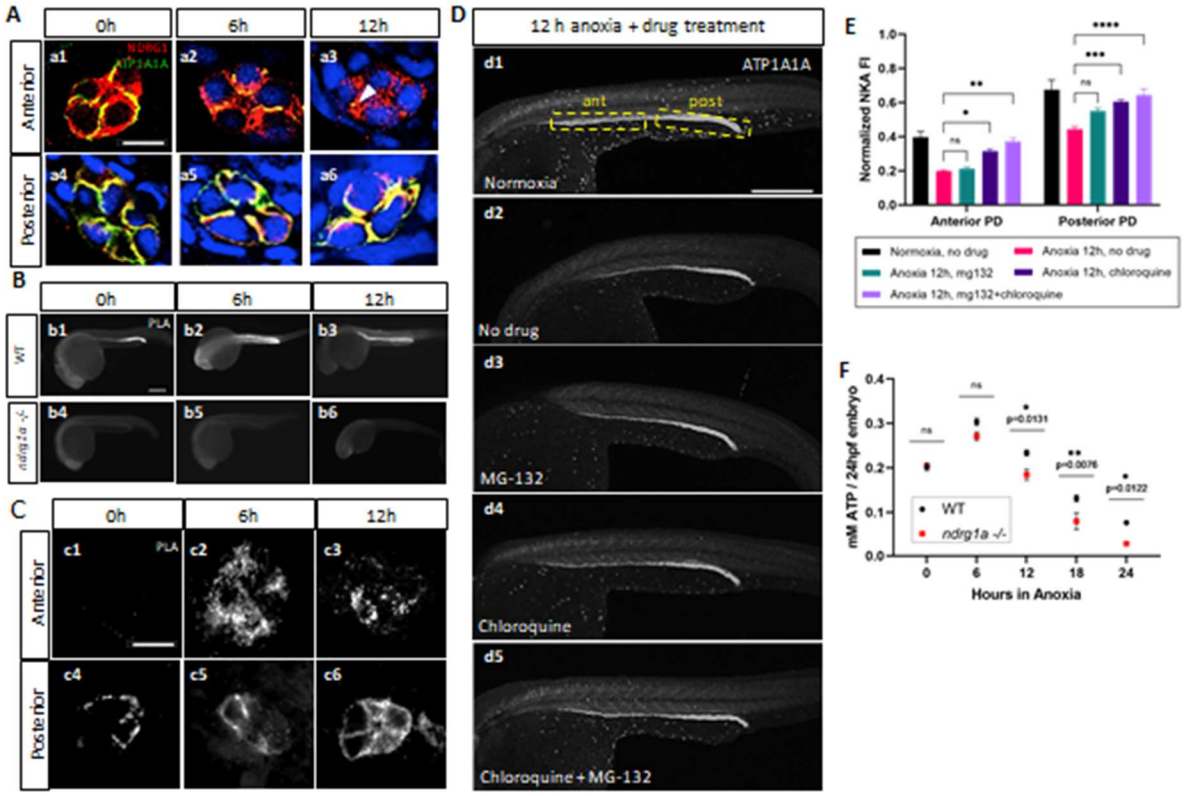

Figure 5. NKA interacts with Ndrg1a under anoxia and is degraded via lysosomal and proteasomal pathways to preserve ATP.

(A) Cross sections of WT embryos exposed to anoxia for 0 h (a1, a4), 6 h (a2, a5) and 12 h (a3, a6) and immunolabeled with anti-ATP1A1A (green) and anti-Ndrg1a (red). (a1-a3) Anterior pronephric duct. (a4-a6) Posterior pronephric duct. Scale bar = 10 µm. n = average of 3 embryos per experimental group; each experiment was repeated 2 times. (B) Lateral views of WT (b1-b3) and *ndrg1a*$^{-/-}$ (b4-b6) embryos labeled using whole-mount proximity ligation assay (PLA) to reveal Ndrg1a and ATP1A1A interaction. Embryos were exposed to 0 h (b1, b4), 6 h (b2, b5), and 12 h (b3, b6) of anoxia. Scale bar = 300 µm. n = average of 3 embryos per experimental group; each experiment was repeated 3 times. (C) Cross sections through the anterior (c1-c3) and posterior (c4-c6) pronephric duct of WT embryos treated as in (b1-b4). Scale bar = 10 µm. (D) Lateral views of WT embryos exposed to 0 h (d1) or 12 h of anoxia (d2-d5) in presence or absence of MG-132 (100uM, proteasome inhibitor), or Chloroquine (10 mM, autophagy inhibitor), or both and immunolabeled using anti-ATP1A1A. n = average of 4 embryos per experimental group; each experiment was repeated 2 times. Scale bar 200 µm. Annotation: yellow boxes show where anterior and posterior pronephric duct measurements were taken. (E) Quantification of ATP1A1A fluorescence intensity in the pronephric duct of embryos subjected to the same anoxia and drug treatments as shown in. Anterior PD: 7% increase in anoxia 12 h, mg132 vs anoxia 12 h, no drug p > 0.9999 ns; 59% increase in anoxia 12 h, chloroquine vs anoxia 12 h, no drug p = 0.0298 *; 87% increase in anoxia 12 h

mg132+chloroquine vs anoxia 12 h, no drug p = 0.0013 **. Posterior PD: 24% increase in anoxia 12 h, mg132 vs anoxia 12 h, no drug p=0.0640 ns, 36% increase in anoxia 12 h, chloroquine vs anoxia 12 h, no drug p = 0.0002 ***, 45% increase in anoxia 12 h mg132+chloroquine vs anoxia 12 h, no drug p < 0.0001 ****. (F) Quantification of total ATP concentration per WT embryo or *ndrg1a*$^{-/-}$ mutant exposed to 0, 6, 12, 18 and 24 h of anoxia. A significant difference between WT and mutants was observed for 12, 18 and 24 h of anoxia (Two-way ANOVA analysis was performed; 0 h WT vs. *ndrg1a*$^{-/-}$: p value > 0.9999, ns; 6 h WT vs. *ndrg1a*$^{-/-}$: p value = 0.3192, ns; 12 h WT vs. *ndrg1a*$^{-/-}$: p value = 0.0131, *; 18 h WT vs. *ndrg1a*$^{-/}$: p value =0.0076, **; 24 h WT vs. *ndrg1a*$^{-/-}$: p value = 0.0122, *). n = average of 15-20 embryos per experimental group; each experiment was repeated 2 times.

To test whether Ndrg1a may bind to ATP1A1A, we adapted the proximity ligation assay (PLA) for use on whole-mount zebrafish embryos. PLA, uses antibodies to two proteins of interest associated with DNA primers; a productive PCR product is produced and detected by fluorescent labeling only when the two antibodies are within less than 40 nm, suggesting that the two target proteins are in close physical proximity and may interact (Weibrecht et al., 2010). PLA performed on anoxia-treated embryos using anti-NDRG1 and anti-ATP1A1A antibodies revealed a low signal in the PD for the 0 h anoxia time point (Fig. 5b1, c1, c4), which noticeably increased by 6 and 12 h of anoxia (Fig. 5b2, b3, c2, c3, c5, c6). Cross sections further showed that the PLA signal in the anterior PD was scattered, localizing to subcortical and possibly intracellular storage compartments (Fig. 5c2, c3), whereas it appeared mostly associated with the cell cortex in the posterior PD (Fig. 5c5, c6). No PLA signal was detected in *ndrg1a*$^{-/-}$ mutants, confirming that the assay is specific for Ndrg1a-ATP1A1A interaction (Fig. 5b4-b6).

The ability to detect strong PLA signal after 12 h of anoxia, a time point that correlates with significantly reduced ATP1A1A levels in the PD, is consistent with the high level of sensitivity of this assay and indicates that interaction between Ndrg1a and ATP1A1A is enhanced by hypoxia.

NKA is downregulated via lysosomal and proteasomal degradation pathways

While ATP1A1A protein levels are not fully depleted following prolonged anoxia, they are greatly reduced. Degradation of transmembrane proteins usually occurs through the lysosome, although these proteins, including potentially NKA, can also be targeted to the proteosome (Helenius, Dada, & Sznajder, 2010; Hirsch & Ploegh, 2000). Hence,

blocking lysosomal or/and proteasomal degradation is expected to enhance ATP1A1A levels in embryos exposed to anoxia. To determine the ATP1A1A degradation route, WT embryos were exposed to anoxia (12 h) and simultaneously incubated in either MG-132 (26S proteasome inhibitor) or Chloroquine (autophagy inhibitor) (Mathai, Meijer, & Simonsen, 2017) or a combination thereof, and immunolabeled using anti-ATP1A1A. Measurements of fluorescence intensity showed that either drug slightly enhanced ATP1A1A levels in the PD relative to control embryos (12 h anoxia, no drug) (Fig. 5d2-d4 E) (Anterior PD: 7% increase in anoxia 12 h, mg132 vs anoxia 12 h, no drug $p > 0.9999$ ns; 59% increase in anoxia 12 h, chloroquine vs anoxia 12 h, no drug $p = 0.0298$ *; Posterior PD: 24% increase in anoxia 12 h, mg132 vs anoxia 12 h, no drug $p = 0.0640$ ns, 36% increase in anoxia 12 h, chloroquine vs anoxia 12 h, no drug $p = 0.0002$ ***), but the combined use of both drugs had the strongest effect relative to control embryos (12 h anoxia, no drug) (Fig. 5d5 E) (Anterior PD: 87% increase in anoxia 12 h mg132+chloroquine vs anoxia 12 h, no drug $p = 0.0013$ **; Posterior PD: 45% increase in anoxia 12 h mg132+chloroquine vs anoxia 12 h, no drug $p < 0.0001$ ****). These results suggest that ATP1A1A is partially degraded following prolonged anoxia via both lysosomal and proteasomal pathways. It is possible that Ndrg1a mediates both degradation pathways given that previous studies have identified three subunits of the 26S proteasome (Tu et al., 2007) and lysosomal-associated membrane protein 1 (LAMP1) (Liu et al., 2018) as putative NDRG1 binding partners.

Ndrg1a preserves ATP levels under severe hypoxia

Hypoxia-induced downregulation of NKA is thought to be a key aspect of metabolic suppression, the ultimate goal of which is to preserve cellular energy (Bogdanova et al.,

2016; Buck & Hochachka, 1993; Gusarova et al., 2011). To assess whether the activity of Ndrg1a contributes to the establishment of hypometabolism, the total level of ATP (from whole embryo lysates) was quantified using a luminescent ATP assay (Fig. 5F). We found that ATP levels were similar between WT and *ndrg1a*$^{-/-}$ mutants under normoxia (0 h anoxia time point). Surprisingly, ATP concentration transiently increased in embryos of both genotypes (6 h anoxia) (WT 0 h vs 6 h: $p < 0.0001$ ****; ndrg1a$^{-/-}$ 0 h vs 6 h: $p < 0.0001$ ****) before steadily declining with additional time points in anoxia. However, depletion of total ATP was more pronounced in *ndrg1a* mutants than in WT embryos following 12, 18, and 24 h of anoxia.

These results suggest that Ndrg1a-mediated downregulation of NKA promotes energy conservation during a time window spanning 12- 24 h of anoxia exposure and hence contributes to organismal adaptation to prolonged hypoxia. The transient rise in ATP for the 6 h anoxia time point is possibly due to sustained oxidative phosphorylation and an increase in glycolysis.

Lactate as a candidate proximal signal for metabolic suppression

Thus far, our data suggest that activation of Ndrg1a accelerates NKA degradation following prolonged anoxia. However, the proximal signal that activates Ndrg1a downstream of anoxia is unknown. We reasoned that this signal could be a small molecule whose levels accumulate following hypoxia exposure. To gain insight into the identity of this putative signal, we carried out metabolite profiling using pre-gastrula zebrafish embryos. Early embryos have a relatively homogenous cell population, facilitating the identification of candidate small molecules. Furthermore, they arrest

rapidly following anoxia exposure (Padilla & Roth, 2001), which provides a convenient read out for metabolic suppression. We therefore carried out metabolite profiling using dome-stage WT embryos subjected to 1 h of anoxia and age- and developmental stage-matched controls raised under normoxic conditions. Following extraction of metabolites, mass spectrometry was performed to identify small molecules whose levels are either up or down regulated (Fig. 6A-C). This analysis revealed three candidate ions, sulfite, sulfate and lactate, which lied outside of the 99th percentile confidence interval for outliers (a-c in Fig. 6A). We chose to further pursue lactate, given that this metabolite, the end product of glycolysis, was previously shown to bind to NDRG3 in hypoxic cancer cells, resulting in NDRG3 stabilization and activation of Ras-Erk signaling (Lee et al., 2015).

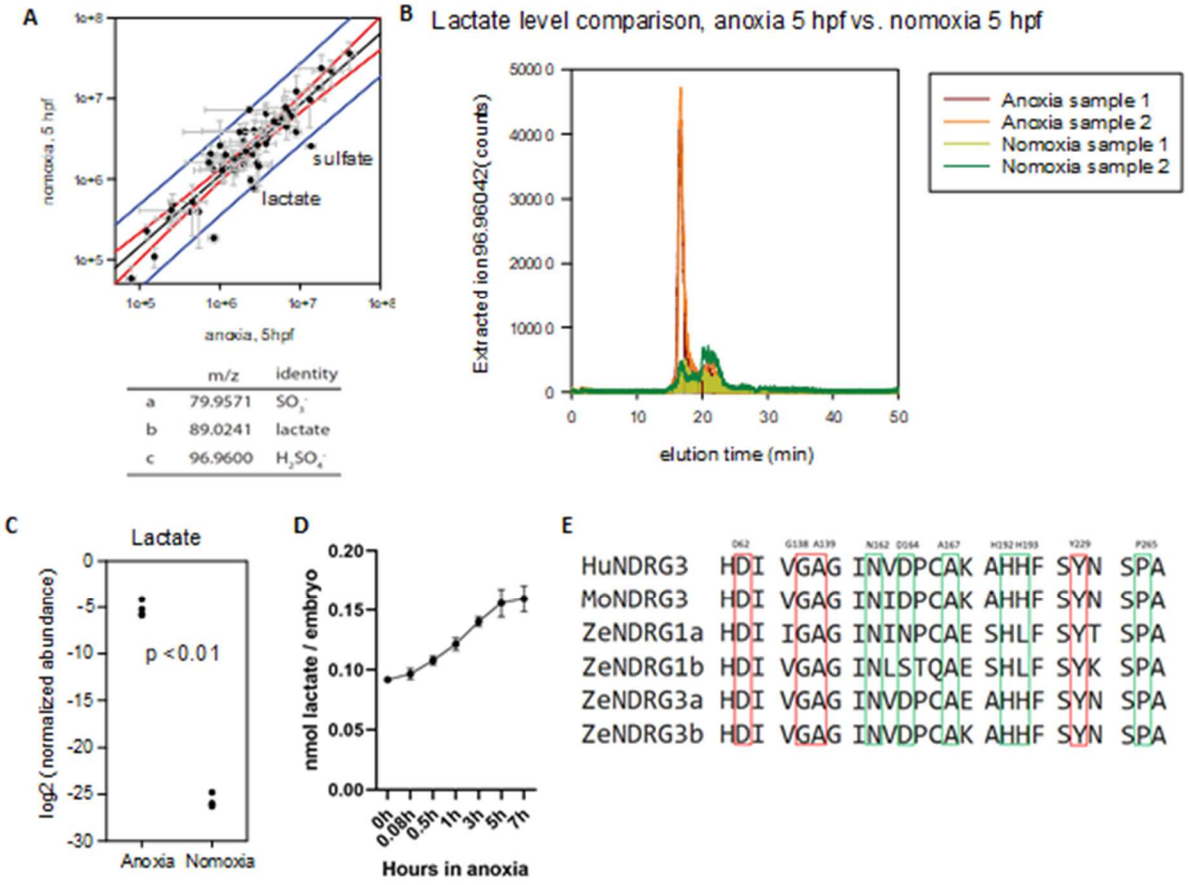

Figure 6. Lactate concentration increases under anoxia

(A, top) Metabolites enriched in anoxia-treated embryos relative to normoxic controls. Y axis: metabolite levels (integrated ion counts) in extracts from sphere stage (4 hpf) embryos exposed to 1 hour of anoxia; X axis: metabolite levels (integrated ion counts) in extracts from age-matched (5 hpf) normoxic controls. The red lines show the predicted correlation line (99% confidence). Blue lines demarcate outliers (99% confidence). Three potential outliers (a, b and c) were identified. n = 10 embryos per sample and 2 technical repeats. (A, bottom) Identity of the three outliers (a,-c) that are significantly enriched in the anoxia-treated sample. (B) Extracted ion counts for different elution timepoints are shown for two extracts from sphere stage (4 hpf) embryos exposed to 1 h of anoxia (orange and red lines) and two control samples from 5 hpf normoxic embryos (yellow and green lines). The peak corresponds to lactate. (C) Comparison of lactate levels (highest peak intensity) in extracts from sphere stage (4 hpf) embryo exposed to 1 h of anoxia and 5 hpf normoxic controls reveals an 18 fold increase (unpaired t test; $p < 0.01$). (D) Fluorometric lactate assay showing lactate concentration (nmol lactate/embryo) in whole embryo extracts from 24 hpf WT embryos exposed to increasing durations of anoxia (0-7 hours). n = average of 20 embryos per experimental group; each experiment was repeated 3 times. (E) Alignment of members of the NDRG family revealing lactate-docking residues, identified in Lee et al (2015). Green residues represent amino acids that

are critical for the interaction between NDRG and lactate, while red residues represent other potentially important lactate docking sites.

Lactate accumulation in anoxic samples was verified by measuring HILIC LC-MS extracted ion counts (Fig. 6B) and quantified using integrated ion count areas (Fig. 6C). To test whether an increase in L-lactate also occurs in older 24 hpf embryos and determine the temporal profile of lactate accumulation, we performed a lactate fluorometric assay (Fig. 6D). This analysis revealed that lactate concentration increased linearly with time in anoxia, consistent with previous observations (Podrabsky, Lopez, Fan, Higashi, & Somero, 2007; Van Heel, 2001; Virani & Rees, 2000). This conserved response reflects a shift from oxidative phosphorylation to anaerobic respiration.

Inhibition of oxidative-phosphorylation increases lactate and induces ATP1A1A degradation

A protein alignment of members of the human, mouse and zebrafish NDRG family revealed that the NDRG3 amino acid residues previously implicated in lactate binding (Lee et al., 2015) are conserved across members of this family (Fig. 6E), suggesting that lactate may also bind to and possibly activate NDRG1.

We next asked whether lactate may be sufficient to promote ATP1A1A degradation under normoxic conditions. Sodium azide, an electron transport chain inhibitor, was used to increase endogenous lactate levels as previously shown (Oginuma et al., 2017) and was confirmed to be effective (WT 158% increase, *ndrg1a*$^{-/-}$ 140% increase) (Fig. 7A). We then tested whether exposure of WT embryos to sodium azide (6, 12, 18, 24 h duration) under normal oxygen caused a decrease in ATP1A1A levels (Fig. 7B). This analysis revealed that NKA levels were indeed reduced in response to sodium azide treatment (WT anterior PD: 73% reduction of NKA level between 0 h and 24 h

anoxia; WT posterior PD: 63% reduction of NKA level between 0 h and 24 h anoxia) (Fig. 7C-D). If Ndrg1a is activated downstream of sodium azide, we would expect that ATP1A1A levels would not be reduced in *ndrg1a*$^{-/-}$- mutants exposed to this drug. Analysis of sodium azide treated *ndrg1a*$^{-/-}$ mutants immunolabeled with anti-ATP1A1A revealed that NKA levels were comparably higher in mutants than in WT embryos for the same treatment groups (*ndrg1a*$^{-/-}$ anterior PD: 20% reduction of NKA level between 0 h and 24 h anoxia; *ndrg1a*$^{-/-}$ posterior PD: 7.5% reduction of NKA level between 0 h and 24 h anoxia) (Fig. 7C-D), corroborating with this prediction.

Consistent with the ability of sodium azide to downregulate NKA under normoxic conditions, we also observed that azide treated embryos exhibited enhanced Ndrg1a-ATP1A1A interaction, as PLA labeling increased proportionately with the duration of the treatment (Fig 7E, e1-4). In contrast, *ndrg1a*$^{-/-}$ mutants subjected to the same treatment had no PLA signal, confirming the specificity of the PLA assay (Fig 7e5). These data are consistent with lactate being a proximal signal that contributes to NKA downregulation by promoting Ndrg1a-ATP1A1A interaction.

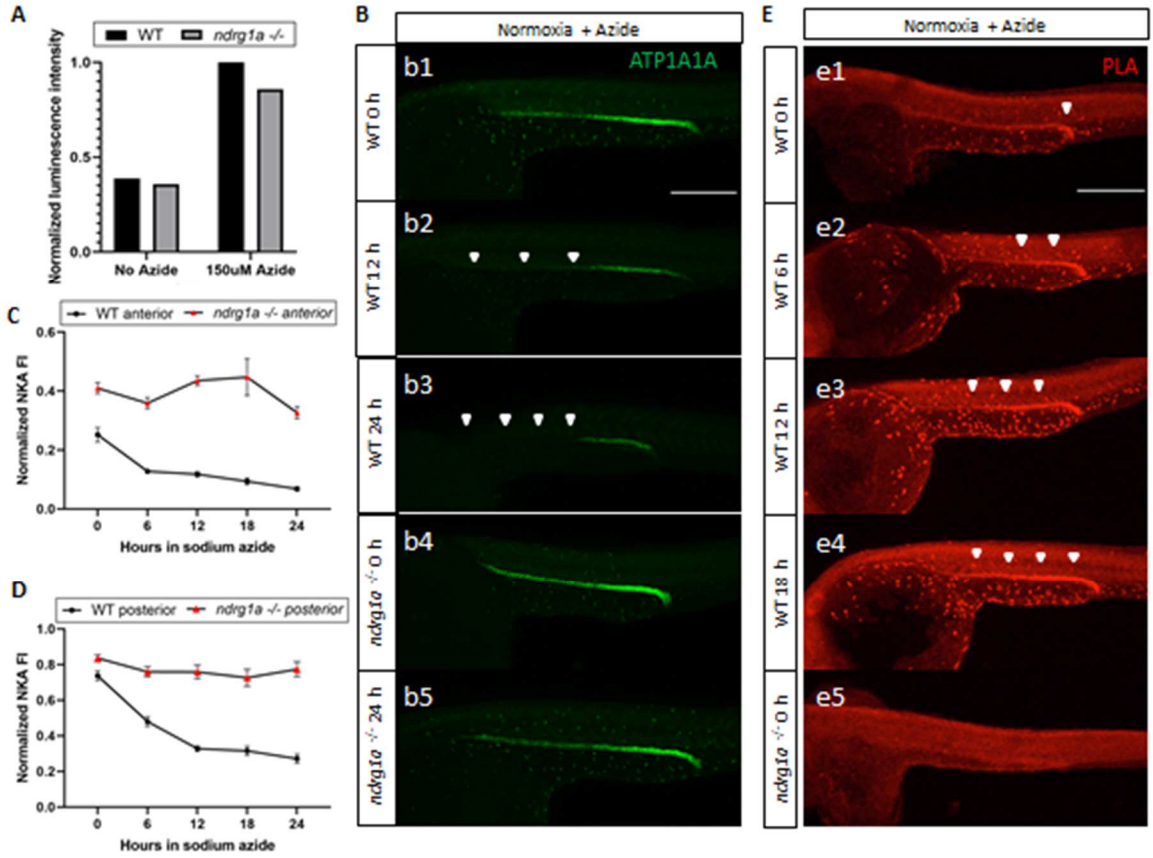

Figure 7. Lactate concentration increases following sodium azide treatment under normoxia and correlates with ATP1A1A downregulation

(A) Fluorometric lactate assay showing normalized lactate fluorescence intensity in whole embryo extracts from WT embryos and *ndrg1a*$^{-/-}$ mutants raised under normoxic conditions and exposed to sodium azide for 9 h. Embryos were 24 hpf at the time of treatment and untreated embryos were stage-matched to drug-treated embryos. n = average of 15 embryos per experimental group; experiment was performed once. (B) Lateral views of WT embryos and *ndrg1a*$^{-/-}$ mutants exposed at 24 hpf to increasing duration of azide under normoxia: (b1-5) 0 h; (b1, b4) 12 h; (b3, 5) 24 h and immunolabeled to reveal ATP1A1A. n = average of 3 embryos per experimental group. Scale bar 300 µm. Arrowheads indicate decreased signal. (C-D) Normalized fluorescence intensity in the (C) anterior and (D) posterior pronephric duct of WT embryos and *ndrg1a*$^{-/-}$ mutants. Embryos were exposed at 24 hpf to increasing duration of azide under normoxia (0, 6, 12, 18 and 24 h) and immunolabeled to reveal ATP1A1A levels. n = average of 3 pronephric ducts per experimental group. (E) Lateral views of WT embryos (e1-4) and an *ndrg1a*$^{-/-}$ mutant (e5) labeled using whole-mount proximity ligation assay (PLA) to reveal Ndrg1a and ATP1A1A interaction. Embryos were raised under normoxic conditions in the presence (6, 12 and 18 h exposure) or absence of sodium azide. n =

average of 3 embryos per experimental group; each experiment was repeated 2 times. Annotations: arrowheads point to PLA signal.

DISCUSSION

Increasing evidence indicates that members of the NDRG family of α−β hydrolases are implicated in the hypoxia response (Melotte et al., 2010). However, the mechanisms by which they function in the physiological adaptation of normal cells to low oxygen are, for the most part, unknown. We uncover here a novel and essential role for Ndrg1a in promoting long-term adaptation to hypoxia via metabolic suppression. Overall, our findings support a model whereby prolonged and severe hypoxia activates or enhances Ndrg1a signaling in the zebrafish embryo, possibly via lactate binding. Activated Ndrg1a accelerates the rate of endocytosis and degradation of the energy-demanding NKA pump in the PD and ionocytes, thereby preserving ATP. The high level of homology between NDRG1 in vertebrates along with evidence pointing towards conserved molecular interactions, suggest that the proposed model for Ndrg1a signaling may be broadly applicable.

Ndrg1a as a molecular switch for long-term adaptation to hypoxia

Given that the molecular cascade leading to ATP1A1A internalization and degradation is triggered by prolonged anoxia and dependent on *ndrg1a*, we propose that Ndrg1a functions as a molecular switch for long-term adaptation to hypoxia. The mechanisms underlying Ndrg1a activation have not been fully elucidated, however two non-mutually exclusive models can be envisaged, which we have coined quantitative vs. qualitative. In the quantitative model, Ndrg1a normoxic activity is enhanced in response to hypoxia, possibly via post-translational modifications (PTM) or/and transcriptional up-regulation

of *ndrg1a* (Le et al., under revision). Consistent with this model, we have shown that *ndrg1a* is required to maintain normoxic levels of NKA in the plasma membrane and to accelerate NKA degradation under hypoxia. Others have reported on similar NDRG1-dependent regulation of LDLR and E-Cadherin levels under normal oxygen (Kachhap et al., 2007; Pietiainen et al., 2013), however it is unknown whether such activities are enhanced under hypoxia.

In the qualitative model, Ndrg1a acquires new properties under hypoxia due to a PTM or binding to a small molecule, which brings about a change in protein conformation or/and binding partner affinity. In support of this model, a previous study showed that binding of lactate to NDRG3 in hypoxic cancer cells is sufficient to stabilize NDRG3 and activate Raf-ERK signaling (Lee et al., 2015). We have shown that sodium azide treatment, which blocks oxidative-phosphorylation and increases the intracellular concentration of lactate, is sufficient to induce ATP1A1A degradation under normoxic conditions and exerts this function in an Ndrg1a-dependent manner. While several metabolites could function downstream of sodium azide as effectors of this response, our data point to lactate as a prime candidate.

There is currently no consensus on the molecular role of activated NDRG1 (Melotte et al., 2010), however we favor the idea that Ndrg1a functions as an adapter protein to link protein-binding partners together. Indeed, there is a growing list of NDRG1 binding partners that localize to several cellular compartments (Tu et al., 2007). Our findings suggest that one the protein complexes that NDRG1 could bring together under hypoxic conditions includes ATP1A1A, endosomal components or/and protein degradation machinery.

Hypoxia-induced NKA downregulation as a mechanism to preserve ATP

The NKA isoforms that are expressed in the kidney are essential for the active translocation of Na^+ and K^+ ions across the membrane and in the secondary active transport of other solutes, including glucose (Katz, 1982). The cost of operating NKA is considerable, and hence an evolutionarily conserved response to hypoxia is to downregulate this pump to conserve ATP. Mechanisms of downregulation include reducing pump activity (inactivation via several redox-sensitive modifications) and/or triggering its endocytosis and degradation (Bogdanova et al., 2016; Buck & Hochachka, 1993; Gusarova et al., 2011). In the zebrafish, downregulation of NKA is a slow response to prolonged anoxia, taking place over the course of several hours. This response correlates with ATP preservation and is most likely delayed because it is a last resort for the cell.

In order for NKA downregulation to be considered a hypoxia adaptation, it would have to be reversible upon return to normoxia, which we have confirmed. The cellular source of the post-anoxia protein is unknown, but may involve intracellular stores of endocytosed NKA or/and protein synthesized *de novo*. The former could provide an immediate source of NKA for rapid restoration of pump activity, while the latter, a more delayed response, could fully replenish the cell's NKA supply.

Context-specific function of NDRG1

Our data support a physiological role for *ndrg1a* in hypoxia-induced NKA degradation. The NKA pump plays an important role in freshwater teleosts such as zebrafish. These fish are faced with the challenge of potential over-hydration and salt depletion, since their

body fluids are hyperosmotic with respect to the environment. To compensate for the tendency towards water influx, zebrafish excrete large volumes of water and limit NaCl loss via reabsorption of Na^+ and Cl^- in the kidney distal (collecting) duct and bladder, and also through ionocyte-dependent absorption of these ions from the environment (Takvam, Wood, Kryvi, & Nilsen, 2021). Consistent with these findings, zebrafish NKA is expressed more highly in the posterior PD, where its activity may power the bulk of Na^+ reabsorption. PLA further revealed regional differences in the manner in which NKA is regulated in the anterior and posterior PD, as ATP1A1A and Ndrg1a appear to interact in posterior cells even under normoxic conditions. It is possible that owing to the high level of activity of NKA in the posterior tubules, there is a build up of lactate in these cells. If correct, constitutive Ndrg1a-ATP1A1A interaction in posterior cells may prime them for a more effective response to hypoxia.

Studies in amphibians show that NDRG1 controls cell differentiation of endodermal organs (Kyuno et al., 2003; Zhang et al., 2013), with no indication of a physiological role for this protein. It is unclear what accounts for the difference in NDRG1 function between teleosts and amphibians, but one possibility is the increased number of *Ndrg* paralogs in zebrafish (6 NDRGs in zebrafish versus 4 in *Xenopus laevis*). This increase might have enabled functional diversification of some members of the NDRG family and for *ndrg1a* in particular to evolve a role in hypoxia adaptation. However, there is ample evidence in mouse and human cells that NDRG1 is hypoxia-responsive (Melotte et al., 2010), making this an unlikely explanation. Alternatively, *ndrg1a* may be required for PD and ionocyte differentiation but its function is masked by other members of the NDRG family that compensate for *ndrg1a* LOF.

NDRG1 and ion homeostasis

While NKA degradation preserves ATP, the loss of this pump can cause a rise in intracellular Na^+ concentration and subsequent water influx, culminating in cellular edema (Bogdanova, Grenacher, Nikinmaa, & Gassmann, 2005; Leaf, 1956; Mudge, 1951). However, hypoxia-tolerant organisms are thought to counter NKA depletion with a general reduction in membrane permeability via blockage of leak and water channels (Boutilier, 2001; Doll, Hochachka, & Reiner, 1991; LaMacchia & Roth, 2015; Lutz & Nilsson, 1997). The underlying mechanisms for this phenomenon, known as channel arrest, have remained controversial, especially with regards to the identity of the proximal signal that triggers channel arrest (Buck & Hochachka, 1993; Hochachka & Lutz, 2001).

PD cells and ionocytes in zebrafish embryos exposed to prolonged anoxia do not show overt signs of cellular edema (Fig. 3D and 4A), suggesting that channel arrest may apply to this organism. We further speculate that NDRG1 may negatively regulate ion transporters in zebrafish embryos, in addition to mediating NKA degradation. Indeed, *ndrg1a*$^{-/-}$ mutants exposed to prolonged anoxia develop severe edema. Moreover, NDRG1 is known to interact with ion transporters CLNS1A and SLC25A6 and ion transport regulator FXYD (Arystarkhova, Bouley, Liu, & Sweadner, 2017; Yang, Kang, Hsu, Lin, & Lee, 2016) and the level of several ion transporters in cichlids exposed to high salinity was shown to be inversely proportional to that of NDRG1 (Kultz, Li, Gardell, & Sacchi, 2013). If correct, the implication of this prediction is that NDRG1 could function as a master switch that coordinates both metabolic suppression/energy preservation (NKA downregulation) and ion homeostasis (reduction in membrane permeability).

Given that human NDRG1 is expressed in the kidney as well as other metabolically-demanding tissues (Melotte et al., 2010) and interacts with NKA and several ion transporters, it is intriguing to consider whether NDRG1-lactate signaling could be modulated to mitigate the cellular damage caused by hypoxic injury.

Thus, we propose the following overall molecular model for Ndrg1a signaling under anoxia (Fig. 8). In response to prolonged anoxia, lactate levels rise. Correlating with lactate increase, we observed we observe that Ndrg1a-ATP1A1A interact, coinciding with ATP1A1A downregulation under prolonged anoxia, which is Ndrg1a-dependent. Lastly, Ndrg1a signaling results in tissue protection and survival of embryos under prolonged anoxia.

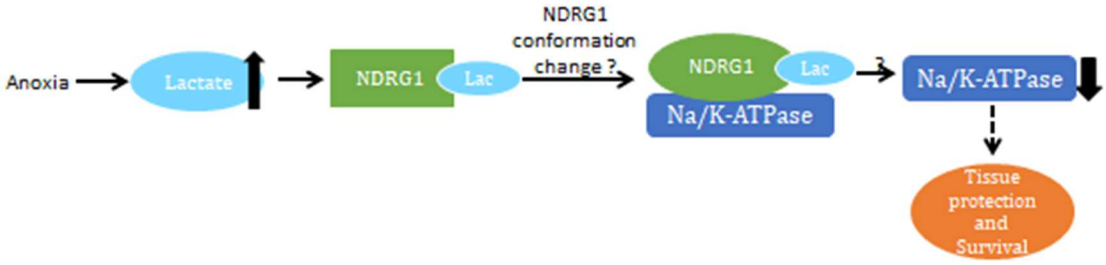

Figure 8. NDRG1: A model representing NDRG1 as a molecular switch for cellular adaptation to hypoxia.
Anoxia induces an increase in lactate, which correlates with Ndrg1 and ATP1A1A interaction and ATP1A1A downregulation in an Ndrg1a-dependent manner. The downregulation of ATP1A1A is beneficial for the organism as it provides tissue protection and survival under prolonged anoxia.

ACKNOWLEDGEMENTS

We would like to acknowledge M. Van Doren, D. Eisenmann, S. Miller, P. Robinson and B. Weinstein for their helpful comments on our manuscript. We would also like to acknowledge T. deCarvalho and S. Larson for help with imaging during the covid pandemic. This project was supported by funding from the Department of Defense (W81XWH-16-1-0466) and the National Institute of Health/NICHD (R21HD089476) to R. Brewster and Y.-S. Lee. We thank T. Addo for contributing to the analysis of *ndrg1a* function. A. Gabel, B. Canales and A. Osei-Ntansah were supported by a National Institute of Health /NIGMS MARC U*STAR (T34 HHS 00001) National Research Service Award to UMBC. S. Viswanathan was supported in part by a grant to UMBC from the Howard Hughes Medical Institute through the HHMI Adaptation Project. Polina Kassir was supported by Experimental Learning Award through the Sondheim Public Affairs Scholars Program.

COMPETING INTERESTS

The authors confirm that there is no financial or non-financial competing interests.

REFERENCES

1. Angst, E., Sibold, S., Tiffon, C., Weimann, R., Gloor, B., Candinas, D., & Stroka, D. (2006). Cellular differentiation determines the expression of the hypoxia-inducible protein NDRG1 in pancreatic cancer. *Br J Cancer, 95*(3), 307-313. doi:10.1038/sj.bjc.6603256
2. Arystarkhova, E., Bouley, R., Liu, Y. B., & Sweadner, K. J. (2017). Impaired AQP2 trafficking in Fxyd1 knockout mice: A role for FXYD1 in regulated vesicular transport. *PLoS One, 12*(11), e0188006. doi:10.1371/journal.pone.0188006
3. Bellot, G., Garcia-Medina, R., Gounon, P., Chiche, J., Roux, D., Pouyssegur, J., & Mazure, N. M. (2009). Hypoxia-induced autophagy is mediated through hypoxia-inducible factor induction of BNIP3 and BNIP3L via their BH3 domains. *Mol Cell Biol, 29*(10), 2570-2581. doi:10.1128/MCB.00166-09
4. Blasiole, B., Canfield, V., Degrave, A., Thisse, C., Thisse, B., Rajarao, J., & Levenson, R. (2002). Cloning, mapping, and developmental expression of a sixth zebrafish Na,K-ATPase alpha1 subunit gene (atp1a1a.5). *Mech Dev, 119 Suppl 1*, S211-214. doi:10.1016/s0925-4773(03)00118-7
5. Bogdanova, A., Grenacher, B., Nikinmaa, M., & Gassmann, M. (2005). Hypoxic responses of Na+/K+ ATPase in trout hepatocytes. *J Exp Biol, 208*(Pt 10), 1793-1801. doi:10.1242/jeb.01572
6. Bogdanova, A., Petrushanko, I. Y., Hernansanz-Agustin, P., & Martinez-Ruiz, A. (2016). "Oxygen Sensing" by Na,K-ATPase: These Miraculous Thiols. *Front Physiol, 7*, 314. doi:10.3389/fphys.2016.00314

7. Bosc, L. V., Resta, T., Walker, B., & Kanagy, N. L. (2010). Mechanisms of intermittent hypoxia induced hypertension. *J Cell Mol Med, 14*(1-2), 3-17. doi:10.1111/j.1582-4934.2009.00929.x
8. Boutilier, R. G. (2001). Mechanisms of cell survival in hypoxia and hypothermia. *J Exp Biol, 204*(Pt 18), 3171-3181. Retrieved from https://www.ncbi.nlm.nih.gov/pubmed/11581331
9. Buck, L. T., & Hochachka, P. W. (1993). Anoxic suppression of Na(+)-K(+)-ATPase and constant membrane potential in hepatocytes: support for channel arrest. *Am J Physiol, 265*(5 Pt 2), R1020-1025. doi:10.1152/ajpregu.1993.265.5.R1020
10. Canfield, V. A., Loppin, B., Thisse, B., Thisse, C., Postlethwait, J. H., Mohideen, M. A., . . . Levenson, R. (2002). Na,K-ATPase alpha and beta subunit genes exhibit unique expression patterns during zebrafish embryogenesis. *Mech Dev, 116*(1-2), 51-59. doi:10.1016/s0925-4773(02)00135-1
11. Cangul, H. (2004). Hypoxia upregulates the expression of the NDRG1 gene leading to its overexpression in various human cancers. *BMC Genet, 5*, 27. doi:10.1186/1471-2156-5-27
12. Caruso, R. P., Levinson, B., Melamed, J., Wieczorek, R., Taneja, S., Polsky, D., . . . Osman, I. (2004). Altered N-myc downstream-regulated gene 1 protein expression in African-American compared with caucasian prostate cancer patients. *Clin Cancer Res, 10*(1 Pt 1), 222-227. doi:10.1158/1078-0432.ccr-0604-3

13. Chen, B., Nelson, D. M., & Sadovsky, Y. (2006). N-myc down-regulated gene 1 modulates the response of term human trophoblasts to hypoxic injury. *J Biol Chem, 281*(5), 2764-2772. doi:10.1074/jbc.M507330200
14. Choi, S. J., Oh, S. Y., Kim, J. H., Sadovsky, Y., & Roh, C. R. (2007). Increased expression of N-myc downstream-regulated gene 1 (NDRG1) in placentas from pregnancies complicated by intrauterine growth restriction or preeclampsia. *Am J Obstet Gynecol, 196*(1), 45 e41-47. doi:10.1016/j.ajog.2006.08.029
15. Christou-Savina, S., Beales, P. L., & Osborn, D. P. (2015). Evaluation of zebrafish kidney function using a fluorescent clearance assay. *J Vis Exp*(96), e52540. doi:10.3791/52540
16. Dengler, F. (2020). Activation of AMPK under Hypoxia: Many Roads Leading to Rome. *Int J Mol Sci, 21*(7). doi:10.3390/ijms21072428
17. Doll, C. J., Hochachka, P. W., & Reiner, P. B. (1991). Channel arrest: implications from membrane resistance in turtle neurons. *Am J Physiol, 261*(5 Pt 2), R1321-1324. doi:10.1152/ajpregu.1991.261.5.R1321
18. Douglas, R. M., Ryu, J., Kanaan, A., Del Carmen Rivero, M., Dugan, L. L., Haddad, G. G., & Ali, S. S. (2010). Neuronal death during combined intermittent hypoxia/hypercapnia is due to mitochondrial dysfunction. *Am J Physiol Cell Physiol, 298*(6), C1594-1602. doi:10.1152/ajpcell.00298.2009
19. Draper, J., Enot, D. P., Parker, D., Beckmann, M., Snowdon, S., Lin, W., & Zubair, H. (2009). Metabolite signal identification in accurate mass metabolomics data with MZedDB, an interactive m/z annotation tool utilising predicted

ionisation behaviour 'rules'. *BMC Bioinformatics, 10*, 227. doi:10.1186/1471-2105-10-227

20. Drummond, I. A., Majumdar, A., Hentschel, H., Elger, M., Solnica-Krezel, L., Schier, A. F., . . . Fishman, M. C. (1998). Early development of the zebrafish pronephros and analysis of mutations affecting pronephric function. *Development, 125*(23), 4655-4667. Retrieved from https://www.ncbi.nlm.nih.gov/pubmed/9806915
21. Elmonem, M. A., Berlingerio, S. P., van den Heuvel, L. P., de Witte, P. A., Lowe, M., & Levtchenko, E. N. (2018). Genetic Renal Diseases: The Emerging Role of Zebrafish Models. *Cells, 7*(9). doi:10.3390/cells7090130
22. Guillemin, K., & Krasnow, M. A. (1997). The hypoxic response: huffing and HIFing. *Cell, 89*(1), 9-12. doi:10.1016/s0092-8674(00)80176-2
23. Gusarova, G. A., Trejo, H. E., Dada, L. A., Briva, A., Welch, L. C., Hamanaka, R. B., . . . Sznajder, J. I. (2011). Hypoxia leads to Na,K-ATPase downregulation via Ca(2+) release-activated Ca(2+) channels and AMPK activation. *Mol Cell Biol, 31*(17), 3546-3556. doi:10.1128/MCB.05114-11
24. Helenius, I. T., Dada, L. A., & Sznajder, J. I. (2010). Role of ubiquitination in Na,K-ATPase regulation during lung injury. *Proc Am Thorac Soc, 7*(1), 65-70. doi:10.1513/pats.200907-082JS
25. Hirsch, C., & Ploegh, H. L. (2000). Intracellular targeting of the proteasome. *Trends Cell Biol, 10*(7), 268-272. doi:10.1016/s0962-8924(00)01768-2

26. Hickman C. P., Trump B. F. (1969). "The kidney," in Fish Physiology, eds Hoar W. S., Randall D. J. (Cambridge, CA: Academic;) 91–239. 10.1016/S1546-5098(08)60083-7

27. Hochachka, P. W., & Lutz, P. L. (2001). Mechanism, origin, and evolution of anoxia tolerance in animals. *Comp Biochem Physiol B Biochem Mol Biol, 130*(4), 435-459. doi:10.1016/s1096-4959(01)00408-0

28. Hwang, P. P., & Chou, M. Y. (2013). Zebrafish as an animal model to study ion homeostasis. *Pflugers Arch, 465*(9), 1233-1247. doi:10.1007/s00424-013-1269-1

29. Inoue, D., & Wittbrodt, J. (2011). One for all--a highly efficient and versatile method for fluorescent immunostaining in fish embryos. *PLoS One, 6*(5), e19713. doi:10.1371/journal.pone.0019713

30. Kachhap, S. K., Faith, D., Qian, D. Z., Shabbeer, S., Galloway, N. L., Pili, R., . . . Carducci, M. A. (2007). The N-Myc down regulated Gene1 (NDRG1) Is a Rab4a effector involved in vesicular recycling of E-cadherin. *PLoS One, 2*(9), e844. doi:10.1371/journal.pone.0000844

31. Katz, A. I. (1982). Renal Na-K-ATPase: its role in tubular sodium and potassium transport. *Am J Physiol, 242*(3), F207-219. doi:10.1152/ajprenal.1982.242.3.F207

32. Kim, K. T., Ongusaha, P. P., Hong, Y. K., Kurdistani, S. K., Nakamura, M., Lu, K. P., & Lee, S. W. (2004). Function of Drg1/Rit42 in p53-dependent mitotic spindle checkpoint. *J Biol Chem, 279*(37), 38597-38602. doi:10.1074/jbc.M400781200

33. Kimmel, C. B., Ballard, W. W., Kimmel, S. R., Ullmann, B., & Schilling, T. F. (1995). Stages of embryonic development of the zebrafish. *Dev Dyn, 203*(3), 253-310. doi:10.1002/aja.1002030302

34. Kultz, D., Li, J., Gardell, A., & Sacchi, R. (2013). Quantitative molecular phenotyping of gill remodeling in a cichlid fish responding to salinity stress. *Mol Cell Proteomics, 12*(12), 3962-3975. doi:10.1074/mcp.M113.029827

35. Kurdistani, S. K., Arizti, P., Reimer, C. L., Sugrue, M. M., Aaronson, S. A., & Lee, S. W. (1998). Inhibition of tumor cell growth by RTP/rit42 and its responsiveness to p53 and DNA damage. *Cancer Res, 58*(19), 4439-4444. Retrieved from https://www.ncbi.nlm.nih.gov/pubmed/9766676

36. Kyuno, J., Fukui, A., Michiue, T., & Asashima, M. (2003). Identification and characterization of Xenopus NDRG1. *Biochem Biophys Res Commun, 309*(1), 52-57. doi:10.1016/s0006-291x(03)01522-5

37. Lachat, P., Shaw, P., Gebhard, S., van Belzen, N., Chaubert, P., & Bosman, F. T. (2002). Expression of NDRG1, a differentiation-related gene, in human tissues. *Histochem Cell Biol, 118*(5), 399-408. doi:10.1007/s00418-002-0460-9

38. LaMacchia, J. C., & Roth, M. B. (2015). Aquaporins-2 and -4 regulate glycogen metabolism and survival during hyposmotic-anoxic stress in Caenorhabditis elegans. *Am J Physiol Cell Physiol, 309*(2), C92-96. doi:10.1152/ajpcell.00131.2015

39. Leaf, A. (1956). On the mechanism of fluid exchange of tissues in vitro. *Biochem J, 62*(2), 241-248. doi:10.1042/bj0620241

40. Lee, D. C., Sohn, H. A., Park, Z. Y., Oh, S., Kang, Y. K., Lee, K. M., . . . Yeom, Y. I. (2015). A lactate-induced response to hypoxia. *Cell, 161*(3), 595-609. doi:10.1016/j.cell.2015.03.011

41. Liu, X., Salokas, K., Tamene, F., Jiu, Y., Weldatsadik, R. G., Ohman, T., & Varjosalo, M. (2018). An AP-MS- and BioID-compatible MAC-tag enables comprehensive mapping of protein interactions and subcellular localizations. *Nat Commun, 9*(1), 1188. doi:10.1038/s41467-018-03523-2

42. Lutz, P. L., & Nilsson, G. E. (1997). Contrasting strategies for anoxic brain survival--glycolysis up or down. *J Exp Biol, 200*(Pt 2), 411-419. Retrieved from https://www.ncbi.nlm.nih.gov/pubmed/9050250

43. Mathai, B. J., Meijer, A. H., & Simonsen, A. (2017). Studying Autophagy in Zebrafish. *Cells, 6*(3). doi:10.3390/cells6030021

44. Melotte, V., Qu, X., Ongenaert, M., van Criekinge, W., de Bruine, A. P., Baldwin, H. S., & van Engeland, M. (2010). The N-myc downstream regulated gene (NDRG) family: diverse functions, multiple applications. *FASEB J, 24*(11), 4153-4166. doi:10.1096/fj.09-151464

45. Mendelsohn, B. A., Kassebaum, B. L., & Gitlin, J. D. (2008). The zebrafish embryo as a dynamic model of anoxia tolerance. *Dev Dyn, 237*(7), 1780-1788. doi:10.1002/dvdy.21581

46. Mudge, G. H. (1951). Electrolyte and water metabolism of rabbit kidney slices; effect of metabolic inhibitors. *Am J Physiol, 167*(1), 206-223. doi:10.1152/ajplegacy.1951.167.1.206

47. Oginuma, M., Moncuquet, P., Xiong, F., Karoly, E., Chal, J., Guevorkian, K., & Pourquie, O. (2017). A Gradient of Glycolytic Activity Coordinates FGF and Wnt Signaling during Elongation of the Body Axis in Amniote Embryos. *Dev Cell, 40*(4), 342-353 e310. doi:10.1016/j.devcel.2017.02.001

48. Padilla, P. A., & Roth, M. B. (2001). Oxygen deprivation causes suspended animation in the zebrafish embryo. *Proc Natl Acad Sci U S A, 98*(13), 7331-7335. doi:10.1073/pnas.131213198

49. Park, H., Adams, M. A., Lachat, P., Bosman, F., Pang, S. C., & Graham, C. H. (2000). Hypoxia induces the expression of a 43-kDa protein (PROXY-1) in normal and malignant cells. *Biochem Biophys Res Commun, 276*(1), 321-328. doi:10.1006/bbrc.2000.3475

50. Peers, C., Dallas, M. L., Boycott, H. E., Scragg, J. L., Pearson, H. A., & Boyle, J. P. (2009). Hypoxia and neurodegeneration. *Ann N Y Acad Sci, 1177*, 169-177. doi:10.1111/j.1749-6632.2009.05026.x

51. Pietiainen, V., Vassilev, B., Blom, T., Wang, W., Nelson, J., Bittman, R., . . . Ikonen, E. (2013). NDRG1 functions in LDL receptor trafficking by regulating endosomal recycling and degradation. *J Cell Sci, 126*(Pt 17), 3961-3971. doi:10.1242/jcs.128132

52. Pirahanchi, Y., Jessu, R., & Aeddula, N. R. (2021). Physiology, Sodium Potassium Pump. In *StatPearls*. Treasure Island (FL).

53. Podrabsky, J. E., Lopez, J. P., Fan, T. W., Higashi, R., & Somero, G. N. (2007). Extreme anoxia tolerance in embryos of the annual killifish Austrofundulus

limnaeus: insights from a metabolomics analysis. *J Exp Biol, 210*(Pt 13), 2253-2266. doi:10.1242/jeb.005116

54. Roh, C. R., Budhraja, V., Kim, H. S., Nelson, D. M., & Sadovsky, Y. (2005). Microarray-based identification of differentially expressed genes in hypoxic term human trophoblasts and in placental villi of pregnancies with growth restricted fetuses. *Placenta, 26*(4), 319-328. doi:10.1016/j.placenta.2004.06.013
55. Schmajuk, G., Sierakowska, H., & Kole, R. (1999). Antisense oligonucleotides with different backbones. Modification of splicing pathways and efficacy of uptake. *J Biol Chem, 274*(31), 21783-21789. doi:10.1074/jbc.274.31.21783
56. Semenza, G. L. (2001). HIF-1, O(2), and the 3 PHDs: how animal cells signal hypoxia to the nucleus. *Cell, 107*(1), 1-3. doi:10.1016/s0092-8674(01)00518-9
57. Semenza, G. L. (2012). Hypoxia-inducible factors: mediators of cancer progression and targets for cancer therapy. *Trends Pharmacol Sci, 33*(4), 207-214. doi:10.1016/j.tips.2012.01.005
58. Shaw, E., McCue, L. A., Lawrence, C. E., & Dordick, J. S. (2002). Identification of a novel class in the alpha/beta hydrolase fold superfamily: the N-myc differentiation-related proteins. *Proteins, 47*(2), 163-168. doi:10.1002/prot.10083
59. Shi, X. H., Larkin, J. C., Chen, B., & Sadovsky, Y. (2013). The expression and localization of N-myc downstream-regulated gene 1 in human trophoblasts. *PLoS One, 8*(9), e75473. doi:10.1371/journal.pone.0075473
60. Shu, S., Wang, Y., Zheng, M., Liu, Z., Cai, J., Tang, C., & Dong, Z. (2019). Hypoxia and Hypoxia-Inducible Factors in Kidney Injury and Repair. *Cells, 8*(3). doi:10.3390/cells8030207

61. Sibold, S., Roh, V., Keogh, A., Studer, P., Tiffon, C., Angst, E., . . . Stroka, D. (2007). Hypoxia increases cytoplasmic expression of NDRG1, but is insufficient for its membrane localization in human hepatocellular carcinoma. *FEBS Lett, 581*(5), 989-994. doi:10.1016/j.febslet.2007.01.080

62. Song, Y., Oda, Y., Hori, M., Kuroiwa, K., Ono, M., Hosoi, F., . . . Tsuneyoshi, M. (2010). N-myc downstream regulated gene-1/Cap43 may play an important role in malignant progression of prostate cancer, in its close association with E-cadherin. *Hum Pathol, 41*(2), 214-222. doi:10.1016/j.humpath.2009.07.011

63. Storey, K. B., & Storey, J. M. (2007). Tribute to P. L. Lutz: putting life on 'pause'--molecular regulation of hypometabolism. *J Exp Biol, 210*(Pt 10), 1700-1714. doi:10.1242/jeb.02716

64. Takvam, M., Wood, C. M., Kryvi, H., & Nilsen, T. O. (2021). Ion Transporters and Osmoregulation in the Kidney of Teleost Fishes as a Function of Salinity. *Front Physiol, 12*, 664588. doi:10.3389/fphys.2021.664588

65. Tu, L. C., Yan, X., Hood, L., & Lin, B. (2007). Proteomics analysis of the interactome of N-myc downstream regulated gene 1 and its interactions with the androgen response program in prostate cancer cells. *Mol Cell Proteomics, 6*(4), 575-588. doi:10.1074/mcp.M600249-MCP200

66. Van Heel, T. I., Van Den Thillart, G., Vianen, G.J., Steffens, A.B., & Van Kampen, M. (2001). Plasma Lactate and Stress Hormones in Common Carp (Cyprinus Carpio) and Rainbow Trout (Oncorhynchus Mykiss) During Stepwise Decreasing Oxygen Levels. *Netherlands Journal of Zoology, 51*(1), 33-50.

67. Vianen, G.J. & Thillart, Guido & Kampen, M. & Heel, T.I. & Steffens, A.B.. (2001). Plasma Lactate and Stress Hormones in Common Carp (Cyprinus Carpio) and Rainbow Trout (Oncorhynchus Mykiss) During Stepwise Decreasing Oxygen Levels. Netherlands Journal of Zoology. 51. 33-50. 10.1163/156854201X00035.

68. Virani, N. A., & Rees, B. B. (2000). Oxygen consumption, blood lactate and inter-individual variation in the gulf killifish, Fundulus grandis, during hypoxia and recovery. *Comp Biochem Physiol A Mol Integr Physiol, 126*(3), 397-405. doi:10.1016/s1095-6433(00)00219-1

69. Weibrecht, I., Leuchowius, K. J., Clausson, C. M., Conze, T., Jarvius, M., Howell, W. M., . . . Soderberg, O. (2010). Proximity ligation assays: a recent addition to the proteomics toolbox. *Expert Rev Proteomics, 7*(3), 401-409. doi:10.1586/epr.10.10

70. Wodopia, R., Ko, H. S., Billian, J., Wiesner, R., Bartsch, P., & Mairbaurl, H. (2000). Hypoxia decreases proteins involved in epithelial electrolyte transport in A549 cells and rat lung. *Am J Physiol Lung Cell Mol Physiol, 279*(6), L1110-1119. doi:10.1152/ajplung.2000.279.6.L1110

71. Won, S. J., Kim, D. Y., & Gwag, B. J. (2002). Cellular and molecular pathways of ischemic neuronal death. *J Biochem Mol Biol, 35*(1), 67-86. doi:10.5483/bmbrep.2002.35.1.067

72. Xie, H., & Simon, M. C. (2017). Oxygen availability and metabolic reprogramming in cancer. *J Biol Chem, 292*(41), 16825-16832. doi:10.1074/jbc.R117.799973

73. Yang, W. K., Kang, C. K., Hsu, A. D., Lin, C. H., & Lee, T. H. (2016). Different Modulatory Mechanisms of Renal FXYD12 for Na(+)-K(+)-ATPase between Two Closely Related Medakas upon Salinity Challenge. *Int J Biol Sci, 12*(6), 730-745. doi:10.7150/ijbs.15066

74. Zhang, T., Guo, X., & Chen, Y. (2013). Retinoic acid-activated Ndrg1a represses Wnt/beta-catenin signaling to allow Xenopus pancreas, oesophagus, stomach, and duodenum specification. *PLoS One, 8*(5), e65058. doi:10.1371/journal.pone.0065058

CHAPTER 2 SPECIAL THANKS

During my completion of Ndrg1a-NKA work, I have been fortunate enough to work with many undergraduate students as well as collaborators. I have listed their contributions to this work below in alphabetical order (Last name).

- Bryanna Canales; Assisted with lactate measurements in anoxia treated embryos using lactate assay kit
- Austin Gabel; Performed metabolomics study with Young-sam Lee - specifically, collected anoxia treated embryos and provided samples to Young-sam Lee
- Lois Kang; Assisted with CRISPR mutant sequencing.
- Polina Kassir; Assisted with NKA downregulation reversibility experiments
- Young-sam Lee (collaborator from Kentucky Med); Performed mass-spectrometry and analyzed metabolomics data, made final figures
- Afia Osei-Ntansah; Assisted with sectioning and imaging of immunolabeled samples
- Neil Tran; Assisted with gathering data for pericardial edema experiments
- Anya Viswanathan; Assisted with performing kidney clearance assay under anoxia

CHAPTER 3: CONCLUSIONS AND FUTURE DIRECTIONS

Chapter 3 of my dissertation thesis is organized around the three major findings from Chapter 2:

I. NDRG1 promotes tissue and organismal protection during long term exposure to hypoxia

II. NDRG1 downregulates the ATP-demanding sodium potassium ATPase pump under hypoxia

III. Blockage of oxidative phosphorylation is a proximal signal downstream of hypoxia that can activate Ndrg1

Within each of the sections outlined above, a detailed discussion of related topics is further examined along with future research directions.

I. NDRG1 promotes tissue and organismal protection during long-term exposure to hypoxia

My thesis work has demonstrated that NDRG1 promotes tissue and organismal protection following exposure to prolonged anoxia. *ndrg1a* mutants begin to show signs of tissue damage and death only after prolonged anoxia (12 hours of anoxia or more) (**Figure 2 - Chapter 2**). However, 12 h of anoxia is a very harsh treatment compared to hypoxia that embryos would normally encounter in their natural environment.

It is likely that more commonly, mild to moderate hypoxia may be what most organisms face in nature. In addition, natural hypoxia exposure may be shorter in

duration. Thus, there must be other hypoxia-responsive molecules that are activated under acute, mild hypoxia.

These observations suggest that NDRG1 is implicated in long term adaptation to severe hypoxia and that other signaling molecules, such as HIF and AMPK may mediate responses to more acute and moderate hypoxia in the zebrafish embryo. In the section below, NDRG is described in relation to other hypoxia-responsive molecules that complete the entire picture of the hypoxia response as the intensity and duration of oxygen deprivation increases.

I.1.Relation of NDRG1 to other mediators of (short and long term) hypoxia adaptation

As a reminder, my experiments exposed normoxic embryos to anoxia without any intermediary mild/moderate hypoxia steps, which is quite different from the gradual worsening of hypoxic conditions that embryos might encounter in the wild. Indeed, there are other hypoxia adaptive responses that are mounted during the mild and moderate hypoxia that may be activated prior to anoxia responses such as NDRG1-mediated NKA downregulation.

In a recent study using an invertebrate, the bearded fireworm (*Hermodice carunculata*), it was shown that HIF-1a is differentially regulated depending on the severity of hypoxia (Grime et al., 2021). The authors observed that the HIF-1a subunit was upregulated only during the mild hypoxia phase (4.5 ± 0.25 mg O_2 L^{-1} [64% of normoxia level]) and was subsequently downregulated under moderate hypoxia (2.5 ± 0.25 mg O_2 L^{-1} [36% of normoxia level]). Consistent with the above finding, additional studies suggest that HIF is a hypoxia-responsive transcription factor

that is only activated under mild hypoxia (Hochachka and Lutz, 2001; Semenza, 2001a,b; Guillemin and Krasnow, 1997; Lavista-Llanos et al., 2002), establishing HIF as an early mediator of the hypoxia response. This makes sense given that HIF is an oxygen sensor whose regulation reflects the concentration of environmental oxygen. In addition, given that HIF is a transcription factor that initiates the upregulation of target genes, an energy-demanding process, it follows that HIF is activated under hypoxic conditions that are compatible with the production of sufficient energy to fuel transcription and translation.

AMPK is another well-studied hypoxia-responsive molecule. Since a detailed description of the regulation and function of AMPK under hypoxia was provided in the Introduction, I will focus here mainly on how AMPK relates to hypoxia-responsive molecules such as HIF. First, a study reported by De Theije et al., demonstrated that AMPK may be activated under acute hypoxia (short-term) and become inhibited under prolonged hypoxia (chronic) (De Theije et al., 2018). This places AMPK in the same activation time frame as HIF. In fact, given the protective effects that AMPK and HIF confer under hypoxia, it has been hypothesized that there is crosstalk between these signaling molecules. Most relevant to my thesis, AMPK has been shown to post-translationally regulate ion transporters (see Chapter 3, section II.3. below for additional discussion), while HIF targets the same ion transporters at the transcriptional level (Siques et al., 2018; Tan et al., 2012; Dengler et al., 2019; Kles and Tappenden, 2002). Despite the strong evidence for cross-talk between HIF and AMPK (Salle-Lefort et al., 2016; Abdel et al., 2017; Jung et al., 2008; Minet et al., 2001; Kietzmann et al., 2016; Chandel et al., 2000), an equal number of studies have failed to identify an interaction (Laderoute et al., 2006; Fukuyama et al., 2007; Salminen et al., 2016) or reported an

inhibitory relationship between the two (Faubert et al., 2013; Lyu et al., 2018; Zadra et al., 2015; Seo et al., 2016), suggesting the presence of complex regulatory mechanisms that may be context-specific. Regardless, both AMPK and HIF play a concomitant role in providing protection against hypoxia. While both proteins are activated during the mild, acute hypoxia, AMPK acts to regulate proteins that mediate immediate, short-term adaptation, while HIF regulates transcription of genes useful for hypoxia for long term adaptation.

Given that the enhancer region of *NDRG1* contains HRE, *ndrg1* is likely to be regulated by this transcription factor under hypoxia. Thus, in the early stages of hypoxia, both HIF and AMPK are activated by their respective proximal signals. For HIF, it is the decrease in oxygen level that allows the alpha subunit to escape the hydroxylation and ubiquitination post-translational modifications and be stabilized. With regards to AMPK, the increase in AMP/ATP ratio or rise in ROS following the onset of hypoxia activates a cascade of phosphorylation. Once stabilized, HIF acts as a transcription factor to upregulate necessary genes involved in angiogenesis and glycolysis that allow cells to survive hypoxia. Meanwhile, AMPK may phosphorylate additional kinases or directly phosphorylate cellular targets such as ion transporters thereby triggering their endocytosis and degradation (Gusarova et al., 2009). As these initial hypoxia-responsive signaling pathways are activated, one of the genes upregulated by HIF, *NDRG1* (Wang et al., 2008; Wang et al., 2013), becomes translated and may be further modified by lactate binding (Lee et al., 2015). Interestingly, additional targets of HIF include lactate dehydrogenase (*ldha*) and other genes involved in the glycolysis pathway, which contribute to lactate production. Once translated and potentially modified by lactate, NDRG1 could be

activated to function as an independent, downstream molecule of the AMPK signaling pathway that mediates the downregulation of NKA, among many other potential pathways. Additional discussion between the interaction between NDRG1 and AMPK is examined in Chapter 3, section II.3, below.

II. NDRG1 downregulates the ATP-demanding NKA pump under hypoxia.

My thesis work has demonstrated that NDRG1 is required for the downregulation of the NKA pump following prolonged hypoxia. This finding opens up several interesting possibilities for future research, some of which are translational. One direction would be to investigate whether other NDRG family members have conserved roles in regulating NKA. Given the conserved alpha-beta hydrolase motifs in NDRG members, it is possible that other NDRG members may downregulate NKA under stressful conditions in a tissue-specific manner. Another interesting research topic would be to investigate whether NDRG1 can regulate other ion transporters or even other energetically-demanding molecules belonging to different classes of proteins under hypoxia. A detailed discussion of each of these future directions is provided below.

II.1. Role of NDRGs in other tissues and cell types

NDRG1 is expressed in the pronephros and ionocytes and plays an important role in preserving ATP and promoting survival in these tissues. In Chapter Two, I demonstrated that NDRG1 interacts directly with NKA following prolonged anoxia and is required for NKA intracellular storage or degradation. I propose that this hypoxia response is adaptive and beneficial for tissues in which NDRG1 is expressed and the organism as a whole.

Given that the other NDRG family members (Ndrg1b, 2, 3a, 3b, and 4) are expressed in tissues and organs (Chapter 1, Section III.4) that are more ATP-demanding than the kidney (brain, heart, muscle), it raises the question of whether other members of this family play similar ATP-conserving and survival-promoting roles comparable to NDRG1 in their respective tissues. Considering the specific physiological oxygen concentrations and demands of different tissues and organs, it is possible that NDRGs are tuned specially to the needs of the cells in which they are expressed. It will therefore be interesting to investigate whether NDRGs in other tissues interact with NKA following hypoxia. In addition, future studies should determine whether NDRGs can regulate the expression of NKA to conserve ATP and promote survival.

II.2. Can NDRG1 mediate channel arrest via downregulation of leak channels?

Although this section was covered in Chapter 2, a more detailed discussion is provided below. The degradation of NKA alone can cause edema and therefore is not expected to be adaptive unless it is coupled with a reduction in membrane permeability via downregulation of other ion channels as a two-pronged approach to achieve metabolic suppression and ion homeostasis. There is indirect evidence for channel arrest in zebrafish and we hence hypothesize that Ndrg1a could mediate both energy conservation and reduction in membrane permeability.

To maintain ion homeostasis, anoxia-tolerant organisms are known to reduce membrane permeability via inhibition or reduction in the amount of ion and water channels in response to low oxygen. (Doll, Hochachka, & Reiner, 1991; LaMacchia & Roth, 2015b; Lutz & Nilsson, 1997). This adaptation, known as “the channel arrest

hypothesis" appears to be conserved in zebrafish. The most promising evidence is that the embryos exposed to prolonged anoxia, which downregulate the NKA, do not develop edema. Literature-based evidence also indicates that NDRG1a may mediate channel arrest in addition to down-regulating Na-K-ATPase. In addition, calcium uptake through the epithelial Ca2+ channel (ECAC), is inhibited under low oxygen in zebrafish embryos (Kwong et al., 2016).

A proteomics study in prostate cancer cells identified 58 putative NDRG1-interacting partners, including ATP1a1 (the α subunit of Na^+-K^+-ATPase), CLNS1A (a chloride current regulator), and SLC25A6 (solute carrier family 25) (Tu, Yan, Hood, & Lin, 2007a). Secondly, a recent study investigating molecular adaptation to salinity in cichlid fish noted an inverse correlation between the level of NDRG1, which was reduced in high salinity, and several ion transporters that were up-regulated (Kültz, Li, Gardell, & Sacchi, 2013). These observations raise the possibility that NDRG1 serves as a master regulator for controlling both metabolic suppression (e.g. NKA downregulation) and ion homeostasis (reduction in membrane permeability). It would therefore be interesting to investigate the possible role of NDRG1 as the master regulator of ion transporters under hypoxia.

II.3. Relationship between NDRG1 and AMPK in NKA downregulation.

The downregulation of NKA under hypoxia has been reported to be mediated by AMPK by several studies modeling acute lung disease (Gusarova et al., 2009; Gusarova et al., 2011; Tan et al., 2012). However, the impact of AMPK signaling on NKA levels is context-dependent as other studies have also linked AMPK activation with NKA

stabilization and stimulation (Xiao et al., 2019; Benziane et al., 2012). With respect to the studies implicating AMPK in the downregulation of the sodium-potassium pump under hypoxia, it would be interesting to determine whether NDRG1 is implicated in this molecular pathway, given that the catalytic subunit of AMPK, Prkaa1, is expressed in the pronephros.

First, it is important to understand more generally how NKA is processed for degradation under hypoxia. Many studies have already identified key molecules and PTMs that are required prior to NKA endocytosis and degradation under hypoxia. Two studies showed that protein kinase C zeta (PKC-zeta) directly phosphorylates the alpha1 subunit, ATP1a, at the Ser-18 position (Dada et al., 2003; Chibalin et al., 1999). Furthermore, it was found that mitochondrial (ROS), which are elevated under hypoxia, are sufficient to activate PKC-zeta and trigger endocytosis (Dada et al., 2003). Another report indicated that hypoxia-induced mitochondrial ROS activates the AMPK alpha1 isoform, which directly phosphorylates protein kinase C zeta at the Thr410, resulting in in NKA phosphorylation and endocytosis (Gusarova et al., 2009). Furthermore, another study confirmed that in addition to phosphorylation, endocytosis of NKA was dependent on the ubiquitination of four lysine residues adjacent to Ser-18 on ATP1a (Dada et al., 2007). Interestingly, short-term hypoxia did not reduce the total level of NKA, but it altered the abundance of ATP1a in the membrane (Dada et al., 2003). In contrast, long term hypoxia led to a decrease in total NKA levels (Comellas et al., 2006). These findings suggest that acute hypoxia results in possible endocytosis of NKA, but is not sufficient for its degradation, and that degradation only occurs under prolonged or severe hypoxia. Furthermore, it was found that proteasomal and lysosomal inhibitors can

prevent NKA degradation (Comellas et al., 2006). The figure below summarizes the main steps implicated in hypoxia-induced NKA degradation in human lung cells.

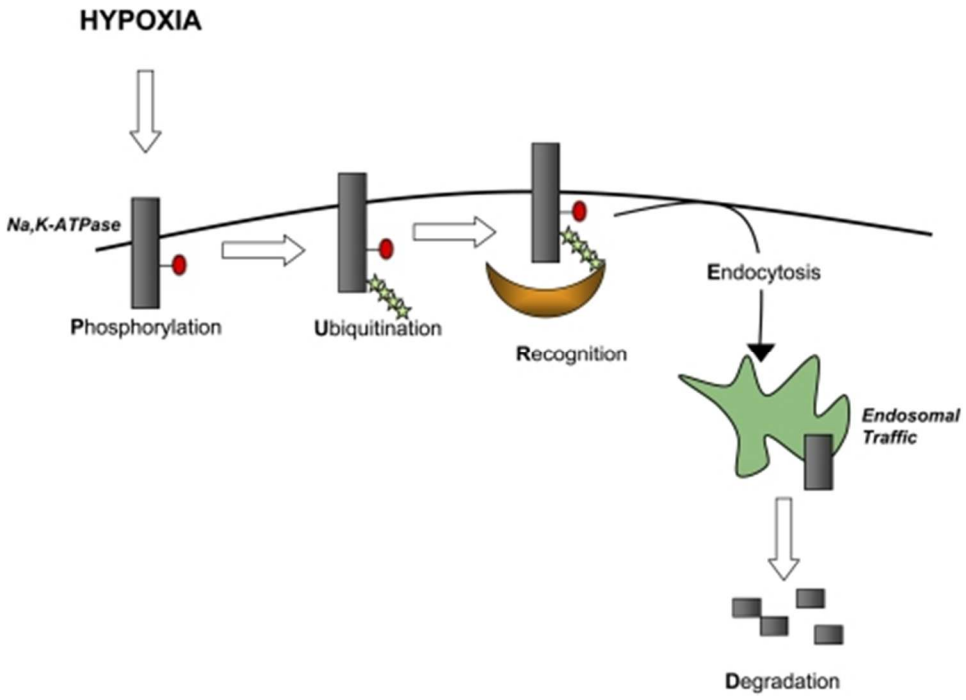

Figure 3.1. Steps required for the degradation of the NKA under hypoxia. The degradation of the NKA under hypoxia follows the PURED pathway: P - Phosphorylation, U - Ubiquitination, R - Recognition, E - Endocytosis, D - Degradation. Image from Helenius et al., 2010.

Of course, the findings described above from the acute lung injury model have to be tested in zebrafish, specifically in zebrafish pronephros. However, we can make an informed model about how NDRG1 may function in zebrafish pronephros and ionocytes based on the findings from these studies.

So where does NDRG1 fit in this molecular pathway? A key paper describing the role of NDRG1 in regulating LDLR revealed a potential role of NDRG1 in regulating membrane proteins. In the study by Pietiainen et al., authors found that silencing NDRG1 in epithelial cells resulted in increased ubiquitination of LDLR, but its degradation was reduced (Pietiainen et al., 2013). Furthermore, LDLR receptor abundance was reduced at the plasma membrane, but was increased in EEA1-positive endosomes. These findings suggest three important roles for NDRG1 in regulating plasma membrane proteins such as LDLR. First, NDRG1 does not play a role in the ubiquitination of LDLR as in the absence of NDRG1, the LDLR were still ubiquitinated. Second, NDRG1 is not required for the endocytosis of LDLR to the EEA1 associated endosomes as LDLR was still endocytosed when NDRG1 was silenced. Third, this study reveals that NDRG1 may be involved in the downstream pathways from the EEA1 associated endosomes that regulate the degradation of LDLR as in the absence of NDRG1, LDLR that were ubiquitinated and endocytosed did not get degraded. Thus based on the LDLR paper (Pietiainen et al., 2013), NDRG1 may not play a role in the ubiquitination of the sodium-potassium pump nor play any post-translational modifications upstream of ubiquitination, including phosphorylation. In addition, this may mean that NDRG1 does not play a role in the initial endocytosis of the sodium-potassium pump, which may be different from my findings with respect to NKA where the protein is not endocytosed in *ndrg1a*-/- mutants

following anoxia. Lastly, in the absence of NDRG1, the NKA is not degraded - which we observe in our studies as well. Thus, with respect to how NDRG1 signaling may be linked with the activity of the AMPK, it appears that AMPK tags the protein for degradation, and NDRG1, in its capacity as a vesicle trafficking regulator and hypoxia sensitive protein, recognizes the tagged protein and orchestrates its endocytosis for either storage or degradation.

Again, this is a potential model and experiments must be performed to confirm this model. We cannot assume that the AMPK is even implicated in NKA degradation in zebrafish. Although the alpha subunit of AMPK is expressed in the pronephros, there is no evidence for its expression in the ionocytes where NKA is also expressed. However, if AMPK is implicated in the downregulation of NKA, it would be very interesting because both AMPK and NDRG1 would function as "oxygen sensors." It is as if the system has multiple checks and balances to ensure that the NKA is not endocytosed and degraded by mistake.

II.4. Does Ndrg3a play a complementary role to Ndrg1a?

In zebrafish, The expression of Ndrg1a and Ndrg3a overlap in the kidney and ionocytes (Le et al., unpublished). However this apparent co-localization is deceptive as sections through the PD reveal that these proteins in fact have a distinct subcellular distribution. Specifically, a key difference in the localization of Ndrg3a is its localization at the apical pole in contrast to that of Ndrg1a, which is broadly distributed throughout the cytosol and cortex. This raises the interesting possibility that NDRGs have specialized functions in regulating distinct subsets of ion transporters and pumps. In renal cells, ion transporters

localize to either the basolateral or apical side - depending on the role that these proteins play in the cell. Given the high homology between Ndrg1a and Ndrg3a coupled with the role of Ndrg1a in downregulating NKA in the basolateral membrane, a potential model is that Ndrg3a downregulates other ion transporters or proteins in the apical membrane. One way to investigate this would be to first identify a potential ion transporter or a protein that interacts with Ndrg3a then investigate an interaction between these proteins. Lastly using LOF tools, the requirement of Ndrg3a in regulating the levels of its binding partner under low O2 conditions can be tested. If Ndrg1a and Ndrg3a are indeed not functionally redundant, a prediction is that the double mutant phenotype would be more severe than either single mutant phenotype alone.

II.5. Role of Ndrg1a in recycling NKA to the membrane post-hypoxia

Since Ndrg1a is an oxygen sensor implicated in NKA endocytosis and intracellular trafficking, it is feasible that Ndrg1a also mediates the recruitment of NKA to the plasma membrane during re-oxygenation.

Although the sodium-potassium pump is already properly localized to the plasma membrane in *ndrg1a* morphants and mutants under normoxia - suggesting that the *de novo* synthesized NKA trafficking to the plasma membrane is not Ndrg1a dependent, hence Ndrg1a may not play a role in the insertion of de novo synthesized ATP1a following reoxygenation.

However, it is possible that Ndrg1a participates in recycling the previously synthesized NKA that are stored in intracellular vesicles or compartments following hypoxia. One experiment to tease apart the role of Ndrg1a in NKA recruitment back to

the membrane following hypoxia would be to deplete the Ndrg1a protein post-hypoxia. Although somewhat technically challenging, an auxin-inducible degrons could be used to conditionally degrade Ndrg1a protein (Yesbolatova et al., 2020; Yamaguchi et al., 2019). Furthermore, to identify the origin of the NKA returning to the membrane following hypoxia, we could use either a protein translation inhibitor such as cycloheximide or a recycling endosome inhibitor.

II.6. Identify the Ndrg1a normoxic and hypoxic interactome and explore the role of NDRG1 as an adapter protein

Several studies have demonstrated that unlike canonical alpha-beta hydrolases, NDRG family members do not contain the catalytic amino acids to be a functional alpha-beta hydrolase. Although the most recent crystal structure study (Mustonen et al., 2020) revealed putative catalytic amino acid presence for the NDRG1, it is still unclear whether NDRG1 may function as a canonical alpha-beta hydrolase (Detail in Chapter 1, section III).

Another study investigating the role of a plant alpha-beta hydrolase, Gibberellin receptor (GID1), which also lacks the alpha-beta hydrolase catalytic domain, provided important insight into the molecular role for this class of hydrolase proteins. In this study, the authors found that GID1 functions as an adapter protein, whose role is to serve as a bridge between several target proteins including 26s proteasome components **(Figure 3.2)** (Mindrebo et al., 2016). Specifically, once the gibberellin hormone binds to the GID1, this NDRG homolog is able to interact with DELLA - the GRAS family transcriptional repressor that represses gibberellin gene pathways. Following the

formation of the GID1-DELLA complex, the E2 ubiquitin conjugation enzyme and E3 ubiquitin-ligase complex are recruited to tag the DELLA protein for degradation. This results in the release of gibberellin hormone signaling inhibition by DELLA and the transcription of genes under gibberellin control occurs. Hence, it is possible that Ndrg1a functions as a similar adapter protein to degrade inhibitors of specific gene transcription, thereby modulating gene expression.

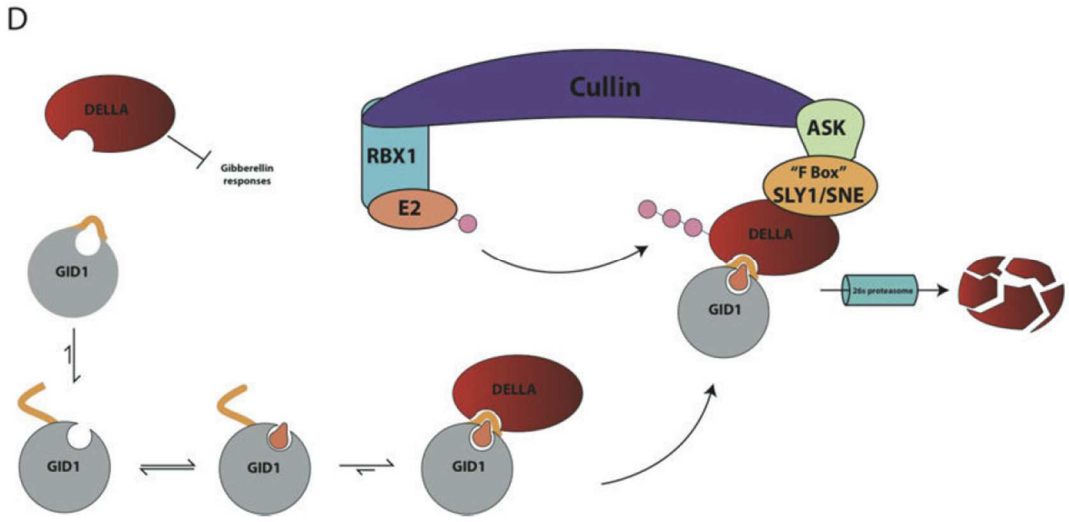

Figure 3.2. Gibberellin hormone-Gibberellin receptor (GID1) signaling pathway. Upon gibberellin hormone binding by the GID1, the GID1-gibberellin complex changes in its conformation and interacts with the DELLA proteins. DELLA proteins are GRAS family transcriptional repressors - named for the conserved DELLA sequence in their N-terminus. The GID1-DELLA complex is then further recruited to SCF (SKP1-like Cul1 F-box) E3 ubiquitin-ligase complex. Subsequently, FBOX proteins are recruited, which are responsible for recruiting E3 ligase substrates destined for 26s proteasomal degradation via polyubiquitination. Specifically, the DELLA proteins are degraded by the 26s proteasome. Interestingly, this degradation allows transcription of genes under gibberellin hormone signaling. Image from Mindrebo et al., 2016.

Our results reveal that NDRG1 and NKA are binding partners and their interaction is increased following exposure to hypoxia or blockage of oxidative phosphorylation. Furthermore, a prostate cancer study investigating NDRG1 binding partners revealed a suite of molecules that are involved in many different aspects of cell function, including cell proliferation, cell adhesion and polarity, transcription, translation, and proteasomal degradation (Tu et al., 2007). In light of this finding, it is tempting to hypothesize that NDRG1 functions as an adapter protein to bring together NKA and components of the proteasomal or lysosomal complex, resulting in NKA degradation under hypoxia. Furthermore, Ndrg1a may mediate the degradation of other energy-demanding proteins such as those involved in transcription or translation to conserve ATP under hypoxia. A future direction of interest would be to investigate whether, in addition NKA, Ndrg1a regulates the level of other proteins under hypoxia.

In particular, it would be worthwhile to directly compare Ndrg1a binding partners under normoxic and hypoxic conditions, using co-IP mass spectrometry. This would not only identify potential new binding partners, but also provide insight on how Ndrgs function. We would be able to assess whether Ndrg1a functions in a similar manner under hypoxia and normoxia or whether Ndrg1a gaines a novel function under hypoxia (via enhanced affinity for distinct binding partners) or both. This experiment builds on the previously described quantitative vs qualitative model.

III. Blockage of oxidative phosphorylation produces lactate as a proximal signal that may activate NDRG1

Considering that the signaling pathway for NKA degradation in the zebrafish pronephros and ionocytes occurs in response to prolonged anoxia, in an *ndrg1a*-dependent manner, we propose that Ndrg1a functions as a molecular switch for hypoxia adaptation. According to the quantitative and qualitative models presented in Chapter One, activation of this switch could either enhance normoxic function of Ndrg1a (quantitative model) or result in altered properties of Ndrg1a (qualitative model). The signaling pathway underlying the activation of Ndrg1a is not understood completely, but it is likely to involve a combination of transcriptional upregulation of *ndrg1a* and ligand binding. One such ligand interaction may be lactate, previously demonstrated to bind to and stabilize NDRG3 in cancer cells, ultimately resulting in the activation of the Raf-ERK signaling pathway and enhanced hypoxia adaptation in cancer cells (Lee et al., 2015).

In Chapter Two, I demonstrated that in zebrafish embryos, increasing intracellular lactate via azide treatment is sufficient to induce NKA degradation under normoxic conditions, similar to the degradation of NKA observed under prolonged anoxia. Hence, lactate may be a proximal signal that activates Ndrg1a according to the qualitative model. However, the effects of azide treatment is not specific to lactate, it may also produce ROS, among other signaling molecules. Hence, the effect of sodium azide treatment may be the culmination of several signaling pathways that are activated following the blockage of the oxidative phosphorylation. Perhaps, injecting lactate directly into the embryo may allow us to address whether lactate alone can downregulate NKA under normoxia.

It would be interesting to test whether lactate alone could precondition cells for enhanced hypoxia adaptation via priming Ndrg1a-NKA interaction under normoxic

conditions. Several observations lend indirect support to the feasibility of this therapeutic approach. Ndrg1-NKA appear to constitutively interact in the posterior PD, which expresses higher levels of NKA than the anterior PD. NKA is likely to be more active in the posterior PD than the anterior PD given that this the region where the majority of Na^+ is reabsorbed owing to NKA activity (Takvam et al., 2021) Hence, the posterior PD may have higher levels of lactate production that could confer pre-conditioning and protection to these cells.

III.1. Other proximal signals that can activate NDRG1

As previously mentioned, normoxic treatment with sodium azide results in elevated lactate levels, which correlate with the degradation of NKA. However, considering that azide is an electron transport chain blocker, lactate may not be the only byproduct of sodium azide application under normoxia. For one, ROS can certainly be produced under normoxia with the blockage of the ETC. As discussed in Chapter 3, section II.3, ROS can trigger AMPK activation, which in turn results in NKA phosphorylation. Subsequently, this can result in potential interaction with its downstream partners that are involved in vesicle trafficking such as the NDRG1. In addition, other potential proximal signaling molecules may be produced in response to ETC blockage or hypoxia.

In our mass-spectrometry study that identified lactate as one of the metabolites that was up-regulated under anoxia, there were several other metabolites whose levels also changed significantly, including SO3- and H2SO4-. It is possible that these metabolites also regulate Ndrg1a activity downstream of hypoxia. Alternatively, they may be involved in other, Ndrg1a-independent adaptive responses. To more directly

identify small molecules that bind to and regulate Ndrg1a, we could use gel filtration chromatography-mass spectrometry . This approach would entail extracting metabolites from zebrafish embryos treated with either anoxia or normoxia (control) and combine them with recombinant Ndrg1a protein. Metabolites that are bound to Ndrg1a could be separated from unbound metabolites using gel filtration chromatography. The remaining metabolites (those that are bound to Ndrg1a) would then be identified by mass spectrometry.

IV. CHAPTER 3 REFERENCES

1. Abdel Malik, R.; Zippel, N.; Frömel, T.; Heidler, J.; Zukunft, S.; Walzog, B.; Ansari, N.; Pampaloni, F.; Wingert, S.; Rieger, M.A.; et al. AMP-Activated Protein Kinase α2 in Neutrophils Regulates Vascular Repair via Hypoxia-Inducible Factor-1α and a Network of Proteins Affecting Metabolism and Apoptosis. Circ. Res. 2017, 120, 99–109
2. Benziane B, Björnholm M, Pirkmajer S, Austin RL, Kotova O, Viollet B, Zierath JR, Chibalin AV. Activation of AMP-activated protein kinase stimulates Na+,K+-ATPase activity in skeletal muscle cells. J Biol Chem. 2012 Jul 6;287(28):23451-63. doi: 10.1074/jbc.M111.331926. Epub 2012 May 18. PMID: 22610379; PMCID: PMC3390622.
3. Chandel, N.S.; McClintock, D.S.; Feliciano, C.E.; Wood, T.M.; Melendez, J.A.; Rodriguez, A.M.; Schumacker, P.T. Reactive oxygen species generated at mitochondrial complex III stabilize hypoxia-inducible factor-1alpha during hypoxia: A mechanism of O2 sensing. J. Biol. Chem. 2000, 275, 25130–25138
4. Chibalin AV, Ogimoto G, Pedemonte CH, Pressley TA, Katz AI, Féraille E, Berggren PO, Bertorello AM. Dopamine-induced endocytosis of Na+,K+-ATPase is initiated by phosphorylation of Ser-18 in the rat alpha subunit and Is responsible for the decreased activity in epithelial cells. J Biol Chem. 1999 Jan 22;274(4):1920-7. doi: 10.1074/jbc.274.4.1920. PMID: 9890946.
5. Comellas AP, Dada LA, Lecuona E, Pesce LM, Chandel NS, Quesada N, Budinger GR, Strous GJ, Ciechanover A, Sznajder JI. Hypoxia-mediated

degradation of Na,K-ATPase via mitochondrial reactive oxygen species and the ubiquitin-conjugating system. Circ Res. 2006 May 26;98(10):1314-22. doi: 10.1161/01.RES.0000222418.99976.1d. Epub 2006 Apr 13. PMID: 16614303.

6. Dada LA, Chandel NS, Ridge KM, Pedemonte C, Bertorello AM, Sznajder JI. Hypoxia-induced endocytosis of Na,K-ATPase in alveolar epithelial cells is mediated by mitochondrial reactive oxygen species and PKC-zeta. J Clin Invest. 2003 Apr;111(7):1057-64. doi: 10.1172/JCI16826. PMID: 12671055; PMCID: PMC152585.
7. Dada LA, Welch LC, Zhou G, Ben-Saadon R, Ciechanover A, Sznajder JI. Phosphorylation and ubiquitination are necessary for Na,K-ATPase endocytosis during hypoxia. Cell Signal. 2007 Sep;19(9):1893-8. doi: 10.1016/j.cellsig.2007.04.013. Epub 2007 May 5. PMID: 17532187; PMCID: PMC2039720.
8. Dengler, F.; Gäbel, G. The Fast Lane of Hypoxic Adaptation: Glucose Transport Is Modulated via A HIF-Hydroxylase-AMPK-Axis in Jejunum Epithelium. Int. J. Mol. Sci. 2019, 20, 4993.
9. De Theije, C.C.; Schols, A.M.W.J.; Lamers, W.H.; Neumann, D.; Köhler, S.E.; Langen, R.C.J. Hypoxia impairs adaptation of skeletal muscle protein turnover- and AMPK signaling during fasting-induced muscle atrophy. PLoS ONE 2018, 13, e0203630.
10. Doll, C. J., Hochachka, P. W., & Reiner, P. B. (1991). Channel arrest: implications from membrane resistance in turtle neurons. The American Journal of Physiology, 261(5), R1321–R1324.

11. Faubert, B.; Boily, G.; Izreig, S.; Griss, T.; Samborska, B.; Dong, Z.; Dupuy, F.; Chambers, C.; Fuerth, B.J.; Viollet, B.; et al. AMPK is a negative regulator of the Warburg effect and suppresses tumor growth in vivo. Cell Metab. 2013, 17, 113–124.

12. Fukuyama, Y.; Ohta, K.; Okoshi, R.; Suehara, M.; Kizaki, H.; Nakagawa, K. Hypoxia induces expression and activation of AMPK in rat dental pulp cells. J. Dent. Res. 2007, 86, 903–907.

13. Grimes, C.J., Petersen, L.H. & Schulze, A. Differential gene expression indicates modulated responses to chronic and intermittent hypoxia in corallivorous fireworms (*Hermodice carunculata*). *Sci Rep* 11, 11110 (2021). https://doi.org/10.1038/s41598-021-90540-9

14. Guillemin K, Krasnow MA. The hypoxic response: huffing and HIFing. Cell. 1997 Apr 4;89(1):9-12. doi: 10.1016/s0092-8674(00)80176-2. PMID: 9094708.

15. Gusarova GA, Dada LA, Kelly AM, Brodie C, Witters LA, Chandel NS, Sznajder JI. Alpha1-AMP-activated protein kinase regulates hypoxia-induced Na,K-ATPase endocytosis via direct phosphorylation of protein kinase C zeta. Mol Cell Biol. 2009 Jul;29(13):3455-64. doi: 10.1128/MCB.00054-09. Epub 2009 Apr 20. PMID: 19380482; PMCID: PMC2698765.

16. Gusarova GA, Trejo HE, Dada LA, et al. Hypoxia leads to Na,K-ATPase downregulation via Ca(2+) release-activated Ca(2+) channels and AMPK activation. *Mol Cell Biol*. 2011;31(17):3546-3556. doi:10.1128/MCB.05114-11

17. Helenius IT, Dada LA, Sznajder JI. Role of ubiquitination in Na,K-ATPase regulation during lung injury. *Proc Am Thorac Soc*. 2010;7(1):65-70. doi:10.1513/pats.200907-082JS

18. Hochachka PW, Lutz PL. Mechanism, origin, and evolution of anoxia tolerance in animals. Comp Biochem Physiol B Biochem Mol Biol. 2001 Dec;130(4):435-59. doi: 10.1016/s1096-4959(01)00408-0. PMID: 11691622.

19. Jung, S.-N.; Yang, W.K.; Kim, J.; Kim, H.S.; Kim, E.J.; Yun, H.; Park, H.; Kim, S.S.; Choe, W.; Kang, I.; et al. Reactive oxygen species stabilize hypoxia-inducible factor-1 alpha protein and stimulate transcriptional activity via AMP-activated protein kinase in DU145 human prostate cancer cells. Carcinogenesis 2008, 29, 713–721

20. Kietzmann, T.; Mennerich, D.; Dimova, E.Y. Hypoxia-Inducible Factors (HIFs) and Phosphorylation: Impact on Stability, Localization, and Transactivity. Front. Cell Dev. Biol. 2016, 4, 11.

21. Kles, K.A.; Tappenden, K.A. Hypoxia differentially regulates nutrient transport in rat jejunum regardless of luminal nutrient present. Am. J. Physiol. Gastrointest. Liver Physiol. 2002, 283, G1336–G1342.

22. Kültz, D., Li, J., Gardell, A., & Sacchi, R. (2013). Quantitative Molecular Phenotyping of Gill Remodeling in a Cichlid Fish Responding to Salinity Stress. Molecular & Cellular Proteomics, 12(12), 3962–3975. https://doi.org/10.1074/mcp.M113.029827

23. Kwong, R. W. M., Kumai, Y., Tzaneva, V., Azzi, E., Hochhold, N., Robertson, C., … Perry, S. F. (2016). Inhibition of calcium uptake during hypoxia in

developing zebrafish is mediated by hypoxia-inducible factor. The Journal of Experimental Biology, 219(24), 3988–3995. https://doi.org/10.1242/jeb.148700

24. Laderoute, K.R.; Amin, K.; Calaoagan, J.M.; Knapp, M.; Le, T.; Orduna, J.; Foretz, M.; Viollet, B. 5'-AMP-activated protein kinase (AMPK) is induced by low-oxygen and glucose deprivation conditions found in solid-tumor microenvironments. Mol. Cell. Biol. 2006, 26, 5336–5347.
25. LaMacchia, J. C., & Roth, M. B. (2015b). Cellular Responses to Hypoxia Aquaporins-2 and -4 regulate glycogen metabolism and survival during hyposmotic-anoxic stress in Caenorhabditis elegans. American Journal of Physiology. Cell Physiology, 309, C92–C96. https://doi.org/10.1152/ajpcell.00131.2015
26. Lavista-Llanos S, Centanin L, Irisarri M, Russo DM, Gleadle JM, Bocca SN, Muzzopappa M, Ratcliffe PJ, Wappner P. Control of the hypoxic response in Drosophila melanogaster by the basic helix-loop-helix PAS protein similar. Mol Cell Biol. 2002 Oct;22(19):6842-53. doi: 10.1128/MCB.22.19.6842-6853.2002. PMID: 12215541; PMCID: PMC134029.
27. Lutz, P. L., & Nilsson, G. E. (1997). Contrasting strategies for anoxic brain survival--glycolysis up or down. The Journal of Experimental Biology, 200(Pt 2), 411–419.
28. Lyu, X.; Wang, J.; Guo, X.; Wu, G.; Jiao, Y.; Faleti, O.D.; Liu, P.; Liu, T.; Long, Y.; Chong, T.; et al. EBV-miR-BART1-5P activates AMPK/mTOR/HIF1 pathway via a PTEN independent manner to promote glycolysis and angiogenesis in nasopharyngeal carcinoma. PLoS Pathog. 2018, 14, e1007484. [

29. Minet, E.; Michel, G.; Mottet, D.; Raes, M.; Michiels, C. Transduction pathways involved in Hypoxia-Inducible Factor-1 phosphorylation and activation. Free Radic. Biol. Med. 2001, 31, 847–855
30. Pietiäinen V, Vassilev B, Blom T, Wang W, Nelson J, Bittman R, Bäck N, Zelcer N, Ikonen E. NDRG1 functions in LDL receptor trafficking by regulating endosomal recycling and degradation. J Cell Sci. 2013 Sep 1;126(Pt 17):3961-71. doi: 10.1242/jcs.128132. Epub 2013 Jun 26. PMID: 23813961.
31. Rybnikova E, Samoilov M. Current insights into the molecular mechanisms of hypoxic pre- and postconditioning using hypobaric hypoxia. Front Neurosci. 2015 Oct 23;9:388. doi: 10.3389/fnins.2015.00388. PMID: 26557049; PMCID: PMC4615940.
32. Sallé-Lefort, S.; Miard, S.; Nolin, M.-A.; Boivin, L.; Paré, M.-È.; Debigaré, R.; Picard, F. Hypoxia upregulates Malat1 expression through a CaMKK/AMPK/HIF-1α axis. Int. J. Oncol. 2016, 49, 1731–1736.
33. Salminen, A.; Kaarniranta, K.; Kauppinen, A. AMPK and HIF signaling pathways regulate both longevity and cancer growth: The good news and the bad news about survival mechanisms. Biogerontology 2016, 17, 655–680. [
34. Semenza GL. HIF-1 and mechanisms of hypoxia sensing. Curr Opin Cell Biol. 2001 Apr;13(2):167-71. doi: 10.1016/s0955-0674(00)00194-0. PMID: 11248550.
35. Semenza GL. HIF-1, O(2), and the 3 PHDs: how animal cells signal hypoxia to the nucleus. Cell. 2001 Oct 5;107(1):1-3. doi: 10.1016/s0092-8674(01)00518-9. PMID: 11595178.

36. Seo, K.; Seo, S.; Ki, S.H.; Shin, S.M. Sestrin2 inhibits hypoxia-inducible factor-1α accumulation via AMPK-mediated prolyl hydroxylase regulation. Free Radic. Biol. Med. 2016, 101, 511–523.

37. Sharp FR, Ran R, Lu A, et al. Hypoxic preconditioning protects against ischemic brain injury. *NeuroRx*. 2004;1(1):26-35. doi:10.1602/neurorx.1.1.26

38. Siques, P.; Brito, J.; Flores, K.; Ordenes, S.; Arriaza, K.; Pena, E.; León-Velarde, F.; López de Pablo, Á.L.; Gonzalez, M.C.; Arribas, S. Long-Term Chronic Intermittent Hypobaric Hypoxia Induces Glucose Transporter (GLUT4) Translocation Through AMP-Activated Protein Kinase (AMPK) in the Soleus Muscle in Lean Rats. Front. Physiol. 2018, 9, 799

39. Takvam M, Wood CM, Kryvi H, Nilsen TO. Ion Transporters and Osmoregulation in the Kidney of Teleost Fishes as a Function of Salinity. *Front Physiol*. 2021;12:664588. Published 2021 Apr 20. doi:10.3389/fphys.2021.664588

40. Tan CD, Smolenski RT, Harhun MI, et al. AMP-activated protein kinase (AMPK)-dependent and -independent pathways regulate hypoxic inhibition of transepithelial Na+ transport across human airway epithelial cells. British Journal of Pharmacology. 2012 Sep;167(2):368-382. DOI: 10.1111/j.1476-5381.2012.01993.x.

41. Tu, L. C., Yan, X., Hood, L., & Lin, B. (2007a). Proteomics Analysis of the Interactome of N-myc Downstream Regulated Gene 1 and Its Interactions with the Androgen Response Program in Prostate Cancer Cells. Molecular & Cellular Proteomics, 6(4), 575–588. https://doi.org/10.1074/mcp.M600249-MCP200

42. Xiao, J., Zhu, S., Guan, H. *et al.* AMPK alleviates high uric acid-induced Na+-K+-ATPase signaling impairment and cell injury in renal tubules. *Exp Mol Med* 51, 1–14 (2019). https://doi.org/10.1038/s12276-019-0254-y

43. Zadra, G.; Batista, J.L.; Loda, M. Dissecting the Dual Role of AMPK in Cancer: From Experimental to Human Studies. Mol. Cancer Res. 2015, 13, 1059–1072.

APPENDIX

I. Background

Many experiments have been performed in an attempt to tease apart the hypoxia proximal molecular signal for developmental arrest in the zebrafish embryo. In this section, I have outlined early hypoxia studies that have not been published but which nevertheless provide interesting insights into hypoxia adaptation. In addition, I have included several findings that contributed to our understanding of NDRG1-NKA but were not included in Chapter 2

II. Generation of *ndrg1a* mutant

The early stages of the NDRG1-NKA study relied heavily on the usage of morpholino to knockdown NDRG1 to study its role under hypoxia. However, with the advent of the CRISPR technology and the ever progressing standards of the zebrafish field, it became necessary to establish a stable *ndrg1a* CRISPR mutant to further characterize Ndrg1a function. Initial thought processes in generating the *ndrg1a* mutants were as follows. First, the guide RNAs that *guide* the Cas9 protein to the genomic site for double stranded cut were designed such that they targeted either early exons or exon-intron junctions. This would allow premature truncation of the NDRG1 protein. Three separate gRNAs were used to target specific genomic locations (2 exon-intron junctions and 1 exon) to increase the likelihood of successful mutant creation. As our results indicate, the exon-intron junction gRNAs were successful in triggering improper splicing, resulting in the deletion of middle exons (Figure A.1). We further confirmed this using an antibody against the middle portion of the NDRG1, which did not detect NDRG1 signal in

western blots or embryos labeled using whole-mount immunofluorescence (Chapter 2, Supplementary figure 1). The CRISPR reaction was so efficient that we observed over 75% complete knockout in F0 (CRISPR RNP injected embryos) somatic cells. The diagram below shows how the F0 CRISPR RNP injected fish were processed to isolate out a homozygous mutant *ndrg1a*, which we named ndrg1a^{mbc1}.

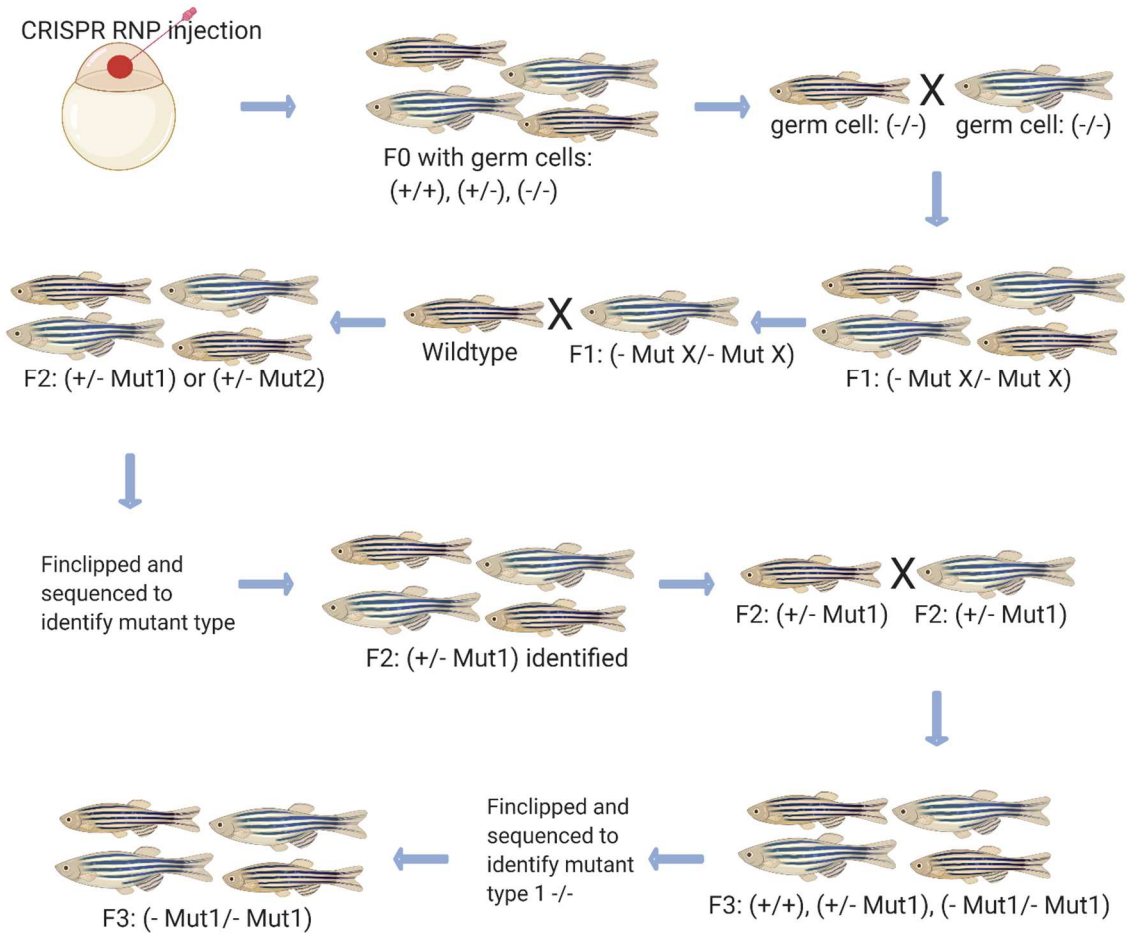

Figure A.1. Schematic of how CRISPR *ndrg1a* homozygous mutant were generated F0 embryos were injected with ribonucleoprotein complexes consisting of 3 gRNAs. The F0 fish were raised to adults and mated 1:1 (male:female) to identify individuals whose germ cells were knocked out for *ndrg1a*. Male and a female germline *ndrg1a* knockout fish were crossed to establish F1 line with (*ndrg1a* mutation 1/mutation 2). F1 individuals were outcrossed to wild type fish to isolate *ndrg1a* mutation 1 or mutation 2 (F2). The F2 individuals (+/*ndrg1a* mut 1 or mut 2) were fin clipped and sequenced to identify mutant alleles. All of the F2 with (+/ *ndrg1a* mutation type 1) were collected and intercrossed to produce F3, whose genetic combinations could be one of: (+/+, +/*ndrg1a* mutation1, or *ndrg1a* mutation 1/*ndrg1a* mutation 1). The F3 individuals were fin clipped and sequenced to identify the homozygous *ndrg1a* -/- with mutation type 1. Image made on Biorender.

III. Development of proximity ligation assay (PLA)

During the early stages of Ndrg1a characterization, it became important to determine whether Ndrg1a was a potential binding partner of NKA in the zebrafish PDand ionocytes. At the time, there was a study which revealed that in human prostate cancer cells, NDRG1 could directly bind to the alpha subunit of NKA, however this was not known to occur in zebrafish.

Early attempts at understanding the interaction between Ndrg1a and NKA relied on i*n situ* hybridization and immunofluorescence experiments, but these results could not definitively provide evidence for interaction between Ndrg1a and the NKA.

Folllowing several unsuccessful attempts to verify Ndrg1a-NKA interaction, we turned to the proximity ligation assay (PLA). This technique allows visualization of the location of potential interactions between two molecules of interest that can be detected by antibodies. However, the established protocol was optimized for cell culture work only and when this protocol was used on the wholemount zebrafish embryo, it resulted in little to no signaling. Thus, through extensive optimization, a new PLA protocol was established to visualize *in situ* potential protein-protein interactions. The protocol below is part of the PLA methods publication manuscript currently in progress.

TITLE

Using Proximity Ligation Assay (PLA) to detect *in situ* protein-protein interactions in the pronephris duct of the zebrafish embryo

ABSTRACT

Understanding the spatial and temporal distribution of protein-protein interactions can reveal important insights into protein function. The *Danio rerio* (zebrafish) is an indispensable vertebrate model organism for studying protein-protein interactions, given its transparency, external embryogenesis, and amenability to different molecular tools. Here, we demonstrate that the proximity ligation assay (PLA) technique used in conjunction with IF can reveal novel spatial-temporal protein-protein interactions in the developing PD of the zebrafish embryo. Results show that proteins that appear to spatially overlap using IF are more clearly detected using PLA. Described here is a protocol for PLA to detect protein-protein interactions in the developing PD of the zebrafish embryo.

INTRODUCTION

Proteins function byinteracting with other proteins in the cell. The binding partners of a protein can reveal the protein's function and its signaling pathway. Such protein-protein interactions (PPIs) form an extensive network of signaling pathways that specify a cell's particular function in the broader context, such as in tissue or organs.

Zebrafish (D. *rerio*) is a vertebrate model organism that is amenable to studying protein-protein interactions. Given its transparent and external embryogenesis coupled with a wide variety of molecular tools available, the zebrafish model organism is a good candidate for visualizing PPIs on the whole organism level.

Given the popularity of zebrafish as a model system, several techniques to study PPIs have already been developed. Co-immunoprecipitation from homogenized zebrafish samples has been established previously to study PPI. However, this technique has

downsides. First, using the homogenized zebrafish sample introduces artificial protein-protein interactions after the lysis of different tissue types that normally do not interact with each other. Second, immunoprecipitation does not address the location of the PPIs.

In addition, co-immunolabeling and analysis of the overlapping ROIs is often used to provide evidence for PPIs. However, this technique also can be misleading due to lack of specificity of the antibody or broad protein distribution that reveal spatial overlap but not direct interaction

The proximity ligation assay (PLA) is a solution to the problems identified above. PLA, similar to immunofluorescence, uses primary antibodies to visualize the proteins of interest. A specialized set of complementary secondary antibodies attached to oligonucleotide probes are used to target the primary antibodies, which are then ligated and fluorescently amplified to visualize the location of the potential PPi.

METHODS AND MATERIALS

DAY 0

1. Zebrafish husbandry

1. Zebrafish are fed daily and kept in zebrafish system water made up of Instant Ocean salt dissolved at 550uS with pH 7.5 and 28.5 degrees Celsius.

2. Spawning and collection of embryos

1. On the afternoon before the experiment, adult zebrafish males and females are placed in a zebrafish spawning tank in a 2:2 ratio with dividers that separate males from females.

2. On the morning of the experiment, dividers are pulled to initiate spawning activity. The spawning event is allowed to occur for 30 minutes before the adults are removed from tanks and embryos collected.

3. The embryos are then placed in a petri dish with the zebrafish system water in the 28.5 degree Celsius incubator overnight until the desired developmental stage is reached (24-48 hours-post-fertilization).

3. Dechorionation and fixation

1. Manually dechorionate 24-48 hpf zebrafish embryos using a pair of forceps under a brightfield microscope. hpf

2. Transfer the dechorionated embryos into a 1.5 ml Eppendorf tube.

3. Remove excess zebrafish system water from the Eppendorf tube. Be careful not to damage the embryos during this process.

4. For 24-48 hpf zebrafish embryos, apply 1 ml of 4% paraformaldehyde (PFA). Incubate at room temperature for 1 hour on a gentle nutator.

5. Remove as much 4% PFA as possible and rinse once with 1ml of 1x PBS for 5 min at room temperature.

DAY 1

4. Blocking

1. Transfer the embryo(s) to a 96-well plate. Separate different experimental groups into each well (limit to 6 embryos per well).

2. Remove as much of the 1ml of 1x PBS from the last step and block embryos with 40 uL of the Duolink blocking reagent (Table of Materials) for 3 hours at room temperature, rotating at 80 RPM.

5. Primary antibody incubation

1. Mix the Duolink antibody diluent (Table of Materials) well by vortexing for 5 seconds.
2. Dilute the primary antibodies against the proteins of interest in the Duolink antibody diluent at (1:100) concentration. Each sample well receives 40 uL of primary antibody solution. Note: It is important to pre-determine the primary antibodies' concentration using an immunofluorescence experiment. The optimization of antibody concentration will determine the PLA results. The primary antibodies should also be from different hosts matched up with the Duolink secondary antibodies (PLA probes).
3. Remove the Duolink blocking solution from the previous step and add 40 uL of primary antibody solution to the wells and incubate overnight at room temperature at 80 RPM.

DAY 2

6. Secondary antibody (PLA probe) incubation

1. Vortex PLUS and MINUS PLA probes (Table of Materials) and dilute the probes 1:5 in the Duolink antibody diluent (Table of Materials). Each sample well will receive 40 uL of secondary antibody solution.
2. Remove primary antibody solution

3. Wash three times with 1x Wash buffer A (Table of Materials) for 30 minutes at room temperature at 80 RPM.

4. Remove the last 1x Wash buffer A and add 40 uL of secondary antibody solution (PLA probes diluted to 1:5 in Duolink antibody diluent) to each well and incubate overnight at room temperature at 80 RPM.

5. After the overnight incubation, move the samples to 37 degrees Celsius incubator for an additional 3 hours still.

DAY 3

7. Ligation

1. Dilute the 5x Duolink ligation buffer (Table of Materials) 1:5 in water to make the ligation solution and mix well. Each sample will take 40 ul of the dilution solution. For each 40ul dilution solution, add 1 ul ligase.

2. Remove the secondary antibody solution and wash each sample three times at 30 minutes each with 1x Wash buffer A (Table of Materials) at room temperature at 80 RPM.

3. Remove the last 1x Wash buffer A and incubate embryos in the ligation solution for 3 hours at room temperature at 80 RPM followed by a still incubation at 37 degrees Celsius for 3 hours.

8. Amplification

1. Remove the ligation solution from the last step.

2. Wash the samples three times for 30 minutes in 1x Wash Buffer A at room temperature at 80 RPM.

3. Dilute 5x amplification buffer (Table of Materials) 1:5 in water to make the amplification solution and mix well. Each sample will take 40 uL of the amplification solution. For each 40 ul amplification solution, add 0.5 ul polymerase.

4. Remove the last 1x Wash buffer A and add the amplification solution and incubate samples for 3 hours at room temperature at 80 RPM, followed by a still incubation at 37 degrees Celsius for 3 hours.

9. Washes

1. Wash samples three times with 100 uL of 1x Wash Buffer B (Table of Materials) for 30 minutes at room temperature at 80 RPM in the dark.

2. Remove the last 1x Wash Buffer B and add 100 uL of 0.01x Wash Buffer B (Table of Materials) for 5 minutes in the dark at room temperature at 80 RPM.

3. Remove the last 0.01x Wash Buffer B and add the final 0.01x Wash Buffer B as a storage buffer.

10. Image acquisition

Note: depending on the Duolink PLA kit purchased, the fluorescence must be detected on the fluorescent microscope's appropriate channel.

IV. Using PLA to detect an Ndrg1a binding partner: Proliferating cell nuclear antigen (PCNA)

Proliferating cell nuclear antigen (PCNA) is often used as a molecular marker to detect cells in the S phase of the cell cycle. Thus, cells expressing PCNA actively synthesize DNA in the nucleus (Leonardi et al., 1992). In addition, PCNA has been shown to play a role in DNA repair (Shivji et al., 1992; Essers et al., 2005).

Interestingly, PCNA was identified in a prostate cancer study performed by Tu and colleagues to identify binding partners of NDRG1 (Tu et al., 2007). To test the newly established PLA protocol on a potential Ndrg1a interacting partner in zebrafish (other than ATP1A1A), PCNA was chosen as a candidate. Using the protocol outlined above, the PLA experiment was performed and confirmed the mass spectrometry study by Tu et al. showing Ndrg1a and PCNA interaction in zebrafish (Figure A.2). Interestingly, the Ndrg1a and PCNA interaction appears to be maintained over anoxia. Given that Ndrg1a downregulates ATP demanding proteins such as NKA under anoxia, it will be interesting to test whether Ndrg1a can downregulate PCNA under anoxia.

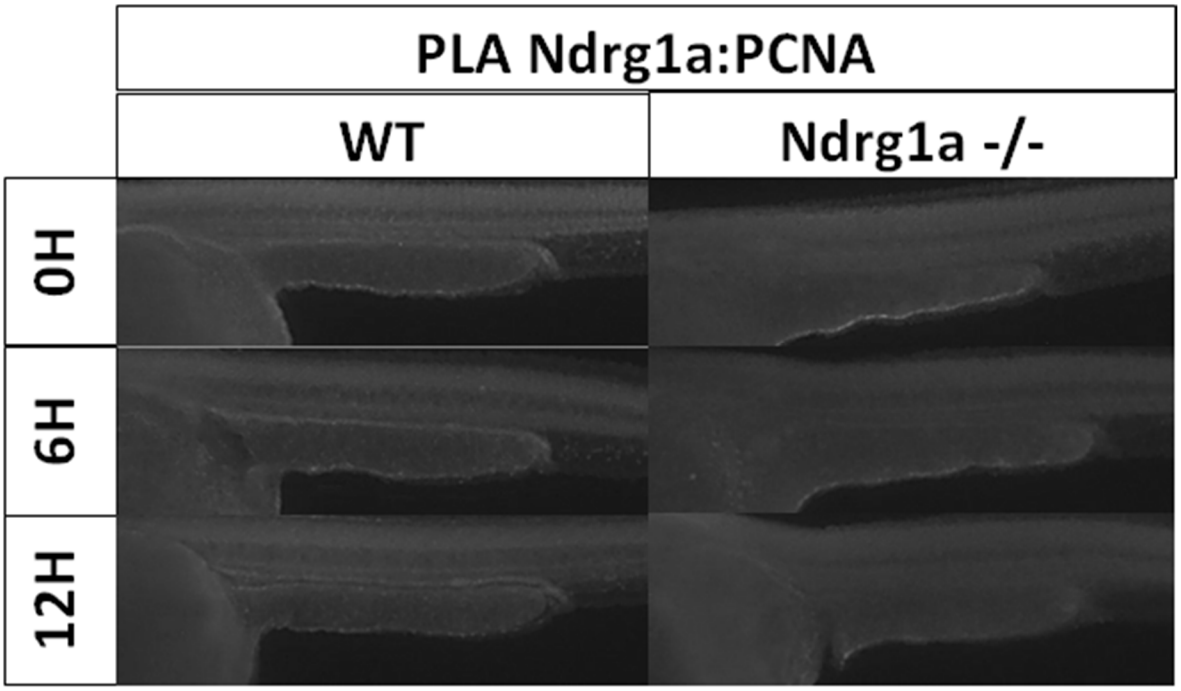

Figure A.2. PLA between Ndrg1a and PCNA under increasing duration of anoxia reveals interaction between Ndrg1a and PCNA. PLA between Ndrg1a and PCNA was performed on 24hpf embryos treated with 0, 6, 12h of anoxia. PLA results show interaction between Ndrg1a and PCNA in WT embryos (left), but no interaction was observed in Ndrg1a mutants (right).

V. Creation of *ndrg3a* mutant

Ndrg1a is broadly expressed in the cytosol and the plasma membrane in the pronephros. However, Ndrg3a is expressed on the apical surface of the pronephros. In order to test the hypothesis that Ndrg3a may play a role in downregulating ion transporters and other energy demanding protein at the apical membrane of the pronephros, CRISPR RNPs have been injected into the animal pole of WT F0 embryos to create CRISPR *ndrg3a* mutants.

The following gRNAs have been used for generation of *ndrg3a* mutants:

gRNA1:

/AlTR1/rCrArArGrCrCrUrCrUrGrCrUrGrArCrCrUrArCrArGrUrUrUrUrArGrArGrCrUrArUrGrCrU/AlTR2/

gRNA2:

/AlTR1/rGrUrCrArCrArUrGrGrArGrCrArCrArCrCrGrUrGrGrUrUrUrUrArGrArGrCrUrArUrGrCrU/AlTR2/

gRNA3:

/AlTR1/rCrArArUrCrUrUrGrUrGrGrArCrArUrUrGrUrGrArGrUrUrUrUrArGrArGrCrUrArUrGrCrU/AlTR2/

Using the NDRG3 antibody (Novus Biologicals, cat# NBP1-86054), I have confirmed the knockout of Ndrg3a in a handful of the F0 embryos injected with the *ndrg3a* CRISPR RNP solution (Figure A.3).

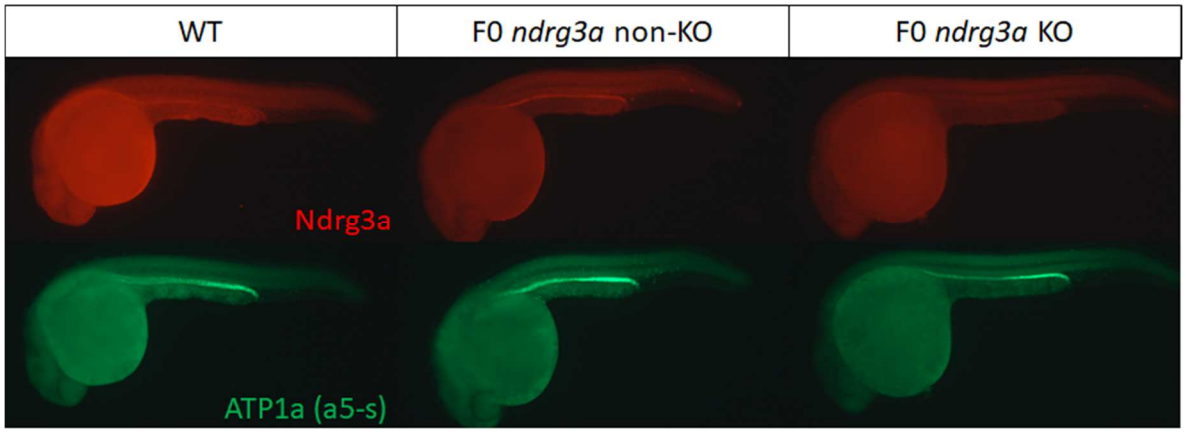

Figure A.3. Immunofluorescence of WT, F0 *ndrg3a* non-KO and KO mutants. Embryos were injected with *ndrg3a* CRISPR RNP solution into the animal pole at 1 cell stage. At 24hpf, embryos were fixed and prepared for immunofluorescence. Immunofluorescence reveals knockout of Ndrg3a in a handful of embryos in the somatic cells of injected F0 embryos. From left to right, WT, F0 *ndrg3a* non-KO embryos, and F0 *ndrg3a* knockout embryos are shown. The F0 *ndrg3a* non-KO embryos show expression of Ndrg3a similar to the WT. All embryos expressed ATP1A in the pronephros, indicating that *ndrg3a* may not be required for initial differentiation of the pronephros up to 24hpf stage of development.

VI. Hydrogen sulfide studies

One prominent working model of oxygen sensing involves a molecule known as hydrogen sulfide (H2S). In the H2S-mediated oxygen sensing model, endogenous H2S is produced in response to decreasing oxygen level where the level of H2S is inversely proportional to the level of oxygen by a balancing activity between H2S production and its oxidation in the mitochondria (Kimura, 2013; Olson, 2011, 2015; Olson et al., 2013). Also, H2S is known to bind to complex IV in the ETC, similar to the chemical ETC blockers that Gitlin laboratory and a group in Novartis had used to block the ETC (Cooper & Brown, 2008) (Figure). In addition, sodium azide, a chemical we used to raise lactate in normoxic embryos, also targets the complex IV in the ETC. In zebrafish, there are three main enzymes which produce endogenous H2S, cystathionine-β-synthase (CBS), cystathionine-γ-lyase (CSE), and 3-mercaptopyruvate sulfurtransferase (3-MST) (Hammers et al., 2015). In zebrafish, CBS and CSE both have two paralogs, while 3-MST only has one. In addition, mRNA expression data from the Zebrafish Information Network (ZFIN) showed that mRNA of CBS and CSE are expressed from the early stages of zebrafish development; while no mRNA expression data exists for 3-MST.

Exogenous H2S causes developmental delay in normoxic embryos.

At the time, I wanted to link the potential oxygen sensor, H2S, with the lactate accumulation as observed under anoxia in order to test whether H2S signaling can potentially activate Ndrgs. As discussed previously, evidence indicates that blockage of ETC causes developmental arrest – suggesting that endogenous signaling molecules may function in this capacity in response to anoxia. First I wanted to test whether H2S alone

can induce developmental arrest in zebrafish embryos. To investigate whether H2S may be a proximal signal to arrest, 4hpf stage zebrafish embryos were subjected to varying concentrations of H2S under normoxia. Preliminary data showed that too much H2S killed the embryos, while too little H2S did not have an effect; however, an optimal concentration was identified, which elicited developmental arrest (Figure A.4). Although the concentration of H2S used in this experiment was much higher than the known physiological concentration of H2S, it was reasoned that much more exogenous H2S must be used to observe the effect of H2S under normoxia as 1. H2S is a highly volatile gas molecule that is easily off-gassed from the media, 2. Embryos are covered in a protective outer shell known as the chorion which reduces H2S penetration and, 3. H2S must further pass through the membrane and cytoplasm to the ETC in the mitochondria. These embryos were able to resume normal development once returned to normoxic water without H2S. For future studies, it would be interesting to test whether H2S treated embryos have increased lactate levels and H2S alone can lead to Ndrg1a-NKA interaction under normoxia.

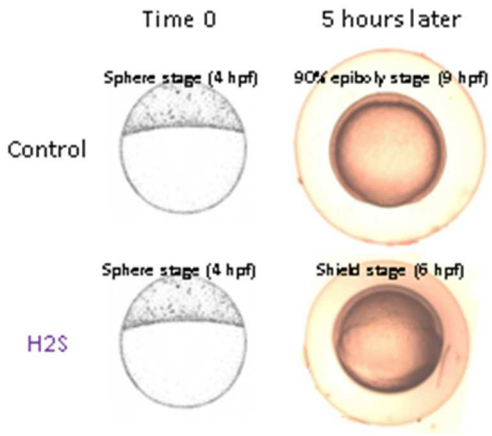

Figure A.4. Exogenous H2S treatment results in delayed development in zebrafish embryos. 4hpf embryos were treated with H2S. H2S treated embryos only developed to 6hpf equivalent developmental stage.

Intriguingly, a previous study demonstrated treatment of H2S in the renal tubular epithelial cells induced an internalization of the sodium potassium pump and the mechanism responsible for this internalization is triggered by sulfhydrolation PTM of cysteines 797 and 798 on the epidermal growth factor receptors (EGFR) (Ge et al., 2014). Interestingly, H2S also inhibited sodium hydrogen exchanger-3 (NHE3) activity in renal tubular epithelial cells. It will be very interesting to test what role H2S plays in regulating ion transporter activity under hypoxia.

VII. Contribution to the *ndrg* expression paper

I was able to contribute to the work investigating the expression pattern of different *ndrg* family members led by Nguyet Le and Timothy Hufford. Specifically, I have contributed to the characterization of Ndrg1a protein expression following increasing duration of anoxia and post-reoxygenation. The latest version of the *ndrg* expression paper entitled, “Differential Expression and Hypoxia-mediated Regulation of the N-myc Downstream Regulated Gene Family" is attached below.

i. **Differential Expression and Hypoxia-mediated Regulation of the N-myc Downstream Regulated Gene Family**

ii. **Hypoxia Regulation of *ndrgs***

iii. Nguyet Le[#1], Timothy M. Hufford[#1], Jong S. Park[1], and Rachel M. Brewster[1*]

iv. 1. Department of Biological Sciences, University of Maryland Baltimore County,

Baltimore, Maryland 21250, USA

# These authors contributed equally to the manuscript

v. * Corresponding author: Department of Biological Sciences, University of Maryland

Baltimore County, Baltimore, Maryland 21250, USA

E-mail: brewster@umbc.edu

Tel: 410-455-3570

vi. **NON-STANDARD ABBREVIATIONS**

NDRG: N-myc downstream regulated gene

HIF-1α: Hypoxia-inducible factor 1 alpha

HRE: Hypoxia response element

PHD2: Prolyl hydroxylase domain protein 2

VHL: von Hippel-Lindau protein

EPO: Erythropoietin

VEGF: Vascular endothelial growth factor

CREB: cAMP-response element binding protein

Myc: Myelocytomatosis proto-oncogene, basic helix-loop-helix transcription factor

NF-kB: Nuclear factor kappa-light-chain-enhancer of activated B cells

STAT: Signal transducer and activator of transcription

Drg1: Downregulated gene 1

Cap43: Calcium-associated protein 43 kDa

Rit42: Reduced in tumor, 42 kDa

RTP: Reducing agents and tunicamycin-responsive protein

PROXY-1: Protein regulated by oxygen 1

AP-1/2: Activator proteins 1 & 2

LAMP1: Lysosomal-associated membrane protein 1

Rab4: Ras-related protein Rab-4A

TNF-α: Tumor necrosis factor alpha

WISH: Wholemount *in situ* hybridization

Igfbp-1: Insulin-like growth factor-binding protein 1

vii. ACKNOWLEDGMENTS

We would like to acknowledge P. Chowdhary and B. Weinstein for their helpful comments on our manuscript. We would also like to acknowledge T. deCarvalho and S. Larson for imaging our samples during the COVID-19 pandemic that limited access to the Keith Porter Imaging Facility. This project was supported by funding from the Department of Defense (W81XWH-16-1-0466) and the National Institute of Health/NICHD (R21HD089476) to R. Brewster. N. Le was supported by a National Institute of Health /NIGMS MARC U*STAR (T34 HHS 00001) National Research Service Award to UMBC. T. Hufford was supported by CBI (NIGMS/NIH T32 GM066706) and IMSD (NIGMS/NIH T32 GM055036) training grants.

viii. CONFLICT OF INTEREST STATEMENT

The authors confirm that there are no conflicts of interest in connection with this article.

ix. AUTHOR CONTRIBUTIONS

N. Le executed the WISH and qPCR experiments and analyzed the data; T. Hufford executed qPCR experiments and validation, plotted and analyzed the qPCR data; J. Park optimized and validated immunolabeling reagents, performed immunolabeling experiments, and analyzed the data; and R. Brewster planned and oversaw the project and analyzed the data; N. Le wrote the first draft of the manuscript, T. Hufford and R. Brewster edited the manuscript.

x. ABSTRACT

Many organisms rely on oxygen to generate cellular energy (adenosine triphosphate or ATP). During severe hypoxia, the production of ATP decreases, leading to cell damage or death. Conversely, excessive oxygen causes oxidative stress that is equally damaging to cells. To mitigate pathological outcomes, organisms have evolved mechanisms to adapt to fluctuations in oxygen levels. Zebrafish embryos are remarkably hypoxia-tolerant, surviving anoxia (zero oxygen) for hours in a hypometabolic, energy-conserving state. To begin to unravel underlying mechanisms, we analyze here the distribution of the N-myc Downstream Regulated Gene (*ndrg*) family, *ndrg1-4,* and their transcriptional response to hypoxia. These genes have been primarily studied in cancer cells and hence little is understood about their normal function and regulation. We show here using *in situ* hybridization that *ndrgs* are expressed in metabolically-demanding organs of the zebrafish embryo, such as the brain, kidney, and heart. To investigate whether *ndrgs* are hypoxia-responsive, we exposed embryos to different durations and severity of hypoxia

and analyzed transcript levels. We observed that *ndrgs* are differentially regulated by hypoxia and that *ndrg1a* has the most robust response, with a nine-fold increase following prolonged anoxia. We further show that this treatment resulted in maintained expression of *ndrg1a* in the kidney, ionocytes, and epiphysis, enhanced expression in the inner ear and *de novo* expression in tissues where *ndrg1a* is not observed under normoxia (somites, head vasculature and mechanosensory cells). These findings provide an entry point into understanding the role of this conserved gene family in hypoxia adaptation of normal cells.

KEYWORDS

NDRG, hypoxia, hypometabolism, gene expression, zebrafish

xi. INTRODUCTION

Earth's atmosphere is composed of approximately 21 percent oxygen (O_2). Aerobic organisms use this environmental O_2 to produce ATP during oxidative phosphorylation. Hence fluctuations in O_2 levels, either up or down, can have very detrimental outcomes for aerobic organisms. Severe hypoxia causes a decrease in ATP production due to diminished activity of the electron transport chain. Given that ATP fuels energy-

demanding processes in the cell, its reduction can lead to cellular damage or death (1-4) . Thus, hypoxia, hypoxemia or ischemia, is a contributing cause to many disease states in humans, including pulmonary vascular disease, acute kidney injury, neurodegenerative disease, and stroke (5-10). Conversely, excessive O_2 is equally, if not more harmful as it causes oxidative stress due to reactive oxygen species production that is damaging to macromolecules, including lipids, proteins, and nucleic acid (11-13).

To mitigate these adverse consequences, aerobic organisms have evolved mechanisms to adapt to low O_2 and maintain homeostasis. Such adaptations optimize access to O_2 by increasing red blood cell count and angiogenesis and altering energy metabolism in part by switching from oxidative phosphorylation to glycolysis (14, 15). In addition, cells conserve energy when exposed to chronic and severe hypoxia by reducing their metabolic rate. The latter is accomplished via suppression or arrest of energetically-demanding processes such as cell division, transcription and translation and down-regulating the activity of the sodium-potassium ATPase pump (16-23). While metabolic suppression has primarily been studied in organisms considered anoxia-tolerant, including painted turtles, crucian carp, naked mole rats and hibernating ground squirrels (16, 24), it is likely to also be utilized in other organisms as well, albeit to a lesser extent. Zebrafish (*Danio rerio*) embryos maintain homeostasis under anoxia (zero O_2) by entering into a hypometabolic state characterized by reversible developmental and physiological arrest, which enables them to survive for up to 50 hours (25, 26). This protective response is developmentally regulated, with older embryos being less tolerant to anoxia (26).

Despite the necessity to conserve energy via suppression of transcription and translation, genes that are vital for the hypoxia response are in fact transcriptionally up-regulated under hypoxia (27-30). Such up-regulation is mediated by several transcription factors, the best studied of which is the Hypoxia-Inducible Factor-1α (HIF-1α) (31-33). Under normoxic conditions (normoxia), the HIF-1α subunit is hydroxylated by prolyl hydroxylase domain protein 2 (PHD2), marking it for degradation by the von Hippel-Lindau protein (VHL). However, when O_2 levels are reduced, PHD2 activity is inhibited and stabilized HIF-1α binds to the HIF-1β subunit and translocates to the nucleus to regulate transcription. Upon entry into the nucleus, HIF-α/β heterodimers bind the hypoxia-response element (HRE). Even though this sequence is abundant in the genome, fewer than 1% of potential HRE sites are bound by the HIF complex under hypoxia, suggesting the existence of another layer of regulation (34-37). HIFs directly activate genes that mediate metabolic reprogramming from oxidative phosphorylation to glycolysis (38, 39) and genes that increase the available O_2 supply, such as *EPO*, *VEGF* and its receptors (40). Other HIF targets are implicated in autophagy, apoptosis, redox homeostasis, inflammation and immunity, stemness and self-renewal, metastasis and invasion (35, 39, 41, 42). In addition to HIFs, several other transcription factors are known to influence the hypoxia response, including CREB, Myc, NF-kB, and STATs, which engage in cross-regulatory interactions with HIFs (32).

Members of the N-myc downstream regulated gene (NDRGs) family are also hypoxia-responsive. The mammalian family consists of 4 members, *NDRG1-4*, while the zebrafish genome with its third round of genome duplication, encodes 6 paralogues, *ndrg1a*, *1b*, *2*, *3a*, *3b*, and *4* (43). NDRGs are highly conserved across metazoans and the

sequence homology is in fact greater for specific members of the family across different species (> 80%) than between NDRG family members of the same species, which share ~ 57–65% amino acid identity (44). NDRGs belong to the α/β-hydrolase family, however they are thought to be enzymatically inactive, lacking a critical catalytic triad (45). NDRG1 (formerly known as Drg1, Cap43, Rit42, RTP, and PROXY-1) contains three tandem repeats (GTRSRSHTSE) near its C-terminal and a phosphopantetheine sequence, which are two unique features that make it distinct from other NDRG family members. NDRG1 is thought to function as a tumor suppressor (46). However, the absence of cancer resultant from germline mutations in humans (47) and targeted knockout in mice (48), suggests that *NDRG1* may rather be involved in cancer progression (metastasis) rather than initiation (49-54). Human NDRG1 interacts with numerous other proteins in human cancer and other cell lines, including actin, Clathrin and associated proteins AP-1 and AP-2, Caveolin-1, Kinesin, LAMP1, Rab4, and 26S proteasome components (49, 51, 55, 56), consistent with a possible role in regulating vesicle trafficking (56, 57). *NDRG1* and *NDRG2* transcript levels increase under hypoxia, as these genes have HIF-1α binding sites (hypoxia-response elements or HREs) in their promoters (58-61). However, NDRG regulation under hypoxic conditions is complex and does not depend solely on HIF-1α, as several other transcription factors (62, 63) and *NDRG1* long non-coding RNA itself (64, 65) have also been implicated. *NDRG4* is transcriptionally up-regulated under hypoxia in cancer cells, however in a TNF-α/NF-κB rather than a HIF-1α -dependent manner (66). In contrast, NDRG3 is regulated post-translationally in hypoxic cancer cells, via lactate binding, which stabilizes the protein and promotes cell proliferation and angiogenesis

(67). These findings indicate that NDRGs are regulated at the transcriptional and post-translational levels in response to hypoxia and promote adaptation to low O_2.

To date, NDRGs have mostly been studied in cancer cells and far less is known about their normal role and regulation. However, significant insights into their function are likely to result from the recently solved crystal structures of *NDRG1, 2,* and *3* (68-70). While all members of this family can be regulated in response to fluctuations in O_2 levels, it is unclear what range and duration of hypoxia they respond to. Lastly, even though the spatial distribution of *NDRG* family members has been analyzed in zebrafish (71, 72) and frog (*Xenopus laevis and tropicalis*) embryos (43, 73, 74) and mammals (75-83), it is unclear whether their spatial distribution changes under low O_2. We report here on the spatial distribution of members of the zebrafish Ndrg family and their regulation in response to hypoxia.

MATERIALS AND METHODS

Zebrafish

Zebrafish (*Danio rerio*) were raised and housed at 27°C on a 14/10 hour light/dark cycle. Zebrafish used in this study were the wild-type AB strain. Embryos were obtained by breeding male/female pairs. Maintenance of zebrafish and experimental procedures on larvae and adult zebrafish were performed in accordance with the protocol approved by the Institutional Animal Care and Use Committee (IACUC) at the University of Maryland Baltimore County. Zebrafish embryos (raised in normoxia) were staged and

sorted according to Kimmel *et al.* 1995 (84). See Supplementary Figure 2 for staging of anoxia-treated embryos.

Hypoxia & anoxia treatments

For wholemount *in situ* hybridization (WISH), 24 hours post-fertilization (24 hpf) zebrafish embryos were dechorionated and then placed in 100 mm petri dish (CellTreat, Pepperell, MA, USA, Cat# 229663) containing 0% or 3% O_2 system water in an O_2 control glove box (Plas-Labs, Lansing, MI, USA model # 856-HYPO) set at 0% or 3% O_2 and 27°C. Following hypoxia treatment, embryos were placed into 1.5mL microcentrifuge tubes (~ 20 embryos/tube) with excess water removed. Embryos in each microcentrifuge tube were removed from the chamber and fixed in 4% paraformaldehyde (PFA) in phosphate buffer saline (PBS) (Thermo Scientific, Waltham, MA, USA Cat# J19943-K2) at 4°C overnight. Fixed embryos were rinsed in absolute methanol (Thermo Fisher Scientific, Waltham, MA, USA, CAS# 67-56-1) for 10 min at room temperature and stored in absolute methanol at -20° C.

For Real-time PCR (qPCR), stage-matched control embryos were placed in 100 mm petri dishes containing 0% or 3% O_2 system water, placed in the O_2 control glove box set at 0% or 3% O_2 and 27°C. Following 4 h and 8 h of treatment, single embryos were placed into 1.5 mL microcentrifuge tubes (Stellar Scientific Ltd Co, Albuquerque, NM, USA, Cat# T17-100) with excess water removed. Single embryos in the microcentrifuge tubes were taken out of the chamber, flash frozen in liquid nitrogen, and stored at -80°C for total RNA extraction. Embryos raised under normoxic conditions

were used as stage-matched controls for 3% O_2 (27 hpf for 4 h and 30.5 hpf for 8 h) and anoxia (26 hpf for 4 h and 27 hpf for 8 h) treatments.

Riboprobe synthesis

The PCR template was cDNA synthesized from total RNA extracted from a combination of 6 hpf, 24 hpf and 48 hpf zebrafish embryos. RNA extraction was performed with the QuickRNA MicroPrep Kit (Zymo Research, Irvine, CA, USA Cat#R1051) and cDNA synthesis was carried out using the iScript cDNA Synthesis Kit (Bio-Rad, Hercules, CA, USA Cat# 1708890) according to the manufacturers' instructions.

PCR reactions were prepared using 1 µl of diluted (1:5) cDNA as template in a total volume of 50 µl. Primer concentrations were 10 µM for each oligonucleotide. PCR-fragments were produced using a C1000 Thermal Cycler (Bio-Rad, Hercules, CA, USA Cat#1851148) and Phusion-Polymerase (Thermo Scientific, Vilnius, LT, F530S) (35 cycles and 57°C annealing temperature). PCR-fragments were gel-purified using Micro Bio-Spin P-30 Gel columns Tris Buffer (RNase-free)(Bio-Rad, Hercules, CA, USA Cat#7326250) and subsequently, 300-500 ng were used as template DNA to synthesize antisense RNA probes using *in vitro* transcription with the mMESSAGE mMACHINE T7 Transcription Kit (Thermo Fisher Scientific, Carlsbad, CA, USA Cat#AM1344), incorporating digoxigenin (DIG)-UTP via a DIG-labelling kit (Roche, Mannheim, Germany Cat#11277073910).

To avoid amplification of regions of homology between *ndrg* members, all oligonucleotide primer pairs were designed against the 3'UTR of each gene, with the exception of *ndrg2* for which the primer pairs targeted the coding region (spanning exons

11-16) as well as the 3'UTR, as specified in Li *et al.* 2016 (71). For antisense probes, a T7 promoter sequence **(5'- TAATACGACTCACTATAG-3')** was added to the 5' end of each reverse primer. The following primer sets were used to amplify cDNA for 35 cycles as follows:

ndrg1a forward: 5'-ACCAATCAGTTCTGACTGTGCTGC-3'

ndrg1a reverse: 5'-

TAATACGACTCACTATAGCACTCCCAACATGGAAAACGCAGA-3'

ndrg1b forward: 5'-ACACGCCTCAGCAGTTTAATCTGG-3'

ndrg1b reverse: 5'-

TAATACGACTCACTATAGCTCACTGAAGTCTTGCACAACCAG-3'

ndrg2 forward: 5'-ACAACACGTTCAAATGCCCG-3'

ndrg2 reverse: 5'-**TAATACGACTCACTATAG**GGAAGACATGAGCTGGCTGT-3'

ndrg3a forward: 5'-GGTCTTCCAACTGGTTTGAGATGC-3'

ndrg3a reverse: 5'-

TAATACGACTCACTATAGTGAGAACCAGTGGACAGTGACACT-3'

ndrg3b forward: 5'-GCCAGAGAGTGCTGGTCTAATGAA-3'

ndrg3b reverse: 5'-

TAATACGACTCACTATAGCCGAGACATGCTAATCAGTAGCTC-3'

ndrg4 forward: 5'-GACTTGCGTCAGGGATGATAACCT-3'

ndrg4 reverse: 5'-

TAATACGACTCACTATAGGAATGAGTGAGAGCAAGGGCCGAT-3'

Wholemount RNA *in situ* hybridization

Normoxic controls were fixed at desired stages (shield, 15 somites, 24 hpf, and 48 hpf) in 4% PFA in PBS (Thermo Scientific, Waltham, MA, USA Cat# J19943-K2) at 4°C overnight. Anoxia-exposed 24 hpf embryos were treated as described in the anoxia treatment section above. To prevent pigmentation from masking the WISH signal, embryos fixed after 24 hpf were incubated in 0.003% 1-phenyl-2-thiourea (PTU) (Sigma-Aldrich, Milwaukee, WI, USA Cat# P7629-100G) at 24 hpf until the time of fixation. WISH was performed on both normoxic and anoxic embryos using DIG labeled antisense probes according to the specifications published by Thisse and Thisse (2008) (85). Briefly, embryos were rinsed in PBS (137 mM NaCl, 2.7 mM KCl, 8.8 mM Na2HPO4) with 0.1% Tween-20 (Sigma-Aldrich, Milwaukee, WI, USA CAS# 9005-64-5). Proteinase K (10 µg/ml)(Sigma-Aldrich, Milwaukee, WI, USA CAS# 39450-01-6) treatment was performed for 10 min (24 hpf), 12 min (27 hpf control and 24 hpf + anoxia-treated), and 30 min (48 hpf) embryos. Embryos were then hybridized with DIG labeled antisense probes (*in situ* hybridization mix with 5% Dextran Sulfate (EMD Millipore Corp., Billerica, MA, USA Cat#S4030)) at 70°C overnight. Following hybridization, excess probe was removed by washing embryos in a saline-sodium citrate (SSC) series (Thermo Fisher Scientific, Waltham, MA, USA, Cat# AM9763). For probe detection, alkaline phosphatase-conjugated antibody (Roche Diagnostics, Mannheim, Germany Cat# 11093274910) diluted (1:5,000) in pre-incubation (PI) buffer (PBS, 0.1% Tween 20, 2% sheep serum, 2mg/ml BSA (Thermo Fisher Scientific, Waltham, MA,

USA, CAS# 9048-46-8) was added and incubated at 4°C overnight. 5-bromo-4-chloro-3-indolyl-phosphate (BCIP) (Roche, Mannheim, Germany Cat#11383221001) was used in conjunction with nitro blue tetrazolium (NBT) (Roche, Mannheim, Germany Cat#11383213001) for the colorimetric detection of alkaline phosphatase activity. When the signal was optimal, the reaction was stopped by washing in PBS with 0.1% Tween-20 and rinsed in 4% PFA overnight.

Vibratome sectioning, microscopy, and imaging

Following WISH, embryos were embedded in 4% low melt agarose (IBI Scientific, Peosta, IA, USA, Cat# IB70050) in PBS (100 g/ml) and sectioned using a vibratome (Vibratome,1500) set at 40µm thickness. Cross sections were mounted on glass slides in 50% glycerol (Sigma-Aldrich, Milwaukee, WI, USA, Cat# G7757-1GA) under cover slips.

Zebrafish embryos were mounted for imaging from a lateral or dorsal view on slides, in a drop of 4% w/v methylcellulose (Sigma Aldrich, Milwaukee, WI, USA, Cat# 274437-500G) in 1X E3 medium (5mM NaCl, 0.17mM KCl, 0.33mM CaCl2, and 0.33mM MgSO4)(for zebrafish embryo). Bright-field images were captured using an AxioCam HRc 503 CCD camera mounted on an Axioskop (Carl Zeiss, Oberkochen, Germany). Images were corrected for brightness and contrast along the entire image, and for comparison of normoxia and anoxia treated embryos the images were adjusted equally.

Real-time quantitative PCR

RNA extractions and cDNA synthesis were carried out using single embryos collected at the appropriate developmental stage for the stage-matched controls and immediately following treatment for anoxia- and 3% O_2-treated embryos. RNA extractions were performed using the QuickRNA MicroPrep Kit (Zymo Research, Irvine, CA, USA Cat#R1051). cDNA was synthesized from 100 ng total RNA using iScript cDNA Synthesis Kit (Bio-Rad, Hercules, CA, USA Cat# 1708890) according to the manufacturers' instructions. The cDNA samples were diluted 1:10 with nuclease-free water (Life Technologies Corp., Austin, TX, USA, Cat# AM9937). qPCR experiments were carried out with a CFX96 Touch Real-time qPCR Detection System (Bio-Rad, Hercules, CA, USA) using the SsoAdvanced Universal SYBR Green Supermix (Bio-Rad, Hercules, CA, USA Cat# 172-5271).

We tested a panel of candidate reference genes for the q-PCR analysis, including *ef1a*, *b-actin*, *rpl0*, *rpl13a*, and *ube2a*, which were previously demonstrated to be stable across zebrafish developmental stages and/or following harsh chemical treatments (27, 86-88). Among these, *rpl0*, *rpl13a*, and *ube2a* did not amplify sufficient cDNA in 40 cycles and were not pursued further. *ef1a* and *b-actin* have both been used as reference genes for zebrafish hypoxia studies specifically (27, 87) and their transcripts were sufficiently abundant at 24 hpf. We selected *ef1a* for all experiments described below. Oligonucleotide primer pairs spanned regions common to all *ndrg* splice variants, with the exception of *ndrg1b* and *ndrg2*, which only have one variant. The PCR primer efficiency of each primer pair was assessed using cDNA dilution curves and values of 96-104% were obtained for all except *ndrg1b*, which did not amplify efficiently (consistent with the lack of gene expression at 24 hpf observed using WISH and reported by others

(89)). Amplification specificity was determined following each run as the presence of a single melt peak for each transcript. The following primer sets were designed using Primer-BLAST and used to amplify cDNA for 40 cycles:

ndrg1a forward: 5'-ATCATGCAGCACTTCGCTGT-3'

ndrg1a reverse: 5'-CAATAGCCATGCCGATCACA-3'

ndrg1b forward: 5'-CATGGGCTACATGCCCTCTG-3'

ndrg1b reverse: 5'- TGACCCGATGAACTGTGCTC-3'

ndrg2 forward: 5'-AGCTGGAAAGAAAGTGCGAGA-3'

ndrg2 reverse: 5'-TTTACGCCGTCCGCTTATGT-3'

ndrg3a forward: 5'-GGACTAGCAATCTTGTGGAC-3'

ndrg3a reverse: 5'-TCTCGATTCCGAGGTCTTGA-3'

ndrg3b forward: 5'-GTCAGGCTTGATGATGGATG-3'

ndrg3b reverse: 5'-CCCTCTCAAAGTCACATGAAGG-3'

ndrg4 forward: 5'-AGCCAGCTATTCTGACCTAC-3'

ndrg4 reverse: 5'-GATATCCTTGAGGCATCTGG-3'

ef1α forward: 5'- TACCCTCCTCTTGGTCGCTT-3'

ef1α reverse: 5'- TGGAACGGTGTGATTGAGGG-3'

Reactions were run in triplicate with 7-8 biological replicates, using 1 µl of diluted cDNA as template in a reaction volume of 20 µl. For all *ndrg4* reactions, 2 ul of stock cDNA was used as template. Primer stock concentrations were 10 µM and working concentrations were 0.5 µM for each oligonucleotide (Thermo Fisher Scientific, Waltham, MA, USA). The following annealing temperatures were used for each target gene primer set: 57.0°C for *ndrg1a,* 56.6°C for *ndrg2,* 53.0°C for *ndrg3a,* 55.0°C for *ndrg3b,* and 51.0°C for *ndrg4.* Evaluation of results was performed with the CFX96 Touch RT-PCR Detection System program (Bio-Rad, Hercules, CA, USA) and using GraphPad Prism 8 & 9 software (Prism, San Diego, CA, USA). The presence of outliers was assessed using both Grubbs' (alpha = 0.05) and ROUT (Q = 1%) methods. Outliers identified with both Grubbs' (alpha = 0.05) and ROUT (Q = 1%) methods and were further inspected and handled as follows (90, 91). Outliers with Ct values that could not be attributed to experimental error (improper dilution, amplification failure) for a particular group were included, as the variation could be attributed to biological variation. Outliers with Ct values over 40 (e.g. a technical replicate for which amplification did not occur properly) were not further analyzed, and any biological replicates for which two or more technical replicates of the reference or target gene failed to amplify were entirely excluded from the analysis.

RESULTS

The spatial distribution of the *ndrg* family during early development

The zebrafish genome encodes 6 homologs of the *ndrg* family: *ndrg1a* (ENSDARG00000032849), *ndrg1b* (ENSDARG00000010420), *ndrg2* (ENSDARG00000011170), *ndrg3a* (ENSDARG00000013087), *ndrg3b* (ENSDARG00000010052), and *ndrg4* (ENSDARG00000103937). To characterize the members of the *ndrg* family, we began by determining their spatial distribution in early-stage zebrafish embryos, using wholemount *in situ* hybridization (WISH). Since several members of this family contain large overlapping coding sequences (53-65% homology), riboprobes were designed that bind to non-conserved regions in the 3'UTR of all *ndrgs,* with the exception of *ndrg2*. Due to issues with the amplification of the *ndrg2* 3'UTR, we used instead a riboprobe complementary to the coding region and 3'UTR of this gene that has low homology with other *ndrg* members (71).

At the shield stage (6 hpf), *ndrg1a* expression is ubiquitous (Fig. 1A). During segmentation (15-somites), *ndrg1a* becomes restricted to the pronephric ducts (embryonic kidney) and ionocytes (also known as mucous cells) (Fig. 1B, C); these cell types serve the common function of maintaining osmotic homeostasis by filtering ions across the plasma membrane. *ndrg1a* is also observed in the yolk at this stage of development (Fig. 1B). At 24 hpf *ndrg1a* is weakly expressed in the epiphysis (embryonic gland that produces melatonin), in addition to the pronephric duct, ionocytes and caudal vein (Fig. 1D, E) and by 48 hpf, *ndrg1a* is observed in corpuscles of Stannius (endocrine glands in the kidney), liver, intestinal bulb, retina, and other brain regions (Fig. 1F, G). The expression of *ndrg1b* is very dynamic. At the shield stage, it is ubiquitously expressed (Fig. 1H), while by 15-somites and 24 hpf, it is no longer detected (Fig. 1I-L). In contrast, at 48 hpf, *ndrg1b* is strongly expressed in the retina (Fig. 1M,N). The expression of *ndrg2* is ubiquitous at

shield stage (Fig. 2A) and remains broadly distributed by 15-somites, in the embryo proper and the yolk (Fig. 2B, C). At 24 hpf, *ndrg2* is strongly expressed in the brain, retina, spinal cord and intermediate cell mass of the mesoderm (where hematopoiesis occurs) (Fig. 2D, E). At 48 hpf, *ndrg2* expression expands to the pectoral fin buds, somites and the heart, with basal levels observed throughout the embryo (Fig. 2F, G). *ndrg3a* is broadly expressed at the shield stage (Fig. 3A) and is observed in the head region and pronephric ducts at 15-somites (Fig. 3B, C). At 24 hpf (Fig. 3D, E), *ndrg3a* is also seen in pharyngeal pouches, pectoral fin buds and somites. By 48 hpf, *ndrg3a* signal is detected in the brain, cranial placodes, and the spinal cord in addition to the pronephric ducts and associated corpuscles of Stannius (Fig. 3F, G). *ndrg3b* signal is not detected between shield stage and 24 hpf (Fig. H-L); however, at 48 hpf it is observed in the brain and, at lower levels, in pectoral fin buds (Fig. 3K,L). At the shield stage, *ndrg4* is expressed ubiquitously (Fig. 2H) but becomes enriched in somites by the 15-somites stage (Fig. 2I, J). At 24 hpf and 48 hpf (Fig. 2K-N), *ndrg4* transcript is detected in the brain, the heart, the cranial placodes, the somites, the spinal cord, the pectoral fin buds, the intermediate cell mass of the mesoderm, and proctodeum.

Normoxic control groups that account for hypoxia-induced developmental delays

To gain an understanding of the transcriptional regulation of *ndrgs* in response to low O_2, we exposed 24 hpf embryos to two different hypoxic conditions (3% and 0% O_2) for 4 or 8 hours and analyzed transcript levels using qPCR (results presented in section below). Given that O_2 deprivation delays or arrests zebrafish development, an important consideration for these experiments is the appropriate normoxic control group to use, which we have designated as: time zero, age-matched and staged-matched normoxic

controls. Time zero controls are embryos that are the same age as the experimental group at the onset of treatment (i.e. 24 hpf). Age-matched controls are the same age (hpf) as the experimental groups (28 hpf for embryos subjected to 4 hours of hypoxia and 32 hpf for embryos exposed to 8 hours of hypoxia. Stage-matched controls are embryos at the same developmental stage as the experimental groups exposed to 4 or 8 hours of hypoxia; the stage of development varies depending on the severity of the treatment, as embryos arrest faster under anoxia.

With respect to anoxia, when using time zero controls, qPCR results revealed that transcript levels were significantly up-regulated for *ndrg1a* following 4 and 8 hours of treatment (3 and 8-fold up-regulation, respectively), while other members of the *ndrg* family increased to a lesser extent (2-fold or less) (Fig. S1A). In contrast, the use of age-matched controls resulted in a different outcome, with *ndrg1a* and *3a* being significantly up-regulated following 4 and 8 hours of anoxia while *ndrg2*, *3b* and *4* were down-regulated (Fig. S1B). These differences in transcript levels using time zero and age-matched normoxic controls are most likely explained by dynamic gene expression during development, consistent with RNA Seq repository data (EMBL Zebrafish Expression Atlas)(89) showing that *ndrg* expression levels change significantly between 24 and 48 hpf. Based on these observations, the most appropriate normoxic control would be one that takes into account the developmental stage of the experimental group, i.e. a stage-matched control.

Several criteria were used to match the developmental stages of experimental groups: the overall length of the embryo, the length of the yolk extension, head curvature, and level of pigmentation of the eye and the body (Fig. S2). Based on these criteria, the

following normoxic control groups were selected (where = indicates "best matched to"): 26 hpf normoxic control = 24 hpf embryo exposed to 4 h of anoxia (or 24 hpf + 4 h anoxia) (Fig. S2A and B), 27 hpf normoxic control = 24 hpf + 8 h of anoxia (Fig. S2C and D), 27 hpf normoxic control = 24 hpf + 4 h 3% O_2 (Fig. S2E and F), 30.5 hpf normoxic control = 24 hpf + 8 h 3% O_2 (Fig. S2G and H).

Differential regulation of members of the *ndrg* family in response to low oxygen

Cells adapt in distinct manners to varying levels of O_2. Hypoxia (mild to severe) generally elicits metabolic reprogramming via HIF-1α-dependent transcriptional up-regulation of key genes that mediate the adaptive response (14, 15). In contrast, anoxia-tolerance involves metabolic arrest, during which most ATP-demanding processes are suppressed, except for those that are essential for survival (16, 24). To gain an understanding of the range of hypoxia conditions that elicit *ndrg* up-regulation and identify the members of this family that may promote hypoxia adaptation, we subjected embryos to hypoxia (3% O_2) or anoxia (0% O_2) for 4 or 8 hours.

In response to 4 hours of 3% O_2, the transcript levels of none of the *ndrg* family members were significantly altered (Fig. 4A). After 8 hours of 3% O_2, *ndrg1a* was moderately up-regulated (1.91-fold). The expression of other members was not significantly altered (Fig. 4B).

Following 4 hours of anoxia, *ndrg1a* and *ndrg3a* were up-regulated (1.68-fold and 1.49-fold, respectively). In contrast, *ndrg2* was significantly down-regulated (-0.45 fold, respectively), while *ndrg3b* and *ndrg4* expression were not significantly altered (Fig. 5A). By 8 hours of anoxia, *ndrg1a* was further up-regulated 9.27-fold, and we also

observed a slight up-regulation of *ndrg3a* (1.88-fold) (Fig. 5B). *ndrg2* was down-regulated (-0.5-fold), and *ndrgb3b* and *ndrg4* did not significantly change following 8 hours of anoxia (Fig. 5B).

Overall, these data reveal that the *ndrg* family is differentially regulated in response to low O_2. *ndrg1a* is the most hypoxia-responsive member of the family during early development and is transcriptionally up-regulated in response to severe and prolonged O_2 deprivation. This finding is consistent with a previous study in cancer cells revealing that members of the NDRG family mediate long-term adaptation to hypoxia (67). Despite the lack of reported HIF-1α binding sites in its promoter region, *ndrg3a* transcript levels also appear to be up-regulated under anoxia. *ndrg1b* levels were extremely low at the stages used in this qPCR analysis (Fig. 1K, L) and were not further analyzed. Other members of the *ndrg* family may not be hypoxia-responsive at 24 hpf, at least not at the transcriptional level.

The spatial distribution of *ndrg1a* changes in response to anoxia

To confirm that *ndrg1a* is indeed hypoxia-responsive and determine if any changes in its spatial distribution occur following the most stringent hypoxia treatment, we performed WISH using 24 hpf embryos that were exposed to 8 hours of anoxia. Even though WISH is not a quantitative method to assess gene expression levels, we reasoned that the amount of transcript can at least be directly compared if control (stage-matched) and experimental (anoxia-treated) embryos are processed simultaneously during the color reaction step of WISH.

Following prolonged anoxia, *ndrg1a* transcript is retained, possibly enhanced, in the pronephric duct, ionocytes, endodermal organs (liver, intestine) and epiphysis but is noticeably elevated in the inner ear (otic vesicle) (Fig. 6B, B', B", C, D, F, F"). Interestingly, *ndrg1a* signal is also observed in tissues where this gene is not normally expressed (or expressed at levels that are below the detection limit) under normoxic conditions. Among these tissues, the head vasculature was prominently labeled in anoxia-treated embryos, namely: the primordial midbrain channel (pmbc), the primordial hindbrain channel (phbc), the mid-cerebral vein (mcb) and the aortic arch (aa) (Fig 6B, B', F, F'). Although variable in levels between embryos and experiments (possibly correlating with the duration of the color reaction), *ndrg1a* transcript is also seen in a segmentally-repeated pattern in the trunk (Fig. 6A", B", C, E", F") that appears to correspond to somites. The mesoderm-expanded expression explains the thickened anterior-posteriorly oriented stripes of *ndrg1a* label observed from a dorsal view (Fig 6C,D). Furthermore, in samples where the labeling is generally stronger, *ndrg1a* transcript also becomes apparent in the lateral line primordium, a migrating epithelial placode that deposits a series of mechanosensory hair cell organ progenitors along the flank of the embryo (Fig. 6C'). These observations were categorized into mild (Fig. 6D, D'), moderate (Fig. 6B-B", F-F"), and severe (Fig. 6C, C') transcriptional response patterns.

Cross sections of control and anoxia-treated embryos confirmed the anoxia-induced expression of *ndrg1a* in otic vesicles (Fig. 6G, H) and at basal levels throughout the somites, with some puncta of more intense label (Fig. 6I, J). In addition, the sections revealed elevated expression of *ndrg1a* in the caudal aorta and vein (Fig. 6I, J).

To see whether these observed changes in *ndrg1a* expression at the mRNA level correspond with those of protein expression, we performed immunolabeling of Ndrg1a following exposure to anoxia and re-oxygenation post-anoxia. We extended our duration of anoxia beyond 8 hours to include 12 hours of treatment, anticipating that it may take time to sufficiently detect increased protein expression. We observed that following 8 hours of anoxia, Ndrg1a protein is expressed in visibly more ionocytes. This is consistent with the enhanced expression of mRNA in ionocytes following 8 hours anoxia. Following 12 hours anoxia, protein expression did not change very much from 8 hours. However, 12 hours of anoxia followed by 3 and 6 hours of reoxygenation provided intriguing increases in protein expression patterns. We observed overall increased expression throughout the head and anterior trunk regions of the embryo, consistent with the *in situ* results. Specifically, increased expression in the otic vesicle, dorsal aorta, and hatching gland were noticeably increased following re-oxygenation.

Immunolabeling of control, anoxia-treated, and re-oxygenated embryos confirmed anoxia-enhanced expression of Ndrg1a in ionocytes. Additionally, re-oxygenation-induced expression of Ndrg1a was observed in otic vesicles, dorsal aorta, and hatching gland.

In summary, this analysis revealed that, following prolonged anoxia, *ndrg1a* transcript is maintained or enhanced in tissues in which it is present under normoxic conditions (pronephric duct, ionocytes and epiphysis) and expanded to additional tissues (vasculature, otic vesicles, and somites). These increases in tissue expression were found to correspond to protein expression during anoxia exposure and during re-oxygenation. The overall increase in *ndrg1a* across multiple tissues accounts for the dramatic 9-fold

up-regulation in transcript observed using qPCR (Fig. 5B). These findings reveal hypoxia-dependent transcriptional regulation of *ndrg1a* in an intact, developing organism and identify tissues in which *ndrg1a* and other members of this family may play a protective role following severe and prolonged hypoxia.

DISCUSSION

Expression of *ndrg* family members during early development

WISH analysis of the *ndrg* family shows that during early development (shield), *ndrgs* are broadly expressed, with the exception of *ndrg3b* that is below detection levels (shield to 24 hpf). The overlapping expression of *ndrg1a, 1b, 2, 3a, and 4* suggests that these genes may be functionally redundant. From mid-somitogenesis onward, *ndrgs* acquire more distinct spatial distribution patterns, consistent with previous studies revealing expression of members of this family in different cell types in the mouse brain (75) and organs/tissues of *Xenopus laevis* and *tropicalis* embryos (43, 73, 74).

The distribution of *ndrgs* is quite similar in fish and amphibian (*Xenopus tropicalis*) embryos. *ndrg1a* is observed in the eye, pronephric duct, the intestinal bulb, and the liver of zebrafish and *Xenopus* embryos (43, 73, 74). However, *ndrg1a* distribution in *Xenopus* appears broader than that of zebrafish, as it is also reported in the frog notochord, branchial arches, and pancreas. Similarly to the expression pattern of zebrafish *ndrg2*, the distribution of *Xenopus ndrg2* is enriched in the nervous system; although there are also clear differences between these organisms since zebrafish *ndrg2* is

in the heart prominent in somites while *Xenopus ndrg2* is found throughout the epidermis (43). Zebrafish *ndrg3a* and *Xenopus ndrg3* are both present in cranial placodes and spinal cord, but the former also localizes in the pharyngeal pouches, pronephric duct, and somites while the latter is enriched in the heart and otic vesicles (43). *ndrg4* is expressed throughout the nervous system in both zebrafish and *Xenopus*, but only observed in the zebrafish intermediate cell mass and proctodeum, and the *Xenopus* pronephric duct (43). Overall, these expression patterns suggest that the function of Ndrgs is at least partially conserved between fish and amphibians.

ndrgs respond differentially to hypoxia

While transcription is an energy-demanding process that is suppressed under severe hypoxia (17), genes that mediate hypoxia adaptation are generally up-regulated (14, 15). Our qPCR data reveal that among the *ndrg* family members, *ndrg1a* is the most hypoxia-responsive and that prolonged (8 hours) anoxia elicits the strongest increase in transcript levels. These findings corroborate with data from previous studies revealing that zebrafish and mammalian NDRG1 have HREs in their promoter region and are up-regulated in a HIF-1α-dependent manner in response to hypoxia (59, 92). *ndrg3*a is also up-regulated under anoxic conditions, albeit to a lesser extent than *ndrg1a* and does not have confirmed HREs, suggesting that other transcription factors contribute to its up-regulation. We observed very high Ct values for *ndrg1b* in our qPCR experiments (data not shown), suggesting the presence of very little transcript. The low levels of *ndrg1b* and *ndrg4* at 24 hpf were also reported previously from an RNA-seq analysis of zebrafish across developmental stages (89). Our *in situ* results for *ndrg1b* also suggest low expression levels around 24 hpf (Fig. 1K, L), with expression becoming first noticeable

by 48 hpf in the retina. This spatio-temporal expression profile of *ndrg1b* has also been corroborated with previously published data (93).

Our qPCR data also revealed that *ndrg2*, *3b,* and *4* are either unchanged or down-regulated, which can be explained in several ways. Unchanged values may reflect that the transcripts are stabilized, as previously reported for other genes (94), or that the rates of synthesis and degradation are equally matched. Down-regulation could be due to mRNA decay exceeding the rate of synthesis or active repression of gene expression to conserve ATP (16, 17, 94-96). However, repression seems unlikely, as it is generally reserved for genes whose protein products are required for energetically-demanding processes (e.g. *elongation factor 5A* that mediates translation) (17). Given that HREs have been reported in zebrafish *ndrg1a, 1b* and human *NDRG2* regulatory regions (58, 92), it is surprising that our qPCR analysis revealed that transcript levels of *ndrg2* are either unchanged or decreased under low O_2. It is also possible that a milder hypoxia treatment may be required to elicit up-regulation of *ndrg2*. Surprisingly, we also did not observe significant changes in *ndrg4* transcript levels. Zebrafish *ndrg4* plays essential roles in regulating cardiomyocyte growth and proliferation (72), processes that must be suppressed under anoxia. *NDRG4* may be regulated by other hypoxia-responsive transcription factors (97) and may also be responsive to milder conditions than those studied here (98, 99). Indeed, a previous study revealed that hypoxia (5%) but not anoxia exposure of 24 hpf zebrafish embryos, caused the up-regulation of *igfbp-1*, *epo* and *vegf* (87). Another explanation is that hypoxia-induced transcriptional regulation is dynamic and up-regulation of these genes may occur at later developmental stages, as was previously shown for *igfbp-1 and vegf* that are up-regulated in hypoxia-exposed 36 hpf, but not 24 hpf embryos (87).

ndrg1a is up-regulated in metabolically-demanding tissues following prolonged anoxia

Previous studies using human cancer cells (59, 60) or homogenous cell lines (trophoblasts) (100) have revealed that *NDRG1* is up-regulated in response to hypoxia. However, little is known about how this response is orchestrated across multiple tissues of a whole organism. Using WISH, we investigated the distribution of *ndrg1a* in 24 hpf zebrafish embryos exposed to 8 hours of anoxia, a treatment that elicits the most robust increase in *ndrg1a* transcript. Given that these conditions are very stringent, we reasoned that any tissue/organ in which *ndrg1a* levels are significantly increased must require the activity of this protein to adapt to low O_2.

Our study revealed that, following anoxia, *ndrg1a* is up-regulated in the epiphysis and possibly the pronephric duct, ionocytes, and endodermal organs (although the WISH procedure was not sensitive enough to detect an increase relative to the already high normoxic levels of *ndrg1a* in these cells). The epiphysis, also known as the pineal gland, receives information about the light-dark cycle from the environment and produces the hormone melatonin in response to this information. Melatonin has multiple cellular functions, including reducing oxidative stress (101), which is elevated under hypoxia and can cause cell death (102). In addition to responding to light-dark stimuli, the pineal is also hypoxia-responsive, as stabilized Hif-1α modulates clock gene expression in zebrafish pineal cells (103, 104). Given that *ndrg1a* is a Hif-1α target, it is possible that Ndrg1a is implicated in the regulation of clock genes and melatonin production under low O_2 (105). The liver is quite effective at taking up O_2 and is normally well supplied by the bloodstream; nevertheless, it is susceptible to hypoxic injury and associated

complications (106). In contrast, the intestine normally experiences wide fluctuations in O_2 throughout the day with some regions becoming hypoxic. Genes that aid in the maintenance of the hypoxic intestine are HIF-1α-regulated, providing a potential explanation for the expression of *ndrg1a* in this tissue (107, 108)**.** The function of *ndrg1a* in the pronephric duct and ionocytes is unclear, but these cells rely on the metabolically-demanding sodium-potassium ATPase pump to maintain ionic gradients and hence are likely to be sensitive to O_2 depletion (109).

In addition to enhanced expression of *ndrg1a* in the epiphysis, we also observed expansion of *ndrg1a* distribution to tissues/organs where it is not present under normoxic conditions, namely the inner ear (otic vesicles), head vasculature, and somites. Previous studies have demonstrated that mutations in *NDRG1* are associated with Charcot-Marie-Tooth disease type 4D (CMT4D) (83), a demyelinating neuropathy that causes hearing loss in humans. Furthermore, hypoxia can cause hearing loss (110-113); thus it is possible that Ndrg1a protects the inner ear or/and connected auditory nerve fibers from hypoxia-induced damage. Vascular sprouting is a well-documented hypoxic response to maximize O_2 delivery (114). NDRG1 was previously shown to mediate endothelial cell migration under intermittent hypoxia (115), raising the question of whether its up-regulation under anoxia serves a similar purpose in head vasculature. Somites give rise to skeletal muscle cells, which experience cellular hypoxia and lactic acidosis during exercise that is further exacerbated by environmental hypoxia (116). It is possible that Ndrg1a protects muscle cells from acidosis or promotes hypometabolism in these cells.

Even though other members of the *ndrg* family are not transcriptionally up-regulated under anoxia (or at least not as significantly as *ndrg1a*), there is evidence that

they can be post-translationally modified in response to hypoxia (67, 117-119). In this regard, it is interesting that *ndrg2, 3a, 3b and 4* are expressed in the pectoral fin buds, which are known to play a respiratory role in fish (120, 121). Furthermore, these genes are expressed in several metabolically-demanding tissues, including the brain, spinal cord, heart, and kidney.

In summary, we have shown that *ndrgs* are distributed across a range of hypoxia-sensitive/responsive tissues and that the levels of *ndrg1a* and *3a* are selectively increased following prolonged exposure to anoxia. Future studies will address whether members of this family promote hypoxia adaptation of the tissues and organs in which they are expressed.

xiv. FIGURE LEGENDS

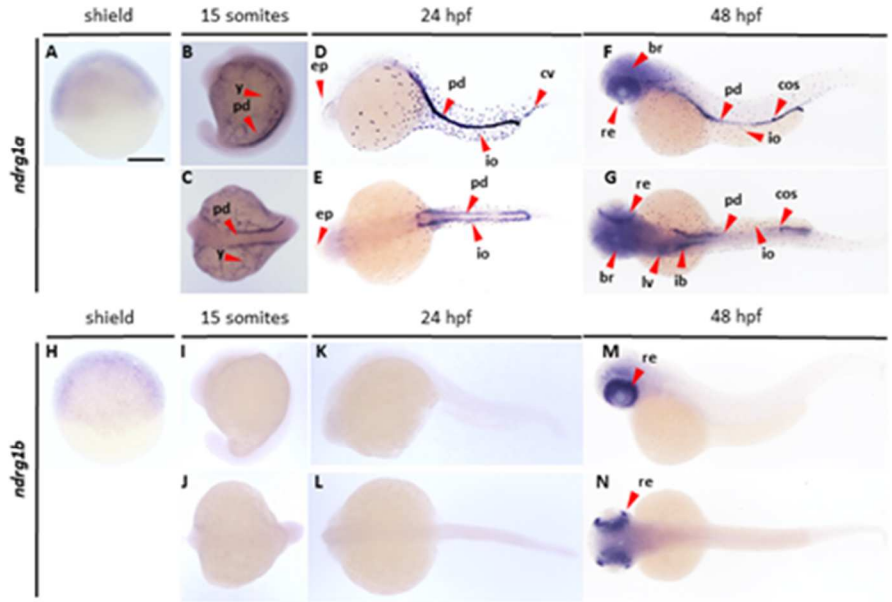

Figure 1. Gene expression analysis of *ndrg1*. WISH analysis revealing the distribution of *ndrg1a* (A-G) and *ndrg1b* (H-N) transcripts in zebrafish embryos at shield (A, H), 15 somites (B, C, I, J), 24 hpf (D, E, K, L) and 48 hpf (F, G, M, N) stages, imaged from lateral (A, B, D, F, H, I, K, M) and dorsal (C, E, G, J, L, N) views. Abbreviations: br (brain), cv (caudal vein), ep (epiphysis), cos (corpuscles of Stannius), ib (intestinal bulb), io (ionocyte), lv (liver), pd (pronephric ducts), re (retina), and y (yolk). Scale bar, 250 μm.

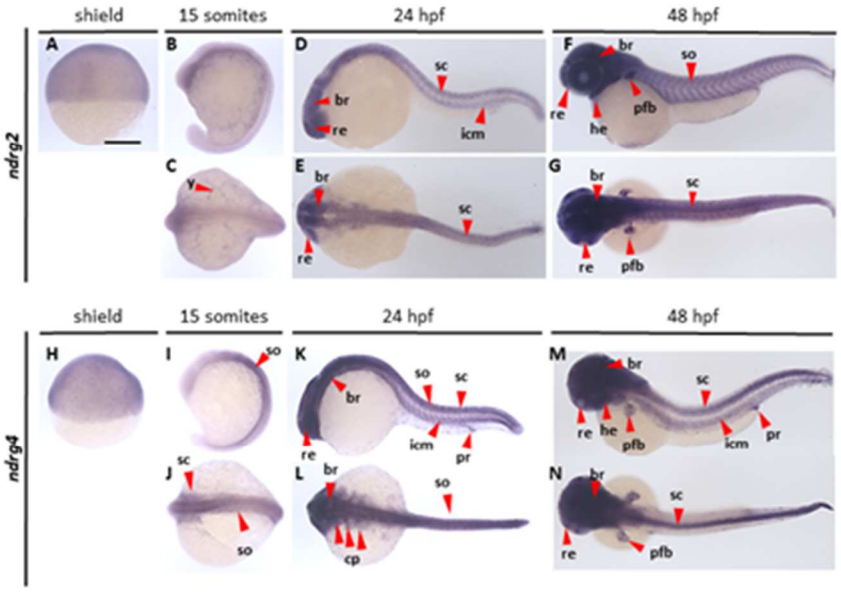

Figure 2. Gene expression analysis of *ndrg2* and *ndrg4*. WISH analysis revealing the distribution of *ndrg2* (A-F) and *ndrg4* (G-L) *transcripts* in zebrafish embryos at shield (A, G), 15 somites (B, H), 24 hpf (C, D, I, J) and 48 hpf (E, F, K, L) stages, imaged from lateral (A-C, E, G-I, K) and dorsal (D, F, J, L) views. Abbreviations: br (brain), cp (cranial placodes), he (heart), icm (intermediate cell mass of mesoderm), pfb (pectoral fin buds), pr (proctodeum), re (retina), sc (spinal cord), and so (somites). Scale bar, 250 μm.

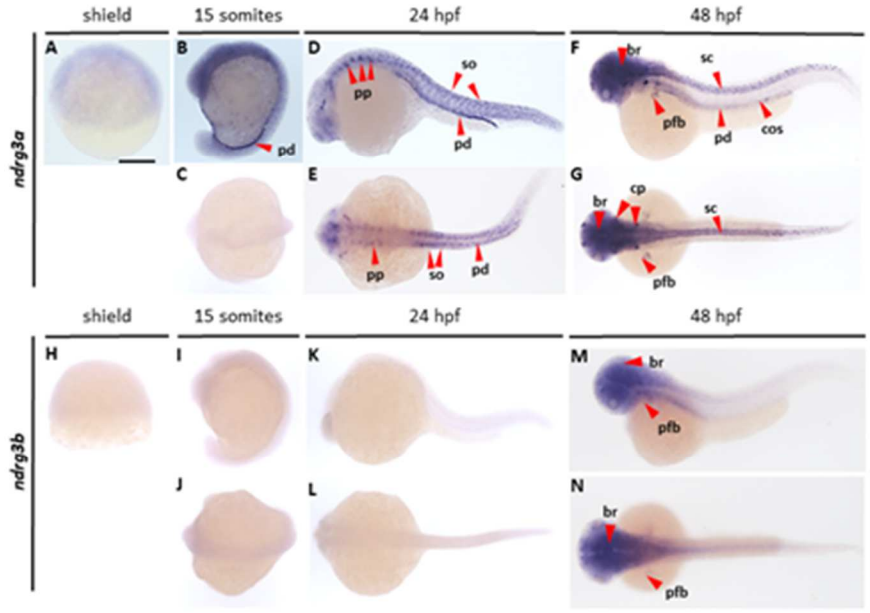

Figure 3. Gene expression analysis of *ndrg3*. WISH analysis revealing the distribution of *ndrg3a* (A-G) *and ndrg3b* (H-N) transcripts in zebrafish embryos at shield (A, G), 15 somites (A, H), 24 hpf (D, E, K, L) and 48 hpf (F, G, M, N) stages, imaged from lateral (A, B, D, F, H, I, K, M) and dorsal (C, E, G, J, L, N) views) and 48 hpf (F, G, M, N) stages, imaged from lateral (A, B, D, F, H, I, K, M) and dorsal (C, E, G, J, L, N) views. Abbreviations: br (brain), cos (corpuscles of Stannius), cp (cranial placodes), pfb (pectoral fin buds), pp (pharyngeal pouches), pd (pronephric ducts), sc (spinal cord), and so (somites). Scale bar, 250 µm.

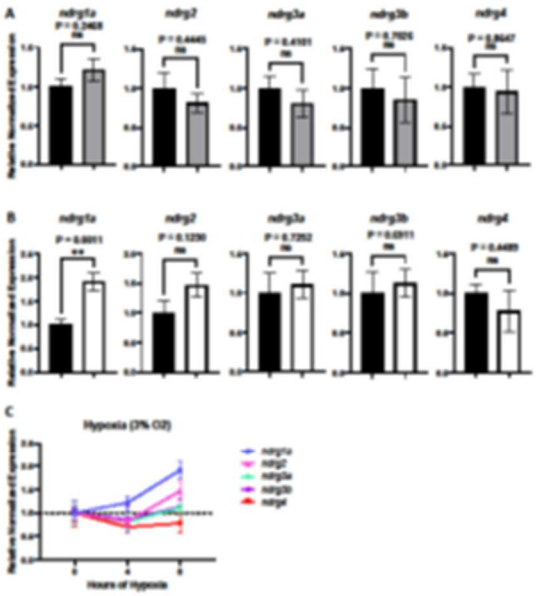

Figure 4. Changes in *ndrg* transcript levels in response to hypoxia (3% oxygen). (A, B) Real-time qPCR analysis of 24 hpf zebrafish embryos exposed to 4 h (A, grey bars) or 8 h (B, white bars) of hypoxia relative to normoxic (stage-matched) controls (A, B, black bars) normalized to *ef1a*. (C) Plotted graphical summary of qPCR results. The y-axis in the graphs represents the relative normalized expression of each gene. All fold changes were derived using the formula, $2^{-(\Delta\Delta CT)}$. represent standard error of the mean (SEM). Significance was obtained using the unpaired, two-tailed t-test with Welch's Correction. $^{**}p < 0.01$. Reactions were run in triplicate with 7-8 biological replicates (n = 7-8).

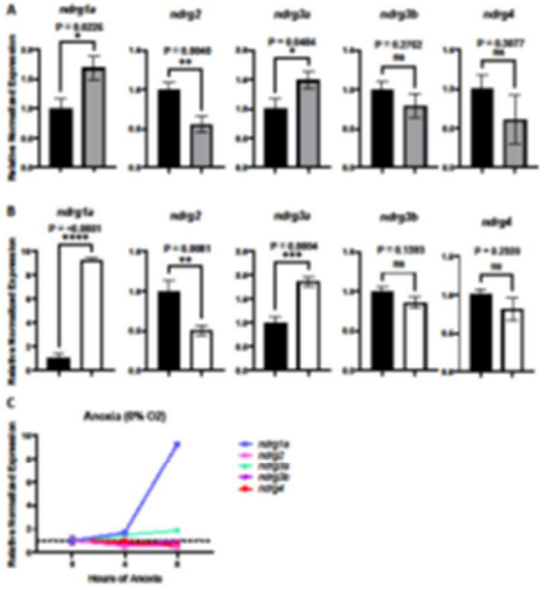

Figure 5. Changes in *ndrg* transcript levels in response to anoxia (0% oxygen). Real-time qPCR analysis of 24 hpf zebrafish embryos exposed to 4 h (A, grey bars) or 8 h (B, white bars) of anoxia relative to normoxic (stage-matched) controls (A, B, black bars) normalized to *ef1a*. (C) Plotted graphical summary of qPCR results. The y-axis in the graphs represents the relative normalized expression of each gene. All fold changes were derived using the formula, $2^{-(\Delta\Delta CT)}$. represent standard error of the mean (SEM). Significance was obtained using the unpaired, two-tailed t-test with Welch's Correction. *$p < 0.05$, **$p < 0.01$, ***$p < 0.0005$, ****$p < 0.0001$. Reactions were run in triplicate with 7-8 biological replicates (n = 7-8).

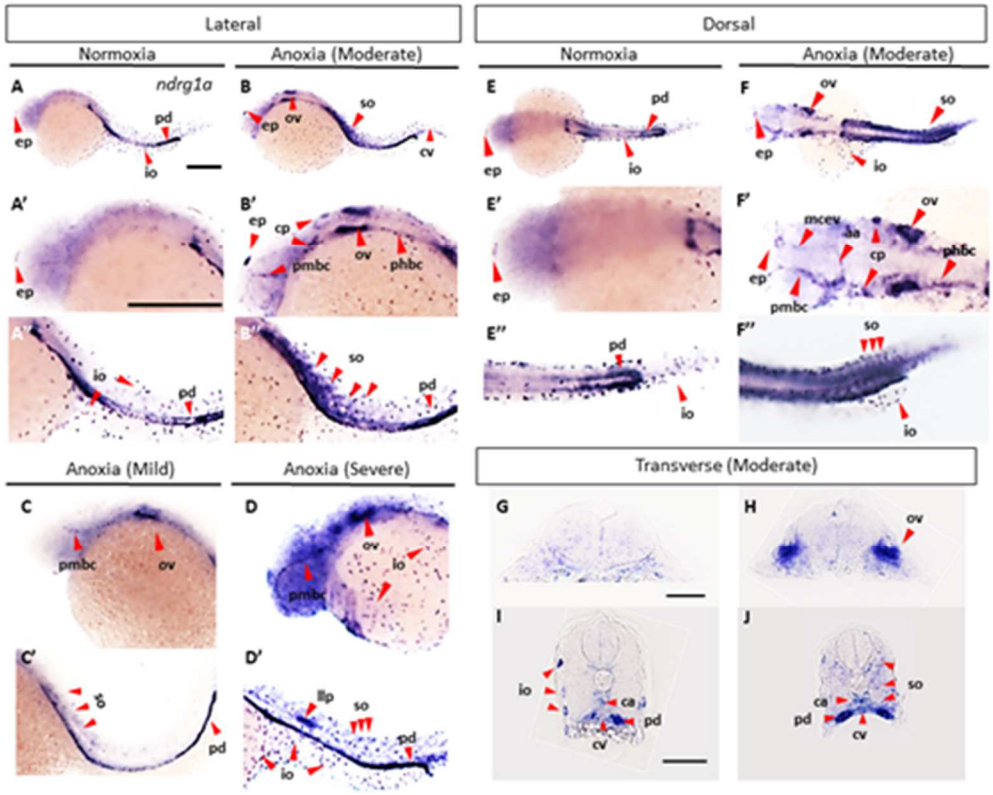

Figure 6. Analysis of *ndrg1a* expression in zebrafish embryos following 8h of anoxia. WISH analysis revealing the distribution of *ndrg1a* transcript in 24 hpf zebrafish embryo exposed to 8h of anoxia (B-B", C-C', D-D', F-F", H, J) relative to normoxic (stage-matched controls) (A-A'', E-E'', G, I) imaged from a lateral view (A-D'), a dorsal view (E-F") and cross sectional (G-J) views through the otic vesicles (G,H) and the trunk (I,J). (A'-B", E-F" are magnified views of (A,B,E,F). The severe (C,C') and mild (D,D') transcriptional responses are included to compare with the moderate response (B-B", F-F"). Abbreviations: aa (aortic arch), cv (caudal vein), ep (epiphysis), io (ionocyte), llp (lateral line primordium), mcev (mid-cerebral vein), ov (otic vesicle), pcv (posterior cardinal vein), phbc (primordial hindbrain channel), pmbc (primordial midbrain channel), and pd (pronephric ducts), and so (somites). The experiment was repeated in triplicate, with 8 embryos representative of the group imaged. Scale bar in A,A', 250 µm. Scale bar in E,G, 50 µm.

SUPPLEMENTAL FIGURE LEGENDS

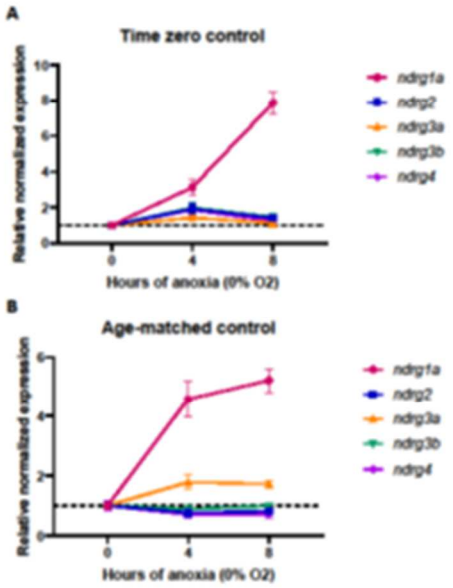

Figure S1. Real-time qPCR using time zero and age-matched controls. Real-time qPCR analysis of *ndrg* transcript levels in 24 hpf zebrafish embryos exposed to anoxia for 4 or 8 hours. Expression levels were normalized to reference gene *ef1a*. (A) Use of time 0 (24 hpf)normoxic controls. (B) Use of age-matched (28 hpf for 4 h anoxia and 32 hpf for 8 h anoxia) normoxic controls. The y-axis represents the log2 fold changes in expression of each gene. The dotted horizontal line represents the baseline to which values were normalized. All fold changes were derived using the formula, $2^{-(\Delta\Delta CT)}$. Reactions were run in triplicate with 8 biological replicates (n=8). Bars represent standard error (SE).

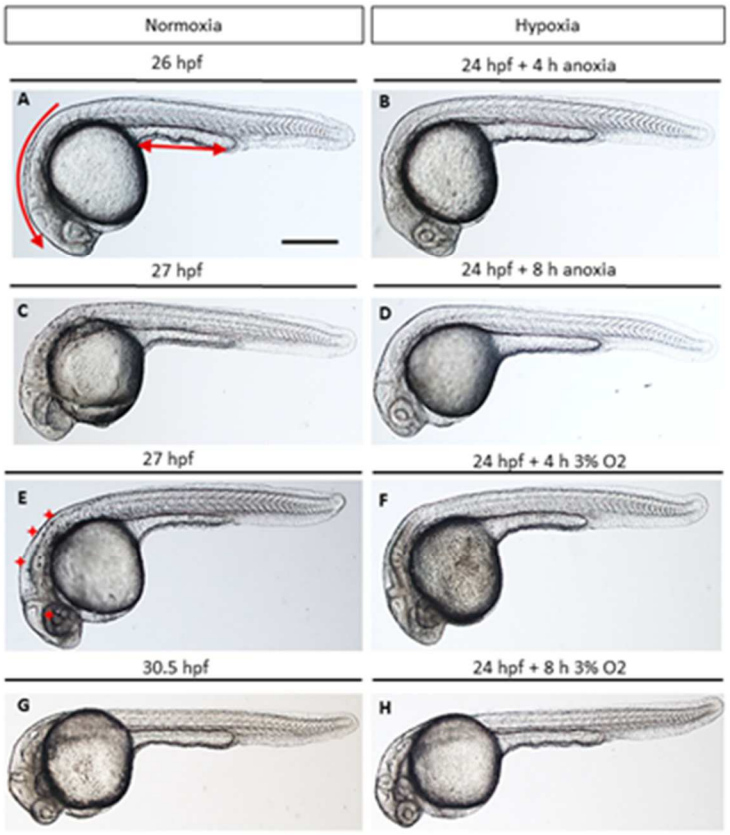

Figure S2. Identification of developmental stage-matched normoxic control for anoxia (0% oxygen) and hypoxia (3% oxygen). 24 hpf embryos were treated in 0% O2 (B,D) or 3% O2 (F,H) for 4 h and 8 h. Images of normoxic embryos were taken every 0.5 h interval. 26 hpf embryo (A) shows similar morphology to 24 hpf + 4 h anoxia treated embryos and 27 hpf embryo (C) shows similar morphology to 24 hpf + 8 h anoxia treated embryos. 27 hpf embryo (E) shows similar morphology to 24 hpf + 4 h 3% O2 treated embryos and 30.5 hpf embryo (G) shows similar morphology to 24 hpf + 8 h 3% O2 treated embryos. Annotations (A) of yolk extension (double-arrow), head curvature (curved arrow), and pigmentation of eye (straight arrow)(Created with BioRender.com). Scale bar, 250 µm.

Figures below show our current ongoing work for submission (where I have contributed)

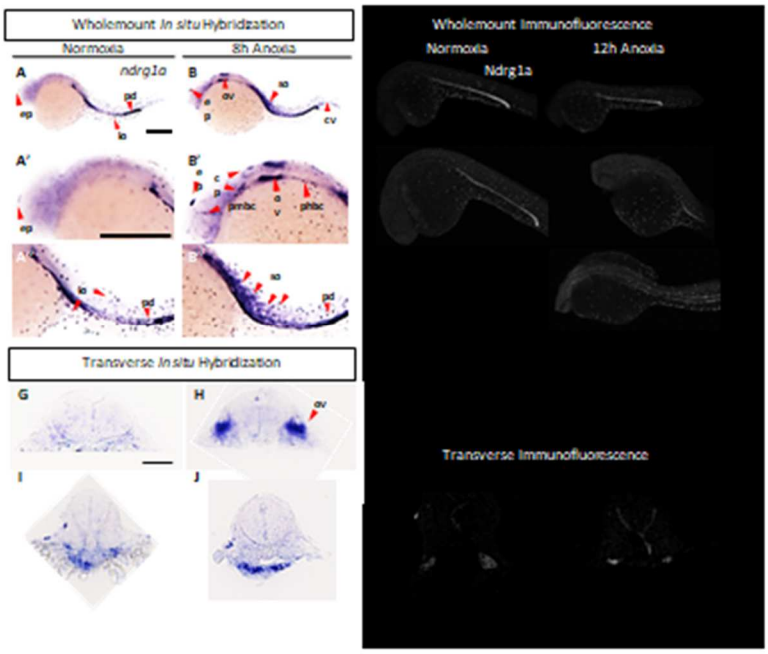

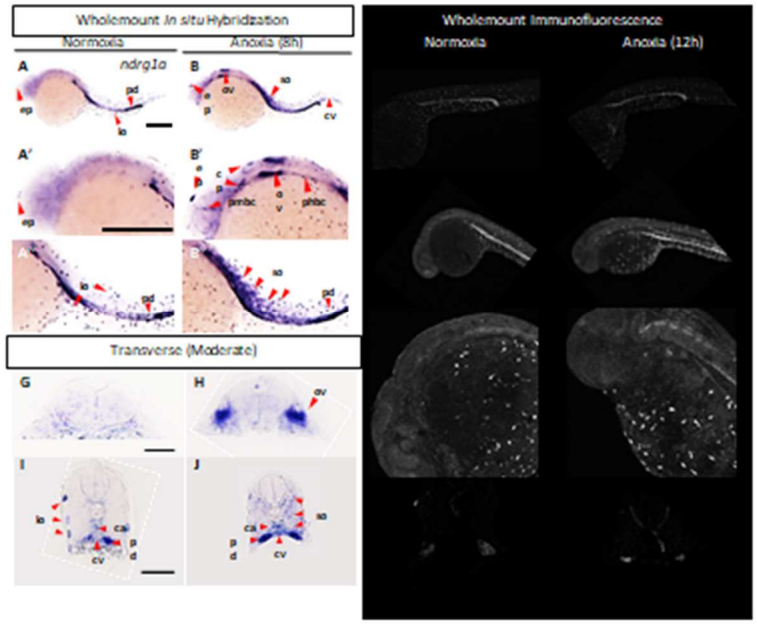

Currently, in-progress figures including the Ndrg1a protein work.

xii. REFERENCES

1. Banasiak, K. J., Xia, Y., and Haddad, G. G. (2000) Mechanisms underlying hypoxia-induced neuronal apoptosis. *Progress in Neurobiology* **62**, 215-249

2. Nakajima, W., Ishida, A., Lange, M. S., Gabrielson, K. L., Wilson, M. A., Martin, L. J., Blue, M. E., and Johnston, M. V. (2000) Apoptosis Has a Prolonged Role in the Neurodegeneration after Hypoxic Ischemia in the Newborn Rat. *The Journal of Neuroscience* **20**, 7994-8004

3. Hu, B. R., Liu, C. L., Ouyang, Y., Blomgren, K., and Siesjö, B. K. (2000) Involvement of Caspase-3 in Cell Death after Hypoxia–Ischemia Declines during Brain Maturation. *Journal of Cerebral Blood Flow & Metabolism* **20**, 1294-1300

4. Guo, M.-F., Yu, J.-Z., and Ma, C.-G. (2011) Mechanisms related to neuron injury and death in cerebral hypoxic ischaemia. *Folia Neuropathologica* **49**, 79-87

5. Vohwinkel, C. U., Hoegl, S., and Eltzschig, H. K. (2015) Hypoxia signaling during acute lung injury. *Journal of Applied Physiology* **119**, 1157-1163

6. Cummings, K. W., and Bhalla, S. (2015) Pulmonary Vascular Diseases. *Clinics in Chest Medicine* **36**, 235-248

7. Tanaka, S., Tanaka, T., and Nangaku, M. (2014) Hypoxia as a key player in the AKI-to-CKD transition. *American Journal of Physiology-Renal Physiology* **307**, F1187-F1195

8. Peers, C., Dallas, M. L., Boycott, H. E., Scragg, J. L., Pearson, H. A., and Boyle, J. P. (2009) Hypoxia and Neurodegeneration. *Annals of the New York Academy of Sciences* **1177**, 169-177

9. Ferdinand, P., and Roffe, C. (2016) Hypoxia after stroke: a review of experimental and clinical evidence. *Experimental & Translational Stroke Medicine* **8**

10. Eltzschig, H. K., and Eckle, T. (2011) Ischemia and reperfusion—from mechanism to translation. *Nature Medicine* **17**, 1391-1401

11. Malek, M., and Nematbakhsh, M. (2015) Renal ischemia/reperfusion injury; from pathophysiology to treatment. *J Renal Inj Prev* **4**, 20-27

12. Cadenas, S. (2018) ROS and redox signaling in myocardial ischemia-reperfusion injury and cardioprotection. *Free Radical Biology and Medicine* **117**, 76-89

13. Granger, D. N., and Kvietys, P. R. (2015) Reperfusion injury and reactive oxygen species: The evolution of a concept. *Redox Biology* **6**, 524-551

14. Semenza, G. L. (2013) HIF-1 mediates metabolic responses to intratumoral hypoxia and oncogenic mutations. *Journal of Clinical Investigation* **123**, 3664-3671

15. Xie, H., and Simon, M. C. (2017) Oxygen availability and metabolic reprogramming in cancer. *Journal of Biological Chemistry* **292**, 16825-16832

16. Storey, K. B., and Storey, J. M. (2007) Tribute to P. L. Lutz: putting life on 'pause'--molecular regulation of hypometabolism. *J Exp Biol* **210**, 1700-1714

17. Cavadas, M. A. S., Cheong, A., and Taylor, C. T. (2017) The regulation of transcriptional repression in hypoxia. *Exp Cell Res* **356**, 173-181

18. Van Den Beucken, T., Magagnin, M. G., Jutten, B., Seigneuric, R., Lambin, P., Koritzinsky, M., and Wouters, B. G. (2011) Translational control is a major contributor to hypoxia induced gene expression. *Radiotherapy and Oncology* **99**, 379-384

19. Wouters, B. G., Van Den Beucken, T., Magagnin, M. G., Koritzinsky, M., Fels, D., and Koumenis, C. (2005) Control of the hypoxic response through regulation of mRNA translation. *Seminars in Cell & Developmental Biology* **16**, 487-501

20. Koritzinsky, M., Seigneuric, R., Magagnin, M. G., Beucken, T. V. D., Lambin, P., and Wouters, B. G. (2005) The hypoxic proteome is influenced by gene-specific changes in mRNA translation. *Radiotherapy and Oncology* **76**, 177-186

21. Ortmann, B., Druker, J., and Rocha, S. (2014) Cell cycle progression in response to oxygen levels. *Cellular and Molecular Life Sciences* **71**, 3569-3582

22. Lees, G. J. (1991) Inhibition of sodium-potassium-ATPase: a potentially ubiquitous mechanism contributing to central nervous system neuropathology. *Brain Research Reviews* **16**, 283-300

23. Helenius, I. T., Dada, L. A., and Sznajder, J. I. (2010) Role of Ubiquitination in Na,K-ATPase Regulation during Lung Injury. *Proceedings of the American Thoracic Society* **7**, 65-70

24. Larson, J., Drew, K. L., Folkow, L. P., Milton, S. L., and Park, T. J. (2014) No oxygen? No problem! Intrinsic brain tolerance to hypoxia in vertebrates. *Journal of Experimental Biology* **217**, 1024-1039

25. Padilla, P. A., and Roth, M. B. (2001) Oxygen deprivation causes suspended animation in the zebrafish embryo. *Proceedings of the National Academy of Sciences* **98**, 7331-7335

26. Mendelsohn, B. A., Kassebaum, B. L., and Gitlin, J. D. (2008) The zebrafish embryo as a dynamic model of anoxia tolerance. *Developmental Dynamics* **237**, 1780-1788

27. Ton, C., Stamatiou, D., and Liew, C. C. (2003) Gene expression profile of zebrafish exposed to hypoxia during development. *Physiol Genomics* **13**, 97-106

28. Woods, I. G., and Imam, F. B. (2015) Transcriptome analysis of severe hypoxic stress during development in zebrafish. *Genom Data* **6**, 83-88

29. Julian, C. G. (2017) Epigenomics and human adaptation to high altitude. *J Appl Physiol (1985)* **123**, 1362-1370

30. Storey, K. B. (2007) Anoxia tolerance in turtles: metabolic regulation and gene expression. *Comp Biochem Physiol A Mol Integr Physiol* **147**, 263-276

31. Semenza, G. L. (2001) HIF-1 and mechanisms of hypoxia sensing. *Current Opinion in Cell Biology* **13**, 167-171

32. Nakayama, K., and Kataoka, N. (2019) Regulation of Gene Expression under Hypoxic Conditions. *International Journal of Molecular Sciences* **20**, 3278

33. Dengler, V. L., Galbraith, M. D., and Espinosa, J. M. (2014) Transcriptional regulation by hypoxia inducible factors. *Critical Reviews in Biochemistry and Molecular Biology* **49**, 1-15

34. Schödel, J., Mole, D. R., and Ratcliffe, P. J. (2013) Pan-genomic binding of hypoxia-inducible transcription factors. *Biological Chemistry* **394**, 507-517

35. Mole, D. R., Blancher, C., Copley, R. R., Pollard, P. J., Gleadle, J. M., Ragoussis, J., and Ratcliffe, P. J. (2009) Genome-wide Association of Hypoxia-inducible Factor (HIF)-1α and HIF-2α DNA Binding with Expression Profiling of Hypoxia-inducible Transcripts. *Journal of Biological Chemistry* **284**, 16767-16775

36. Xia, X., and Kung, A. L. (2009) Preferential binding of HIF-1 to transcriptionally active loci determines cell-type specific response to hypoxia. *Genome Biology* **10**, R113

37. Schödel, J., Oikonomopoulos, S., Ragoussis, J., Pugh, C. W., Ratcliffe, P. J., and Mole, D. R. (2011) High-resolution genome-wide mapping of HIF-binding sites by ChIP-seq. *Blood* **117**, e207-e217

38. Benita, Y., Kikuchi, H., Smith, A. D., Zhang, M. Q., Chung, D. C., and Xavier, R. J. (2009) An integrative genomics approach identifies Hypoxia Inducible Factor-1 (HIF-1)-target genes that form the core response to hypoxia. *Nucleic Acids Research* **37**, 4587-4602

39. Semenza, G. L. (2012) Hypoxia-inducible factors: mediators of cancer progression and targets for cancer therapy. *Trends in Pharmacological Sciences* **33**, 207-214

40. Takeda, N., Maemura, K., Imai, Y., Harada, T., Kawanami, D., Nojiri, T., Manabe, I., and Nagai, R. (2004) Endothelial PAS Domain Protein 1 Gene Promotes Angiogenesis Through the Transactivation of Both Vascular Endothelial Growth Factor and Its Receptor, Flt-1. *Circulation Research* **95**, 146-153

41. Wenger, R. H., Stiehl, D. P., and Camenisch, G. (2005) Integration of Oxygen Signaling at the Consensus HRE. *Science's STKE* **2005**, re12-re12

42. Chi, J.-T., Wang, Z., Nuyten, D. S. A., Rodriguez, E. H., Schaner, M. E., Salim, A., Wang, Y., Kristensen, G. B., Helland, Å., Børresen-Dale, A.-L., Giaccia, A., Longaker, M. T., Hastie, T., Yang, G. P., Van De Vijver, M. J., and Brown, P. O. (2006) Gene Expression Programs in Response to Hypoxia: Cell Type Specificity and Prognostic Significance in Human Cancers. *PLoS Medicine* **3**, e47

43. Zhong, C., Zhou, Y. K., Yang, S. S., Zhao, J. F., Zhu, X. L., Chen, H. H., Chen, P. C., Huang, L. Q., and Huang, X. (2015) Developmental expression of the N-myc downstream regulated gene (Ndrg) family during Xenopus tropicalis embryogenesis. *Int J Dev Biol* **59**, 511-517

44. Melotte, V., Qu, X., Ongenaert, M., van Criekinge, W., de Bruine, A. P., Baldwin, H. S., and van Engeland, M. (2010) The N-myc downstream regulated gene (NDRG) family: diverse functions, multiple applications. *FASEB J* **24**, 4153-4166

45. Shaw, E., McCue, L. A., Lawrence, C. E., and Dordick, J. S. (2002) Identification of a novel class in the α/β hydrolase fold superfamily: The N-myc differentiation-related proteins. *Proteins: Structure, Function, and Bioinformatics* **47**, 163-168

46. Wang, B., Li, J., Ye, Z., Li, Z., and Wu, X. (2014) N-myc downstream regulated gene 1 acts as a tumor suppressor in ovarian cancer. *Oncol Rep* **31**, 2279-2285

47. Kalaydjieva, L., Gresham, D., Gooding, R., Heather, L., Baas, F., de Jonge, R., Blechschmidt, K., Angelicheva, D., Chandler, D., Worsley, P., Rosenthal, A., King, R. H., and Thomas, P. K. (2000) N-myc downstream-regulated gene 1 is mutated in hereditary motor and sensory neuropathy-Lom. *Am J Hum Genet* **67**, 47-58

48. Taketomi, Y., Sunaga, K., Tanaka, S., Nakamura, M., Arata, S., Okuda, T., Moon, T. C., Chang, H. W., Sugimoto, Y., Kokame, K., Miyata, T., Murakami, M., and Kudo, I. (2007) Impaired mast cell maturation and degranulation and attenuated allergic responses in Ndrg1-deficient mice. *J Immunol* **178**, 7042-7053

49. Kachhap, S. K., Faith, D., Qian, D. Z., Shabbeer, S., Galloway, N. L., Pili, R., Denmeade, S. R., DeMarzo, A. M., and Carducci, M. A. (2007) The N-Myc down regulated Gene1 (NDRG1) Is a Rab4a effector involved in vesicular recycling of E-cadherin. *PLoS One* **2**, e844

50. Sun, J., Zhang, D., Bae, D. H., Sahni, S., Jansson, P., Zheng, Y., Zhao, Q., Yue, F., Zheng, M., Kovacevic, Z., and Richardson, D. R. (2013) Metastasis suppressor, NDRG1, mediates its activity through signaling pathways and molecular motors. *Carcinogenesis* 34, 1943-1954

51. Mi, L., Zhu, F., Yang, X., Lu, J., Zheng, Y., Zhao, Q., Wen, X., Lu, A., Wang, M., Zheng, M., Ji, J., and Sun, J. (2017) The metastatic suppressor NDRG1 inhibits EMT, migration and invasion through interaction and promotion of caveolin-1 ubiquitylation in human colorectal cancer cells. *Oncogene* **36**, 4323-4335

52. Merlot, A. M., Porter, G. M., Sahni, S., Lim, E. G., Peres, P., and Richardson, D. R. (2019) The metastasis suppressor, NDRG1, differentially modulates the endoplasmic reticulum stress response. *Biochim Biophys Acta Mol Basis Dis* **1865**, 2094-2110

53. Kovacevic, Z., and Richardson, D. R. (2006) The metastasis suppressor, Ndrg-1: a new ally in the fight against cancer. *Carcinogenesis* **27**, 2355-2366

54. Jin, R., Liu, W., Menezes, S., Yue, F., Zheng, M., Kovacevic, Z., and Richardson, D. R. (2014) The metastasis suppressor NDRG1 modulates the phosphorylation and nuclear translocation of beta-catenin through mechanisms involving FRAT1 and PAK4. *J Cell Sci* **127**, 3116-3130

55. Tu, L. C., Yan, X., Hood, L., and Lin, B. (2007) Proteomics Analysis of the Interactome of N-myc Downstream Regulated Gene 1 and Its Interactions with the Androgen Response Program in Prostate Cancer Cells. *Molecular & Cellular Proteomics* **6**, 575-588

56. Pietiainen, V., Vassilev, B., Blom, T., Wang, W., Nelson, J., Bittman, R., Back, N., Zelcer, N., and Ikonen, E. (2013) NDRG1 functions in LDL receptor trafficking by regulating endosomal recycling and degradation. *J Cell Sci* **126**, 3961-3971

57. Askautrud, H. A., Gjernes, E., Gunnes, G., Sletten, M., Ross, D. T., Børresen-Dale, A. L., Iversen, N., Tranulis, M. A., and Frengen, E. (2014) Global Gene Expression Analysis Reveals a Link between NDRG1 and Vesicle Transport. *PLoS ONE* **9**, e87268

58. Wang, L., Liu, N., Yao, L., Li, F., Zhang, J., Deng, Y., Liu, J., Ji, S., Yang, A., Han, H., Zhang, Y., Zhang, J., Han, W., and Liu, X. (2008) NDRG2 is a new HIF-1 Target Gene Necessary for Hypoxia-Induced Apoptosis in A549 Cells. *Cellular Physiology and Biochemistry* **21**, 239-250

59. Wang, Q., Li, L.-H., Gao, G.-D., Wang, G., Qu, L., Li, J.-G., and Wang, C.-M. (2013) HIF-1α up-regulates NDRG1 expression through binding to NDRG1 promoter, leading to proliferation of lung cancer A549 cells. *Molecular Biology Reports* **40**, 3723-3729

60. Cangul, H. (2004) Hypoxia upregulates the expression of the NDRG1 gene leading to its overexpression in various human cancers. *BMC Genet* **5**, 27

61. Cangul, H., Salnikow, K., Yee, H., Zagzag, D., Commes, T., and Costa, M. (2002) Enhanced overexpression of an HIF-1/hypoxia-related protein in cancer cells. *Environ Health Perspect* **110 Suppl 5**, 783-788

62. Ellen, T. P., Ke, Q., Zhang, P., and Costa, M. (2008) NDRG1, a growth and cancer related gene: regulation of gene expression and function in normal and disease states. *Carcinogenesis* **29**, 2-8

63. Said, H. M., Safari, R., Al-Kafaji, G., Ernestus, R. I., Lohr, M., Katzer, A., Flentje, M., and Hagemann, C. (2017) Time- and oxygen-dependent expression and regulation of NDRG1 in human brain cancer cells. *Oncol Rep* **37**, 3625-3634

64. Yeh, C. C., Luo, J. L., Nhut Phan, N., Cheng, Y. C., Chow, L. P., Tsai, M. H., Chuang, E. Y., and Lai, L. C. (2018) Different effects of long noncoding RNA NDRG1-OT1 fragments on NDRG1 transcription in breast cancer cells under hypoxia. *RNA Biol* **15**, 1487-1498

65. Lin, H. C., Yeh, C. C., Chao, L. Y., Tsai, M. H., Chen, H. H., Chuang, E. Y., and Lai, L. C. (2018) The hypoxia-responsive lncRNA NDRG-OT1 promotes NDRG1 degradation via ubiquitin-mediated proteolysis in breast cancer cells. *Oncotarget* **9**, 10470-10482

66. Lee, G. Y., Chun, Y.-S., Shin, H.-W., and Park, J.-W. (2016) Potential role of the N-MYC downstream-regulated gene family in reprogramming cancer metabolism under hypoxia. *Oncotarget* **7**, 57442-57451

67. Lee, D. C., Sohn, H. A., Park, Z. Y., Oh, S., Kang, Y. K., Lee, K. M., Kang, M., Jang, Y. J., Yang, S. J., Hong, Y. K., Noh, H., Kim, J. A., Kim, D. J., Bae, K. H., Kim, D. M., Chung, S. J., Yoo, H. S., Yu, D. Y., Park, K. C., and Yeom, Y. I. (2015) A lactate-induced response to hypoxia. *Cell* **161**, 595-609

68. Mustonen, V., Muruganandam, G., Loris, R., Kursula, P., and Ruskamo, S. Crystal and solution structure of NDRG1, a membrane-binding protein linked to myelination and tumour suppression. *The FEBS Journal* **n/a**

69. Hwang, J., Kim, Y., Kang, H. B., Jaroszewski, L., Deacon, A. M., Lee, H., Choi, W. C., Kim, K. J., Kim, C. H., Kang, B. S., Lee, J. O., Oh, T. K., Kim, J. W., Wilson, I. A., and Kim, M. H. (2011) Crystal structure of the human N-Myc downstream-regulated gene 2 protein provides insight into its role as a tumor suppressor. *J Biol Chem* **286**, 12450-12460

70. Kim, K. R., Kim, K. A., Park, J. S., Jang, J. Y., Choi, Y., Lee, H. H., Lee, D. C., Park, K. C., Yeom, Y. I., Kim, H.-J., and Han, B. W. (2020) Structural and Biophysical Analyses of Human N-Myc Downstream-Regulated Gene 3 (NDRG3) Protein. *Biomolecules* **10**, 90

71. Li, R. A., Traver, D., Matthes, T., and Bertrand, J. Y. (2016) Ndrg1b and fam49ab modulate the PTEN pathway to control T-cell lymphopoiesis in the zebrafish. *Blood* **128**, 3052-3060

72. Qu, X., Jia, H., Garrity, D. M., Tompkins, K., Batts, L., Appel, B., Zhong, T. P., and Baldwin, H. S. (2008) ndrg4 is required for normal myocyte proliferation during early cardiac development in zebrafish. *Developmental Biology* **317**, 486-496

73. Kyuno, J., Fukui, A., Michiue, T., and Asashima, M. (2003) Identification and characterization of Xenopus NDRG1. *Biochem Biophys Res Commun* **309**, 52-57

74. Zhang, T., Guo, X., and Chen, Y. (2013) Retinoic acid-activated Ndrg1a represses Wnt/beta-catenin signaling to allow Xenopus pancreas, oesophagus, stomach, and duodenum specification. *PLoS One* **8**, e65058

75. Okuda, T., Kokame, K., and Miyata, T. (2008) Differential expression patterns of NDRG family proteins in the central nervous system. *J Histochem Cytochem* **56**, 175-182

76. Schonkeren, S. L., Massen, M., van der Horst, R., Koch, A., Vaes, N., and Melotte, V. (2019) Nervous NDRGs: the N-myc downstream–regulated gene family in the central and peripheral nervous system.

77. Hu, X. L., Liu, X. P., Deng, Y. C., Lin, S. X., Wu, L., Zhang, J., Wang, L. F., Wang, X. B., Li, X., Shen, L., Zhang, Y. Q., and Yao, L. B. (2006) Expression analysis of the NDRG2 gene in mouse embryonic and adult tissues. *Cell Tissue Res* **325**, 67-76

78. Mitchelmore, C., Büchmann-Møller, S., Rask, L., West, M. J., Troncoso, J. C., and Jensen, N. A. (2004) NDRG2: a novel Alzheimer's disease associated protein. *Neurobiol Dis* **16**, 48-58

79. Jin, P. P., Xia, F., Ma, B. F., Li, Z., Zhang, G. F., Deng, Y. C., Tu, Z. L., Zhang, X. X., and Hou, S. X. (2019) Spatiotemporal expression of NDRG2 in the human fetal brain. *Ann Anat* **221**, 148-155

80. Maeda, A., Hongo, S., and Miyazaki, A. (2004) Genomic organization, expression, and comparative analysis of noncoding region of the rat Ndrg4 gene. *Gene* **324**, 149-158

81. Nakada, N., Hongo, S., Ohki, T., Maeda, A., and Takeda, M. (2002) Molecular characterization of NDRG4/Bdm1 protein isoforms that are differentially regulated during rat brain development. *Brain Res Dev Brain Res* **135**, 45-53

82. Zhou, R. H., Kokame, K., Tsukamoto, Y., Yutani, C., Kato, H., and Miyata, T. (2001) Characterization of the human NDRG gene family: a newly identified member, NDRG4, is specifically expressed in brain and heart. *Genomics* **73**, 86-97

83. Berger, P., Sirkowski, E. E., Scherer, S. S., and Suter, U. (2004) Expression analysis of the N-Myc downstream-regulated gene 1 indicates that myelinating Schwann cells are the primary disease target in hereditary motor and sensory neuropathy-Lom. *Neurobiol Dis* **17**, 290-299

84. Kimmel, C. B., Ballard, W. W., Kimmel, S. R., Ullmann, B., and Schilling, T. F. (1995) Stages of embryonic development of the zebrafish. *Dev Dyn* **203**, 253-310

85. Thisse, C., and Thisse, B. (2008) High-resolution in situ hybridization to whole-mount zebrafish embryos. *Nature Protocols* **3**, 59-69

86. McCurley, A. T., and Callard, G. V. (2008) Characterization of housekeeping genes in zebrafish: male-female differences and effects of tissue type, developmental stage and chemical treatment. *BMC Molecular Biology* **9**, 102

87. Robertson, C. E., Wright, P. A., Köblitz, L., and Bernier, N. J. (2014) Hypoxia-inducible factor-1 mediates adaptive developmental plasticity of hypoxia tolerance in zebrafish, Danio rerio. *Proc Biol Sci* **281**

88. Xu, H., Li, C., Zeng, Q., Agrawal, I., Zhu, X., and Gong, Z. (2016) Genome-wide identification of suitable zebrafish Danio rerio reference genes for normalization of gene expression data by RT-qPCR. *Journal of Fish Biology* **88**, 2095-2110

89. White, R. J., Collins, J. E., Sealy, I. M., Wali, N., Dooley, C. M., Digby, Z., Stemple, D. L., Murphy, D. N., Billis, K., Hourlier, T., Füllgrabe, A., Davis, M. P., Enright, A. J., and Busch-Nentwich, E. M. (2017) A high-resolution mRNA expression time course of embryonic development in zebrafish. *eLife* **6**, e30860

90. Burns, M. J., Nixon, G. J., Foy, C. A., and Harris, N. (2005) Standardisation of data from real-time quantitative PCR methods - evaluation of outliers and comparison of calibration curves. *BMC Biotechnol* **5**, 31

91. Motulsky, H. J., and Brown, R. E. (2006) Detecting outliers when fitting data with nonlinear regression - a new method based on robust nonlinear regression and the false discovery rate. *BMC Bioinformatics* **7**, 123

92. Greenald, D., Jeyakani, J., Pelster, B., Sealy, I., Mathavan, S., and van Eeden, F. J. (2015) Genome-wide mapping of Hif-1alpha binding sites in zebrafish. *BMC Genomics* **16**, 923

93. Takita, S., Wada, Y., and Kawamura, S. (2016) Effects of NDRG1 family proteins on photoreceptor outer segment morphology in zebrafish. *Scientific Reports* **6**, 36590

94. Teodoro, R. O., and O'Farrell, P. H. (2003) Nitric oxide-induced suspended animation promotes survival during hypoxia. *EMBO J* **22**, 580-587

95. Johnson, A. B., Denko, N., and Barton, M. C. (2008) Hypoxia induces a novel signature of chromatin modifications and global repression of transcription. *Mutat Res* **640**, 174-179

96. Cavadas, M. A. S., Mesnieres, M., Crifo, B., Manresa, M. C., Selfridge, A. C., Keogh, C. E., Fabian, Z., Scholz, C. C., Nolan, K. A., Rocha, L. M. A., Tambuwala, M. M., Brown, S., Wdowicz, A., Corbett, D., Murphy, K. J., Godson, C., Cummins, E. P., Taylor, C. T., and Cheong, A. (2016) REST is a hypoxia-responsive transcriptional repressor. *Scientific Reports* **6**, 31355

97. Cummins, E. P., and Taylor, C. T. (2005) Hypoxia-responsive transcription factors. *Pflugers Arch* **450**, 363-371

98. Wen, L., Liu, L., Tong, L., Li, J., Zhang, K., Zhang, Q., and Li, C. (2019) NDRG4 prevents cerebral ischemia/reperfusion injury by inhibiting neuronal apoptosis. *Genes & Diseases* **6**, 448-454

99. Xing, Y., Tang, B., Zhu, C., Li, W., Li, Z., Zhao, J., Gong, W. D., Wu, Z. Q., Zhu, C. C., and Zhang, Y. Q. (2016) N-myc downstream-regulated gene 4, up-regulated by tumor necrosis factor-α and nuclear factor kappa B, aggravates cardiac ischemia/reperfusion injury by inhibiting reperfusion injury salvage kinase pathway. *Basic Res Cardiol* **111**, 11

100. Chen, B., Nelson, D. M., and Sadovsky, Y. (2006) N-myc down-regulated gene 1 modulates the response of term human trophoblasts to hypoxic injury. *J Biol Chem* **281**, 2764-2772

101. Claustrat, B., and Leston, J. (2015) Melatonin: Physiological effects in humans. *Neurochirurgie* **61**, 77-84

102. Niizuma, K., Endo, H., and Chan, P. H. (2009) Oxidative stress and mitochondrial dysfunction as determinants of ischemic neuronal death and survival. *J Neurochem* **109 Suppl 1**, 133-138

103. Chilov, D., Hofer, T., Bauer, C., Wenger, R. H., and Gassmann, M. (2001) Hypoxia affects expression of circadian genes PER1 and CLOCK in mouse brain. *FASEB J* **15**, 2613-2622

104. Pelster, B., and Egg, M. (2018) Hypoxia-inducible transcription factors in fish: expression, function and interconnection with the circadian clock. *J Exp Biol* **221**

105. Reiter, R. J., Mayo, J. C., Tan, D. X., Sainz, R. M., Alatorre-Jimenez, M., and Qin, L. (2016) Melatonin as an antioxidant: under promises but over delivers. *J Pineal Res* **61**, 253-278

106. Ebert, E. C. (2006) Hypoxic liver injury. *Mayo Clin Proc* **81**, 1232-1236

107. Zheng, L., Kelly, C. J., and Colgan, S. P. (2015) Physiologic hypoxia and oxygen homeostasis in the healthy intestine. A Review in the Theme: Cellular Responses to Hypoxia. *Am J Physiol Cell Physiol* **309**, C350-360

108. Singhal, R., and Shah, Y. M. (2020) Oxygen battle in the gut: Hypoxia and hypoxia-inducible factors in metabolic and inflammatory responses in the intestine. *J Biol Chem* **295**, 10493-10505

109. Bogdanova, A., Petrushanko, I. Y., Hernansanz-Agustin, P., and Martinez-Ruiz, A. (2016) "Oxygen Sensing" by Na,K-ATPase: These Miraculous Thiols. *Front Physiol* **7**, 314

110. Mazurek, B., Haupt, H., Georgiewa, P., Klapp, B. F., and Reisshauer, A. (2006) A model of peripherally developing hearing loss and tinnitus based on the role of hypoxia and ischemia. *Med Hypotheses* **67**, 892-899

111. Olivetto, E., Simoni, E., Guaran, V., Astolfi, L., and Martini, A. (2015) Sensorineural hearing loss and ischemic injury: Development of animal models to assess vascular and oxidative effects. *Hear Res* **327**, 58-68

112. Sonbay Yilmaz, N. D., Saka, C., Oktay Arslan, B., Aygener Yesilyurt, N., Saka, D., Ardic, S., and Akin, I. (2019) The effect of hypoxia on hearing function. *Turk J Med Sci* **49**, 1450-1454

113. Sanchez-Garcia, M. A., Zottoli, S. J., and Roberson, L. M. (2019) Hypoxia Has a Lasting Effect on Fast-Startle Behavior of the Tropical Fish Haemulon plumieri. *Biol Bull* **237**, 48-62

114. Krock, B. L., Skuli, N., and Simon, M. C. (2011) Hypoxia-induced angiogenesis: good and evil. *Genes Cancer* **2**, 1117-1133

115. Toffoli, S., Delaive, E., Dieu, M., Feron, O., Raes, M., and Michiels, C. (2009) NDRG1 and CRK-I/II are regulators of endothelial cell migration under Intermittent Hypoxia. *Angiogenesis* **12**, 339-354

116. Gladden, L. B. (2004) Lactate metabolism: a new paradigm for the third millennium. *The Journal of Physiology* **558**, 5-30

117. Sugiki, T., Murakami, M., Taketomi, Y., Kikuchi-Yanoshita, R., and Kudo, I. (2004) N-myc downregulated gene 1 is a phosphorylated protein in mast cells. *Biol Pharm Bull* **27**, 624-627

118. Murray, J. T., Campbell, D. G., Morrice, N., Auld, G. C., Shpiro, N., Marquez, R., Peggie, M., Bain, J., Bloomberg, G. B., Grahammer, F., Lang, F., Wulff, P., Kuhl, D., and Cohen, P. (2004) Exploitation of KESTREL to identify NDRG family members as physiological substrates for SGK1 and GSK3. *Biochem J* **384**, 477-488

119. Burchfield, J. G., Lennard, A. J., Narasimhan, S., Hughes, W. E., Wasinger, V. C., Corthals, G. L., Okuda, T., Kondoh, H., Biden, T. J., and Schmitz-Peiffer, C. (2004) Akt mediates insulin-stimulated phosphorylation of Ndrg2: evidence for cross-talk with protein kinase C theta. *J Biol Chem* **279**, 18623-18632

120. Zimmer, A. M., Mandic, M., Rourke, K. M., and Perry, S. F. (2020) Breathing with fins: do the pectoral fins of larval fishes play a respiratory role? *Am J Physiol Regul Integr Comp Physiol* **318**, R89-R97

121. Hale, M. E. (2014) Developmental change in the function of movement systems: transition of the pectoral fins between respiratory and locomotor roles in zebrafish. *Integr Comp Biol* **54**, 238-249

VIII. Summary

Currently, the molecular mechanisms that initiate and maintain hypometabolic state in zebrafish embryos are mostly unknown. However, it is clear that when hypometabolism is established, it confers the zebrafish embryos the ability to survive under low O2 conditions – possibly by decreasing the ATP demand to meet the lowered O2 supply. Most likely, there are several, parallel hypoxia adaptive signaling pathways that are triggered in response to hypoxia/anoxia, which orchestrate the induction of hypometabolism. Ultimately, understanding these mechanisms in zebrafish embryos may reveal potential therapeutic targets for the prevention and treatment of ischemic injuries.

IX. APPENDIX REFERENCES

(Excluding references used in "Differential Expression and Hypoxia-mediated Regulation of the N-myc Downstream Regulated Gene Family" manuscript; The references for the above mentioned manuscript is listed separately as part of the publication manuscript above)

1. Cooper, C. E., & Brown, G. C. (2008). The inhibition of mitochondrial cytochrome oxidase by the gases carbon monoxide, nitric oxide, hydrogen cyanide and hydrogen sulfide: Chemical mechanism and physiological significance. *Journal of Bioenergetics and Biomembranes*. https://doi.org/10.1007/s10863-008-9166-6
2. Essers J, Theil AF, Baldeyron C, van Cappellen WA, Houtsmuller AB, Kanaar R, Vermeulen W (2005). "Nuclear dynamics of PCNA in DNA replication and repair". *Mol. Cell. Biol*. **25** (21): 9350–9359.
3. Ge SN, Zhao MM, Wu DD, Chen Y, Wang Y, Zhu JH, Cai WJ, Zhu YZ, Zhu YC. Hydrogen sulfide targets EGFR Cys797/Cys798 residues to induce Na(+)/K(+)-ATPase endocytosis and inhibition in renal tubular epithelial cells and increase sodium excretion in chronic salt-loaded rats. Antioxid Redox Signal. 2014 Nov 20;21(15):2061-82. doi: 10.1089/ars.2013.5304. Epub 2014 May 8. PMID: 24684506; PMCID: PMC4215382.
4. Hammers, M. D., Taormina, M. J., Cerda, M. M., Montoya, L. A., Seidenkranz, D. T., Parthasarathy, R., & Pluth, M. D. (2015). A Bright Fluorescent Probe for H2S Enables Analyte-Responsive, 3D Imaging in Live Zebrafish Using Light

Sheet Fluorescence Microscopy. *Journal of the American Chemical Society*, *137*(32), 10216–23. https://doi.org/10.1021/jacs.5b04196

5. Kimura, H. (2013). Hydrogen Sulfide and its Therapeutic Applications. *Hydrogen Sulfide and Its Therapeutic Applications*, 1–207. https://doi.org/10.1007/978-3-7091-1550-3
6. Leonardi E, Girlando S, Serio G, Mauri FA, Perrone G, Scampini S, Dalla Palma P, Barbareschi M (1992). "PCNA and Ki67 expression in breast carcinoma: correlations with clinical and biological variables". *J. Clin. Pathol*. **45** (5): 416–419.
7. Olson, K. R. (2011). Hydrogen sulfide is an oxygen sensor in the carotid body. *Respiratory Physiology & Neurobiology*, *179*, 103–110. https://doi.org/10.1016/j.resp.2011.09.010
8. Olson, K. R. (2015). Hydrogen sulfide as an oxygen sensor. *Antioxidants & Redox Signaling*, *22*(5), 377–97. https://doi.org/10.1089/ars.2014.5930
9. Olson, K. R., Deleon, E. R., Gao, Y., Hurley, K., Sadauskas, V., Batz, C., & Stoy, G. F. (2013). Thiosulfate: a readily accessible source of hydrogen sulfide in oxygen sensing. *American Journal of Physiology. Regulatory, Integrative and Comparative Physiology*, *305*(6), R592-603. https://doi.org/10.1152/ajpregu.00421.2012
10. Shivji KK, Kenny MK, Wood RD (April 1992). "Proliferating cell nuclear antigen is required for DNA excision repair". *Cell*. **69** (2): 367–74.
11. Tu LC, Yan X, Hood L, Lin B. Proteomics analysis of the interactome of N-myc downstream regulated gene 1 and its interactions with the androgen response

program in prostate cancer cells. Mol Cell Proteomics. 2007 Apr;6(4):575-88. doi: 10.1074/mcp.M600249-MCP200. Epub 2007 Jan 12. PMID: 17220478.